Weak decays beyond leading logarithms

Gerhard Buchalla*

Theoretical Physics Department, Fermi National Accelerator Laboratory, P.O. Box 500, Batavia, Illinois 60510

Andrzej J. Buras†

Physik Department, Technische Universität München, D-85748 Garching, Germany and Max-Planck-Institut für Physik, Werner-Heisenberg-Institut, Föhringer Ring 6, D-80805 München, Germany

Markus E. Lautenbacher‡

Physik Department, Technische Universität München, D-85748 Garching, Germany and Stanford Linear Accelerator Center Theory Group, Stanford University, P.O. Box 4349, Stanford, California 94309
Received 6 June 1996

We review the present status of QCD corrections to weak decays beyond the leading-logarithmic approximation, including particle-antiparticle mixing and rare and *CP*-violating decays. After presenting the basic formalism for these calculations we discuss in detail the effective Hamiltonians of all decays for which the next-to-leading-order corrections are known. Subsequently, we present the phenomenological implications of these calculations. The values of various parameters are updated, in particular the mass of the newly discovered top quark. One of the central issues in this review are the theoretical uncertainties related to renormalization-scale ambiguities, which are substantially reduced by including next-to-leading-order corrections. The impact of this theoretical improvement on the determination of the Cabibbo-Kobayashi-Maskawa matrix is then illustrated. [S0034-6861(96)00304-2]

CONTENTS

*Electronic address: buchalla@fnth20.fnal.gov
†Electronic address: buras@feynman.t30.physik.tu-muenchen.de
‡Electronic address: lauten@feynman.t30.physik.tu-muenchen.de

I. INTRODUCTION

In our present day understanding, weak interactions show the most complicated and diversified pattern of all the fundamental forces of nature. The standard model of strong and electroweak interactions is capable of successfully describing a large amount of experimental information quantitatively and even more information

qualitatively. However, there are many unanswered questions that still remain, and many of them, such as electroweak symmetry breaking and the origin of fermion masses and quark mixing, are closely related to weak interactions. In addition, the discrete space-time symmetries C, P, and T (charge, parity, and time) are respected by the strong and electromagnetic interactions, but not by the weak interaction. For these reasons, much effort has been spent on developing a theoretical understanding of the weak interaction. An excellent laboratory for this enterprise is provided by the very rich phenomenology of weak meson decays.

In this article, we review the subject of next-to-leading-order QCD corrections to weak meson decays. The careful investigation of these decays is mandatory for further testing of the standard model. Of particular importance is the determination of all Cabbibo-Kobayashi-Maskawa. (CKM) parameters to an accuracy that will test the consistency of the standard model, including the unitarity of the CKM matrix and its compatibility with the quark masses. Many interesting issues within this context remain unresolved, for example, direct CP violation in nonleptonic K decays, CP violation patterns in the B system, and the rare K and B decays that are sensitive to the effects of virtual heavy particles, such as the top quark. As experiments achieve better resolution and discover more rare decay channels, the corresponding theory has to become more precise as well, so that the new experimental results can be efficiently used to obtain improved determinations of the parameters in the standard model and consequently to allow improved predictions for future experiments.

Since hadrons are involved in all the decays we are interested in here, QCD effects are unavoidable and must be quantitatively understood. To accomplish this task one employs two tools of quantum field theory, the operator product expansion (OPE) (Wilson and Zimmermann, 1972) and the renormalization group (Stueckelberg and Petermann, 1953; Gell-Mann and Low, 1954; Ovsyannikov, 1956; Callan Jr., 1970; Symanzik, 1970; 't Hooft, 1973; Weinberg, 1973). In the OPE, an amplitude A for a process such as a weak decay may be represented as (Witten, 1977)

$$A=\langle\mathcal{H}_{\rm eff}\rangle=\sum_i C_i(\mu,M_W)\langle Q_i(\mu)\rangle. \tag{1.1}$$

Here Q_i are local operators and C_i are the Wilson coefficients. Both the C_i and Q_i depend on the QCD renormalization scale μ, and C_i depends on the mass of the W boson and the masses of other heavy particles such as the top quark as well. One can view the expression of $\Sigma_i C_i Q_i$ more intuitively as an effective Hamiltonian for the process considered, with Q_i the effective vertices and C_i the corresponding coupling constants.

The essential point about the OPE is that it separates the full problem into two distinct parts, the long-distance contributions contained in the operator matrix elements and the short-distance physics described by the Wilson coefficients. The renormalization scale μ separating the two regimes is typically chosen to be of the order of 1 GeV for kaon decays and a few GeV for the decays of D and B mesons. The physical amplitude A, however, cannot depend on μ. The μ dependence of the Wilson coefficients has to cancel the μ dependence present in $\langle Q_i(\mu)\rangle$. In other words it is a matter of choice what exactly belongs to the matrix elements and what to the coefficient functions. This cancellation of μ dependence generally involves several terms in the expansion in Eq. (1.1).

The long-distance part in Eq. (1.1) deals with low-energy strong interactions and therefore poses a very difficult problem. Many approaches, like lattice gauge theory, $1/N$ expansion, QCD and hadronic sum rules, or chiral perturbation theory, have been used in the past to obtain qualitative insight and some quantitative estimates of relevant hadronic matrix elements. In addition heavy-quark effective theory and heavy-quark expansions have been widely used for B decays. Despite these efforts the problem is not yet solved satisfactorily.

In general in weak decays of mesons the hadronic matrix elements constitute the most important source of theoretical uncertainty. There are, however, a few special examples of semileptonic rare decays (K^+, $K_L\to\pi^0\nu\bar{\nu}$, $B\to X_s\nu\bar{\nu}$), where matrix elements needed can be extracted from well-measured leading decays, calculated perturbatively, or, as in the case of $B_s\to\mu\bar{\mu}$, expressed fully in terms of meson decay constants. Thus the problem of long-distance QCD can almost be completely avoided. This makes these decay modes very attractive from a theoretical point of view, although, due to very small branching ratios, they are quite difficult to access experimentally.

In contrast to the long-distance contributions the short-distance QCD interaction can be analyzed systematically using well-established field-theoretical methods. Due to the asymptotic freedom of QCD the strong-interaction effects at short distances are calculable in perturbation theory in the strong coupling $\alpha_s(\mu)$. In fact $\alpha_s(\mu)$ is small enough in the full range of relevant short-distance scales of $\mathcal{O}(M_W)$ down to $\mathcal{O}(1\ \text{GeV})$ to serve as a reasonable expansion parameter. However, the presence of large logarithms $\ln(M_W/\mu)$ multiplying $\alpha_s(\mu)$, where $\mu=\mathcal{O}(1\ \text{GeV})$, in the calculation of the coefficients $C_i(\mu,M_W)$ spoils the validity of the usual perturbation series. This is a characteristic feature of renormalizable quantum field theories when vastly different scales are present. It is therefore necessary to perform a renormalization-group analysis that allows an efficient summation of logarithmic terms to all orders in perturbation theory. In this way the usual perturbation theory is replaced by a renormalized-group improved perturbation theory in which the leading order corresponds to summing the leading logarithmic terms $\sim[\alpha_s\ln(M_W/\mu)]^n$. Then at next to leading order (NLO), all terms of the form $\sim\alpha_s[\alpha_s\ln(M_W/\mu)]^n$ are summed in addition, and so on.

The evaluation of the short-distance coefficients in the renormalized-group improved perturbation theory is only a part of the entire problem, but one should stress that it is still indispensible to analyze this part systemati-

TABLE I. Processes for which NLO QCD corrections have been calculated.

Decay	Reference
$\Delta F=1$ decays	
Current-current operators	(Altarelli *et al.*, 1981), (Buras and Weisz, 1990)
QCD penguin operators	(Buras *et al.*, 1993), (Buras *et al.*, 1993a), (Ciuchini, Franco, Martinelli, and Reina, 1994)
Electroweak penguin operators	(Buras *et al.*, 1993), (Buras *et al.*, 1993a), (Ciuchini, Franco, Martinelli, and Reina, 1994)
Magnetic penguin operators	(Misiak and Münz, 1995)
$B(B\to Xe\nu)$	(Altarelli *et al.*, 1981), (Buchalla, 1993), (Bagan *et al.*, 1994), (Bagan, Ball, Fiol, and Gosdzinsky, 1995),
Inclusive $\Delta S=1$	(Jamin and Pich, 1994)
Particle-antiparticle mixing	
η_1	(Herrlich and Nierste, 1994)
η_2,η_B	(Buras *et al.*, 1990)
η_3	(Herrlich and Nierste, 1995a)
Rare K- and B-meson decays	
$K_L^0\to\pi^0\nu\bar{\nu}$, $B\to l^+l^-$, $B\to X_s\nu\bar{\nu}$	(Buchalla and Buras, 1993a)
$K^+\to\pi^+\nu\bar{\nu}$, $K_L\to\mu^+\mu^-$	(Buchalla and Buras, 1994a)
$K^+\to\pi^+\mu\bar{\mu}$	(Buchalla and Buras, 1994b)
$K_L\to\pi^0e^+e^-$	(Buras, Lautenbacher, Misiak, and Münz, 1994)
$B\to X_se^+e^-$	(Misiak, 1995), (Buras and Münz, 1995)

cally; the effective Hamiltonians resulting from the short-distance analysis provide the necessary basis for any further computation of weak-decay amplitudes. The long-distance matrix elements can be treated separately and will hopefully be known with desired accuracy one day.

It is worth noting that the short-distance QCD contributions by themselves already have an important impact on weak-decay processes. In nonleptonic K decays, for example, they help to explain the famous $\Delta I=1/2$ rule, and they generate penguin operators that are relevant for ε'/ε. They suppress the semileptonic branching ratio in heavy-quark decays and produce a significant enhancement of the weak radiative process $B\to X_s\gamma$.

Starting with the pioneering work of Galliard and Lee (1974a) and Altarelli and Maiani (1974), who calculated the first leading-logarithmic-order QCD effects in weak decays, considerable efforts have been devoted to the calculation of short-distance QCD corrections to weak-meson decay processes. The analysis has been extended to a large variety of particular modes. Of special interest are processes sensitive to the virtual contribution of heavy quarks, like the top quark. A classic example of this type is the work of Galliard and Lee (1974b), which analyzed K^0-$\bar{K}^0$ mixing and estimated the charm quark mass prior to its discovery, based on the dependence of the $\Delta S=2$ transition on virtual charm. This calculation is the prototype for present-day analyses of virtual-top contributions in B^0-$\bar{B}^0$ mixing, rare decays, and CP violation, which are similar in spirit.

Until 1989 most calculations were done in the leading-logarithmic approximation (Vainshtein *et al.*, 1977; Gilman and Wise, 1979, 1980; Guberina and Peccei, 1980), with the exception of Altarelli *et al.* (1981), where the first NLO calculation in the theory of weak decays was presented. Currently, effective Hamiltonians are available to NLO for the most important and interesting cases, as is given in Table I, due to a series of publications beginning with the work of Burns and Weisz (1990).

Aside from general increases in accuracy inherent with going to the next higher order in a perturbation series expansion, there are several important reasons for performing these very involved and complicated calculations of next to leading order:

(i) The NLO approximation tests the validity of the perturbation theory. In leading order, the ultimate result is $\mathcal{O}(1)$, whereas, at NLO, one first obtains an $\mathcal{O}(\alpha_s)$ correction relative to the leading order, and one can check whether it is small enough to justify the perturbative approach.

(ii) The QCD has a scale parameter $\Lambda_{\overline{\rm MS}}$, but it cannot be interpreted meaningfully in weak decays without going to NLO.

(iii) Due to renormalization-group invariance, the physical amplitudes of decays do not depend on the exact scales at which quark masses are defined. However, by truncating a perturbation series, renormalization-group invariance is broken, resulting in scale-dependent ambiguities in the final answer. These can be reduced

considerably by going to NLO.

(iv) The Wilson coefficients are renormalization-scheme-dependent quantities. The scheme dependence is first "felt" at NLO, whereas the leading order is completely insensitive to this important feature. In particular, this issue is essential for a proper matching of the short-distance contributions to the long-distance matrix elements as obtained from lattice calculations.

(v) Certain decays, e.g., $K_L \to \pi^0 e^+ e^-$ and $B \to X_s e^+ e^-$, are only sensitive to the top-quark mass at the next to leading order.

This review article can conceptually be divided into three parts, "basic concepts," "technical calculations," and "phenomenological applications." This division is given in the hope of making the review as readable as possible for a wide audience of physicists.

The first part, Secs. II and III, introduces basic concepts that are utilized in the remainder of the review. Section II describes important aspects of the standard model as they relate to weak decays. In particular, the CKM matrix is shown in two common parametrizations, and the unitarity triangle is described. Section III outlines the basic formalism for the calculation of QCD effects in weak decays. Beginning with the idea of effective field theories, we introduce the techniques of the operator product expansion (OPE) and renormalization group (RG). The Wilson coefficients C_i are computed for local operators Q_i in the leading-logarithmic and next-to-leading-logarithmic approximations. In order to calculate C_i, one must evaluate one-loop and two-loop anomalous dimensions of Q_i, and, more generally, anomalous-dimension matrices that describe mixing of Q_i under renormalization. General formulas are obtained for C_i and the anomalous dimensions of Q_i. Section III.F contains the "master equations" for C_i, including next-to-leading-order corrections. In particular, the μ and renormalization-scheme dependences are discussed, and we show how they are cancelled by those present in the hadronic matrix elements.

The second part, comprised of Secs. IV–XV, is a compendium of effective Hamiltonians for weak decays for which next-to-leading-order corrections have been calculated (see Table I). We also include the $b \to s\gamma$ and $b \to sg$ transitions, which, while not known to NLO, deserve special attention. Initial conditions, $C_i(M_W)$, are given, as are a list of all one- and two-loop anomalous-dimension matrices, and tables of C_i as functions of $\Lambda_{\overline{\rm MS}}$, m_t, and the renormalization schemes considered. $\Lambda_{\overline{\rm MS}}$ is the QCD scale, and m_t the mass of the top quark. Using the results and general procedure of Sec. III, we examine similarities and differences between the different decays. In addition, Sec. XIV describes the penguin box expansion, a version of OPE well suited to study the top-quark mass dependence of weak decays, and Sec. XV introduces heavy-quark effective theory, showing the applications of this formalism to short-distance QCD corrections. Section XV also includes a summary of some important NLO results obtained in heavy-quark effective theory.

TABLE II. Electroweak charges Q, Y, and the third component of the weak isospin T_3 for quarks and leptons in the standard model.

	ν_L^e	e_L^-	e_R^-	u_L	d_L	u_R	d_R
Q	0	−1	−1	2/3	−1/3	2/3	−1/3
T_3	1/2	−1/2	0	1/2	−1/2	0	0
Y	−1	−1	−2	1/3	1/3	4/3	−2/3

The final part of this review (Secs. XVI–XXVI) presents the phenomenological perspective of weak decays and can be followed without a deep reading of the second part, although Sec. IV is a good reference to understand the general ideas. In Sec. XVI, comments are made about input parameters, Sec. XVII is an overview of the leading inclusive B-meson decays, and Sec. XVIII investigates the unitarity triangle as well as other important quantities that will be applied in the remaining sections. Sections XIX–XXVI analyze particular decays, their uncertainties with and without NLO corrections, and their significance to the standard model and its parameters.

II. STANDARD ELECTROWEAK MODEL

A. Particles and interactions

Throughout this review we will work in the context of the three-generation model of quarks and leptons, which is based on the gauge group $\mathrm{SU}(3)\otimes\mathrm{SU}(2)_L\otimes\mathrm{U}(1)_Y$ spontaneously broken down to $\mathrm{SU}(3)\otimes\mathrm{U}(1)_Q$. Here Y and Q denote the weak-hypercharge and the electric-charge generators, respectively. SU(3) represents the symmetry of QCD, which will be discussed in more detail in the following section. Here we review certain features of the electroweak part of the standard model that will be important for the present considerations.

The left-handed leptons and quarks are put in $\mathrm{SU}(2)_L$ doublets

$$\begin{pmatrix} \nu_e \\ e^- \end{pmatrix}_L, \quad \begin{pmatrix} \nu_\mu \\ \mu^- \end{pmatrix}_L, \quad \begin{pmatrix} \nu_\tau \\ \tau^- \end{pmatrix}_L, \tag{2.1}$$

$$\begin{pmatrix} u \\ d' \end{pmatrix}_L, \quad \begin{pmatrix} c \\ s' \end{pmatrix}_L, \quad \begin{pmatrix} t \\ b' \end{pmatrix}_L \tag{2.2}$$

with the corresponding right-handed fields transforming as singlets under $\mathrm{SU}(2)_L$. The primes are discussed below. The relevant electroweak charges Q, Y, and the third component of the weak isospin T_3 are collected in Table II.

The electroweak interactions of quarks and leptons are mediated by the massive weak gauge bosons $W^\pm$ and Z^0 and by the photon A. These interactions are summarized by the Lagrangian

$$\mathcal{L}_{\rm int} = \mathcal{L}_{CC} + \mathcal{L}_{\rm NC}, \tag{2.3}$$

where

$$\mathcal{L}_{CC}=\frac{g_2}{2\sqrt{2}}\,(J_\mu^+ W^{+\mu}+J_\mu^- W^{-\mu}) \tag{2.4}$$

describes the *charged current* interactions and

$$\mathcal{L}_{\rm NC}=eJ_\mu^{em}A^\mu+\frac{g_2}{2\cos\Theta_W}J_\mu^0 Z^\mu \tag{2.5}$$

the *neutral current* interactions. Here e is the QED coupling constant, g_2 is the $SU(2)_L$ coupling constant, and Θ_W is the Weinberg angle. The currents are given as follows

$$J_\mu^+=(\bar{u}d')_{V-A}+(\bar{c}s')_{V-A}+(\bar{t}b')_{V-A}+(\bar{\nu}_e e)_{V-A}+(\bar{\nu}_\mu\mu)_{V-A}+(\bar{\nu}_\tau\tau)_{V-A}, \tag{2.6}$$

$$J_\mu^{em}=\sum_f Q_f\bar{f}\gamma_\mu f, \tag{2.7}$$

$$J_\mu^0=\sum_f \bar{f}\gamma_\mu(v_f-a_f\gamma_5)f, \quad \text{with} \tag{2.8}$$

$$v_f=T_3^f-2Q_f\sin^2\Theta_W, \quad a_f=T_3^f, \tag{2.9}$$

and Q_f and T_3^f denote the charge and the third component of the weak isospin of the left-handed fermion f_L. $(V-A)$ refers to $\gamma_\mu(1-\gamma_5)$.

In the discussion of weak decays an important role is played by the Fermi constant

$$\frac{G_F}{\sqrt{2}}=\frac{g_2^2}{8M_W^2}, \tag{2.10}$$

which has the value

$$G_F=1.16639\times10^{-5}\ \text{GeV}^{-2}. \tag{2.11}$$

Other values of the relevant parameters will be collected in the Appendix.

The interactions between the gauge bosons are standard and can be found in any textbook on gauge theories.

The primes in Eq. (2.2) indicate that the weak eigenstates (d',s',b') are not equal to the corresponding mass eigenstates (d,s,b) but rather are linear combinations of the latter. This is expressed through the relation

$$\begin{pmatrix} d' \\ s' \\ b' \end{pmatrix}=\begin{pmatrix} V_{ud} & V_{us} & V_{ub} \\ V_{cd} & V_{cs} & V_{cb} \\ V_{td} & V_{ts} & V_{tb} \end{pmatrix}\begin{pmatrix} d \\ s \\ b \end{pmatrix}, \tag{2.12}$$

where the unitary matrix connecting these two sets of states is the Cabibbo-Kobayashi-Maskawa (CKM) matrix. Many parametrizations of this matrix have been proposed in the literature. In this review we will use two parametrizations: the standard parametrization recommended by the Particle Data Group and the Wolfenstein parametrization.

B. Standard parametrization

Let us introduce the notation $c_{ij}=\cos\theta_{ij}$ and $s_{ij}=\sin\theta_{ij}$ with i and j being quark generation labels $(i,j=1,2,3)$. The standard parametrization is then given as follows (Particle Data Group, 1994)

$$V=\begin{pmatrix} c_{12}c_{13} & s_{12}c_{13} & s_{13}e^{-i\delta} \\ -s_{12}c_{23}-c_{12}s_{23}s_{13}e^{i\delta} & c_{12}c_{23}-s_{12}s_{23}s_{13}e^{i\delta} & s_{23}c_{13} \\ s_{12}s_{23}-c_{12}c_{23}s_{13}e^{i\delta} & -s_{23}c_{12}-s_{12}c_{23}s_{13}e^{i\delta} & c_{23}c_{13} \end{pmatrix}, \tag{2.13}$$

where δ is the phase necessary for CP violation. c_{ij} and s_{ij} can all be chosen to be positive, and δ may vary in the range $0\leq\delta\leq2\pi$. However, the measurements of CP violation in K decays force δ to be in the range $0<\delta<\pi$.

The extensive phenomenology of the last few years has shown that s_{13} and s_{23} are small numbers, $\mathcal{O}(10^{-3})$ and $\mathcal{O}(10^{-2})$, respectively. Consequently, to an excellent accuracy, $c_{13}\approx c_{23}\approx1$ and the four independent parameters are

$$s_{12}=|V_{us}|, \quad s_{13}=|V_{ub}|, \quad s_{23}=|V_{cb}|, \quad \delta, \tag{2.14}$$

with the phase δ extracted from CP-violating transitions or loop processes sensitive to $|V_{td}|$. The latter fact is based on the observation that, for $0\leq\delta\leq\pi$, there is a one-to-one correspondence between δ and $|V_{td}|$ given by

$$|V_{td}|=\sqrt{a^2+b^2-2ab\,\cos\delta}, \quad a=|V_{cd}V_{cb}|, \quad b=|V_{ud}V_{ub}|. \tag{2.15}$$

C. Wolfenstein parametrization beyond leading order

We will also use the Wolfenstein parametrization (Wolfenstein, 1983). It is an approximate parametrization of the CKM matrix in which each element is expanded as a power series in the small parameter $\lambda=|V_{us}|=0.22$.

$$V=\begin{pmatrix} 1-\frac{\lambda^2}{2} & \lambda & A\lambda^3(\varrho-i\eta) \\ -\lambda & 1-\frac{\lambda^2}{2} & A\lambda^2 \\ A\lambda^3(1-\varrho-i\eta) & -A\lambda^2 & 1 \end{pmatrix}+\mathcal{O}(\lambda^4), \tag{2.16}$$

where the four independent parameters are

$$\lambda, \quad A, \quad \varrho, \quad \eta. \tag{2.17}$$

The Wolfenstein parametrization has several nice fea-

tures. It offers a very transparent geometrical representation of the structure of the CKM matrix and allows one to derive several analytic results to be discussed below. This turns out to be very useful in the phenomenology of rare decays and of CP violation.

When using the Wolfenstein parametrization one should remember that it is an approximation and that in certain situations neglecting $\mathcal{O}(\lambda^4)$ terms may give wrong results. How does one find $\mathcal{O}(\lambda^4)$ and higher order terms? Since Eq. (2.16) is only an approximation, the *exact* definition of λ is not unique by terms of the neglected order $\mathcal{O}(\lambda^4)$. This is the reason why different $\mathcal{O}(\lambda^4)$ terms can be found in the literature. They simply correspond to different definitions of the expansion parameter λ. Obviously the physics does not depend on this choice. Here it suffices to find an expansion in λ that allows for simple relations between the parameters in Eqs. (2.14) and (2.17). This will also restore the unitarity of the CKM matrix, which in the Wolfenstein parametrization as given in Eq. (2.16) is not satisfied exactly.

To this end we go back to Eq. (2.13) and impose the relations (Buras, Lautenbacher, and Ostermaier, 1994)

$$s_{12}=\lambda, \quad s_{23}=A\lambda^2, \quad s_{13}e^{-i\delta}=A\lambda^3(\varrho-i\eta) \tag{2.18}$$

to *all orders* in λ. In view of the comments made above this can certainly be done. It follows that

$$\varrho=\frac{s_{13}}{s_{12}s_{23}}\cos\delta, \quad \eta=\frac{s_{13}}{s_{12}s_{23}}\sin\delta. \tag{2.19}$$

We observe that Eqs. (2.18) and (2.19) simply represent the change of variables from Eqs. (2.14) to (2.17). Making this change of variables in the standard parametrization (2.13), we find that the CKM matrix as a function of (λ,A,ϱ,η) satisfies unitarity exactly. We also note that, in view of $c_{13}=1-\mathcal{O}(\lambda^6)$, the relations between s_{ij} and $|V_{ij}|$ in Eq. (2.14) are satisfied to high accuracy. The relations in Eq. (2.19) have been first used in Schmidtler and Schubert (1992). However, the improved treatment of the unitarity triangle presented below goes beyond the analysis of these authors.

The procedure outlined above automatically gives the corrections to the Wolfenstein parametrization in Eq. (2.16). Indeed expressing Eq. (2.13) in terms of Wolfenstein parameters using Eq. (2.18) and then expanding in powers of λ, we recover the matrix in Eq. (2.16) and in addition find explicit corrections of $\mathcal{O}(\lambda^4)$ and higher-order terms. V_{ub} remains unchanged. The corrections to V_{us} and V_{cb} appear only at $\mathcal{O}(\lambda^7)$ and $\mathcal{O}(\lambda^8)$, respectively. For many practical purposes the corrections to the real parts can also be neglected. The essential corrections to the imaginary parts are

$$\Delta V_{cd}=-iA^2\lambda^5\eta, \quad \Delta V_{ts}=-iA\lambda^4\eta. \tag{2.20}$$

These two corrections have to be taken into account in the discussion of CP violation. On the other hand the imaginary part of V_{cs}, which in our expansion in λ appears only at $\mathcal{O}(\lambda^6)$, can be fully neglected.

In order to improve the accuracy of the unitarity triangle discussed below we will also include the $\mathcal{O}(\lambda^5)$ correction to V_{td}, which gives

$$V_{td}=A\lambda^3(1-\bar{\varrho}-i\bar{\eta}) \tag{2.21}$$

with

$$\bar{\varrho}=\varrho\left(1-\frac{\lambda^2}{2}\right), \quad \bar{\eta}=\eta\left(1-\frac{\lambda^2}{2}\right). \tag{2.22}$$

In order to derive analytic results we need accurate explicit expressions for $\lambda_i=V_{id}V_{is}^*$, where $i=c,t$. We have

$$\mathrm{Im}\lambda_t=-\mathrm{Im}\lambda_c=\eta A^2\lambda^5, \tag{2.23}$$

$$\mathrm{Re}\lambda_c=-\lambda\left(1-\frac{\lambda^2}{2}\right), \tag{2.24}$$

$$\mathrm{Re}\lambda_t=-\left(1-\frac{\lambda^2}{2}\right)A^2\lambda^5(1-\bar{\varrho}). \tag{2.25}$$

To an accuracy of 0.2% expressions (2.23) and (2.24) represent the exact formulas obtained using Eq. (2.13). Equation (2.25) deviates by at most 2% from the exact formula in the full range of parameters considered. In order to keep the analytic expressions in the phenomenological applications in a transparent form we have dropped a small $\mathcal{O}(\lambda^7)$ term in deriving Eq. (2.25). After inserting Eqs. (2.23)–(2.25) in exact formulas for quantities of interest, further expansion in λ should not be made.

D. Unitarity triangle beyond leading order

The unitarity of the CKM matrix provides us with several relations, of which

$$V_{ud}V_{ub}^*+V_{cd}V_{cb}^*+V_{td}V_{tb}^*=0 \tag{2.26}$$

is the most useful one. In the complex plane Eq. (2.26) can be represented as a triangle, the so-called "unitarity-triangle" (UT). Phenomenologically this triangle is very interesting, as it simultaneously involves the elements V_{ub}, V_{cb}, and V_{td}, the values of which are currently in dispute.

In the usual analyses of the unitarity triangle only terms $\mathcal{O}(\lambda^3)$ are kept in Eq. (2.26) (Dib *et al.*, 1990; Buras and Harlander, 1992; Harris and Rosner, 1992; Nir, 1992; Schmidtler and Schubert, 1992; Ali and London, 1995). It is, however, straightforward to include the next-to-leading-$\mathcal{O}(\lambda^5)$ terms (Buras, Lautenbacher, and Ostermaier, 1994). We note first that

$$V_{cd}V_{cb}^*=-A\lambda^3+\mathcal{O}(\lambda^7). \tag{2.27}$$

Thus, to an excellent accuracy, $V_{cd}V_{cb}^*$ is real with $|V_{cd}V_{cb}^*|=A\lambda^3$. Keeping $\mathcal{O}(\lambda^5)$ corrections and rescaling all terms in Eq. (2.26) by $A\lambda^3$, we find

$$\frac{1}{A\lambda^3}V_{ud}V_{ub}^*=\bar{\varrho}+i\bar{\eta}, \quad \frac{1}{A\lambda^3}V_{td}V_{tb}^*=1-(\bar{\varrho}+i\bar{\eta}) \tag{2.28}$$

with $\bar{\varrho}$ and $\bar{\eta}$ defined in Eq. (2.22). Thus we can represent Eq. (2.26) as the unitarity triangle in the complex $(\bar{\varrho},\bar{\eta})$ plane. This is shown in Fig. 1. The length of the side CB that lies on the real axis is unity when Eq. (2.26)

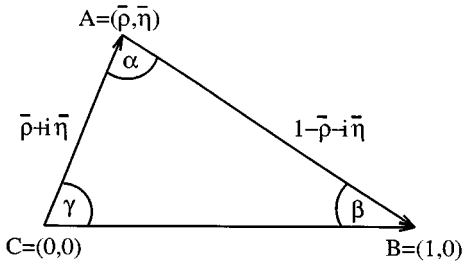

FIG. 1. Unitarity triangle in the complex $(\bar{\varrho},\bar{\eta})$ plane.

is rescaled by $V_{cd}V_{cb}^*$. We observe that, beyond the leading order in λ, the point A *does not* correspond to (ϱ,η) but to $(\bar{\varrho},\bar{\eta})$. Clearly, within 3% accuracy, $\bar{\varrho}=\varrho$ and $\bar{\eta}=\eta$. Yet in the distant future the accuracy of experimental results and theoretical calculations may improve considerably, so that the more accurate formulation given here will be appropriate.

Using simple trigonometry one can calculate $\sin(2\phi_i)$, $\phi_i=\alpha,\beta,\gamma$, in terms of $(\bar{\varrho},\bar{\eta})$ with the result

$$\sin 2\alpha=\frac{2\bar{\eta}(\bar{\eta}^2+\bar{\varrho}^2-\bar{\varrho})}{(\bar{\varrho}^2+\bar{\eta}^2)[(1-\bar{\varrho})^2+\bar{\eta}^2]}, \tag{2.29}$$

$$\sin 2\beta=\frac{2\bar{\eta}(1-\bar{\varrho})}{(1-\bar{\varrho})^2+\bar{\eta}^2}, \tag{2.30}$$

$$\sin 2\gamma=\frac{2\bar{\varrho}\,\bar{\eta}}{\bar{\varrho}^2+\bar{\eta}^2}=\frac{2\varrho\,\eta}{\varrho^2+\eta^2}. \tag{2.31}$$

The lengths CA and BA in the rescaled triangle of Fig. 1, to be denoted by R_b and R_t, respectively, are given by

$$R_b\equiv\frac{|V_{ud}V_{ub}^*|}{|V_{cd}V_{cb}^*|}=\sqrt{\bar{\varrho}^2+\bar{\eta}^2}=\left(1-\frac{\lambda^2}{2}\right)\frac{1}{\lambda}\left|\frac{V_{ub}}{V_{cb}}\right|, \tag{2.32}$$

$$R_t\equiv\frac{|V_{td}V_{tb}^*|}{|V_{cd}V_{cb}^*|}=\sqrt{(1-\bar{\varrho})^2+\bar{\eta}^2}=\frac{1}{\lambda}\left|\frac{V_{td}}{V_{cb}}\right|. \tag{2.33}$$

The expressions for R_b and R_t, given here in terms of $(\bar{\varrho},\bar{\eta})$, are excellent approximations. Clearly R_b and R_t can also be determined by measuring two of the angles ϕ_i:

$$R_b=\frac{\sin(\beta)}{\sin(\alpha)}=\frac{\sin(\alpha+\gamma)}{\sin(\alpha)}=\frac{\sin(\beta)}{\sin(\gamma+\beta)}, \tag{2.34}$$

$$R_t=\frac{\sin(\gamma)}{\sin(\alpha)}=\frac{\sin(\alpha+\beta)}{\sin(\alpha)}=\frac{\sin(\gamma)}{\sin(\gamma+\beta)}. \tag{2.35}$$

III. BASIC FORMALISM

A. Renormalization of QCD

As already emphasized in the Introduction, the effects of QCD play an important role in the phenomenology of weak decays of hadrons. In fact, in the theoretical analysis of these decays, the investigation of QCD corrections is the most difficult and involved part. In the present subsection we shall briefly recall basic features of perturbative QCD and its renormalization and concentrate on those aspects that will be needed for the present review. We also take the opportunity to introduce for later reference expressions for the running coupling constant, the running mass, and the corresponding renormalization-group functions.

The Lagrangian density for QCD is

$$\begin{aligned}\mathcal{L}_{\rm QCD}=&-\frac{1}{4}(\partial_\mu A_\nu^a-\partial_\nu A_\mu^a)(\partial^\mu A^{a\nu}-\partial^\nu A^{a\mu})\\&-\frac{1}{2\xi}(\partial^\mu A_\mu^a)^2+\bar{q}(i\not{\partial}-m_q)q+\chi^{a*}\partial^\mu\partial_\mu\chi^a\\&-\frac{g}{2}f^{abc}(\partial_\mu A_\nu^a-\partial_\nu A_\mu^a)A^{b\mu}A^{c\nu}\\&-\frac{g^2}{4}f^{abe}f^{cde}A_\mu^a A_\nu^b A^{c\mu}A^{d\nu}+g\bar{q}_i T_{ij}^a\gamma^\mu q_j A_\mu^a\\&+gf^{abc}(\partial^\mu\chi^{a*})\chi^b A_\mu^c.\end{aligned} \tag{3.1}$$

Here $q=(q_1,q_2,q_3)$ is the color triplet of quark flavor $q=u,d,s,c,b,t$. g is the QCD coupling, A_μ^a the gluon field, χ^a the ghost field, and ξ the gauge parameter. T^a, f^{abc} $(a,b,c=1,\ldots,8)$ are the generators and structure constants of SU(3), respectively. From this Lagrangian one may read off the Feynman rules for QCD, e.g., $igT_{ij}^a\gamma^\mu$, for the quark-gluon vertex.

In order to deal with divergences that appear in quantum (loop) corrections to Green functions, the theory has to be regularized to have an explicit parametrization of the singularities and subsequently renormalized to render the Green functions finite. For these purposes we will employ

(i) Dimensional regularization (DR) by continuation to $D=4-2\varepsilon$ space-time dimensions (Ashmore, 1972; Bollini and Giambiagi, 1972a, 1972b; Cicuta and Montaldi, 1972; 't Hooft and Veltman, 1972a).

(ii) Subtraction of divergences in the minimal subtraction scheme MS ('t Hooft, 1973) or the modified minimal subtraction scheme ($\overline{\rm MS}$) (Bardeen *et al.*, 1978).

To eliminate the divergences one has to renormalize the fields and parameters in the Lagrangian, in general through

$$\begin{aligned}&A_{0\mu}^a=Z_3^{1/2}A_\mu^a,\quad q_0=Z_q^{1/2}q,\quad \chi_0^a=\tilde{Z}_3^{1/2}\chi^a,\\&g_0=Z_g g\mu^\varepsilon,\quad \xi_0=Z_3\xi,\quad m_0=Z_m m.\end{aligned} \tag{3.2}$$

The subscript "0" indicates unrenormalized quantities. The factors Z are the renormalization constants. The scale μ has been introduced to make g dimensionless in $D=4-2\varepsilon$ dimensions. Since we will not consider Green functions with external ghosts, we will not need the ghost-field renormalization. We also do not need the gauge-parameter renormalization if we are dealing with gauge-independent quantities, as, e.g., Wilson-coefficient functions.

A straightforward way to implement renormalization is provided by the counterterm method. Thereby the parameters and fields in the original Lagrangian, which are

to be considered as unrenormalized (bare) quantities, are re-expressed through renormalized ones by means of Eq. (3.2) from the very beginning. For instance, the quark kinetic term becomes

$$\mathcal{L}_F=\bar{q}_0 i\not{\partial} q_0-m_0\bar{q}_0 q_0\equiv\bar{q} i\not{\partial} q-m\bar{q}q+(Z_q-1)\bar{q} i\not{\partial} q -(Z_q Z_m-1)m\bar{q}q. \tag{3.3}$$

The advantage is that only renormalized quantities are present in the Lagrangian. The counterterms, $\sim(Z-1)$, which also appear, can be formally treated as interaction terms that contribute to Green functions calculated in perturbation theory. The Feynman rule for the counterterms in Eq. (3.3), for example, reads (p is the quark momentum)

$$i(Z_q-1)\not{p}-i(Z_q Z_m-1)m. \tag{3.4}$$

The constants Z_i are then determined such that they cancel the divergences in the Green functions according to the chosen renormalization scheme. In an analogous way all renormalization constants can be fixed by considering the appropriate Green functions.

Of central importance for the study of perturbative-QCD effects are the renormalization-group equations, which govern the dependence of renormalized parameters and Green functions on the renormalization scale μ. These differential equations are easily derived from Eq. (3.2) by using the fact that bare quantities are μ independent. In this way one finds that the renormalized coupling $g(\mu)$ obeys (Gross, 1976)

$$\frac{d}{d\ \ln\mu}\,g(\mu)=\beta(\varepsilon,g(\mu)), \tag{3.5}$$

where

$$\beta(\varepsilon,g)=-\varepsilon g-g\,\frac{1}{Z_g}\,\frac{dZ_g}{d\ \ln\mu}\equiv-\varepsilon g+\beta(g), \tag{3.6}$$

which defines the β function. Equation (3.5) is valid in arbitrary dimensions. In four dimensions $\beta(\varepsilon,g)$ reduces to $\beta(g)$. Similarly, the anomalous dimension of the mass γ_m, defined through

$$\frac{dm(\mu)}{d\ \ln\mu}=-\gamma_m(g)m(\mu), \tag{3.7}$$

is given by

$$\gamma_m(g)=\frac{1}{Z_m}\,\frac{dZ_m}{d\ \ln\mu}. \tag{3.8}$$

In the MS ($\overline{\rm MS}$) scheme, where only the pole terms in ε are present in the renormalization constants Z_i, these can be expanded as

$$Z_i=1+\sum_{k=1}^{\infty}\frac{1}{\varepsilon^k}\,Z_{i,k}(g). \tag{3.9}$$

Using Eqs. (3.5) and (3.6) one finds

$$\frac{1}{Z_i}\,\frac{dZ_i}{d\ \ln\mu}=-2g^2\,\frac{\partial Z_{i,1}(g)}{\partial g^2}, \tag{3.10}$$

which allows a direct calculation of the renormalization-group functions from the $1/\varepsilon$-pole part of the renormalization constants. Along these lines one obtains at the two-loop level, which is required for next-to-leading-order calculations,

$$\beta(g)=-\beta_0\,\frac{g^3}{16\pi^2}-\beta_1\,\frac{g^5}{(16\pi^2)^2}. \tag{3.11}$$

In terms of

$$\alpha_s\equiv\frac{g^2}{4\pi} \tag{3.12}$$

we have

$$\frac{d\alpha_s}{d\ \ln\mu}=-2\beta_0\,\frac{\alpha_s^2}{4\pi}-2\beta_1\,\frac{\alpha_s^3}{(4\pi)^2}. \tag{3.13}$$

Similarly, the two-loop expression for the quark-mass anomalous dimension can be written as

$$\gamma_m(\alpha_s)=\gamma_{m0}\,\frac{\alpha_s}{4\pi}+\gamma_{m1}\left(\frac{\alpha_s}{4\pi}\right)^2. \tag{3.14}$$

We also give the $1/\varepsilon$-pole part $Z_{q,1}$ of the quark-field renormalization constant Z_1 to $\mathcal{O}(\alpha_s^2)$, which we will need later on,

$$Z_{q,1}=a_1\,\frac{\alpha_s}{4\pi}+a_2\left(\frac{\alpha_s}{4\pi}\right)^2. \tag{3.15}$$

The coefficients in Eqs. (3.13)–(3.15) are

$$\beta_0=\frac{11N-2f}{3},\quad \beta_1=\frac{34}{3}\,N^2-\frac{10}{3}\,Nf-2C_F f,$$

$$C_F=\frac{N^2-1}{2N}, \tag{3.16}$$

$$\gamma_{m0}=6C_F,\quad \gamma_{m1}=C_F\left(3C_F+\frac{97}{3}\,N-\frac{10}{3}\,f\right), \tag{3.17}$$

$$a_1=-C_F,\quad a_2=C_F\left(\frac{3}{4}\,C_F-\frac{17}{4}\,N+\frac{1}{2}\,f\right), \tag{3.18}$$

where N is the number of colors and f the number of quark flavors. The coefficients are given in the MS ($\overline{\rm MS}$) scheme. However, β_0, β_1, γ_{m0}, and a_1 are scheme independent. The expressions for a_1 and a_2 in Eq. (3.18) are valid in Feynman gauge, $\xi=1$.

At two-loop order the solution of the renormalization-group equation (3.13) for $\alpha_s(\mu)$ can always be written in the form

$$\alpha_s(\mu)=\frac{4\pi}{\beta_0\ln(\mu^2/\Lambda^2)}\left[1-\frac{\beta_1}{\beta_0^2}\,\frac{\ln\ln(\mu^2/\Lambda^2)}{\ln(\mu^2/\Lambda^2)}\right], \tag{3.19}$$

with Λ the QCD scale. Equation (3.19) gives the running coupling constant at NLO. $\alpha_s(\mu)$ vanishes as $\mu/\Lambda\to\infty$ due to asymptotic freedom. We remark that, in accordance with the two-loop accuracy, Eq. (3.19) is valid up to terms of the order $\mathcal{O}(1/\ln^3(\mu^2/\Lambda^2))$. For the purpose of counting orders in $1/\ln(\mu^2/\Lambda^2)$, the double-logarithmic expression $\ln\ln(\mu^2/\Lambda^2)$ may formally be viewed as a constant. Note that an additional term $\sim 1/\ln^2(\mu^2/\Lambda^2)$, which

is of the same order as the next-to-leading-order correction in Eq. (3.19), can always be absorbed into a multiplicative redefinition of Λ. Hence the choice of the form of Eq. (3.19) is possible without restriction, but one should keep in mind that the definition of Λ is related to this particular choice. The introduction of the $\overline{\rm MS}$ scheme and the corresponding definition of $\Lambda_{\overline{\rm MS}}$ and its relation to $\Lambda_{\rm MS}$ is discussed in Section III.F.4.

Finally we write down the two-loop expression for the running quark mass in the MS ($\overline{\rm MS}$) scheme, which results from integrating Eq. (3.7):

$$m(\mu)=m(m)\left[\frac{\alpha_s(\mu)}{\alpha_s(m)}\right]^{\gamma_{m0}/2\beta_0}\left[1+\left(\frac{\gamma_{m1}}{2\beta_0}-\frac{\beta_1\gamma_{m0}}{2\beta_0^2}\right)\times\frac{\alpha_s(\mu)-\alpha_s(m)}{4\pi}\right]. \tag{3.20}$$

B. Operator product expansion in weak decays—preliminaries

Weak decays of hadrons are mediated through the weak interactions of their quark constituents. These hadrons also have strong interactions that have a typical hadronic energy scale of the order of 1 GeV. Our goal is therefore to derive an effective low-energy theory describing the weak interactions of quarks. The formal framework to achieve this is provided by the operator product expansion (OPE) (Wilson and Zimmermann, 1972). In order to introduce the main ideas behind it, let us consider the simple example of the quark-level transition $c\to s u\bar d$, which is relevant for Cabibbo-allowed decays of D mesons. Disregarding QCD effects for the moment, the tree-level W-exchange amplitude for $c\to s u\bar d$ is simply given by

$$A=i\frac{G_F}{\sqrt2}V_{cs}^*V_{ud}\frac{M_W^2}{k^2-M_W^2}(\bar s c)_{V-A}(\bar u d)_{V-A}$$
$$=-i\frac{G_F}{\sqrt2}V_{cs}^*V_{ud}(\bar s c)_{V-A}(\bar u d)_{V-A}+\mathcal{O}\left(\frac{k^2}{M_W^2}\right), \tag{3.21}$$

where $(V-A)$ refers to the Lorentz structure $\gamma_\mu(1-\gamma_5)$.

Since k, the momentum transfer through the W propagator, is very small compared to the W mass M_W, terms of the order $\mathcal{O}(k^2/M_W^2)$ can safely be neglected, and the full amplitude A can be approximated by the first term on the rhs of Eq. (3.21). Now this term may obviously also be obtained from an effective Hamiltonian defined by

$$\mathcal{H}_{\rm eff}=\frac{G_F}{\sqrt2}V_{cs}^*V_{ud}(\bar s c)_{V-A}(\bar u d)_{V-A}+\cdots, \tag{3.22}$$

where the ellipsis denotes operators of higher dimensions, typically involving derivative terms, which can in principle be chosen so as to reproduce terms of higher order in k^2/M_W^2 of the full amplitude given by Eq. (3.21). This exercise already provides us with a simple example of an OPE. The product of two charged-current operators is expanded into a series of local operators whose contributions are weighted by effective coupling constants, the Wilson coefficients.

A more formal basis for this procedure may be given by considering the generating functional for Green functions in the path-integral formalism. The part of the generating functional relevant for the present discussion is, up to an overall normalizing factor, given by

$$Z_W\sim\int[dW^+][dW^-]\exp\left(i\int d^4x\ \mathcal{L}_W\right), \tag{3.23}$$

where $\mathcal{L}_W$ is the Lagrangian density containing the kinetic terms of the W boson field and its interaction with charged currents,

$$\mathcal{L}_W=-\frac{1}{2}(\partial_\mu W_\nu^+-\partial_\nu W_\mu^+)(\partial^\mu W^{-\nu}-\partial^\nu W^{-\mu})$$
$$+M_W^2W_\mu^+W^{-\mu}+\frac{g_2}{2\sqrt2}(J_\mu^+W^{+\mu}+J_\mu^-W^{-\mu}), \tag{3.24}$$

$$J_\mu^+=V_{pn}\bar p\,\gamma_\mu(1-\gamma_5)n,\quad p=(u,c,t)$$
$$n=(d,s,b),\quad J_\mu^-=(J_\mu^+)^\dagger. \tag{3.25}$$

Since we are not interested in Green functions with external W lines, we have not introduced external source terms for the W fields. In the present argument we will furthermore choose the unitary gauge for the W field for definiteness, although physical results do not depend on this choice.

Introducing the operator

$$K_{\mu\nu}(x,y)=\delta^{(4)}(x-y)[g_{\mu\nu}(\partial^2+M_W^2)-\partial_\mu\partial_\nu], \tag{3.26}$$

we may, after discarding a total derivative in the W kinetic term, rewrite Eq. (3.23) as

$$Z_W\sim\int[dW^+][dW^-]$$
$$\times\exp\left[i\int d^4x\ d^4y\ W_\mu^+(x)K^{\mu\nu}(x,y)W_\nu^-(y)\right.$$
$$\left.+i\frac{g_2}{2\sqrt2}\int d^4x\ J_\mu^+W^{+\mu}+J_\mu^-W^{-\mu}\right]. \tag{3.27}$$

The inverse of $K_{\mu\nu}$, denoted by $\Delta_{\mu\nu}$, and defined through

$$\int d^4y\ K_{\mu\nu}(x,y)\Delta^{\nu\lambda}(y,z)=g_\mu^\lambda\delta^{(4)}(x-z) \tag{3.28}$$

is just the W propagator in the unitary gauge,

$$\Delta_{\mu\nu}(x,y)=\int\frac{d^4k}{(2\pi)^4}\Delta_{\mu\nu}(k)e^{-ik(x-y)}, \tag{3.29}$$

$$\Delta_{\mu\nu}(k)=\frac{-1}{k^2-M_W^2}\left(g_{\mu\nu}-\frac{k_\mu k_\nu}{M_W^2}\right). \tag{3.30}$$

Performing the Gaussian functional integration over $W^{\pm}(x)$ in Eq. (3.27) explicitly, we simplify this expression to

$$Z_W \sim \exp\left[-i \int \frac{g_2^2}{8} J_\mu^-(x) \Delta^{\mu\nu}(x,y) J_\nu^+(y) d^4x \; d^4y \right]. \tag{3.31}$$

This result implies a nonlocal action functional for the quarks

$$\mathcal{S}_{nl} = \int d^4x \mathcal{L}_{\rm kin} - \frac{g_2^2}{8} \int d^4x \; d^4y \; J_\mu^-(x) \Delta^{\mu\nu}(x,y) J_\nu^+(y), \tag{3.32}$$

where the first piece represents the quark kinetic terms and the second their charged current interactions.

We can now formally expand this second, nonlocal term in powers of $1/M_W^2$ to yield a series of local interaction operators of dimensions that increase with the order in $1/M_W^2$. To lowest order

$$\Delta^{\mu\nu}(x,y) \approx \frac{g^{\mu\nu}}{M_W^2} \delta^{(4)}(x-y), \tag{3.33}$$

and the second term in Eq. (3.32) becomes

$$-\frac{g_2^2}{8M_W^2} \int d^4x \; J_\mu^-(x) J^{+\mu}(x), \tag{3.34}$$

corresponding to the usual effective charged-current interaction Lagrangian

$$\mathcal{L}_{\rm int,eff} = -\frac{G_F}{\sqrt{2}} J_\mu^- J^{+\mu}(x) = -\frac{G_F}{\sqrt{2}} V_{pn}^* V_{p'n'} (\bar{n} p)_{V-A} (\bar{p}' n')_{V-A}, \tag{3.35}$$

which contains, among other terms, the leading contribution to Eq. (3.22).

The simple considerations we have presented so far already illustrate several of the basic aspects of the general approach.

(i) Formally, the procedure to approximate the interaction term in Eq. (3.32) by Eq. (3.34) is an example of a short-distance OPE. The product of the local operators $J_\mu^-(x)$ and $J_\nu^+(y)$, to be taken at short distances, due to the convolution with the massive, short-range W propagator $\Delta^{\mu\nu}(x,y)$ [see Eq. (3.33)], is expanded into a series of composite local operators, of which the leading term is given by (3.34).

(ii) The dominant contributions in the short-distance expansion come from the operators of lowest dimension. In our case these are four-fermion operators of dimension six, whereas operators of higher dimensions can usually be neglected in weak decays.

(iii) Note that, as far as the charged-current weak interaction is concerned, no approximation is involved in the nonlocal interaction term in Eq. (3.32), except that we do not consider higher-order weak corrections or processes with external W-boson states. Correspondingly, the OPE series into which the nonlocal interaction is expanded is equivalent to the original theory when considered to all orders in $1/M_W^2$. In other words, the full series will reproduce the complete Green functions for the charged-current weak interactions of quarks. The truncation of the operator series then yields a systematic approximation scheme for low-energy processes, neglecting contributions suppressed by powers of k^2/M_W^2. In this way one is able to construct low-energy effective theories for weak decays.

(iv) In going from the full to the effective theory the W boson is removed as an explicit, dynamical degree of freedom. This step is often refered to as "integrating out" the W boson, a terminology which is very obvious in the path-integral language discussed above. Alternatively, one could use the canonical-operator formalism, where the W field, instead of being integrated out, gets "contracted out" through the application of Wick's theorem.

(v) The effective local four-fermion interaction terms are a modern version of the classic Fermi theory of weak interactions.

(vi) An intuitive interpretation of the OPE formalism discussed so far is that, from the point of view of low-energy dynamics, the effects of a short-range exchange force mediated by a heavy boson approximately corresponds to a point interaction.

(vii) The presentation we have given illustrates furthermore that the approach of evaluating the relevant Green functions (or amplitudes) directly in order to construct the OPE, as in Eq. (3.21), actually gives the same result as the more formal technique employing path integrals. While the latter can give some useful insight into the general aspects of the method, the former is more convenient for practical calculations, and we will make use of it throughout the following discussion.

(viii) Up to now we have not talked about the strong interactions among quarks, which of course have to be taken into account. They are described by QCD and can at short distances be calculated in perturbation theory, due to the property of asymptotic freedom of QCD. The corresponding gluon-exchange contributions constitute quantum corrections to the simplified picture sketched above, which can in this sense be viewed as a classical approximation. We will describe the incorporation of QCD corrections and related additional features they imply for the OPE in the following section.

C. OPE and short-distance QCD effects

We will now take up the discussion of QCD quantum corrections at short distances to the OPE for weak decays. A crucial point for this enterprise is the property of asymptotic freedom of QCD. This allows one to treat the short-distance corrections, that is the contribution of hard gluons at energies of the order $\mathcal{O}(M_W)$ down to hadronic scales ≥ 1 GeV, in perturbation theory. In the following, we will always restrict ourselves to the leading dimension-six operators in the OPE and omit the negli-

gible contributions of higher-dimensional operators. Staying with the example of $c\to s\bar{u}d$ transitions, recall that the amplitude without QCD was

$$A_0=-i\,\frac{G_F}{\sqrt{2}}\,V_{cs}^*V_{ud}(\bar{s}_ic_i)_{V-A}(\bar{u}_jd_j)_{V-A}\,, \tag{3.36}$$

where the summation over repeated color indices is understood. This result leads directly to the effective Hamiltonian of Eq. (3.22), where the color indices have been suppressed. If we now include QCD effects, the effective Hamiltonian, constructed to reproduce the low-energy approximation of the exact theory, is generalized to

$$\mathcal{H}_{\rm eff}=\frac{G_F}{\sqrt{2}}\,V_{cs}^*V_{ud}(C_1Q_1+C_2Q_2), \tag{3.37}$$

where

$$Q_1=(\bar{s}_ic_j)_{V-A}(\bar{u}_jd_i)_{V-A}\,, \tag{3.38}$$

$$Q_2=(\bar{s}_ic_i)_{V-A}(\bar{u}_jd_j)_{V-A}\,. \tag{3.39}$$

The essential features of this Hamiltonian are

(i) In addition to the original operator Q_2 (with index 2 for historical reasons) a new operator Q_1 with the same flavor form but different color structure is generated. This is because a gluon linking the two color-singlet weak-current lines can "mix" the color indices due to the following relation for the color charges T^a_{ij}

$$T^a_{ik}T^a_{jl}=-\frac{1}{2N}\,\delta_{ik}\delta_{jl}+\frac{1}{2}\,\delta_{il}\delta_{jk}\,. \tag{3.40}$$

(ii) The Wilson coefficients C_1 and C_2, the coupling constants for the interaction terms Q_1 and Q_2, become calculable nontrivial functions of α_s, M_W, and the renormalization scale μ. If QCD is neglected, they have the trivial form C_1=0 and C_2=1, and Eq. (3.37) reduces to Eq. (3.22).

In order to obtain the final result for the Hamiltonian of Eq. (3.37), we have to calculate the coefficients $C_{1,2}$. These are determined by the requirement that the amplitude A in the full theory be reproduced by the corresponding amplitude in the effective theory [Eq. (3.37)], thus

$$A=-i\,\frac{G_F}{\sqrt{2}}\,V_{cs}^*V_{ud}(C_1\langle Q_1\rangle+C_2\langle Q_2\rangle). \tag{3.41}$$

If we calculate the amplitude A and, to the same order in α_s, the matrix elements of operators $\langle Q_1\rangle,\langle Q_2\rangle$, we can obtain C_1 and C_2 via Eq. (3.41). This procedure is called *matching* the full theory onto the effective theory [Eq. (3.37)].

Here we use the term "amplitude" in the meaning of "amputated Green function." Correspondingly, operator matrix elements are—within this perturbative context—amputated Green functions with operator insertion. In a diagrammatic language these amputated Green functions are given by Feynman graphs, but without gluonic self-energy corrections in external legs, like, e.g., in Figs. 2 and 3, for the full and effective theory, respectively. In the present example penguin diagrams do not contribute due to the flavor structure of the $c\to s\bar{u}d$ transition.

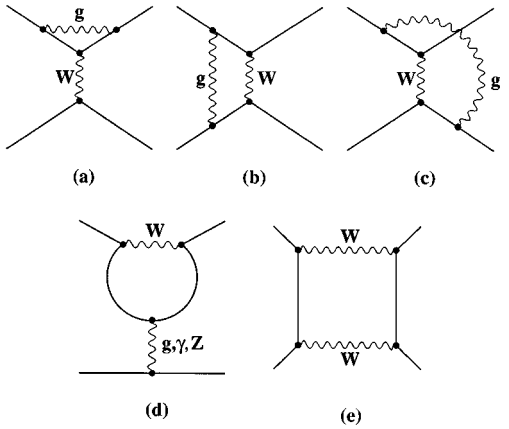

FIG. 2. One-loop current-current (a)–(c), penguin (d), and box (e) diagrams in the full theory. For pure QCD corrections as considered in this section and, e.g., in Sec. VI, the γ and Z^0 contributions in diagram (d) and diagram (e) are absent. Possible left-right or up-down reflected diagrams are not shown.

Evaluating the current-current diagrams of Figs. 2(a)–2(c), we find, for the full amplitude A to $\mathcal{O}(\alpha_s)$,

$$A=-i\,\frac{G_F}{\sqrt{2}}\,V_{cs}^*V_{ud}\left[\left(1+2C_F\,\frac{\alpha_s}{4\pi}\ln\frac{\mu^2}{-p^2}\right)S_2 + \frac{3}{N}\,\frac{\alpha_s}{4\pi}\ln\frac{M_W^2}{-p^2}\,S_2-3\,\frac{\alpha_s}{4\pi}\ln\frac{M_W^2}{-p^2}\,S_1\right]. \tag{3.42}$$

Here we have introduced the spinor amplitudes

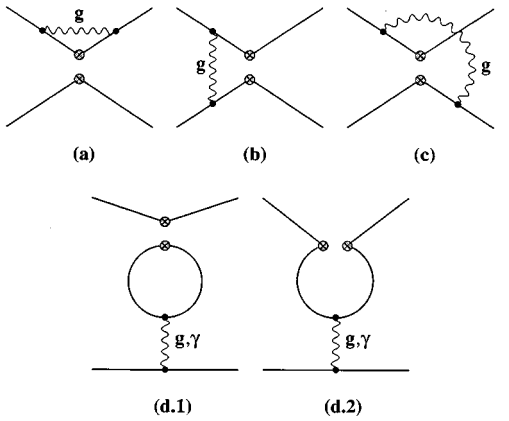

FIG. 3. One-loop current-current (a)–(c) and penguin (d) diagrams contributing to the leading order anomalous dimensions and matching conditions in the effective theory. The 4-vertex "$\otimes\otimes$" denotes the insertion of a 4-fermion operator Q_i. For pure QCD corrections as considered in this section and, e.g., in Sec. VI, the contributions from γ in diagrams (d.1) and (d.2) are absent. Again, possible left-right or up-down reflected diagrams are not shown.

$$S_1=(\bar{s}_i c_j)_{V-A}(\bar{u}_j d_i)_{V-A}, \tag{3.43}$$

$$S_2=(\bar{s}_i c_i)_{V-A}(\bar{u}_j d_j)_{V-A}, \tag{3.44}$$

which are just the tree-level matrix elements of Q_1 and Q_2. We have employed the Feynman gauge (ξ=1) and taken all external quark lines massless and carrying off-shell momentum p. Furthermore we have kept only logarithmic corrections $\sim\alpha_s\cdot\log$ and discarded constant contributions of order $\mathcal{O}(\alpha_s)$, which corresponds to the leading logarithmic approximation. The necessary renormalization of the quark fields in the MS scheme is already incorporated into Eq. (3.42). It has removed a $1/\varepsilon$ singularity in the first term of Eq. (3.42), which therefore carries an explicit μ dependence.

Under the same conditions, the unrenormalized current-current matrix elements of the operators Q_1 and Q_2 are found to be, from Figs. 3(a)–3(c),

$$\begin{aligned}\langle Q_1\rangle^{(0)}=&\left[1+2C_F\frac{\alpha_s}{4\pi}\left(\frac{1}{\varepsilon}+\ln\frac{\mu^2}{-p^2}\right)\right]S_1\\&+\frac{3}{N}\frac{\alpha_s}{4\pi}\left(\frac{1}{\varepsilon}+\ln\frac{\mu^2}{-p^2}\right)S_1\\&-3\frac{\alpha_s}{4\pi}\left(\frac{1}{\varepsilon}+\ln\frac{\mu^2}{-p^2}\right)S_2,\end{aligned} \tag{3.45}$$

$$\begin{aligned}\langle Q_2\rangle^{(0)}=&\left[1+2C_F\frac{\alpha_s}{4\pi}\left(\frac{1}{\varepsilon}+\ln\frac{\mu^2}{-p^2}\right)\right]S_2\\&+\frac{3}{N}\frac{\alpha_s}{4\pi}\left(\frac{1}{\varepsilon}+\ln\frac{\mu^2}{-p^2}\right)S_2\\&-3\frac{\alpha_s}{4\pi}\left(\frac{1}{\varepsilon}+\ln\frac{\mu^2}{-p^2}\right)S_1.\end{aligned} \tag{3.46}$$

Again, the divergences in the first terms are eliminated through field renormalization. However, in contrast to the full amplitude, the resulting expressions are still divergent. Therefore an additional multiplicative renormalization, refered to as *operator renormalization*, is necessary:

$$Q_i^{(0)}=Z_{ij}Q_j. \tag{3.47}$$

Since Eqs. (3.45) and (3.46) each involve both S_1 and S_2, the renormalization constant is in this case a 2×2 matrix Z. The relation between the unrenormalized ($\langle Q_i\rangle^{(0)}$) and the renormalized ($\langle Q_i\rangle$) amputated Green functions is then

$$\langle Q_i\rangle^{(0)}=Z_q^{-2}Z_{ij}\langle Q_j\rangle. \tag{3.48}$$

From Eqs. (3.45), (3.46), and (3.15) in the MS scheme

$$Z=1+\frac{\alpha_s}{4\pi}\frac{1}{\varepsilon}\begin{pmatrix}3/N & -3\\ -3 & 3/N\end{pmatrix}. \tag{3.49}$$

It follows that the renormalized matrix elements $\langle Q_i\rangle$ are given by

$$\begin{aligned}\langle Q_1\rangle=&\left(1+2C_F\frac{\alpha_s}{4\pi}\ln\frac{\mu^2}{-p^2}\right)S_1\\&+\frac{3}{N}\frac{\alpha_s}{4\pi}\ln\left(\frac{\mu^2}{-p^2}\right)S_1-3\frac{\alpha_s}{4\pi}\ln\left(\frac{\mu^2}{-p^2}\right)S_2,\end{aligned} \tag{3.50}$$

$$\begin{aligned}\langle Q_2\rangle=&\left(1+2C_F\frac{\alpha_s}{4\pi}\ln\frac{\mu^2}{-p^2}\right)S_2+\frac{3}{N}\frac{\alpha_s}{4\pi}\ln\left(\frac{\mu^2}{-p^2}\right)S_2\\&-3\frac{\alpha_s}{4\pi}\ln\left(\frac{\mu^2}{-p^2}\right)S_1\end{aligned} \tag{3.51}$$

Inserting $\langle Q_i\rangle$ into Eq. (3.41) and comparing with Eq. (3.42), we derive

$$C_1=-3\frac{\alpha_s}{4\pi}\ln\frac{M_W^2}{\mu^2},\quad C_2=1+\frac{3}{N}\frac{\alpha_s}{4\pi}\ln\frac{M_W^2}{\mu^2}. \tag{3.52}$$

We digress to add a comment on the renormalization of the interaction terms in the effective theory. The commonly used convention is to introduce, via Eq. (3.48), the renormalization constants Z_{ij}, defined to absorb the divergences of the operator matrix elements. It is, however, instructive to view this renormalization in a slightly different, but of course equivalent, way, corresponding to the standard counterterm method in perturbative renormalization. Consider, as usual, the Hamiltonian of the effective theory as the starting point, with fields and coupling constants as bare quantities that are renormalized according to ($q=s,c,u,d$)

$$q^{(0)}=Z_q^{1/2}q, \tag{3.53}$$

$$C_i^{(0)}=Z_{ij}^c C_j. \tag{3.54}$$

Then the Hamiltonian (Eq. 3.37) is essentially [omitting the factor $(G_F/\sqrt{2})V_{cs}^*V_{ud}$]

$$C_i^{(0)}Q_i(q^{(0)})\equiv Z_q^2Z_{ij}^cC_jQ_i\equiv C_iQ_i+(Z_q^2Z_{ij}^c-\delta_{ij})C_jQ_i, \tag{3.55}$$

that is, it can be written in terms of renormalized couplings and fields (C_iQ_i) plus counterterms. The argument $q^{(0)}$ in the first term in Eq. (3.55) indicates that the interaction term Q_i is composed of bare fields. Calculating the amplitude with the Hamiltonian (Eq. 3.55), which includes the counterterms, we get the finite renormalized result

$$Z_q^2Z_{ij}^cC_j\langle Q_i\rangle^{(0)}=C_j\langle Q_j\rangle. \tag{3.56}$$

Hence [compare to Eq. (3.48)]

$$Z_{ij}^c=Z_{ji}^{-1}. \tag{3.57}$$

In short, it is sometimes useful to keep in mind that one can think of the "operator renormalization," which sounds like a new concept, in terms of the completely equivalent, but customary, renormalization of the coupling constants C_i, as in any field theory.

Now that we have presented in quite some detail the derivation of the Wilson coefficients in Eq. (3.52), we shall discuss and interpret the most important aspects of

the short-distance expansion for weak decays, which can be studied very transparently on the explicit example we have given.

(i) First of all we offer a further remark about the phenomenon of operator mixing that we encountered in our example. This occurs because gluonic corrections to the matrix element of the original operator Q_2 are not just proportional to Q_2 itself, but involve the additional structure Q_1 (and vice versa). Therefore, besides a Q_2 counterterm, a counterterm $\sim Q_1$ is needed to renormalize this matrix element—the operators in question are said to mix under renormalization. This, however, is just an algebraic generalization of the usual concepts. Indeed, if we introduce a different operator basis $Q_\pm=(Q_2\pm Q_1)/2$ (with coefficients $C_\pm=C_2\pm C_1$), the renormalization becomes diagonal, and matrix elements of Q_+ and Q_- are renormalized multiplicatively. In this new basis the OPE is given by

$$A\equiv A_+ + A_- = -i\,\frac{G_F}{\sqrt{2}}\,V_{cs}^* V_{ud}(C_+\langle Q_+\rangle + C_-\langle Q_-\rangle), \tag{3.58}$$

where $[S_\pm=(S_2\pm S_1)/2]$,

$$A_\pm = -i\,\frac{G_F}{\sqrt{2}}\,V_{cs}^* V_{ud}\left[\left(1+2C_F\,\frac{\alpha_s}{4\pi}\,\ln\frac{\mu^2}{-p^2}\right)S_\pm + \left(\frac{3}{N}\mp 3\right)\frac{\alpha_s}{4\pi}\ln\left(\frac{M_W^2}{-p^2}\right)S_\pm\right], \tag{3.59}$$

and

$$\langle Q_\pm\rangle = \left(1+2C_F\,\frac{\alpha_s}{4\pi}\,\ln\frac{\mu^2}{-p^2}\right)S_\pm + \left(\frac{3}{N}\mp 3\right)\frac{\alpha_s}{4\pi}\ln\left(\frac{\mu^2}{-p^2}\right)S_\pm, \tag{3.60}$$

$$C_\pm = 1+\left(\frac{3}{N}\mp 3\right)\frac{\alpha_s}{4\pi}\,\ln\frac{M_W^2}{\mu^2}. \tag{3.61}$$

(ii) In the calculation of the amplitude A in Eq. (3.42) and of the matrix elements in Eqs. (3.45) and (3.46), the off-shell momentum p of the external quark legs represents an infrared regulator. The logarithmic infrared divergence of the gluon correction diagrams [Figs. 2(a)–2(c) and 3(a)–3(c)] as $p^2\to 0$ is evident from Eqs. (3.42), (3.45), and (3.46). A similar observation can be made for the M_W dependence of the full amplitude A. We see that Eq. (3.42) is logarithmically divergent in the limit $M_W\to\infty$. This behavior is reflected in the ultraviolet divergences (persisting after field renormalization) of the matrix elements [Eqs. (3.45), (3.46)] in the effective theory, whose local interaction terms correspond to the weak interactions in the infinite M_W limit since they are just the leading contribution of the $1/M_W$ operator product expansion. This also implies that the characteristic logarithmic functional dependence of the leading $\mathcal{O}(\alpha_s)$ corrections is closely related to the divergence structure of the effective theory, that is, to the renormalization constants Z_{ij}.

(iii) The most important feature of the OPE is that it provides a factorization of short-distance (Wilson coefficients) and long-distance (operator matrix elements) contributions. This is clearly exhibited in our example. The dependence of the amplitude [Eq. (3.42)] on p^2, representing the long-distance structure of A, is fully contained in the matrix elements of the local operators Q_i [Eqs. (3.50), (3.51)], whereas the Wilson coefficients C_i in Eq. (3.52) are free from this dependence. Essentially, this factorization has the form [see Eqs. (3.59)–(3.61)]

$$\left(1+\alpha_s G\,\ln\frac{M_W^2}{-p^2}\right)=\left(1+\alpha_s G\,\ln\frac{M_W^2}{\mu^2}\right)\times\left(1+\alpha_s G\,\ln\frac{\mu^2}{-p^2}\right), \tag{3.62}$$

that is, amplitude=coefficient function×operator matrix element. Thus the logarithm on the lhs is split according to

$$\ln\frac{M_W^2}{-p^2}=\ln\frac{M_W^2}{\mu^2}+\ln\frac{\mu^2}{-p^2}. \tag{3.63}$$

Since the logarithmic behavior results from the integration over some virtual loop momentum, we may, roughly speaking, rewrite this as

$$\int_{-p^2}^{M_W^2}\frac{dk^2}{k^2}=\int_{\mu^2}^{M_W^2}\frac{dk^2}{k^2}+\int_{-p^2}^{\mu^2}\frac{dk^2}{k^2}, \tag{3.64}$$

which illustrates that the coefficient contains the contributions from large virtual momenta of the loop correction from scales $\mu\approx 1$ GeV to M_W, whereas the low-energy contributions are separated into the matrix elements.

Of course, the latter cannot be calculated in perturbation theory for transitions between physical meson states. The point is that we have calculated the OPE for unphysical off-shell quark external states only to extract the Wilson coefficients, which we need to construct the effective Hamiltonian of Eq. (3.37). For this purpose the fact that we have considered an unphysical amplitude is irrelevant, since the coefficient functions do not depend on the external states, but rather represent the short-distance structure of the theory. Once we have extracted the coefficients and written down the effective Hamiltonian, the latter can be used, at least in principle, to evaluate the physically interesting decay amplitudes by means of some nonperturbative approach.

(iv) In interpreting the role of the scale μ, we may distinguish two different aspects. From the point of view of the effective theory, μ is just a renormalization scale introduced in the process of renormalizing the effective local interaction terms by the dimensional method. On the other hand, from the point of view of the full theory, μ acts as the scale at which the full contribution is separated into a low-energy and a high-energy part, as is evident from the above discussion. For this reason μ is sometimes also called the factorization scale.

(v) In our case the infrared structure of the amplitude is characterized by the off-shell momentum p. In general one could work with any other arbitrary momentum configuration, on-shell or off-shell, with or without external quark mass, and with infrared divergences regulated by off-shell momenta, quark masses, a fictitious gluon mass, or by dimensional regularization. In the case of off-shell momenta the amplitude is furthermore dependent on the gauge parameter of the gluon field. All these things belong to the infrared or long-distance structure of the amplitude. Therefore the dependence on these choices is the same for the full amplitude and for the operator matrix elements and drops out in the coefficient functions. To check that this is really the case for a particular choice is of crucial importance for practical calculations. On the other hand, one may use this freedom and choose the treatment of external lines according to convenience or taste. However, sometimes it may seem preferable to keep a slightly more inconvenient dependence on external masses and/or gluon gauge in order to have a useful check that this dependence does indeed cancel out for the Wilson coefficients one is calculating.

D. The renormalization group

1. Basic concepts

So far we have computed the Wilson coefficient functions [Eq. (3.61)] in ordinary perturbation theory. This, however, is not sufficient for the problem at hand. The appropriate scale at which to normalize the hadronic matrix elements of local operators is a low-energy scale—low compared to the weak scale M_W—of a few GeV typically. In our example of charm decay $\mu=\mathcal{O}(m_c)$. For such a low scale μ, the logarithm $\ln(M_W^2/\mu^2)$ multiplying $\alpha_s(\mu)$ in Eq. (3.61) becomes large. Although $\alpha_s(\mu)$ by itself is a valid expansion parameter down to scales of $\mathcal{O}(1\text{ GeV})$, this is no longer true for the combination $\alpha_s(\mu)\ln(M_W^2/\mu^2)$. In fact, for our example [Eq. (3.61)] the first-order correction term, for $\mu=1$ GeV, amounts to 65–130%, even though $\alpha_s/4\pi\approx 4\%$. The reason for this breakdown of the naive perturbative expansion lies ultimately in the appearance of largely disparate scales M_W and μ in the problem at hand.

This situation can be considerably improved by employing the method of the renormalization group (RG). The renormalization group is the group of transformations between different choices of the renormalization scale μ. The renormalization-group equations describe the change of renormalized quantities, Green functions, and parameters, with μ in a differential form. As we shall illustrate below, solving these differential equations allows one in the leading logarithmic approximation (LLA), to sum up the terms $[\alpha_s\ln(M_W/\mu)]^n$ to all orders n ($n=0,\ldots,\infty$) in perturbation theory. This leads to the RG-improved perturbation theory. Going one step further in this modified expansion, to the next-to-leading-order logarithmic approximation (NLLA), the summation is extended to all terms $\alpha_s[\alpha_s\ln(M_W/\mu)]^n$, and so on. In this context it is useful to consider $\alpha_s\ln(M_W/\mu)$ with a large logarithm $\ln(M_W/\mu)$ as a quantity of $\mathcal{O}(1)$

$$\alpha_s\ln\frac{M_W}{\mu}=\mathcal{O}(1),\quad \mu\ll M_W. \tag{3.65}$$

Therefore the series of powers of $\alpha_s\ln(M_W/\mu)$ cannot be truncated. Summed to all orders, it yields again a contribution of $\mathcal{O}(1)$. Correspondingly, the next-to-leading-order logarithms $\alpha_s[\alpha_s\ln(M_W/\mu)]^n$ represent an $\mathcal{O}(\alpha_s)$ perturbative correction to the leading term.

The renormalization-group equation for the Wilson coefficient functions follows from the fact that the unrenormalized Wilson coefficients $\vec{C}^{(0)}=Z_c\vec{C}$, $\vec{C}^T=(C_1,C_2)$, are μ independent. Defining the matrix of anomalous dimensions γ by

$$\gamma=Z^{-1}\frac{d}{d\ln\mu}Z \tag{3.66}$$

and recalling that $Z_c^T=Z^{-1}$, we obtain the renormalization-group equation

$$\frac{d}{d\ln\mu}\vec{C}(\mu)=\gamma^T(\alpha_s)\vec{C}(\mu). \tag{3.67}$$

The solution of Eq. (3.67) may formally be written in terms of a μ evolution matrix U as

$$\vec{C}(\mu)=U(\mu,M_W)\vec{C}(M_W). \tag{3.68}$$

From Eqs. (3.49) and (3.66) we have to first order in α_s,

$$\gamma(\alpha_s)=\frac{\alpha_s}{4\pi}\gamma^{(0)}=\frac{\alpha_s}{4\pi}\begin{pmatrix}-6/N & 6\\ 6 & -6/N\end{pmatrix}, \tag{3.69}$$

or, in the diagonal basis,

$$\gamma_\pm(\alpha_s)=\frac{\alpha_s}{4\pi}\gamma_\pm^{(0)},\quad \gamma_\pm^{(0)}=\pm 6\frac{N\mp 1}{N}. \tag{3.70}$$

Note that, if we neglect QCD loop corrections completely, the couplings $\vec{C}$ are independent of μ. The nontrivial μ dependence of $\vec{C}$ expressed in Eq. (3.67) is a genuine quantum effect. It implies an anomalous scaling behavior for the dimensionless coefficients, i.e., one that is different from the classical theory. For this reason the factor γ is called an anomalous (scale) dimension [compare Eq. (3.67) with $(d/d\ln\mu)\mu^n=n\mu^n$ for an n-dimensional μ-dependent term μ^n]. Using Eq. (3.13) the RG equation (3.67) is easily solved with the result

$$C_\pm(\mu)=\left[\frac{\alpha_s(M_W)}{\alpha_s(\mu)}\right]^{\gamma_\pm^{(0)}/2\beta_0}C_\pm(M_W). \tag{3.71}$$

At a scale $\mu_W=M_W$ no large logarithms are present, and $C_\pm(M_W)$ can therefore be calculated in ordinary perturbation theory. From Eq. (3.61) we have, to the order needed for the LLA,

$$C_\pm(M_W)=1. \tag{3.72}$$

Equations (3.71) and (3.72) give the final result for the coefficients in the LLA of the RG-improved perturbation theory.

At this point one should emphasize that the choice of the high-energy matching scale $\mu_W = M_W$ is of course not unique. The only requirement is that the choice of μ_W must not introduce large logarithms, $\ln(M_W/\mu_W)$, in order not to spoil the applicability of the usual perturbation theory. Therefore μ_W should be of $\mathcal{O}(M_W)$. The logarithmic correction in Eq. (3.61) is then $\mathcal{O}(\alpha_s)$ and is neglected in LLA. Then, still, $C_\pm(\mu_W)=1$ and

$$C_\pm(\mu)=\left[\frac{\alpha_s(\mu_W)}{\alpha_s(\mu)}\right]^{\gamma_\pm^{(0)}/2\beta_0} =\left[\frac{\alpha_s(M_W)}{\alpha_s(\mu)}\right]^{\gamma_\pm^{(0)}/2\beta_0}[1+\mathcal{O}(\alpha_s)]. \tag{3.73}$$

A change of μ_W around the value of M_W causes an ambiguity of $\mathcal{O}(\alpha_s)$ in the coefficient. This ambiguity represents a theoretical uncertainty in the determination of $C_\pm(\mu)$. In order to reduce it, it is necessary to go beyond the leading order. At NLO the scale ambiguity is then reduced from $\mathcal{O}(\alpha_s)$ to $\mathcal{O}(\alpha_s^2)$. We will come back to this point below. Presently, we will set $\mu_W = M_W$, but it is important to keep the related uncertainty in mind. Taking into account the leading-order solution of the RG equation (3.13) for the coupling, which can be expressed in the form

$$\alpha_s(m)=\frac{\alpha_s(\mu)}{1+\beta_0[\alpha_s(\mu)/4\pi]\ln(m^2/\mu^2)}, \tag{3.74}$$

we may rewrite Eq. (3.71) as

$$C_\pm(\mu)=\left(\frac{1}{1+\beta_0[\alpha_s(\mu)/4\pi]\ln(M_W^2/\mu^2)}\right)^{\gamma_\pm^{(0)}/2\beta_0}. \tag{3.75}$$

Equation (3.75) contains the logarithmic corrections $\sim\alpha_s\ln(M_W^2/\mu^2)$ to all orders in α_s. This shows very clearly that the leading-logarithmic-order corrections have been summed up to all orders in perturbation theory by solving the RG equation. In particular, if we again expand Eq. (3.75) in powers of α_s, keeping the first term only, we recover Eq. (3.61). This observation demonstrates that the RG method allows one to obtain solutions that go beyond the conventional perturbation theory.

Before concluding this subsection, we would like to introduce two more generalizations of the approach developed so far, which will appear in the general discussion below.

2. Threshold effects in LLA

First we may generalize the renormalization-group evolution from M_W down to $\mu\approx m_c$ to include the threshold effect of heavy quarks like b or t as follows

$$\vec{C}(\mu)=U^{(f=4)}(\mu,\mu_b)U^{(f=5)}(\mu_b,\mu_W)\vec{C}(\mu_W), \tag{3.76}$$

which is valid for the LLA. In our example of the $c\to su\bar{d}$ transition, the top quark gives no contribution at all. Being heavier (but comparable) in mass than the W, it is simply removed from the theory along with the W boson. In a first step the coefficients at the initial scale $\mu_W\approx M_W$ are evolved down to $\mu_b\approx m_b$ in an effective theory with five quark flavors ($f=5$). Then, again in the spirit of the effective field-theory technique, for scales below μ_b, the bottom quark is also removed as an explicit degree of freedom from the effective theory, yielding a new effective theory with only four "active" quark flavors left. The matching corrections between both theories can be calculated in ordinary perturbation theory at the scale μ_b, since, due to $\mu_b\approx m_b$, no large logarithms can occur in this procedure. For the same reason matching corrections of $\mathcal{O}(\alpha_s)$ can be neglected in LLA, and the coefficients at μ_b, $\vec{C}(\mu_b)$, simply serve as the initial values for the RG evolution in the four-quark theory down to $\mu\approx m_c$. In addition, continuity of the running coupling across the threshold μ_b is imposed by the requirement

$$\alpha_{s,f=4}(\mu_b,\Lambda^{(4)})=\alpha_{s,f=5}(\mu_b,\Lambda^{(5)}), \tag{3.77}$$

which defines different QCD scales $\Lambda^{(f)}$ for each effective theory.

Neglecting the b threshold, as we did before [Eq. (3.68)], one may merely perform the full evolution from μ_W to μ in an effective four-flavor theory. It turns out that in some cases the difference of these two approaches is negligible.

We would like to add a comment on this effective-field-theory technique. At first sight the idea to "remove by hand" heavy degrees of freedom may look somewhat artificial. However, it appears quite natural when not viewed from the evolution from high towards low energies but vice versa (which actually corresponds to the historical way). Suppose only the "light" quarks u, d, s, and c were known. Then, in the attempt to formulate a theory of their weak interactions, one would be led to a generalized Fermi theory with four quark coupling constants to be determined somehow. Of course, we are in the lucky position to know the underlying theory in the form of the standard model. Therefore we can actually derive the coupling constants of the low-energy effective theory from "first principles." This is exactly what is achieved technically by going through a series of effective theories, removing heavy degrees of freedom successively by means of a step-by-step procedure.

3. Penguin operators

A second, very important issue is the generation of QCD penguin operators (Vainshtein *et al.*, 1977). Consider, for example, the local operator $(\bar{s}_i u_i)_{V-A}(\bar{u}_j d_j)_{V-A}$, which is directly induced by W-boson exchange. In this case, additional QCD correction diagrams, the penguin diagrams, Figs. 3(d.1) and 3(d.2), with a gluon, contribute, and as a consequence six operators are involved in the mixing under renormalization instead of two. These are

$$Q_1=(\bar{s}_i u_j)_{V-A}(\bar{u}_j d_i)_{V-A},$$
$$Q_2=(\bar{s}_i u_i)_{V-A}(\bar{u}_j d_j)_{V-A},$$
$$Q_3=(\bar{s}_i d_i)_{V-A}\Sigma_q(\bar{q}_j q_j)_{V-A},$$

$$Q_4=(\bar{s}_i d_j)_{V-A}\Sigma_q(\bar{q}_j q_i)_{V-A},$$
$$Q_5=(\bar{s}_i d_i)_{V-A}\Sigma_q(\bar{q}_j q_j)_{V+A},$$
$$Q_6=(\bar{s}_i d_j)_{V-A}\Sigma_q(\bar{q}_j q_i)_{V+A}. \quad (3.78)$$

The sum over q runs over all quark flavors that exist in the effective theory in question. The operators Q_1 and Q_2 are just the ones we have encountered in Sec. III.C, but with the c quark replaced by u. This modified flavor structure gives rise to the gluon penguin-type diagrams shown in Fig. 3(d). Since the gluon coupling is of course flavor conserving, it is clear that penguins cannot be generated from the operator $(\bar{s}c)_{V-A}(\bar{u}d)_{V-A}$. The penguin graphs induce the new local interaction vertices $Q_3,\ldots,Q_6$, which have the same quantum numbers. Their structure is easily understood. The flavor content is determined by the $(\bar{s}d)_{V-A}$ current in the upper part and by a $\Sigma_q(\bar{q}q)_V$ vector current due to the gluon coupling in the lower part. For convenience this vector structure is decomposed into a $(V-A)$ and a $(V+A)$ part. For each of these, two different color forms arise due to the color structure of the exchanged gluon [see Eq. (3.40)]. Together this yields the four operators $Q_3,\ldots,Q_6$. For all operators $Q_1,\ldots,Q_6$ all possible QCD corrections (that is all amputated Green functions with insertion of Q_i) of the current-current [Figs. 3(a)–3(c)] as well as of the penguin type [Figs. 3(d.1) and 3(d.2)] have to be evaluated. In this process no new operators are generated, so that $Q_1,\ldots,Q_6$ form a complete set. They "close under renormalization." In analogy to the case of Sec. III.C the divergent parts of these Green functions determine, after field renormalization, the operator renormalization constants, which in the present case form a 6×6 matrix. The calculation of the corresponding anomalous-dimension matrix and the renormalization-group analysis then proceeds in the usual way. We will see that the inclusion of higher-order electroweak interactions requires the introduction of still more operators.

E. Summary of basic formalism

We think that, after this rather detailed discussion of the methods required for the short-distance calculations in weak decays, it is useful to give a concise summary of the material covered so far. At the same time this may serve as an outline of the necessary procedure for practical calculations. Furthermore, it will also provide a starting point for the extension of the formalism from the LLA considered until now to the NLLA to be presented in the next subsection.

Ultimately our goal is the evaluation of weak-decay amplitudes involving hadrons in the framework of a low-energy effective theory of the form

$$\langle\mathcal{H}_{\rm eff}\rangle=\frac{G_F}{\sqrt{2}}V_{\rm CKM}\langle\vec{Q}^T(\mu)\rangle\vec{C}(\mu).$$

The procedure for this calculation can be divided into the following three steps.

Step 1: Perturbation Theory. Calculation of Wilson coefficients $\vec{C}(\mu_W)$ at $\mu_W\approx M_W$ to the desired order in α_s. Since logarithms of the form $\ln(\mu_W/M_W)$ are not large, this can be performed in ordinary perturbation theory. It amounts to matching the full theory onto a five-quark effective theory.

Step 2: RG-Improved Perturbation Theory. (i) Calculation of the anomalous dimensions of the operators. (ii) Solution of the renormalization-group equation for $\vec{C}(\mu)$. (iii) Evolution of the coefficients from μ_W down to the appropriate low-energy scale μ

$$\vec{C}(\mu)=U(\mu,\mu_W)\vec{C}(\mu_W).$$

Step 3: Nonperturbative Regime. Calculation of hadronic matrix elements $\langle\vec{Q}(\mu)\rangle$, normalized at the appropriate low-energy scale μ, by means of some nonperturbative method.

Important issues in this procedure are

(i) The OPE achieves a factorization of short- and long-distance contributions. Correspondingly, in order to disentangle the short-distance from the long-distance part and to extract $\vec{C}(\mu_W)$ in actual calculations, a proper matching of the full onto the effective theory has to be performed. Similar comments apply to the matching of an effective theory with f quark flavors to a theory with $(f-1)$ flavors during the RG evolution to lower scales. Furthermore, factorization implies that the μ dependence and also the dependence on the renormalization scheme, which appears beyond the leading order, cancel between C_i and $\langle Q_i\rangle$. Since the top quark is integrated out along with the W, the coefficients $\vec{C}(\mu_W)$ in general also contain the full dependence on the top-quark mass m_t.

(ii) A summation of large logarithms by means of the RG method is necessary. More specifically, in the nth order of RG-improved perturbation theory the terms of the form

$$\alpha_s^n(\mu)\left(\alpha_s(\mu)\ln\frac{M_W}{\mu}\right)^k$$

are summed to all orders in k ($k=0,1,2,\ldots$). This approach is justified as long as $\alpha_s(\mu)$ is small enough, which requires that μ not be too low, typically not less than 1 GeV.

F. Wilson coefficients beyond leading order

1. The renormalization-group formalism

We are now going to extend the renormalization-group formalism for the coefficient functions to the next-to-leading-order level. Then we shall discuss important aspects of the resulting formulas, in particular the scale and scheme dependences and their cancellation.

As an example, we consider the calculation for the $\Delta S=1$ effective Hamiltonian for nonleptonic decays, which, without QCD effects and for low energy, is given by

$$\mathcal{H}_{\rm eff}^{\Delta S=1}=\frac{G_F}{\sqrt{2}}\,V_{us}^{*}V_{ud}(\bar{s}u)_{V-A}(\bar{u}d)_{V-A}\,. \tag{3.79}$$

At higher energies of course the charm, bottom, and top quark also have to be taken into account. The Feynman diagrams contributing to $\mathcal{O}(\alpha_s)$ corrections to this Hamiltonian are shown in Figs. 2 and 3. Including current-current as well as penguin-type corrections, the relevant operator basis consists of the six operators in Eq. (3.78).

On the one hand, this particular case is very important by itself, since it provides the theoretical basis for a large variety of different decay modes. On the other hand, we keep the discussion fairly general to exhibit all the important features of a typical case. In addition, the central formulas of this subsection will be used at several places later on, although at times they will be extended or modified to match the specific cases in question. In Secs. IV–XV of this report we will give a more detailed discussion of the Hamiltonians relevant for various decays. Here, we will concentrate on the presentation of the OPE and renormalization-group formalism.

The effective Hamiltonian for nonleptonic decays may be written in general as

$$\mathcal{H}_{\rm eff}=\frac{G_F}{\sqrt{2}}\sum_i\,C_i(\mu)Q_i(\mu)\equiv\frac{G_F}{\sqrt{2}}\,\vec{Q}^{\,T}(\mu)\vec{C}(\mu), \tag{3.80}$$

where the index i runs over all contributing operators, in our example, $Q_1,\ldots,Q_6$ of Eq. (3.78). It is straightforward to apply $\mathcal{H}_{\rm eff}$ to D- and B-meson decays as well by changing the quark flavors appropriately. For the time being we omit CKM parameters, which can be reinserted later on. μ is some low-energy scale of $\mathcal{O}(1\ \text{GeV})$, $\mathcal{O}(m_c)$, and $\mathcal{O}(m_b)$ for K-, D-, and B-meson decays, respectively. The argument μ of the operators $Q_i(\mu)$ means that their matrix elements are to be normalized at scale μ.

The Wilson coefficient functions are given by

$$\vec{C}(\mu)=U(\mu,\mu_W)\vec{C}(\mu_W). \tag{3.81}$$

The coefficients at the scale $\mu_W=\mathcal{O}(M_W)$ can be evaluated in perturbation theory. The evolution matrix U then includes the RG-improved perturbative contributions from the scale μ_W down to μ.

In the first step we determine $\vec{C}(\mu_W)$ from a comparison of the amputated Green function with appropriate external lines in the full theory with the corresponding amplitude in the effective theory. At NLO we have to calculate to $\mathcal{O}(\alpha_s)$, including nonlogarithmic, constant terms. The full amplitude from the current-current and penguin-type diagrams in Fig. 2 is finite after field renormalization and can be written as

$$A=\frac{G_F}{\sqrt{2}}\,\vec{S}^{\,T}\left(\vec{A}^{(0)}+\frac{\alpha_s(\mu_W)}{4\pi}\,\vec{A}^{(1)}\right). \tag{3.82}$$

Here $\vec{S}$ denotes the tree-level matrix elements of the operators $\vec{Q}$. In the effective theory Eq. (3.80) the current-current and penguin corrections of Fig. 3 have to be calculated for all the operators Q_i. In this case, besides the field renormalization, a renormalization of operators is necessary

$$Z_q^2\langle\vec{Q}\rangle^{(0)}=Z\langle\vec{Q}\rangle, \tag{3.83}$$

where the matrix Z absorbs those divergences of the Green functions with operator $\vec{Q}$ insertion that are not removed by the field renormalization. The renormalized matrix elements of the operators can then, to $\mathcal{O}(\alpha_s)$, be written as

$$\langle\vec{Q}(\mu_W)\rangle=\left(1+\frac{\alpha_s(\mu_W)}{4\pi}\,r\right)\vec{S}, \tag{3.84}$$

and the amplitude in the effective theory to the same order becomes

$$A_{\rm eff}=\frac{G_F}{\sqrt{2}}\,\vec{S}^{\,T}\left(1+\frac{\alpha_s(\mu_W)}{4\pi}\,r^T\right)\vec{C}(\mu_W). \tag{3.85}$$

Equating Eqs. (3.82) and (3.85) we obtain

$$\vec{C}(\mu_W)=\vec{A}^{(0)}+\frac{\alpha_s(\mu_W)}{4\pi}\,(\vec{A}^{(1)}-r^T\vec{A}^{(0)}). \tag{3.86}$$

In general $\vec{A}^{(1)}$ in Eq. (3.82) involves logarithms $\ln(M_W^2/-p^2)$, where p denotes some global external momentum for the amplitudes in Fig. 2. On the other hand, the matrix r in Eq. (3.84), characterizing the radiative corrections to $\langle\vec{Q}(\mu_W)\rangle$, includes $\ln(-p^2/\mu_W^2)$. As we have seen in Sec. III.C, these logarithms combine to $\ln(M_W^2/\mu_W^2)$ in the Wilson coefficient of Eq. (3.86). For $\mu_W=M_W$ this logarithm vanishes altogether. For $\mu_W=\mathcal{O}(M_W)$ the expression $\ln(M_W^2/\mu_W^2)$ is a "small logarithm," and the correction $\sim\alpha_s\ln(M_W^2/\mu_W^2)$, which could be neglected in LLA, has to be kept in the perturbative calculation at NLO together with constant pieces of order $\mathcal{O}(\alpha_s)$.

In the second step, the renormalization-group equation for $\vec{C}$

$$\frac{d}{d\,\ln\mu}\,\vec{C}(\mu)=\gamma^T(g)\vec{C}(\mu) \tag{3.87}$$

has to be solved with the boundary condition Eq. (3.86). The solution is written with the help of the U matrix as in Eq. (3.81), where $U(\mu,\mu_W)$ obeys the same equation as $\vec{C}(\mu)$ in Eq. (3.87). The general solution is easily written down iteratively

$$\begin{aligned}U(\mu,m)=1&+\int_{g(m)}^{g(\mu)}dg_1\,\frac{\gamma^T(g_1)}{\beta(g_1)}\\&+\int_{g(m)}^{g(\mu)}dg_1\int_{g(m)}^{g_1}dg_2\,\frac{\gamma^T(g_1)}{\beta(g_1)}\,\frac{\gamma^T(g_2)}{\beta(g_2)}\\&+\cdots,\end{aligned} \tag{3.88}$$

which, using $dg/d\,\ln\mu=\beta(g)$, is readily seen to solve the renormalization-group equation

$$\frac{d}{d\,\ln\mu}\,U(\mu,m)=\gamma^T(g)U(\mu,m). \tag{3.89}$$

The series in Eq. (3.88) can be more compactly expressed by introducing the notion of g ordering

$$U(\mu,m)=T_g\exp\int_{g(m)}^{g(\mu)}dg'\,\frac{\gamma^T(g')}{\beta(g')}, \tag{3.90}$$

where in the case $g(\mu)>g(m)$ the g-ordering operator T_g is defined through

$$\begin{aligned}T_g f(g_1)\cdots f(g_n)=&\sum_{\text{perm}}\Theta(g_{i_1}-g_{i_2})\\&\times\Theta(g_{i_2}-g_{i_3})\cdots\Theta(g_{i_{n-1}}-g_{i_n})\\&\times f(g_{i_1})\cdots f(g_{i_n})\end{aligned} \tag{3.91}$$

and brings about an ordering of the factors $f(g_i)$ such that the coupling constants increase from right to left. The sum in Eq. (3.91) runs over all permutations $\{i_1,\ldots,i_n\}$ of $\{1,2,\ldots,n\}$. The T_g ordering is necessary since, in general, the anomalous-dimension matrices at different couplings do not commute beyond the leading order, i.e., $[\gamma(g_1),\gamma(g_2)]\neq 0$.

At next to leading order we have to keep the first two terms in the perturbative expansions for $\beta(g)$ [see Eq. (3.11)] and $\gamma(g)$,

$$\gamma(\alpha_s)=\gamma^{(0)}\frac{\alpha_s}{4\pi}+\gamma^{(1)}\left(\frac{\alpha_s}{4\pi}\right)^2. \tag{3.92}$$

To this order the evolution matrix $U(\mu,m)$ is given by Buras *et al.* (1992)

$$U(\mu,m)=\left(1+\frac{\alpha_s(\mu)}{4\pi}J\right)U^{(0)}(\mu,m)\left(1-\frac{\alpha_s(m)}{4\pi}J\right). \tag{3.93}$$

$U^{(0)}$ is the evolution matrix in LLA and the matrix J expresses the next-to-leading order corrections to this evolution. We have

$$U^{(0)}(\mu,m)=V\left(\left[\frac{\alpha_s(m)}{\alpha_s(\mu)}\right]^{\vec{\gamma}^{(0)}/2\beta_0}\right)_D V^{-1}, \tag{3.94}$$

where V diagonalizes $\gamma^{(0)T}$,

$$\gamma_D^{(0)}=V^{-1}\gamma^{(0)T}V, \tag{3.95}$$

and $\vec{\gamma}^{(0)}$ is the vector containing the diagonal elements of the diagonal matrix $\gamma_D^{(0)}$. If we define

$$G=V^{-1}\gamma^{(1)T}V \tag{3.96}$$

and a matrix H whose elements are

$$H_{ij}=\delta_{ij}\gamma_i^{(0)}\frac{\beta_1}{2\beta_0^2}-\frac{G_{ij}}{2\beta_0+\gamma_i^{(0)}-\gamma_j^{(0)}}, \tag{3.97}$$

the matrix J is given by

$$J=VHV^{-1}. \tag{3.98}$$

The fact that Eq. (3.93) is indeed a solution of the RG equation (3.89) to the order considered is straightforwardly verified by differentiation with respect to $\ln\mu$. Combining the initial values of Eq. (3.86) with the evolution matrix of Eq. (3.93), we obtain

$$\begin{aligned}\vec{C}(\mu)=&\left(1+\frac{\alpha_s(\mu)}{4\pi}J\right)U^{(0)}(\mu,\mu_W)\\&\times\left(\vec{A}^{(0)}+\frac{\alpha_s(\mu_W)}{4\pi}[\vec{A}^{(1)}-(r^T+J)\vec{A}^{(0)}]\right).\end{aligned} \tag{3.99}$$

Using Eq. (3.99) we can calculate, for example, the coefficients at a scale $\mu=\mu_b=\mathcal{O}(m_b)$ in an effective five-flavor theory, $f=5$. If we have to evolve the coefficients to still lower values, we would like to formulate a new effective theory for $\mu<\mu_b$, where now the b quark is also removed as an explicit degree of freedom. To calculate the coefficients in this new four-flavor theory at the scale μ_b, we have to determine the matching corrections at this scale.

We follow the same principles as in the case of integrating out the W boson and require

$$\langle\vec{Q}_f(m)\rangle^T\vec{C}_f(m)=\langle\vec{Q}_{f-1}(m)\rangle^T\vec{C}_{f-1}(m) \tag{3.100}$$

in the general case of a change from an f-flavor to an $(f-1)$-flavor theory at a scale m. The "full amplitude" on the lhs, which is now in an f-flavor effective theory, is expanded into matrix elements of the new $(f-1)$-flavor theory, multiplied by new Wilson coefficients $\vec{C}_{f-1}$. From Eq. (3.84), determining the matrix elements of operators to $\mathcal{O}(\alpha_s)$, one finds

$$\langle\vec{Q}_f(m)\rangle=\left(1+\frac{\alpha_s(m)}{4\pi}\delta r\right)\langle\vec{Q}_{f-1}(m)\rangle, \tag{3.101}$$

where

$$\delta r=r^{(f)}-r^{(f-1)}. \tag{3.102}$$

In Eq. (3.102) we have made explicit the dependence of the matrix r on the number of quark flavors, which enters in our example via the penguin contributions. From Eqs. (3.100) and (3.101) we find

$$\vec{C}_{f-1}(m)=M(m)\vec{C}_f(m) \tag{3.103}$$

with

$$M(m)=1+\frac{\alpha_s(m)}{4\pi}\delta r^T. \tag{3.104}$$

The general renormalization-group matrix U in Eq. (3.93), now evaluated for $(f-1)$ flavors, can be used to evolve $\vec{C}_{f-1}(m)$ to lower values of the renormalization scale. It is clear that no large logarithms can appear in Eq. (3.104) and that therefore the matching corrections, expressed in the matrix $M(m)$, can be computed in usual perturbation theory. We note that this type of matching correction enters in a nontrivial way for the first time at the NLO level. In the LLA $M\equiv 1$, and one can simply omit the b flavor components in the penguin operators when crossing the b threshold.

We also remark that the correction matrix M introduces a small discontinuity of the coefficients, regarded as functions of μ, at the matching scale m. This is, however, not surprising. In any case the $\vec{C}(\mu)$ are not physical quantities and their discontinuity precisely cancels

the effect of removing the heavy-quark flavor from the operators, which evidently is a "discontinuous" step. Hence physical amplitudes are not affected and indeed the behavior of $\vec{C}$ at the matching scale ensures that the same physical result will be obtained whether we choose to calculate in the f-flavor or in the $(f-1)$-flavor theory for scales near the matching scale m.

To conclude, we shall write down what the typical final result for the coefficient functions at $\mu \approx 1$ GeV, appropriate for K decays, looks like if we combine all the contributions discussed above. Then we can write

$$\vec{C}(\mu) = U_3(\mu,\mu_c)M(\mu_c)U_4(\mu_c,\mu_b)M(\mu_b) \times U_5(\mu_b,\mu_W)\vec{C}(\mu_W), \tag{3.105}$$

where U_f is the evolution matrix for f active flavors. In the following discussion we will not always include the flavor thresholds when writing the expression for the RG evolution. It is clear that they can be added in a straightforward fashion.

2. The calculation of the anomalous dimensions

The matrix of anomalous dimensions is the most important ingredient for the renormalization-group calculation of the Wilson coefficient functions. In the following we will summarize the essential steps of its calculation.

Recall that the evaluation of the amputated Green functions with insertion of the operators $\vec{Q}$ gives the relation

$$\langle \vec{Q} \rangle^{(0)} = Z_q^{-2} Z \langle \vec{Q} \rangle \equiv Z_{\mathrm{GF}} \langle \vec{Q} \rangle, \tag{3.106}$$

where $\langle \vec{Q} \rangle^{(0)}, \langle \vec{Q} \rangle$ denote the unrenormalized and renormalized Green functions, respectively. Z_q is the quark-field renormalization constant, and Z is the renormalization constant matrix of the operators $\vec{Q}$. The anomalous dimensions are given by

$$\gamma(g) = Z^{-1} \frac{d}{d \ln \mu} Z. \tag{3.107}$$

In the MS (or $\overline{\mathrm{MS}}$) scheme the renormalization constants are chosen to absorb the pure pole divergences $1/\varepsilon^k$ ($D=4-2\varepsilon$), but no finite parts. Z can then be expanded in inverse powers of ε as follows

$$Z = 1 + \sum_{k=1}^{\infty} \frac{1}{\varepsilon^k} Z_k(g). \tag{3.108}$$

Using the expression for the β function Eq. (3.6) valid for arbitrary ε, we derive the useful formula (Floratos *et al.*, 1977)

$$\gamma(g) = -2g^2 \frac{\partial Z_1(g)}{\partial g^2} = -2\alpha_s \frac{\partial Z_1(\alpha_s)}{\partial \alpha_s}. \tag{3.109}$$

Similar to Eq. (3.108), we expand

$$Z_q = 1 + \sum_{k=1}^{\infty} \frac{1}{\varepsilon^k} Z_{q,k}(g), \tag{3.110}$$

$$Z_{\mathrm{GF}} = 1 + \sum_{k=1}^{\infty} \frac{1}{\varepsilon^k} Z_{\mathrm{GF},k}(g). \tag{3.111}$$

From the calculation of the unrenormalized Green functions Eq. (3.106) we immediately obtain Z_{GF}. Then what we need to compute $\gamma(g)$ is $Z_1(g)$ Eq. (3.109). From Eqs. (3.106), (3.108), (3.110), and (3.111) we find

$$Z_1 = 2Z_{q,1} + Z_{\mathrm{GF},1}. \tag{3.112}$$

At NLO we have, from the $1/\varepsilon$ poles of the unrenormalized Green functions,

$$Z_{\mathrm{GF},1} = b_1 \frac{\alpha_s}{4\pi} + b_2 \left(\frac{\alpha_s}{4\pi} \right)^2. \tag{3.113}$$

The corresponding expression for the well-known factor $Z_{q,1}$ has been quoted in Eq. (3.15). Using Eqs. (3.15), (3.109), (3.112), and (3.113), we finally obtain for the one- and two-loop anomalous-dimension matrices $\gamma^{(0)}$ and $\gamma^{(1)}$ in Eq. (3.92),

$$\gamma_{ij}^{(0)} = -2[2a_1\delta_{ij} + (b_1)_{ij}], \tag{3.114}$$

$$\gamma_{ij}^{(1)} = -4[2a_2\delta_{ij} + (b_2)_{ij}]. \tag{3.115}$$

Equations (3.114) and (3.115) may be used as recipes to immediately extract the anomalous dimensions from the divergent parts of the unrenormalized Green functions.

3. Renormalization-scheme dependence

A further issue, which becomes important at next to leading order, is the dependence of unphysical quantities, like the Wilson coefficients and the anomalous dimensions, on the choice of the renormalization scheme. This scheme dependence arises because the renormalization prescription involves an arbitrariness in the finite parts to be subtracted together with the ultraviolet singularities. Two different schemes are then related by a finite renormalization. Considering the quantities that we encountered in Sec. III.F.1, the following are independent of the renormalization scheme

$$\beta_0, \quad \beta_1, \quad \gamma^{(0)}, \quad \vec{A}^{(0)}, \quad \vec{A}^{(1)}, \quad r^T + J, \quad \langle \vec{Q} \rangle^T \vec{C}, \tag{3.116}$$

whereas

$$r, \quad \gamma^{(1)}, \quad J, \quad \vec{C}, \quad \langle \vec{Q} \rangle \tag{3.117}$$

are scheme dependent.

In the framework of dimensional regularization, one example of how such a scheme dependence can occur is the treatment of γ_5 in D dimensions. Possible choices are the "naive dimensional regularization" (NDR) scheme with γ_5 taken to be anticommuting or the 't Hooft–Veltman (HV) scheme ('t Hooft and Veltman, 1972b; Breitenlohner and Maison, 1977) with nonanticommuting γ_5. Another example is the use of operators in a color singlet or nonsinglet form, such as

$$Q_2 = (\bar{s}_i u_i)_{V-A} (\bar{u}_j d_j)_{V-A} \quad \text{or}$$
$$\tilde{Q}_2 = (\bar{s}_i d_j)_{V-A} (\bar{u}_j u_i)_{V-A}, \tag{3.118}$$

where i,j are color indices. In $D=4$ dimensions these operators are equivalent since they are related by a Fierz transformation. In the NDR scheme, however, these two choices yield different results for r, $\gamma^{(1)}$, and J and thus constitute two different schemes that are related by a nontrivial finite renormalization. On the other hand, both choices give the same r, $\gamma^{(1)}$, and J if the HV scheme is employed.

Let us now discuss the question of renormalization-scheme dependences in explicit terms in order to obtain an overview on how the scheme dependences arise, how various quantities transform under a change of the renormalization scheme, and how the cancellation of scheme dependences is guaranteed for physically relevant quantities.

First of all, it is clear that the product

$$\langle \vec{Q}(\mu)\rangle^T \vec{C}(\mu), \tag{3.119}$$

representing the full amplitude, is independent of the renormalization scheme chosen. This is simply due to the fact that it is precisely the factorization of the amplitude into Wilson coefficients and matrix elements of operators by means of the operator product expansion that introduces the scheme dependence of $\vec{C}$ and $\langle \vec{Q}\rangle$. In other words, the scheme dependence of $\vec{C}$ and $\langle \vec{Q}\rangle$ represents the arbitrariness one has in splitting the full amplitude into coefficients and matrix elements, and the scheme independence of the combined product Eq. (3.119) is manifest in the construction of the operator product expansion.

More explicitly, these quantities are in different schemes (primed and unprimed), related by

$$\langle \vec{Q}\rangle' = \left(1+\frac{\alpha_s}{4\pi}s\right)\langle \vec{Q}\rangle \quad \vec{C}' = \left(1-\frac{\alpha_s}{4\pi}s^T\right)\vec{C}, \tag{3.120}$$

where s is a constant matrix. Equation (3.120) represents a finite renormalization of $\vec{C}$ and $\langle \vec{Q}\rangle$. From Equation (3.84) we immediately obtain

$$r' = r+s. \tag{3.121}$$

Furthermore, from

$$\langle \vec{Q}(\mu)\rangle^T \vec{C}(\mu) \equiv \langle \vec{Q}(\mu)\rangle^T U(\mu,M_W)\vec{C}(M_W) \tag{3.122}$$

we have

$$U'(\mu,M_W) = \left(1-\frac{\alpha_s(\mu)}{4\pi}s^T\right)U(\mu,M_W) \times \left(1+\frac{\alpha_s(M_W)}{4\pi}s^T\right). \tag{3.123}$$

A comparison with Eq. (3.93) yields

$$J' = J - s^T. \tag{3.124}$$

The renormalization-constant matrix in the primed scheme Z' follows from Eqs. (3.120) and (3.106)

$$Z' = Z\left(1-\frac{\alpha_s}{4\pi}s\right). \tag{3.125}$$

Recalling the definition of the matrix of anomalous dimensions, Eqs. (3.107) and (3.92), we derive

$$\gamma^{(0)\prime} = \gamma^{(0)}, \quad \gamma^{(1)\prime} = \gamma^{(1)} + [s,\gamma^{(0)}] + 2\beta_0 s. \tag{3.126}$$

With these general formulas at hand it is straightforward to clarify the cancellation of scheme dependences in all particular cases. Alternatively, they may be used to transform scheme-dependent quantities from one scheme to another, if desired, or to check the compatibility of results obtained in different schemes.

In particular, from Eqs. (3.121) and (3.124) we immediately verify the scheme independence of the matrix r^T+J. This means that, in the expression for $\vec{C}$ in Eq. (3.99), the factor on the right-hand side of $U^{(0)}$, related to the "upper end" of the evolution, is independent of the renormalization scheme, as it must be. The same is true for $U^{(0)}$. On the other hand, $\vec{C}$ still depends on the renormalization scheme through the matrix J to the left of $U^{(0)}$. As is evident from Eq. (3.120), this dependence is compensated for by the corresponding scheme dependence of the matrix elements of operators, so that a physically meaningful result for the decay amplitudes is obtained. To ensure a proper cancellation of the scheme dependence, the matrix elements have to be evaluated in the same scheme (renormalization, γ_5, form of operators) as the coefficient functions, which is a nontrivial task for the necessary nonperturbative computations. In other words, beyond the leading order the matching between short- and long-distance contributions has to be performed properly not only with respect to the scale μ, but also with respect to the renormalization scheme employed.

4. Discussion

We will now specialize the presentation of the general formalism to the case of a single operator (that is without mixing). This situation is, e.g., relevant for the operators Q_+ and Q_- with four different quark flavors, which we encountered in Sec. III.C. The resulting simplifications are useful in order to display some more details of the structure of the calculation and to discuss the most salient features of the NLO analysis in a transparent way.

In the case where only one single operator contributes, the amplitude in the full theory (dynamical W boson) may be written as [see Eq. (3.82)]

$$A = \frac{G_F}{\sqrt{2}}\left(1+\frac{\alpha_s(\mu_W)}{4\pi}\left[-\frac{\gamma^{(0)}}{2}\ln\frac{M_W^2}{-p^2}+\tilde{A}^{(1)}\right]\right)S, \tag{3.127}$$

where we have made the logarithmic dependence on the W mass explicit. In the effective theory the amplitude reads

$$A_{\rm eff}=\frac{G_F}{\sqrt{2}}\,C(\mu_W)\langle Q(\mu_W)\rangle$$
$$=\frac{G_F}{\sqrt{2}}\,C(\mu_W)\left(1+\frac{\alpha_s(\mu_W)}{4\pi}\right.$$
$$\left.\times\left[\frac{\gamma^{(0)}}{2}\left(\ln\frac{-p^2}{\mu_W^2}+\gamma_E-\ln 4\pi\right)+\tilde{r}\right]\right)S. \quad (3.128)$$

The divergent pole term $1/\varepsilon$ has been subtracted minimally. A comparison of Eqs. (3.127) and (3.128) yields the Wilson coefficient

$$C(\mu_W)=1+\frac{\alpha_s(\mu_W)}{4\pi}\left[-\frac{\gamma^{(0)}}{2}\right.$$
$$\left.\times\left(\ln\frac{M_W^2}{\mu_W^2}+\gamma_E-\ln 4\pi\right)+B\right], \quad (3.129)$$

where

$$B=\tilde{A}^{(1)}-\tilde{r}. \quad (3.130)$$

In the leading logarithmic approximation we had simply $C(\mu_W)=1$. By contrast, at NLO the $\mathcal{O}(\alpha_s)$ correction also has to be taken into account. This correction term exhibits the following new features

(i) The expression $\gamma_E-\ln 4\pi$, which is characteristic to dimensional regularization, appears and is proportional to $\gamma^{(0)}$.

(ii) A constant term B is present, which depends on the factorization scheme chosen.

(iii) An explicit logarithmic dependence on the matching scale μ_W shows up.

We discuss these points one by one.

First, the term $\gamma_E-\ln 4\pi$ is characteristic for the MS scheme. It can be eliminated by going from the MS to the $\overline{\rm MS}$ scheme. This issue is well known in the literature. However, we find it useful to briefly repeat the definition of the $\overline{\rm MS}$ scheme in the present context, since this is an important point for NLO analyses.

Consider the RG solution for the coefficient

$$C(\mu)=\left(1+\frac{\alpha_s(\mu)}{4\pi}J\right)\left[\frac{\alpha_s(\mu_W)}{\alpha_s(\mu)}\right]^{\gamma^{(0)}/2\beta_0}$$
$$\times\left\{1+\frac{\alpha_s(\mu_W)}{4\pi}\left[-\frac{\gamma^{(0)}}{2}\right.\right.$$
$$\left.\left.\times\left(\ln\frac{M_W^2}{\mu_W^2}+\gamma_E-\ln 4\pi\right)+B-J\right]\right\}. \quad (3.131)$$

This represents the solution for the MS scheme. Therefore in Eq. (3.131) $\alpha_s=\alpha_{s,\rm MS}$. The redefinition of $\alpha_{s,\rm MS}$ through

$$\alpha_{s,\rm MS}=\alpha_{s,\overline{\rm MS}}\left(1+\beta_0(\gamma_E-\ln 4\pi)\,\frac{\alpha_{s,\overline{\rm MS}}}{4\pi}\right) \quad (3.132)$$

is a finite renormalization of the coupling, which defines the $\overline{\rm MS}$ scheme. Since

$$[\alpha_{s,\rm MS}(\mu_W)]^{\gamma^{(0)}/2\beta_0}$$
$$\doteq[\alpha_{s,\overline{\rm MS}}(\mu_W)]^{\gamma^{(0)}/2\beta_0}$$
$$\times\left(1+\frac{\gamma^{(0)}}{2}(\gamma_E-\ln 4\pi)\,\frac{\alpha_{s,\overline{\rm MS}}(\mu_W)}{4\pi}\right), \quad (3.133)$$

we see that this transformation eliminates, to the order considered, the $\gamma_E-\ln 4\pi$ term in Eq. (3.131). At the lower end of the evolution the same redefinition yields a factor

$$1-\frac{\gamma^{(0)}}{2}(\gamma_E-\ln 4\pi)\,\frac{\alpha_{s,\overline{\rm MS}}(\mu)}{4\pi}, \quad (3.134)$$

which removes the corresponding factor from the matrix element [see Eq. (3.128)]

$$\langle Q(\mu)\rangle_{\rm MS}\equiv\left(1+\frac{\gamma^{(0)}}{2}(\gamma_E-\ln 4\pi)\,\frac{\alpha_{s,\overline{\rm MS}}(\mu)}{4\pi}\right)$$
$$\times\langle Q(\mu)\rangle_{\overline{\rm MS}}. \quad (3.135)$$

At the next-to-leading-logarithmic-order level we are working at, the transformation [Eq. (3.132)] is equivalent to a redefinition of the scale Λ according to

$$\Lambda^2_{\overline{\rm MS}}=4\pi e^{-\gamma_E}\Lambda^2_{\rm MS}, \quad (3.136)$$

as one can verify with the help of Eq. (3.19). In practice, one can just drop the $(\gamma_E-\ln 4\pi)$ terms in Eq. (3.131). Then $\alpha_s(\mu)$ and Λ correspond to the $\overline{\rm MS}$ scheme. Throughout the present report it is always understood that the transformation to $\overline{\rm MS}$ has been performed. Then

$$C(\mu)=\left(1+\frac{\alpha_s(\mu)}{4\pi}J\right)\left[\frac{\alpha_s(\mu_W)}{\alpha_s(\mu)}\right]^{\gamma^{(0)}/2\beta_0}$$
$$\times\left(1+\frac{\alpha_s(\mu_W)}{4\pi}\left[-\frac{\gamma^{(0)}}{2}\ln\frac{M_W^2}{\mu_W^2}+B-J\right]\right). \quad (3.137)$$

Second, from the issue of the MS-$\overline{\rm MS}$ transformation or, more generally, an arbitrary redefinition of α_s (or Λ), one should distinguish the renormalization-scheme dependence due to the ambiguity in the renormalization of the operator. This ambiguity is called "factorization scheme dependence," and is the scheme dependence we have discussed in Sec. III.F.3. A change in the factorization scheme transforms $\gamma^{(1)}$, B, and J as

$$\gamma^{(1)\prime}=\gamma^{(1)}+2\beta_0 s,\quad B'=B-s,\quad J'=J-s, \quad (3.138)$$

where s is a constant number. This follows from the formulae in Sec. III.F.3 and the definition of B in Eq. (3.130). Note that, in the case of a single operator, the relation between $\gamma^{(1)}$ and J simplifies to

$$J=\frac{1}{2\beta_0}\left(\frac{\beta_1}{\beta_0}\,\gamma^{(0)}-\gamma^{(1)}\right). \quad (3.139)$$

Obviously the scheme dependence cancels in the difference $B-J$ in Eq. (3.137).

Third, due to the explicit μ_W dependence in the $\mathcal{O}(\alpha_s)$

correction term, the coefficient function is, to the order considered, independent of the precise value of the matching scale μ_W, as it must be. Indeed

$$\frac{d}{d\ \ln\mu_W}\ C(\mu)=\mathcal{O}(\alpha_s^2), \tag{3.140}$$

since

$$\frac{d}{d\ \ln\mu_W}\ \alpha_s(\mu_W)=-2\beta_0\ \frac{\alpha_s(\mu_W)^2}{4\pi}+\mathcal{O}(\alpha_s^3). \tag{3.141}$$

In the same way one can also convince oneself that the coefficient function is independent of the heavy-quark threshold scales, up to terms of the neglected order. Of course the dependence on the low energy scale μ remains and has to be matched with the corresponding dependence of the operator matrix element. All the points we have mentioned here also apply in an analogous manner to the case with operator mixing, only the algebra is slightly more complicated. We would like to stress once again that it is only at the NLO level that these features enter the analysis in a nontrivial way, as should be evident from the presentation we have given above.

5. Evanescent operators

Finally, we would like to mention the so called *evanescent* operators. These are operators which exist in $D\neq 4$ dimensions but vanish in $D=4$. It has been stressed by Buras and Weisz (1990) that a correct calculation of two-loop anomalous dimensions requires a proper treatment of these operators. This discussion has been extended by Dugan and Grinstein (1991) and further generalized by Herrlich and Nierste (1995b). In view of the rather technical nature of this aspect, we refer the interested reader to the papers referenced above.

IV. GUIDE TO EFFECTIVE HAMILTONIANS

In order to facilitate the presentation of effective Hamiltonians in weak decays we give a complete compilation of the relevant operators below. Divided into six classes, these operators play a dominant role in the phenomenology of weak decays. The six classes are given as follows

Current-Current Operators [Fig. 4(a)].

$$Q_1=(\bar{s}_i u_j)_{V-A}(\bar{u}_j d_i)_{V-A}, \quad Q_2=(\bar{s}u)_{V-A}(\bar{u}d)_{V-A}. \tag{4.1}$$

QCD Penguin Operators [Fig. 4(b)].

$$Q_3=(\bar{s}d)_{V-A}\sum_q\ (\bar{q}q)_{V-A},$$

$$Q_4=(\bar{s}_i d_j)_{V-A}\sum_q\ (\bar{q}_j q_i)_{V-A}, \tag{4.2}$$

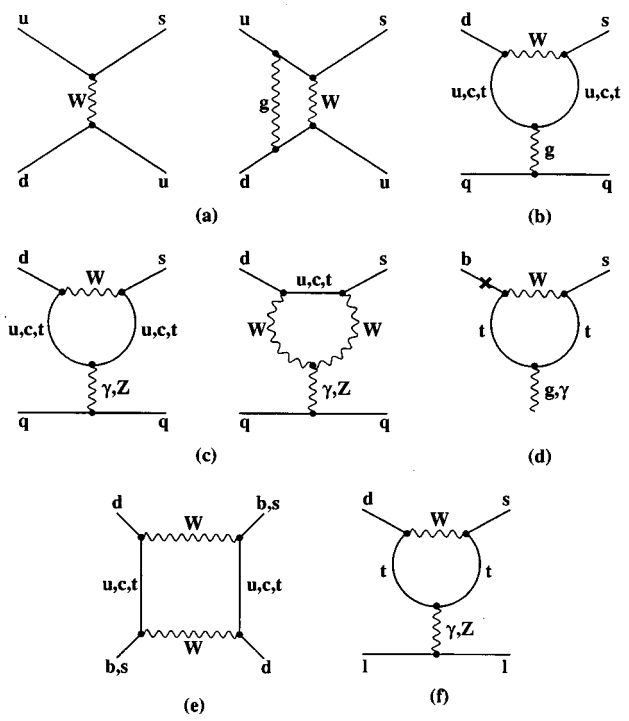

FIG. 4. Typical diagrams in the full theory from which the operators in Eqs. (4.1)–(4.10) originate. The cross in diagram (d) means a mass insertion. It indicates that magnetic penguins originate from the mass term on the external line in the usual QCD or QED penguin diagrams.

$$Q_5=(\bar{s}d)_{V-A}\sum_q\ (\bar{q}q)_{V+A},$$

$$Q_6=(\bar{s}_i d_j)_{V-A}\sum_q\ (\bar{q}_j q_i)_{V+A}. \tag{4.3}$$

Electroweak Penguin Operators [Fig. 4(c)].

$$Q_7=\frac{3}{2}\ (\bar{s}d)_{V-A}\sum_q\ e_q(\bar{q}q)_{V+A},$$

$$Q_8=\frac{3}{2}\ (\bar{s}_i d_j)_{V-A}\sum_q\ e_q(\bar{q}_j q_i)_{V+A}, \tag{4.4}$$

$$Q_9=\frac{3}{2}\ (\bar{s}d)_{V-A}\sum_q\ e_q(\bar{q}q)_{V-A},$$

$$Q_{10}=\frac{3}{2}\ (\bar{s}_i d_j)_{V-A}\sum_q\ e_q(\bar{q}_j q_i)_{V-A}. \tag{4.5}$$

Magnetic Penguin Operators [Fig. 4(d)].

$$Q_{7\gamma}=\frac{e}{8\pi^2}\ m_b\bar{s}_i\sigma^{\mu\nu}(1+\gamma_5)b_i F_{\mu\nu},$$

$$Q_{8G}=\frac{g}{8\pi^2}\ m_b\bar{s}_i\sigma^{\mu\nu}(1+\gamma_5)T^a_{ij}b_j G^a_{\mu\nu}. \tag{4.6}$$

$\Delta S=2$ and $\Delta B=2$ Operators [Fig. 4(e)].

$$Q(\Delta S=2)=(\bar{s}d)_{V-A}(\bar{s}d)_{V-A},$$
$$Q(\Delta B=2)=(\bar{b}d)_{V-A}(\bar{b}d)_{V-A}. \tag{4.7}$$

TABLE III. Compilation of various processes, equation number of the corresponding effective Hamiltonians, and contributing operators.

Process	Cf. Equation	Contributing operators
$\Delta F=1$, $F=B,C,S$ current-current	(5.4)–(5.6)	Q_1, Q_2
$\Delta F=1$ pure QCD	(6.1),(6.32)	$Q_1,\ldots,Q_6$
$\Delta F=1$ QCD and electroweak	(7.1),(7.37)	$Q_1,\ldots,Q_{10}$
$K_L\to\pi^0 e^+e^-$	(8.1)	$Q_1,\ldots,Q_6,Q_{7V},Q_{7A}$
$B\to X_s\gamma$	(9.1)	$Q_1,\ldots,Q_6,Q_{7\gamma},Q_{8G}$
$B\to X_s e^+e^-$	(10.1)	$Q_1,\ldots,Q_6,Q_{7\gamma},Q_{8G},Q_{9V},Q_{10A}$
$K^+\to\pi^+\nu\bar{\nu}$, $(K_L\to\mu^+\mu^-)_{\rm SD}$, $K_L\to\pi^0\nu\bar{\nu}$, $B\to X_{s,d}\nu\bar{\nu}$, $B\to l^+l^-$	(11.4),(11.44),(11.56) (11.57)	$Q(\bar{\nu}\nu), Q(\bar{\mu}\mu)$
K^0-$\bar{K}^0$ mixing	(12.1)	$Q(\Delta S=2)$
B^0-$\bar{B}^0$ mixing	(13.1)	$Q(\Delta B=2)$

Semileptonic Operators [Fig. 4(f)].

$$Q_{7V}=(\bar{s}d)_{V-A}(\bar{e}e)_V, \quad Q_{7A}=(\bar{s}d)_{V-A}(\bar{e}e)_A, \tag{4.8}$$

$$Q_{9V}=(\bar{b}s)_{V-A}(\bar{e}e)_V, \quad Q_{10A}=(\bar{b}s)_{V-A}(\bar{e}e)_A, \tag{4.9}$$

$$Q(\bar{\nu}\nu)=(\bar{s}d)_{V-A}(\bar{\nu}\nu)_{V-A},$$

$$Q(\bar{\mu}\mu)=(\bar{s}d)_{V-A}(\bar{\mu}\mu)_{V-A}, \tag{4.10}$$

where indices in color-singlet currents have been suppressed for simplicity. Here $V\pm A$ refers to the Lorentz structure $\gamma_\mu(1\pm\gamma_5)$.

For illustrative purposes, typical diagrams in the full theory from which the operators of Eqs. (4.1)–(4.10) originate are shown in Fig. 4.

The operators listed above will enter this review in a systematic fashion. We begin in Sec. V with the presentation of the effective Hamiltonians involving the current-current operators Q_1 and Q_2 only. These effective Hamiltonians are given in Eqs. (5.4), (5.5), and (5.6) for $\Delta B=1$, $\Delta C=1$, and $\Delta S=1$ nonleptonic decays, respectively.

In Sec. VI we will generalize the Hamiltonians (5.4) and (5.6) to include the QCD penguin operators Q_3–Q_6. The corresponding expressions are given in Eqs. (6.32) and (6.1), respectively. This generalization does not affect the Wilson coefficients of Q_1 and Q_2.

Next in Sec. VII the $\Delta S=1$ and $\Delta B=1$ Hamiltonians of Sec. VI will be generalized to include the electroweak penguin operators Q_7-Q_{10}. These generalized Hamiltonians are given in Eqs. (7.1) and (7.37) for $\Delta S=1$ and $\Delta B=1$ nonleptonic decays, respectively. The inclusion of the electroweak penguin operators implies the inclusion of QED effects. Consequently, the coefficients of the operators Q_1-Q_6 given in this section will differ slightly from the ones presented in the previous sections.

In Sec. VIII the effective Hamiltonian for $K_L\to\pi^0e^+e^-$ will be presented. It is given in Eq. (8.1). This Hamiltonian can be considered as a generalization of the $\Delta S=1$ Hamiltonian [Eq. (6.1)] presented in Sec. VI to include the semileptonic operators Q_{7V} and Q_{7A}. This generalization does not modify the numerical values of the $\Delta S=1$ coefficients C_i ($i=1,\ldots,6$) given in Sec. VI.

In Sec. IX we will discuss the effective Hamiltonian for $B\to X_s\gamma$, written down in Eq. (9.1). This Hamiltonian can be considered as a generalization of the $\Delta B=1$ Hamiltonian [Eq. (6.32)] to include the magnetic penguin operators $Q_{7\gamma}$ and Q_{8G}. This generalization does not modify the numerical values of the $\Delta B=1$ coefficients C_i ($i=1,\ldots,6$) from Sec. VI.

In Sec. X we present the effective Hamiltonian for $B\to X_s e^+e^-$, given in Eq. (10.1), which can be considered as the generalization of the $B\to X_s\gamma$ Hamiltonian to include the semileptonic operators Q_{9V} and Q_{10A}. The coefficients C_i ($i=1,\ldots,6,7\gamma,8G$) given in Sec. IX are not affected by this generalization.

In Sec. XI the effective Hamiltonians for $K^+\to\pi^+\nu\bar{\nu}$, $K_L\to\mu^+\mu^-$, $K_L\to\pi^0\nu\bar{\nu}$, $B\to X_{s,d}\nu\bar{\nu}$, and $B\to l^+l^-$ will be discussed and are given in Eqs. (11.4), (11.44), (11.56), and (11.57) respectively. Each of these Hamiltonians involves only a single operator, $Q(\nu\bar{\nu})$ or $Q(\mu\bar{\mu})$ for $K^+\to\pi^+\nu\bar{\nu}$, $K_L\to\pi^0\nu\bar{\nu}$, and $K_L\to\mu^+\mu^-$, with analogous operators for $B\to X_{s,d}\nu\bar{\nu}$ and $B\to l^+l^-$.

Finally, Secs. XII and XIII present the effective Hamiltonians for $\Delta S=2$ and $\Delta B=2$ transitions, respectively. These Hamiltonians involve the operators $Q(\Delta S=2)$ and $Q(\Delta B=2)$ and can be found in Eqs. (12.1) and (13.1).

In Table III we give the list of effective Hamiltonians to be presented below, the equations in which they can be found, and the list of operators entering different Hamiltonians.

V. THE EFFECTIVE $\Delta F=1$ HAMILTONIAN: CURRENT-CURRENT OPERATORS

A. Operators

We begin this compendium by presenting the parts of effective Hamiltonians involving the current-current op-

TABLE IV. The coefficient $C_1(\mu)$ for B decays.

	$\Lambda^{(5)}_{\overline{\rm MS}}=140$ MeV			$\Lambda^{(5)}_{\overline{\rm MS}}=225$ MeV			$\Lambda^{(5)}_{\overline{\rm MS}}=310$ MeV		
μ [GeV]	LO	NDR	HV	LO	NDR	HV	LO	NDR	HV
4.0	–0.274	–0.175	–0.211	–0.310	–0.197	–0.239	–0.341	–0.216	–0.264
5.0	–0.244	–0.151	–0.184	–0.274	–0.169	–0.208	–0.300	–0.185	–0.228
6.0	–0.221	–0.133	–0.164	–0.248	–0.148	–0.184	–0.269	–0.161	–0.201
7.0	–0.203	–0.118	–0.148	–0.226	–0.132	–0.166	–0.246	–0.143	–0.181
8.0	–0.188	–0.106	–0.135	–0.209	–0.118	–0.151	–0.226	–0.128	–0.164

erators only. These operators generally will be denoted by Q_1 and Q_2, although their flavor structure depends on the decay considered. To be specific we will consider

$$Q_1=(\bar{b}_i c_j)_{V-A}(\bar{u}_j d_i)_{V-A},$$
$$Q_2=(\bar{b}_i c_i)_{V-A}(\bar{u}_j d_j)_{V-A}, \tag{5.1}$$
$$Q_1=(\bar{s}_i c_j)_{V-A}(\bar{u}_j d_i)_{V-A},$$
$$Q_2=(\bar{s}_i c_i)_{V-A}(\bar{u}_j d_j)_{V-A}, \tag{5.2}$$
$$Q_1=(\bar{s}_i u_j)_{V-A}(\bar{u}_j d_i)_{V-A},$$
$$Q_2=(\bar{s}_i u_i)_{V-A}(\bar{u}_j d_j)_{V-A}, \tag{5.3}$$

for $\Delta B=1$, $\Delta C=1$, and $\Delta S=1$ decays, respectively. Then the corresponding effective Hamiltonians are given by

$$H_{\rm eff}(\Delta B=1)=\frac{G_F}{\sqrt{2}}V_{cb}^*V_{ud}[C_1(\mu)Q_1+C_2(\mu)Q_2], \quad \mu=O(m_b), \tag{5.4}$$

$$H_{\rm eff}(\Delta C=1)=\frac{G_F}{\sqrt{2}}V_{cs}^*V_{ud}[C_1(\mu)Q_1+C_2(\mu)Q_2], \quad \mu=O(m_c), \tag{5.5}$$

$$H_{\rm eff}(\Delta S=1)=\frac{G_F}{\sqrt{2}}V_{us}^*V_{ud}[C_1(\mu)Q_1+C_2(\mu)Q_2], \quad \mu=O(1\ \text{GeV}). \tag{5.6}$$

As we will see in subsequent sections, these Hamiltonians have to be generalized to also include penguin operators. This, however, will not change the Wilson coefficients $C_1(\mu)$ and $C_2(\mu)$, except for small $O(\alpha)$ corrections in a complete analysis that also includes electroweak penguin operators. For this reason it is useful to present the results for $C_{1,2}$ separately, as they can be used in a large class of decays.

When analyzing Q_1 and Q_2 in isolation, it is useful to work with the operators $Q_\pm$ and their coefficients $z_\pm$ defined by

$$Q_\pm=\tfrac{1}{2}(Q_2\pm Q_1), \quad z_\pm=C_2\pm C_1. \tag{5.7}$$

Q_+ and Q_- do not mix under renormalization, and the expression for $z_\pm(\mu)$ is very simple.

B. Wilson coefficients and renormalization-group evolution

The initial conditions for $z_\pm$ at $\mu=M_W$ are obtained using the matching procedure between the full [Figs. 2(a)–2(c)] and effective [Figs. 3(a)–3(c)] theory summarized in Sec. III.F.1. Given the initial conditions for $z_\pm$ at scale $\mu=M_W$,

$$z_\pm(M_W)=1+\frac{\alpha_s(M_W)}{4\pi}B_\pm, \tag{5.8}$$

and using the NLO RG evolution formula [Eq. (3.99)] for the case without mixing, one finds for the Wilson coefficients of $Q_\pm$ at some scale μ

$$z_\pm(\mu)=\left[1+\frac{\alpha_s(\mu)}{4\pi}J_\pm\right]\left[\frac{\alpha_s(M_W)}{\alpha_s(\mu)}\right]^{d_\pm}\times\left[1+\frac{\alpha_s(M_W)}{4\pi}(B_\pm-J_\pm)\right] \tag{5.9}$$

with

$$J_\pm=\frac{d_\pm}{\beta_0}\beta_1-\frac{\gamma_\pm^{(1)}}{2\beta_0}, \quad d_\pm=\frac{\gamma_\pm^{(0)}}{2\beta_0}, \tag{5.10}$$

TABLE V. The coefficient $C_2(\mu)$ for B decays.

	$\Lambda^{(5)}_{\overline{\rm MS}}=140$ MeV			$\Lambda^{(5)}_{\overline{\rm MS}}=225$ MeV			$\Lambda^{(5)}_{\overline{\rm MS}}=310$ MeV		
μ [GeV]	LO	NDR	HV	LO	NDR	HV	LO	NDR	HV
4.0	1.121	1.074	1.092	1.141	1.086	1.107	1.158	1.096	1.120
5.0	1.105	1.062	1.078	1.121	1.072	1.090	1.135	1.080	1.101
6.0	1.093	1.054	1.069	1.107	1.062	1.079	1.118	1.068	1.087
7.0	1.084	1.047	1.061	1.096	1.054	1.069	1.106	1.059	1.077
8.0	1.077	1.042	1.055	1.087	1.047	1.062	1.096	1.052	1.069

TABLE VI. The coefficient $C_1(\mu)$ for K decays and D decays.

	$\Lambda_{\overline{\rm MS}}^{(4)}=215$ MeV			$\Lambda_{\overline{\rm MS}}^{(4)}=325$ MeV			$\Lambda_{\overline{\rm MS}}^{(4)}=435$ MeV		
μ [GeV]	LO	NDR	HV	LO	NDR	HV	LO	NDR	HV
1.00	–0.602	–0.410	–0.491	–0.742	–0.510	–0.631	–0.899	–0.632	–0.825
1.25	–0.529	–0.356	–0.424	–0.636	–0.430	–0.523	–0.747	–0.512	–0.642
1.50	–0.478	–0.319	–0.379	–0.565	–0.378	–0.457	–0.653	–0.439	–0.543
1.75	–0.439	–0.291	–0.346	–0.514	–0.340	–0.410	–0.587	–0.390	–0.478
2.00	–0.409	–0.269	–0.320	–0.475	–0.311	–0.375	–0.537	–0.353	–0.431

where the coefficients β_0 and β_1 of the QCD β function are given by Eq. (3.16). Furthermore, the LO and NLO expansion coefficients for the anomalous dimensions $\gamma_\pm$ of $Q_\pm$ in Eq. (5.10) and the coefficients $B_\pm$ in Eq. (5.8) are given by

$$\gamma_\pm^{(0)}=\pm 12\frac{N\mp 1}{2N}, \tag{5.11}$$

$$\gamma_\pm^{(1)}=\frac{N\mp 1}{2N}\left[-21\pm\frac{57}{N}\mp\frac{19}{3}N\pm\frac{4}{3}f-2\beta_0\kappa_\pm\right], \tag{5.12}$$

$$B_\pm=\frac{N\mp 1}{2N}[\pm 11+\kappa_\pm] \tag{5.13}$$

with N being the number of colors. Here we have introduced the parameter $\kappa_\pm$, which conveniently distinguishes between various renormalization schemes:

$$\kappa_\pm=\begin{cases}0, & \text{NDR},\\ \mp 4, & \text{HV}.\end{cases} \tag{5.14}$$

Thus, using $N=3$ in the following, $J_\pm$ in Eq. (5.10) can also be written as

$$J_\pm=(J_\pm)_{\rm NDR}+\frac{3\mp 1}{6}\kappa_\pm=(J_\pm)_{\rm NDR}\pm\frac{\gamma_\pm^{(0)}}{12}\kappa_\pm. \tag{5.15}$$

Setting $\gamma_\pm^{(1)}$, $B_\pm$, and β_1 to zero, one arrives at the leading logarithmic approximation (Altarelli and Maiani, 1974; Gaillard and Lee, 1974a).

The NLO calculations in the NDR and HV schemes have been presented by Buras and Weisz (1990). In writing Eq. (5.12) we have incorporated the $-2\gamma_J^{(1)}$ correction in the HV scheme resulting from the nonvanishing two-loop anomalous dimension of the weak current,

$$\gamma_J^{(1)}=\begin{cases}0, & \text{NDR},\\ \dfrac{N^2-1}{N}2\beta_0, & \text{HV}.\end{cases} \tag{5.16}$$

The NLO corrections $\gamma_\pm^{(1)}$ in the dimensional-reduction scheme (DRED) have been first considered by Altarelli *et al.* (1981) and later confirmed by Buras and Weisz (1990). Here one has $\kappa_\pm=\mp 6-N$. This value for $\kappa_\pm$ in DRED also incorporates a finite renormalization of α_s in order to work in all schemes with the usual $\overline{\rm MS}$ coupling.

As already discussed in Sec. III.F.3, the expression $(B_\pm-J_\pm)$ is scheme independent. The scheme dependence of the Wilson coefficients $z_\pm(\mu)$ then originates entirely from the scheme dependence of $J_\pm$ at the lower end of the evolution, which can be seen explicitly in Eq. (5.15).

In order to exhibit the μ dependence on the same footing as the scheme dependence, it is useful to rewrite Eq. (5.9) in the case of B decays as follows,

$$z_\pm(\mu)=\left[1+\frac{\alpha_s(m_b)}{4\pi}\tilde{J}_\pm(\mu)\right]\left[\frac{\alpha_s(M_W)}{\alpha_s(m_b)}\right]^{d_\pm}\times\left[1+\frac{\alpha_s(M_W)}{4\pi}(B_\pm-J_\pm)\right] \tag{5.17}$$

with

$$\tilde{J}_\pm(\mu)=(J_\pm)_{\rm NDR}\pm\frac{\gamma_\pm^{(0)}}{12}\kappa_\pm+\frac{\gamma_\pm^{(0)}}{2}\ln\left(\frac{\mu^2}{m_b^2}\right), \tag{5.18}$$

summarizing both the renormalization-scheme dependence and the μ dependence. Note that in the first parentheses in Eq. (5.17) we have set $\alpha_s(\mu)=\alpha_s(m_b)$, since the difference in the scales in this correction is still of higher order. We also note that a change of the renormalization scheme can be compensated for by a change in μ. From Eq. (5.18) we find generally

$$\mu_i^\pm=\mu_{\rm NDR}\exp\left(\mp\frac{\kappa_\pm^{(i)}}{12}\right), \tag{5.19}$$

where i denotes a given scheme. From Eq. (5.14) we then have

$$\mu_{\rm HV}=\mu_{\rm NDR}\exp\left(\frac{1}{3}\right). \tag{5.20}$$

Evidently the change in μ relating HV and NDR[1] is the same for z_+ and z_- and consequently for $C_i(\mu)$.

This discussion shows that a meaningful analysis of the μ dependence of $C_i(\mu)$ can only be made simultaneously with the analysis of the scheme dependence.

The coefficients $C_i(\mu)$ for B decays can now be calculated using

$$C_1(\mu)=\frac{z_+(\mu)-z_-(\mu)}{2},\quad C_2(\mu)=\frac{z_+(\mu)+z_-(\mu)}{2}. \tag{5.21}$$

[1]The relation $\mu_{\rm DRED}^\pm=\mu_{\rm NDR}\exp[(2\pm 1)/4]$ between NDR and DRED is more involved. In any case $\mu_{\rm HV}$ and $\mu_{\rm DRED}^\pm$ are larger than $\mu_{\rm NDR}$.

TABLE VII. The coefficient $C_2(\mu)$ for K decays and D decays.

	$\Lambda_{\overline{\rm MS}}^{(4)}=215$ MeV			$\Lambda_{\overline{\rm MS}}^{(4)}=325$ MeV			$\Lambda_{\overline{\rm MS}}^{(4)}=435$ MeV		
μ [GeV]	LO	NDR	HV	LO	NDR	HV	LO	NDR	HV
1.00	1.323	1.208	1.259	1.422	1.275	1.358	1.539	1.363	1.506
1.25	1.274	1.174	1.216	1.346	1.221	1.282	1.426	1.277	1.367
1.50	1.241	1.152	1.187	1.298	1.188	1.237	1.358	1.228	1.296
1.75	1.216	1.136	1.167	1.264	1.165	1.207	1.313	1.196	1.252
2.00	1.198	1.123	1.152	1.239	1.148	1.185	1.279	1.174	1.221

To this end we set $f=5$ in the formulas above and use the two-loop $\alpha_s(\mu)$ of Eq. (3.19) with $\Lambda\equiv\Lambda_{\overline{\rm MS}}^{(5)}$. The actual numerical values used for $\alpha_s(M_Z)$, or equivalently $\Lambda_{\overline{\rm MS}}^{(5)}$, are collected in the Appendix together with other numerical input parameters.

In the case of D decays and K decays the relevant scales are $\mu=\mathcal{O}(m_c)$ and $\mu=\mathcal{O}(1\ \text{GeV})$, respectively. In order to calculate $C_i(\mu)$ for these cases one has to evolve these coefficients first from $\mu=\mathcal{O}(m_b)$ down to $\mu=\mathcal{O}(m_c)$ in an effective theory with $f=4$. Matching $\alpha_s^{(5)}(m_b)=\alpha_s^{(4)}(m_b)$, we find, to a very good approximation, $\Lambda_{\overline{\rm MS}}^{(4)}=(325\pm110)$ MeV. Unfortunately, the necessity to evolve $C_i(\mu)$ from $\mu=M_W$ down to $\mu=m_c$ in two different effective theories ($f=5$ and $f=4$) and eventually, in the case of K decays with $f=3$ for $\mu<m_c$, makes the formulas for $C_i(\mu)$ in D decays and K decays rather complicated. They can be found in the work of Buras *et al.* (1993b). Fortunately all these complications can be avoided by a simple trick that reproduces these results to better than 1.5%. In order to find $C_i(\mu)$ for 1 GeV $\leqslant\mu\leqslant$2 GeV one can simply use the master formulas given above with $\Lambda_{\overline{\rm MS}}^{(5)}$ replaced by $\Lambda_{\overline{\rm MS}}^{(4)}$ and an "effective" number of active flavors $f=4.15$. This can be verified by comparing the results presented here with those in Tables X and XII, where no "tricks" have been used. The nice feature of this method is that the μ and renormalization-scheme dependences of $C_i(\mu)$ can still be studied in simple terms.

The numerical coefficients $C_i(\mu)$ for B decays are shown in Tables IV and V for different μ and $\Lambda_{\overline{\rm MS}}^{(5)}$. In addition to the results for the NDR and HV renormalization schemes we show the LO values.[2] The corresponding results for K decays and D decays are given in Tables VI and VII.

[2]The results for the DRED scheme can be found in the work of Buras, (1995).

From Tables IV–IX we observe the following.

(i) The scheme dependence of the Wilson coefficients is sizable. This is in particular the case of C_1 which vanishes in the absence of QCD corrections.

(ii) The differences between LO and NLO results in the case of C_1 are large, which shows the importance of next-to-leading-order corrections. In fact, in the NDR scheme, the corrections may be as large as 70%. This comparison of LO and NLO coefficients can, however, be questioned because, for the chosen values of $\Lambda_{\overline{\rm MS}}$, one has $\alpha_s^{(\rm LO)}(M_Z)=0.135\pm0.009$ as compared to $\alpha_s(M_Z)=0.117\pm0.007$ (Bethke, 1994; Webber, 1994). Consequently, the difference in LO and NLO results for C_i originates partly in the change in the value of the QCD coupling.

(iii) In view of the latter fact it is also instructive to show the LO results in which the next-to-leading-order expression for α_s is used. We give some examples in Tables VIII and IX. Now the differences between LO and NLO results is considerably smaller, although still as large as 30–40% in the case of C_1 in the NDR scheme.

(iv) In any case the inclusion of NLO corrections in NDR and HV schemes weakens the impact of QCD on the Wilson coefficients of current-current operators. It is, however, important to keep in mind that such a behavior is specific to the scheme chosen and will in general be different in other schemes, which reflects the unphysical nature of the Wilson coefficient functions.

Our discussion has not invoked HQET (cf. Sec. XV). It is sometimes stated in the literature that at $\mu=m_b$, in the case of B decays, one *must* switch to HQET. In this case for $\mu<m_b$ the anomalous dimensions $\gamma_\pm$ differ from those given above. We should, however, stress that switching to HQET can be done at any $\mu<m_b$, provided the logarithms $\ln(m_b/\mu)$ in $\langle Q_i\rangle$ do not become too large. Similar comments apply to D decays with respect to $\mu=m_c$. Of course the coefficients C_i calculated in HQET for $\mu<m_b$ are different from the coefficients pre-

TABLE VIII. $C_1^{\rm LO}$ and $C_2^{\rm LO}$ for B decays with α_s in NLO.

	$\Lambda_{\overline{\rm MS}}^{(5)}=140$ MeV		$\Lambda_{\overline{\rm MS}}^{(5)}=225$ MeV		$\Lambda_{\overline{\rm MS}}^{(5)}=310$ MeV	
μ [GeV]	C_1	C_2	C_1	C_2	C_1	C_2
4.0	−0.244	1.105	−0.274	1.121	−0.301	1.135
5.0	−0.217	1.091	−0.243	1.105	−0.265	1.116
6.0	−0.197	1.082	−0.220	1.093	−0.239	1.102

TABLE IX. $C_1^{\rm LO}$ and $C_2^{\rm LO}$ for K and D decays with α_s in NLO.

	$\Lambda_{\overline{\rm MS}}^{(4)}=215$ MeV		$\Lambda_{\overline{\rm MS}}^{(4)}=325$ MeV		$\Lambda_{\overline{\rm MS}}^{(4)}=435$ MeV	
μ [GeV]	C_1	C_2	C_1	C_2	C_1	C_2
1.0	–0.524	1.271	–0.664	1.366	–0.851	1.502
1.5	–0.413	1.201	–0.493	1.250	–0.579	1.307
2.0	–0.354	1.165	–0.412	1.200	–0.469	1.235

sented here. However, the corresponding matrix elements $\langle Q_i\rangle$ in HQET are also different so that the physical amplitudes remain unchanged.

VI. THE EFFECTIVE $\Delta F=1$ HAMILTONIAN: INCLUSION OF QCD PENGUIN OPERATORS

In Sec. V we have restricted ourselves to current-current operators when considering QCD corrections to the effective $\Delta F=1$ ($F=B,C,S$) Hamiltonian for weak decays.

As already mentioned in Sec. III.D.3, e.g., for the $\Delta S=1$ case, the special flavor structure of $Q_2=(\bar s u)_{V-A}(\bar u d)_{V-A}$ allows not only for QCD corrections of the current-current type as in Figs. 3(a)–3(c), from which the second current-current operator Q_1 is created. For a complete treatment of QCD corrections, all possible ways of attaching a gluon to the initial weak $\Delta F=1$ transition operator Q_2 have to be taken into account. Therefore attaching gluons to Q_2 in the form of Figs. 3(d.1) and 3(d.2) generates a completely new set of four-quark operators, the so-called QCD penguin operators, usually denoted as $Q_3,\ldots,Q_6$.[3] This procedure is often referred to as inserting Q_2 into type-1 and type-2 penguin diagrams.

The $\Delta S=1$ effective Hamiltonian for $K\to\pi\pi$ at scales $\mu<m_c$ then reads

$$\mathcal{H}_{\rm eff}(\Delta S=1)=\frac{G_F}{\sqrt{2}}V_{us}^*V_{ud}\sum_{i=1}^{6}[z_i(\mu)+\tau\, y_i(\mu)]Q_i \tag{6.1}$$

with

$$\tau=-\frac{V_{ts}^*V_{td}}{V_{us}^*V_{ud}}. \tag{6.2}$$

The set of four-quark operators $\vec{Q}(\mu)$ and Wilson coefficients $\vec{z}(\mu)$ and $\vec{y}(\mu)$ will be discussed one by one in the subsections below.

[3]Obviously, whether or not it is possible to form a closed fermion loop as in a type-1 insertion or to connect the two currents to yield a continuous fermion line as required for a type-2 insertion depends strongly on the flavor structure of the operator considered. For example, for Q_2 only the type-2 penguin diagram contributes. This feature can be exploited to obtain NLO anomalous-dimension matrices in the NDR scheme without the necessity of calculating closed fermion loops with γ_5 (Buras *et al.*, 1993; Buras *et al.*, 1993a).

A. Operators

The basis of four-quark operators for the $\Delta S=1$ effective Hamiltonian in Eq. (6.1) is given in explicit form by

$$\begin{aligned}
Q_1&=(\bar s_i u_j)_{V-A}(\bar u_j d_i)_{V-A}, \qquad (6.3)\\
Q_2&=(\bar s u)_{V-A}(\bar u d)_{V-A},\\
Q_3&=(\bar s d)_{V-A}\sum_q(\bar q q)_{V-A},\\
Q_4&=(\bar s_i d_j)_{V-A}\sum_q(\bar q_j q_i)_{V-A},\\
Q_5&=(\bar s d)_{V-A}\sum_q(\bar q q)_{V+A},\\
Q_6&=(\bar s_i d_j)_{V-A}\sum_q(\bar q_j q_i)_{V+A}.
\end{aligned}$$

As already mentioned, this basis closes under QCD renormalization.

For $\mu<m_c$ the sums over active quark flavors in Eq. (6.3) run over, u, d, and s. However, when $m_b>\mu>m_c$ is considered, $q=c$ also has to be included. Moreover, in this case two additional current-current operators have to be taken into account:

$$Q_1^c=(\bar s_i c_j)_{V-A}(\bar c_j d_i)_{V-A},\quad Q_2^c=(\bar s c)_{V-A}(\bar c d)_{V-A}, \tag{6.4}$$

and the effective Hamiltonian takes the form

$$\mathcal{H}_{\rm eff}(\Delta S=1)=\frac{G_F}{\sqrt{2}}V_{us}^*V_{ud}\Bigg[(1-\tau)\sum_{i=1}^{2}z_i(\mu)(Q_i-Q_i^c)+\tau\sum_{i=1}^{6}v_i(\mu)Q_i\Bigg]. \tag{6.5}$$

B. Wilson coefficients

For the Wilson coefficients $y_i(\mu)$ and $z_i(\mu)$ in Eq. (6.1) one has

$$y_i(\mu)=v_i(\mu)-z_i(\mu). \tag{6.6}$$

The coefficients z_i and v_i are the components of the six-dimensional column vectors $\vec{v}(\mu)$ and $\vec{z}(\mu)$. Their RG evolution is given by

$$\vec{v}(\mu)=U_3(\mu,m_c)M(m_c)U_4(m_c,m_b)M(m_b)\times U_5(m_b,M_W)\vec{C}(M_W), \tag{6.7}$$

$$\vec{z}(\mu)=U_3(\mu,m_c)\vec{z}(m_c). \tag{6.8}$$

Here $U_f(m_1,m_2)$ denotes the full NLO evolution matrix for f active flavors. $M(m_i)$ is the matching matrix at quark threshold m_i given in Eq. (3.104). These two matrices will be discussed in more detail in Secs. VI.C and VI.D, respectively.

The initial values $\vec{C}(M_W)$ necessary for the RG evolution of $\vec{v}(\mu)$ in Eq. (6.7) can be found according to the procedure of matching the effective (Fig. 3) onto the full theory (Fig. 2) as summarized in Sec. III.F. For the NDR scheme one obtains (Buras *et al.*, 1992)

$$C_1(M_W)=\frac{11}{2}\frac{\alpha_s(M_W)}{4\pi}, \tag{6.9}$$

$$C_2(M_W)=1-\frac{11}{6}\frac{\alpha_s(M_W)}{4\pi}, \tag{6.10}$$

$$C_3(M_W)=-\frac{\alpha_s(M_W)}{24\pi}\tilde{E}_0(x_t), \tag{6.11}$$

$$C_4(M_W)=\frac{\alpha_s(M_W)}{8\pi}\tilde{E}_0(x_t), \tag{6.12}$$

$$C_5(M_W)=-\frac{\alpha_s(M_W)}{24\pi}\tilde{E}_0(x_t), \tag{6.13}$$

$$C_6(M_W)=\frac{\alpha_s(M_W)}{8\pi}\tilde{E}_0(x_t), \tag{6.14}$$

where

$$E_0(x)=-\frac{2}{3}\ln x+\frac{x(18-11x-x^2)}{12(1-x)^3}+\frac{x^2(15-16x+4x^2)}{6(1-x)^4}\ln x, \tag{6.15}$$

$$\tilde{E}_0(x_t)=E_0(x_t)-\frac{2}{3}, \tag{6.16}$$

with

$$x_t=\frac{m_t^2}{M_W^2}. \tag{6.17}$$

Here $E_0(x)$ results from the evaluation of the gluon penguin diagrams. The initial values $\vec{C}(M_W)$ in the HV scheme can be found in the work of Buras *et al.* (1992).

In order to calculate the initial conditions $\vec{z}(m_c)$ for $z_i(\mu)$ in Eq. (6.8), one has to consider the difference $Q_2^u-Q_2^c$ of Q_2-type current-current operators, as can be seen explicitly in Eq. (6.5). Due to the Glashow-Iliopoulos-Maiani (GIM) mechanism the coefficients $z_i(\mu)$ of penguin operators Q_i, $i\neq1,2$ are zero in five- and four-flavor theories. The evolution for scales $\mu>m_c$ then involves only the current-current operators $Q_i^u-Q_i^c$, $i=1,2$, with initial conditions at scale $\mu=M_W$

$$z_1(M_W)=C_1(M_W),\quad z_2(M_W)=C_2(M_W). \tag{6.18}$$

$Q_{1,2}^u\equiv Q_{1,2}$ and $Q_{1,2}^c$ do not mix with each other under renormalization. We then find

$$\begin{pmatrix}z_1(m_c)\\ z_2(m_c)\end{pmatrix}=U_4(m_c,m_b)M(m_b)U_5(m_b,M_W)\times\begin{pmatrix}z_1(M_W)\\ z_2(M_W)\end{pmatrix}, \tag{6.19}$$

where this time the evolution matrices $U_{4,5}$ contain only the 2×2 anomalous-dimension submatrices describing the mixing between current-current operators. The matching matrix $M(m_b)$ is then the corresponding 2×2 submatrix of the full 6×6 matrix in Eq. (6.27). For the particular case of Eq. (6.19) it simplifies to a unit matrix. When the charm quark is integrated out, the operators $Q_{1,2}^c$ disappear from the effective Hamiltonian, and the coefficients $z_i(\mu)$, $i\neq1,2$, for penguin operators become nonzero. In order to calculate $z_i(m_c)$ for penguin operators, a proper matching between effective four- and three-quark theories, that is between Eqs. (6.5) and (6.1), has to be made. For the three-quark theory one obtains, in the NDR scheme (Buras *et al.*, 1993b),

$$\vec{z}(m_c)=\begin{pmatrix}z_1(m_c)\\ z_2(m_c)\\ -\alpha_s/(24\pi)F_s(m_c)\\ \alpha_s/(8\pi)F_s(m_c)\\ -\alpha_s/(24\pi)F_s(m_c)\\ \alpha_s/(8\pi)F_s(m_c)\end{pmatrix}, \tag{6.20}$$

where

$$F_s(m_c)=-\tfrac{2}{3}z_2(m_c). \tag{6.21}$$

In the HV scheme $z_{1,2}$ are modified, and one has $F_s(m_c)=0$ or $z_i(m_c)=0$ for $i\neq1,2$.

C. Renormalization-group evolution and anomalous-dimension matrices

The general RG evolution matrix $U(m_1,m_2)$ from scale m_2 down to $m_1<m_2$ in pure QCD is

$$U(m_1,m_2)\equiv T_g\exp\int_{g(m_2)}^{g(m_1)}dg'\,\frac{\gamma_s^T(g'^2)}{\beta(g')}, \tag{6.22}$$

with $\gamma_s(g^2)$ being the full 6×6 QCD anomalous-dimension matrix for $Q_1,\ldots,Q_6$.

For the case at hand it can be expanded in terms of α_s as follows:

$$\gamma_s(g^2)=\frac{\alpha_s}{4\pi}\gamma_s^{(0)}+\frac{\alpha_s^2}{(4\pi)^2}\gamma_s^{(1)}+\cdots. \tag{6.23}$$

Explicit expressions for $\gamma_s^{(0)}$ and $\gamma_s^{(1)}$ will be given below.

From Eq. (6.23) the general QCD evolution matrix $U(m_1,m_2)$ of Eq. (6.22) can be written as in Eq. (3.93) (Buras *et al.*, 1992),

$$U(m_1,m_2)=\left(1+\frac{\alpha_s(m_1)}{4\pi}J\right)U^{(0)}(m_1,m_2)\times\left(1-\frac{\alpha_s(m_2)}{4\pi}J\right), \tag{6.24}$$

where $U^{(0)}(m_1,m_2)$ denotes the evolution matrix in the leading logarithmic approximation and J summarizes the NLO correction to this evolution. Therefore the full matrix $U(m_1,m_2)$ sums logarithms $(\alpha_s t)^n$ and $\alpha_s(\alpha_s t)^n$ with $t=\ln(m_2^2/m_1^2)$. Explicit expressions for $U^{(0)}(m_1,m_2)$ and J are given in Eqs. (3.94)–(3.98).

The LO anomalous-dimension matrix $\gamma_s^{(0)}$ of Eq. (6.23) has the explicit form (Altarelli and Maiani, 1974; Gaillard and Lee, 1974a; Vainshtein *et al.*, 1977; Gilman and Wise, 1979; Guberina and Peccei, 1980)

$$\gamma_s^{(0)}=\begin{pmatrix} \frac{-6}{N} & 6 & 0 & 0 & 0 & 0 \\ 6 & \frac{-6}{N} & \frac{-2}{3N} & \frac{2}{3} & \frac{-2}{3N} & \frac{2}{3} \\ 0 & 0 & \frac{-22}{3N} & \frac{22}{3} & \frac{-4}{3N} & \frac{4}{3} \\ 0 & 0 & 6-\frac{2f}{3N} & \frac{-6}{N}+\frac{2f}{3} & \frac{-2f}{3N} & \frac{2f}{3} \\ 0 & 0 & 0 & 0 & \frac{6}{N} & -6 \\ 0 & 0 & \frac{-2f}{3N} & \frac{2f}{3} & \frac{-2f}{3N} & \frac{-6(-1+N^2)}{N}+\frac{2f}{3} \end{pmatrix}. \tag{6.25}$$

The NLO anomalous-dimension matrix $\gamma_s^{(1)}$ of Eq. (6.23) in the NDR scheme reads (Buras *et al.*, 1992; Ciuchini, Franco, Martinelli, and Reina, 1994)

$$\gamma_{s,\mathrm{NDR}}^{(1)}\big|_{N=3}=\begin{pmatrix} -\frac{21}{2}-\frac{2f}{9} & \frac{7}{2}+\frac{2f}{3} & \frac{79}{9} & -\frac{7}{3} & -\frac{65}{9} & -\frac{7}{3} \\ \frac{7}{2}+\frac{2f}{3} & -\frac{21}{2}-\frac{2f}{9} & -\frac{202}{243} & \frac{1354}{81} & -\frac{1192}{243} & \frac{904}{81} \\ 0 & 0 & -\frac{5911}{486}+\frac{71f}{9} & \frac{5983}{162}+\frac{f}{3} & -\frac{2384}{243}-\frac{71f}{9} & \frac{1808}{81}-\frac{f}{3} \\ 0 & 0 & \frac{379}{18}+\frac{56f}{243} & -\frac{91}{6}+\frac{808f}{81} & -\frac{130}{9}-\frac{502f}{243} & -\frac{14}{3}+\frac{646f}{81} \\ 0 & 0 & \frac{-61f}{9} & \frac{-11f}{3} & \frac{71}{3}+\frac{61f}{9} & -99+\frac{11f}{3} \\ 0 & 0 & \frac{-682f}{243} & \frac{106f}{81} & -\frac{225}{2}+\frac{1676f}{243} & -\frac{1343}{6}+\frac{1348f}{81} \end{pmatrix}. \tag{6.26}$$

In Eqs. (6.25) and (6.26) f denotes the number of active quark flavors at a certain scale μ. The corresponding results for $\gamma_s^{(1)}$ in the HV scheme can either be obtained by direct calculation or by using Eq. (3.126). They can be found in Buras *et al.* (1992), Ciuchini, Franco, Martinelli, and Reina, 1994, where also the N dependence of $\gamma_s^{(1)}$ is given.

D. Quark-threshold matching matrix

As discussed in Sec. III.F.1, in general a matching matrix $M(m)$ has to be included in the RG evolution at NLO when going from a f-flavor effective theory to a $(f-1)$-flavor effective theory at quark threshold $\mu=m$ (Buras *et al.*, 1992, 1993b).

For the $\Delta S=1$ decay $K\to\pi\pi$ in pure QCD, one has (Buras *et al.*, 1992)

$$M(m)=1+\frac{\alpha_s(m)}{4\pi}\,\delta r_s^T. \tag{6.27}$$

At the quark thresholds $m=m_b$ and $m=m_c$, the matrix δr_s is

$$\delta r_s^T=-\tfrac{5}{9}P(0,0,0,1,0,1) \tag{6.28}$$

TABLE X. $\Delta S=1$ Wilson coefficients at $\mu=1$ GeV for $m_t=170$ GeV, $y_1=y_2\equiv 0$.

	$\Lambda^{(4)}_{\overline{\rm MS}}=215$ MeV			$\Lambda^{(4)}_{\overline{\rm MS}}=325$ MeV			$\Lambda^{(4)}_{\overline{\rm MS}}=435$ MeV		
Scheme	LO	NDR	HV	LO	NDR	HV	LO	NDR	HV
z_1	−0.602	−0.407	−0.491	−0.743	−0.506	−0.636	−0.901	−0.622	−0.836
z_2	1.323	1.204	1.260	1.423	1.270	1.362	1.541	1.352	1.515
z_3	0.003	0.007	0.004	0.004	0.013	0.007	0.006	0.022	0.015
z_4	−0.008	−0.022	−0.010	−0.012	−0.034	−0.016	−0.016	−0.058	−0.029
z_5	0.003	0.006	0.003	0.004	0.007	0.004	0.005	0.009	0.005
z_6	−0.009	−0.021	−0.009	−0.013	−0.034	−0.014	−0.018	−0.058	−0.025
y_3	0.029	0.023	0.026	0.036	0.031	0.036	0.045	0.040	0.048
y_4	−0.051	−0.046	−0.048	−0.060	−0.056	−0.059	−0.069	−0.066	−0.072
y_5	0.012	0.004	0.013	0.013	−0.001	0.016	0.014	−0.013	0.020
y_6	−0.084	−0.076	−0.070	−0.111	−0.109	−0.096	−0.145	−0.166	−0.136

with

$$P^T=(0,0,-\tfrac{1}{3},1,-\tfrac{1}{3},1). \tag{6.29}$$

E. Numerical results for the $K\to\pi\pi$ Wilson coefficients in pure QCD

Tables X–XII give the $\Delta S=1$ Wilson coefficients for $Q_1,\ldots,Q_6$ in pure QCD. We observe a visible scheme dependence for all NLO Wilson coefficients. Notably we find $|y_6|$ to be smaller in the HV than in the NDR scheme. In addition, all coefficients, especially z_1 and $y_3,\ldots,y_6$, show a strong dependence on $\Lambda_{\overline{\rm MS}}$.

Next, at NLO the absolute values for $z_{1,2}$ and y_i are suppressed relative to their LO results, except for y_5 in HV and $y_{4,6}$ in NDR for $\mu>m_c$. The latter behavior is related to the effect of the matching matrix $M(m_c)$ absent for $\mu>m_c$. For $y_3,\ldots,y_5$ there is no visible m_t dependence in the range $m_t=(170\pm15)$ GeV. For $|y_6|$ there is a relative variation of $\mathcal{O}(\pm1.5\%)$ for in/decreasing m_t.

Finally, a comment on the Wilson coefficients in the HV scheme as presented here is appropriate. As we have mentioned in Sec. V.B, the two-loop anomalous dimension of the weak current in the HV scheme does not vanish. This peculiar feature of the HV scheme is also felt in $\gamma_s^{(1)}$. The diagonal terms in $\gamma_s^{(1)}$ acquire additional universal large $\mathcal{O}(N^2)$ terms $(44/3)N^2$, which are absent in the NDR scheme. These artificial terms can be removed by working with $\gamma_s^{(1)}-2\gamma_J^{(1)}$ instead of $\gamma_s^{(1)}$. This procedure, adopted in this review and by Buras *et al.* (1993b), effectively corresponds to a finite renormalization of operators that changes the coefficient of $\alpha_s/4\pi$ in $C_2^{\rm HV}(M_W)$ from −13/2 to −7/6. The Rome group (Ciuchini, Franco, Martinelli, and Reina, 1994) has chosen not to make this additional finite renormalization, and consequently their coefficients in the HV scheme differ from the HV coefficients presented here by a universal factor. They can be found by using

$$C^{\rm HV}_{\rm Rome}(\mu)=\left[1-\frac{\alpha_s(\mu)}{4\pi}4C_F\right]C^{\rm HV}(\mu). \tag{6.30}$$

Clearly this difference is compensated for by the corresponding difference in the hadronic matrix elements of the operators Q_i.

F. The $\Delta B=1$ effective Hamiltonian in pure QCD

An important application of the formalism developed in the previous subsections is for the case of B-meson decays. The LO calculation can be found, e.g., in the works of Ponce (1981) and Grinstein (1989), where the importance of NLO calculations has already been pointed out. This section can be viewed as the generalization of Grinstein's analysis beyond the LO approximation. We will focus on the $\Delta B=1$, $\Delta C=0$ part of the effective Hamiltonian, which is of particular interest for the study of CP violation in decays to CP selfconjugate

TABLE XI. $\Delta S=1$ Wilson coefficients at $\mu=m_c=1.3$ GeV for $m_t=170$ GeV and $f=3$ effective flavors. $|z_3|,\ldots,|z_6|$ are numerically irrelevant relative to $|z_{1,2}|$. $y_1=y_2\equiv 0$.

	$\Lambda^{(4)}_{\overline{\rm MS}}=215$ MeV			$\Lambda^{(4)}_{\overline{\rm MS}}=325$ MeV			$\Lambda^{(4)}_{\overline{\rm MS}}=435$ MeV		
Scheme	LO	NDR	HV	LO	NDR	HV	LO	NDR	HV
z_1	−0.518	−0.344	−0.411	−0.621	−0.412	−0.504	−0.727	−0.487	−0.614
z_2	1.266	1.166	1.207	1.336	1.208	1.269	1.411	1.258	1.346
y_3	0.026	0.021	0.024	0.032	0.027	0.031	0.039	0.035	0.040
y_4	−0.050	−0.046	−0.048	−0.059	−0.056	−0.058	−0.068	−0.067	−0.070
y_5	0.013	0.007	0.013	0.015	0.005	0.016	0.016	0.001	0.018
y_6	−0.075	−0.067	−0.062	−0.095	−0.088	−0.079	−0.118	−0.116	−0.102

TABLE XII. $\Delta S=1$ Wilson coefficients at $\mu=2$ GeV for $m_t=170$ GeV. For $\mu>m_c$ the GIM mechanism gives $z_i\equiv 0$, $i=3,\ldots,6$. $y_1=y_2\equiv 0$.

	$\Lambda^{(4)}_{\overline{\rm MS}}=215$ MeV			$\Lambda^{(4)}_{\overline{\rm MS}}=325$ MeV			$\Lambda^{(4)}_{\overline{\rm MS}}=435$ MeV		
Scheme	LO	NDR	HV	LO	NDR	HV	LO	NDR	HV
z_1	−0.411	−0.266	−0.318	−0.477	−0.309	−0.374	−0.541	−0.350	−0.430
z_2	1.199	1.121	1.151	1.240	1.145	1.185	1.282	1.170	1.220
y_3	0.019	0.019	0.018	0.023	0.023	0.022	0.027	0.027	0.026
y_4	−0.040	−0.046	−0.039	−0.046	−0.054	−0.045	−0.052	−0.062	−0.052
y_5	0.011	0.010	0.011	0.012	0.010	0.013	0.013	0.010	0.015
y_6	−0.055	−0.057	−0.047	−0.067	−0.070	−0.056	−0.078	−0.085	−0.067

final states. The part of the Hamiltonian inducing $\Delta B=1$, $\Delta C=\pm 1$ transitions involves no penguin operators and has already been discussed in Sec. V.

At tree-level the effective Hamiltonian of interest here is simply given by

$$\mathcal{H}_{\rm eff}(\Delta B=1) = \frac{G_F}{\sqrt{2}} \sum_{q=u,c} \sum_{q'=d,s} V^*_{qb}V_{qq'}(\bar{b}q)_{V-A}(\bar{q}q')_{V-A}\,. \tag{6.31}$$

The cases $q'=d$ and $q'=s$ can be treated separately and have the same Wilson coefficients $C_i(\mu)$. Therefore we will restrict the discussion to $q'=d$ in the following.

Using unitarity of the CKM matrix, $\xi_u+\xi_c+\xi_t=0$ with $\xi_i=V^*_{ib}V_{id}$, and the fact that $Q^u_{1,2}$ and $Q^c_{1,2}$ have the same initial conditions at $\mu=M_W$, one obtains for the effective $\Delta B=1$ Hamiltonian at scales $\mu=\mathcal{O}(m_b)$,

$$\mathcal{H}_{\rm eff}(\Delta B=1)=\frac{G_F}{\sqrt{2}}\Big\{\xi_c[C_1(\mu)Q^c_1(\mu)+C_2(\mu)Q^c_2(\mu)] + \xi_u[C_1(\mu)Q^u_1(\mu)+C_2(\mu)Q^u_2(\mu)] - \xi_t\sum_{i=3}^{6} C_i(\mu)Q_i(\mu)\Big\}. \tag{6.32}$$

Here

$$Q^q_1=(\bar{b}_iq_j)_{V-A}(\bar{q}_jd_i)_{V-A}\,,$$
$$Q^q_2=(\bar{b}q)_{V-A}(\bar{q}d)_{V-A}\,,$$
$$Q_3=(\bar{b}d)_{V-A}\sum_q (\bar{q}q)_{V-A}\,,$$
$$Q_4=(\bar{b}_id_j)_{V-A}\sum_q (\bar{q}_jq_i)_{V-A}\,,$$
$$Q_5=(\bar{b}d)_{V-A}\sum_q (\bar{q}q)_{V+A}\,,$$
$$Q_6=(\bar{b}_id_j)_{V-A}\sum_q (\bar{q}_jq_i)_{V+A}\,, \tag{6.33}$$

where the summation runs over $q=u,d,s,c,b$.

The corresponding $\Delta B=1$ Wilson coefficients at scale $\mu=\mathcal{O}(m_b)$ are simply given by a truncated version of Eq. (6.7),

$$\vec{C}(m_b)=U_5(m_b,M_W)\vec{C}(M_W). \tag{6.34}$$

Here U_5 is the 6×6 RG evolution matrix of Eq. (6.24) for $f=5$ active flavors. The initial conditions $\vec{C}(M_W)$ are identical to those of Eqs. (6.9)–(6.14) for the $\Delta S=1$ case.

G. Numerical results for the $\Delta B=1$ Wilson coefficients in pure QCD

Table XIII lists the $\Delta B=1$ Wilson coefficients for $Q^{u,c}_1, Q^{u,c}_2, Q_3,\ldots,Q_6$ in pure QCD. C_1, C_4, and C_6 show a $\mathcal{O}(20\%)$ scheme dependence, while this dependence is much weaker for the rest of the coefficients.

Similar to the $\Delta S=1$ case, the numerical values for $\Delta B=1$ Wilson coefficients are sensitive to the value of $\Lambda_{\overline{\rm MS}}$ used to determine α_s for the RG evolution. The sensitivity is less pronounced than in the $\Delta S=1$ case due to the higher value $\mu=\bar{m}_b(m_b)$ of the renormalization scale, and one finds no visible m_t dependence in the range $m_t=(170\pm 15)$ GeV.

TABLE XIII. $\Delta B=1$ Wilson coefficients at $\mu=\bar{m}_b(m_b)=4.40$ GeV for $m_t=170$ GeV.

	$\Lambda^{(5)}_{\overline{\rm MS}}=140$ MeV			$\Lambda^{(5)}_{\overline{\rm MS}}=225$ MeV			$\Lambda^{(5)}_{\overline{\rm MS}}=310$ MeV		
Scheme	LO	NDR	HV	LO	NDR	HV	LO	NDR	HV
C_1	−0.272	−0.164	−0.201	−0.307	−0.184	−0.227	−0.337	−0.202	−0.250
C_2	1.120	1.068	1.087	1.139	1.078	1.101	1.155	1.087	1.113
C_3	0.012	0.012	0.011	0.013	0.013	0.012	0.015	0.015	0.014
C_4	−0.026	−0.031	−0.026	−0.030	−0.035	−0.029	−0.032	−0.038	−0.032
C_5	0.008	0.008	0.008	0.009	0.009	0.009	0.009	0.009	0.010
C_6	−0.033	−0.035	−0.029	−0.038	−0.041	−0.033	−0.042	−0.046	−0.036

VII. THE EFFECTIVE $\Delta F=1$ HAMILTONIAN: INCLUSION OF ELECTROWEAK PENGUIN OPERATORS

In a similar fashion to the creation of the penguin operators $Q_3,\ldots,Q_6$ through QCD corrections, the inclusion of electroweak corrections, shown in Figs. 2(d) and 2(e), generates a set of new operators, the so-called electroweak penguin operators. For the $\Delta S=1$ decay $K\to\pi\pi$ they are usually denoted by $Q_7,\ldots,Q_{10}$.

This means that, although now we will have to deal with more technically involved issues like an extended operator basis or the possibility of mixed QCD–QED contributions, the underlying principles in performing the RG evolution will closely resemble those used in Sec. VI for pure QCD. Obviously, the fundamental step has already been made when going from current-current operators in Sec. V to the inclusion of QCD penguins in Sec. VI. Hence in this section we will, wherever possible, only point out the differences between the pure 6×6 QCD and the combined 10×10 QCD-QED case.

The full $\Delta S=1$ effective Hamiltonian for $K\to\pi\pi$ at scales $\mu<m_c$ is, including QCD and QED corrections,[4]

$$\mathcal{H}_{\rm eff}(\Delta S=1)=\frac{G_F}{\sqrt{2}}V_{us}^*V_{ud}\sum_{i=1}^{10}[z_i(\mu)+\tau\, y_i(\mu)]Q_i(\mu), \tag{7.1}$$

with $\tau=-V_{ts}^*V_{td}/(V_{us}^*V_{ud})$.

A. Operators

The basis of four-quark operators for the $\Delta S=1$ effective Hamiltonian in Eq. (7.1) is given by $Q_1,\ldots,Q_6$ of Eq. (6.3) and the electroweak penguin operators

$$\begin{aligned}
Q_7&=\frac{3}{2}(\bar{s}d)_{V-A}\sum_q e_q(\bar{q}q)_{V+A},\\
Q_8&=\frac{3}{2}(\bar{s}_id_j)_{V-A}\sum_q e_q(\bar{q}_jq_i)_{V+A},\\
Q_9&=\frac{3}{2}(\bar{s}d)_{V-A}\sum_q e_q(\bar{q}q)_{V-A},\\
Q_{10}&=\frac{3}{2}(\bar{s}_id_j)_{V-A}\sum_q e_q(\bar{q}_jq_i)_{V-A}.
\end{aligned} \tag{7.2}$$

Here, e_q denotes the quark electric charge, which reflects the electroweak origin of $Q_7,\ldots,Q_{10}$. The basis $Q_1,\ldots,Q_{10}$ closes under QCD and QED renormalization. Finally, for $m_b>\mu>m_c$, the operators Q_1^c and Q_2^c of Eq. (6.4) have to be included again in a similar way to the case of pure QCD.

[4]In principle, operators $Q_{11}=(g_s/16\pi^2)m_s\bar{s}\sigma_{\mu\nu}T^aG_a^{\mu\nu}(1-\gamma_5)d$ and $Q_{12}=(ee_d/16\pi^2)m_s\bar{s}\sigma_{\mu\nu}F^{\mu\nu}(1-\gamma_5)d$ should also be considered for $K\to\pi\pi$. However, as shown by Bertolini *et al.* (1995a), their numerical contribution is negligible. Therefore Q_{11} and Q_{12} will not be included here for $K\to\pi\pi$.

B. Wilson coefficients

As far as formulas for Wilson coefficients are concerned, the generalization of Sec. VI.B to the present case is to a large extent straightforward.

First, due to the extended operator basis, $\vec{v}(\mu)$ and $\vec{z}(\mu)$ in Eqs. (6.7) and (6.8) are now ten-dimensional column vectors. Furthermore, the substitution

$$U_f(m_1,m_2)\to U_f(m_1,m_2,\alpha)$$

has to be made in the RG evolution equations (6.7), (6.8), and (6.19). Here $U_f(m_1,m_2,\alpha)$ denotes the full 10×10 QCD–QED RG evolution matrix for f active flavors. $U_f(m_1,m_2,\alpha)$ will still be discussed in more detail in Sec. VII.C.

The extended initial values $\vec{C}(M_W)$, including $\mathcal{O}(\alpha)$ corrections and additional entries for $Q_7,\ldots,Q_{10}$, can be obtained from the usual matching procedure between Figs. 2 and 3. They read, in the NDR scheme (Buras *et al.*, 1993b),

$$C_1(M_W)=\frac{11}{2}\frac{\alpha_s(M_W)}{4\pi}, \tag{7.3}$$

$$C_2(M_W)=1-\frac{11}{6}\frac{\alpha_s(M_W)}{4\pi}-\frac{35}{18}\frac{\alpha}{4\pi}, \tag{7.4}$$

$$C_3(M_W)=-\frac{\alpha_s(M_W)}{24\pi}\tilde{E}_0(x_t)+\frac{\alpha}{6\pi}\frac{1}{\sin^2\theta_W}\times[2B_0(x_t)+C_0(x_t)], \tag{7.5}$$

$$C_4(M_W)=\frac{\alpha_s(M_W)}{8\pi}\tilde{E}_0(x_t), \tag{7.6}$$

$$C_5(M_W)=-\frac{\alpha_s(M_W)}{24\pi}\tilde{E}_0(x_t), \tag{7.7}$$

$$C_6(M_W)=\frac{\alpha_s(M_W)}{8\pi}\tilde{E}_0(x_t), \tag{7.8}$$

$$C_7(M_W)=\frac{\alpha}{6\pi}[4C_0(x_t)+\tilde{D}_0(x_t)], \tag{7.9}$$

$$C_8(M_W)=0, \tag{7.10}$$

$$C_9(M_W)=\frac{\alpha}{6\pi}\left[4C_0(x_t)+\tilde{D}_0(x_t)+\frac{1}{\sin^2\theta_W}[10B_0(x_t)-4C_0(x_t)]\right], \tag{7.11}$$

$$C_{10}(M_W)=0, \tag{7.12}$$

where

$$B_0(x)=\frac{1}{4}\left[\frac{x}{1-x}+\frac{x\,\ln x}{(x-1)^2}\right], \tag{7.13}$$

$$C_0(x)=\frac{x}{8}\left[\frac{x-6}{x-1}+\frac{3x+2}{(x-1)^2}\ln x\right], \tag{7.14}$$

$$D_0(x)=-\frac{4}{9}\ln x+\frac{-19x^3+25x^2}{36(x-1)^3}+\frac{x^2(5x^2-2x-6)}{18(x-1)^4}\ln x, \tag{7.15}$$

$$\tilde{D}_0(x_t)=D_0(x_t)-\frac{4}{9}. \tag{7.16}$$

$\tilde{E}_0(x_t)$ and x_t have already been defined in Eqs. (6.16) and (6.17), respectively. Here $B_0(x)$ results from the evaluation of the box diagrams, $C_0(x)$ from the Z^0 penguin, $D_0(x)$ from the photon penguin, and $E_0(x)$ in $\tilde{E}_0(x_t)$ from the gluon penguin diagrams. Θ_W is the Weinberg angle. The initial values $\vec{C}(M_W)$ in the HV scheme are given by Buras *et al.* (1993b).

Finally, the generalization of Eq. (6.20) to the $Q_1,\ldots,Q_{10}$ basis is (Buras *et al.*, 1993b)

$$\vec{z}(m_c)=\begin{pmatrix} z_1(m_c)\\ z_2(m_c)\\ -\alpha_s/(24\pi)F_s(m_c)\\ \alpha_s/(8\pi)F_s(m_c)\\ -\alpha_s/(24\pi)F_s(m_c)\\ \alpha_s/(8\pi)F_s(m_c)\\ \alpha/(6\pi)F_e(m_c)\\ 0\\ \alpha/(6\pi)F_e(m_c)\\ 0 \end{pmatrix}, \tag{7.17}$$

with $F_s(m_c)$ given by Eq. (6.21) and

$$F_e(m_c)=-\frac{4}{9}[3z_1(m_c)+z_2(m_c)]. \tag{7.18}$$

In the HV scheme, in addition to $z_{1,2}$ differing from their NDR values, one has $F_s(m_c)=F_e(m_c)=0$, and, consequently, $z_i(m_c)=0$ for $i\neq 1,2$.

C. Renormalization-group evolution and anomalous-dimension matrices

Besides an extended operator basis the main difference between the pure QCD case of Sec. VI and the present case consists of the additional presence of QED contributions to the RG evolution. This will make the actual formulas for the RG evolution matrices more involved. However, the underlying concepts developed in Secs. V and VI remain the same.

Similar to Eq. (6.22) for pure QCD, the general RG evolution matrix $U(m_1,m_2,\alpha)$ from scale m_2 down to $m_1<m_2$ can be written formally as[5]

$$U(m_1,m_2,\alpha)\equiv T_g\exp\int_{g(m_2)}^{g(m_1)}dg'\,\frac{\gamma^T(g'^2,\alpha)}{\beta(g')}, \tag{7.19}$$

with $\gamma(g^2,\alpha)$ being now the full 10×10 anomalous-dimension matrix including QCD and QED contributions. $\beta(g)$ is defined in Eq. (3.6).

For the case at hand $\gamma(g^2,\alpha)$ can be expanded in the following way

$$\gamma(g^2,\alpha)=\gamma_s(g^2)+\frac{\alpha}{4\pi}\Gamma(g^2)+\cdots, \tag{7.20}$$

with the pure α_s expansion of $\gamma_s(g^2)$ given in Eq. (6.23). The term present due to QED corrections has the expansion

$$\Gamma(g^2)=\gamma_e^{(0)}+\frac{\alpha_s}{4\pi}\gamma_{se}^{(1)}+\cdots. \tag{7.21}$$

Using Eqs. (7.20) and (7.21), we may decompose the general RG evolution matrix $U(m_1,m_2,\alpha)$ of Eq. (7.19) as follows,

$$U(m_1,m_2,\alpha)=U(m_1,m_2)+\frac{\alpha}{4\pi}R(m_1,m_2). \tag{7.22}$$

Here $U(m_1,m_2)$ represents the pure QCD evolution already encountered in Sec. VI but now generalized to an extended operator basis. $R(m_1,m_2)$ describes the additional evolution in the presence of the electromagnetic interaction. $U(m_1,m_2)$ sums the logarithms $(\alpha_s t)^n$ and $\alpha_s(\alpha_s t)^n$ with $t=\ln(m_2^2/m_1^2)$, whereas $R(m_1,m_2)$ sums the logarithms $t(\alpha_s t)^n$ and $(\alpha_s t)^n$.

The formula for $U(m_1,m_2)$ has already been given in Eq. (6.24). The leading-order formula for $R(m_1,m_2)$ is given by Buchalla *et al.* (1990) except that a different overall normalization (a relative factor of -4π in R) has been used there. Here we give the general expression for $R(m_1,m_2)$ (Buras *et al.*, 1993b),

$$R(m_1,m_2)=\int_{g(m_2)}^{g(m_1)}dg'\,\frac{U(m_1,m')\Gamma^T(g')U(m',m_2)}{\beta(g')}\equiv-\frac{2\pi}{\beta_0}V\left(K^{(0)}(m_1,m_2)+\frac{1}{4\pi}\sum_{i=1}^{3}K_i^{(1)}(m_1,m_2)\right)V^{-1}, \tag{7.23}$$

with $g'\equiv g(m')$.

The matrix kernels in Eq. (7.23) are defined by

$$(K^{(0)}(m_1,m_2))_{ij}=\frac{M_{ij}^{(0)}}{a_i-a_j-1}\left[\left(\frac{\alpha_s(m_2)}{\alpha_s(m_1)}\right)^{a_j}\frac{1}{\alpha_s(m_1)}-\left(\frac{\alpha_s(m_2)}{\alpha_s(m_1)}\right)^{a_i}\frac{1}{\alpha_s(m_2)}\right], \tag{7.24}$$

$$(K_1^{(1)}(m_1,m_2))_{ij}=\begin{cases}\dfrac{M_{ij}^{(1)}}{a_i-a_j}\left[\left(\dfrac{\alpha_s(m_2)}{\alpha_s(m_1)}\right)^{a_j}-\left(\dfrac{\alpha_s(m_2)}{\alpha_s(m_1)}\right)^{a_i}\right], & i\neq j\\ M_{ii}^{(1)}\left(\dfrac{\alpha_s(m_2)}{\alpha_s(m_1)}\right)^{a_i}\ln\dfrac{\alpha_s(m_1)}{\alpha_s(m_2)}, & i=j,\end{cases} \tag{7.25}$$

$$K_2^{(1)}(m_1,m_2)=-\alpha_s(m_2)K^{(0)}(m_1,m_2)H, \tag{7.26}$$

[5]We neglect the running of the electromagnetic coupling α, which is a very good approximation (Buchalla *et al.*, 1990).

TABLE XIV. Rows 7–10 of the LO anomalous dimension matrix $\gamma_s^{(0)}$.

(i,j)	1	2	3	4	5	6	7	8	9	10
7	0	0	0	0	0	0	$\frac{6}{N}$	–6	0	0
8	0	0	$\frac{-2(u-d/2)}{3N}$	$\frac{2(u-d/2)}{3}$	$\frac{-2(u-d/2)}{3N}$	$\frac{2(u-d/2)}{3}$	0	$\frac{-6(-1+N^2)}{N}$	0	0
9	0	0	$\frac{2}{3N}$	$-\frac{2}{3}$	$\frac{2}{3N}$	$-\frac{2}{3}$	0	0	$\frac{-6}{N}$	6
10	0	0	$\frac{-2(u-d/2)}{3N}$	$\frac{2(u-d/2)}{3}$	$\frac{-2(u-d/2)}{3N}$	$\frac{2(u-d/2)}{3}$	0	0	6	$\frac{-6}{N}$

$$K_3^{(1)}(m_1,m_2)=\alpha_s(m_1)HK^{(0)}(m_1,m_2) \tag{7.27}$$

with

$$M^{(0)}=V^{-1}\gamma_e^{(0)T}V,$$

$$M^{(1)}=V^{-1}\left(\gamma_{se}^{(1)T}-\frac{\beta_1}{\beta_0}\gamma_e^{(0)T}+[\gamma_e^{(0)T},J]\right)V. \tag{7.28}$$

The matrix H is defined in Eq. (3.97) and β_0,β_1 are defined in Eq. (3.16).

After this formal description we now give explicit expressions for the 10×10 LO and NLO anomalous-dimension matrices $\gamma_s^{(0)}$, $\gamma_e^{(0)}$, $\gamma_s^{(1)}$, and $\gamma_{se}^{(1)}$. The values quoted for the NLO matrices are in the NDR scheme (Buras *et al.*, 1993; Buras *et al.*, 1993a; Ciuchini, Franco, Martinelli, and Reina, 1994). The corresponding results for $\gamma_s^{(1)}$ and $\gamma_{se}^{(1)}$ in the HV scheme can either be obtained by direct calculation or by using the QCD/QED version of Eq. (3.126) given in Buras *et al.* (1993a). They can be found in Buras *et al.* (1993), Buras *et al.* (1993a), Ciuchini *et al.* (1993a), and Ciuchini *et al.* (1994a).

The 6×6 submatrices for $Q_1,\ldots,Q_6$ of the full LO and NLO 10×10 QCD matrices $\gamma_s^{(0)}$ and $\gamma_s^{(1)}$ are identical to the corresponding 6×6 matrices already given in Eqs. (6.25) and (6.26), respectively. $Q_1,\ldots,Q_6$ do not mix to $Q_7,\ldots,Q_{10}$ under QCD, hence

$$[\gamma_s^{(0)}]_{ij}=[\gamma_s^{(1)}]_{ij}=0, \quad i=1,\ldots,6, \quad j=7,\ldots,10. \tag{7.29}$$

The remaining entries for rows 7–10 in $\gamma_s^{(0)}$ (Bijnens and Wise, 1984) and $\gamma_s^{(1)}$ (Buras *et al.*, 1993; Ciuchini, Franco, Martinelli, and Reina, 1994) are given in Tables XIV and XV, respectively. There u and $d(f=u+d)$ denote the number of active up- and down-type quark flavors.

The full 10×10 matrices $\gamma_e^{(0)}$ (Lusignoli, 1989) and $\gamma_{se}^{(1)}$ (Buras *et al.*, 1993a; Ciuchini, Franco, Martinelli, and Reina, 1994) can be found in Tables XVI and XVII, respectively.

TABLE XV. Rows 7–10 of the NLO anomalous dimension matrix $\gamma_s^{(1)}$ for N=3 and NDR.

(i,j)	1	2	3	4	5
7	0	0	$\frac{-61(u-d/2)}{9}$	$\frac{-11(u-d/2)}{3}$	$\frac{83(u-d/2)}{9}$
8	0	0	$\frac{-682(u-d/2)}{243}$	$\frac{106(u-d/2)}{81}$	$\frac{704(u-d/2)}{243}$
9	0	0	$\frac{202}{243}+\frac{73(u-d/2)}{9}$	$-\frac{1354}{81}-\frac{(u-d/2)}{3}$	$\frac{1192}{243}-\frac{71(u-d/2)}{9}$
10	0	0	$-\frac{79}{9}-\frac{106(u-d/2)}{243}$	$\frac{7}{3}+\frac{826(u-d/2)}{81}$	$\frac{65}{9}-\frac{502(u-d/2)}{243}$

(i,j)	6	7	8	9	10
7	$\frac{-11(u-d/2)}{3}$	$\frac{71}{3}-\frac{22f}{9}$	$-99+\frac{22f}{3}$	0	0
8	$\frac{736(u-d/2)}{81}$	$-\frac{225}{2}+4f$	$-\frac{1343}{6}+\frac{68f}{9}$	0	0
9	$-\frac{904}{81}-\frac{(u-d/2)}{3}$	0	0	$-\frac{21}{2}-\frac{2f}{9}$	$\frac{7}{2}+\frac{2f}{3}$
10	$\frac{7}{3}+\frac{646(u-d/2)}{81}$	0	0	$\frac{7}{2}+\frac{2f}{3}$	$-\frac{21}{2}-\frac{2f}{9}$

TABLE XVI. The LO anomalous dimension matrix $\gamma_e^{(0)}$.

(i,j)	1	2	3	4	5	6	7	8	9	10
1	$-\frac{8}{3}$	0	0	0	0	0	$\frac{16N}{27}$	0	$\frac{16N}{27}$	0
2	0	$-\frac{8}{3}$	0	0	0	0	$\frac{16}{27}$	0	$\frac{16}{27}$	0
3	0	0	0	0	0	0	$-\frac{16}{27}+\frac{16N(u-d/2)}{27}$	0	$-\frac{88}{27}+\frac{16N(u-d/2)}{27}$	0
4	0	0	0	0	0	0	$\frac{-16N}{27}+\frac{16(u-d/2)}{27}$	0	$\frac{-16N}{27}+\frac{16(u-d/2)}{27}$	$-\frac{8}{3}$
5	0	0	0	0	0	0	$\frac{8}{3}+\frac{16N(u-d/2)}{27}$	0	$\frac{16N(u-d/2)}{27}$	0
6	0	0	0	0	0	0	$\frac{16(u-d/2)}{27}$	$\frac{8}{3}$	$\frac{16(u-d/2)}{27}$	0
7	0	0	0	0	$\frac{4}{3}$	0	$\frac{4}{3}+\frac{16N(u+d/4)}{27}$	0	$\frac{16N(u+d/4)}{27}$	0
8	0	0	0	0	0	$\frac{4}{3}$	$\frac{16(u+d/4)}{27}$	$\frac{4}{3}$	$\frac{16(u+d/4)}{27}$	0
9	0	0	$-\frac{4}{3}$	0	0	0	$\frac{8}{27}+\frac{16N(u+d/4)}{27}$	0	$-\frac{28}{27}+\frac{16N(u+d/4)}{27}$	0
10	0	0	0	$-\frac{4}{3}$	0	0	$\frac{8N}{27}+\frac{16(u+d/4)}{27}$	0	$\frac{8N}{27}+\frac{16(u+d/4)}{27}$	$-\frac{4}{3}$

D. Quark-threshold matching matrix

Extending the matching matrix $M(m)$ of Eq. (6.27) to the simultaneous presence of QCD and QED corrections yields

$$M(m)=1+\frac{\alpha_s(m)}{4\pi}\,\delta r_s^T+\frac{\alpha}{4\pi}\,\delta r_e^T. \tag{7.30}$$

At scale $\mu=m_b$ the matrices δr_s and δr_e are

$$\delta r_s^T=\frac{5}{18}\,P(0,0,0,-2,0,-2,0,1,0,1), \tag{7.31}$$

$$\delta r_e^T=\frac{10}{81}\,\bar{P}(0,0,6,2,6,2,-3,-1,-3,-1), \tag{7.32}$$

and, at $\mu=m_c$,

$$\delta r_s^T=-\frac{5}{9}\,P(0,0,0,1,0,1,0,1,0,1), \tag{7.33}$$

$$\delta r_e^T=-\frac{40}{81}\,\bar{P}(0,0,3,1,3,1,3,1,3,1) \tag{7.34}$$

with Eq. (6.29) generalized to

$$P^T=(0,0,-\tfrac{1}{3},1,-\tfrac{1}{3},1,0,0,0,0), \tag{7.35}$$

$$\bar{P}^T=(0,0,0,0,0,0,1,0,1,0). \tag{7.36}$$

E. Numerical results for the $K\to\pi\pi$ Wilson coefficients

Tables XVIII–XX give the $\Delta S=1$ Wilson coefficients for $Q_1,\ldots,Q_{10}$ in the mixed case of QCD and QED. The coefficients for the current-current and QCD penguin operators $Q_1,\ldots,Q_6$ are only very weakly affected by the extension of the operator basis to the electroweak penguin operators $Q_7,\ldots,Q_{10}$. Therefore the discussion for $Q_1,\ldots,Q_6$ given in connection with Tables X–XII for the case of pure QCD basically still holds and will not be repeated here. For the remaining coefficients, $Q_7,\ldots,Q_{10}$, one finds a moderate scheme dependence for y_7, y_9, and y_{10}, but a $\mathcal{O}(9\%)$ one for y_8. The notable feature of $|y_6|$ being larger in NDR than in HV still holds, but it is now confronted with an exactly opposite dependence for the other important $\Delta S=1$ Wilson coefficient, y_8, which is enhanced over its LO value. The particular dependence of y_6 and y_8 with respect to scheme, LO/NLO, and m_t (see below) should be kept in mind for the later discussion of ε'/ε in Sec. XIX.

We also note that, in the range of m_t considered here, y_7 is very small, y_9 is essentially unaffected by NLO QCD corrections, and y_{10} is suppressed for $\mu\geqslant m_c$. It should also be stressed that $|y_9|$ and $|y_{10}|$ are substantially larger than $|y_8|$, although, as we will see in the analysis of ε'/ε, the operator Q_8 is more important than Q_9 and Q_{10} for this ratio. One infers from Tables XVIII–XX that also in the mixed QCD/QED case, the Wilson coefficients show a strong dependence on $\Lambda_{\overline{\rm MS}}$.

In contrast to the coefficients $y_3,\ldots,y_6$ for QCD penguins, $y_7,\ldots,y_{10}$ for the electroweak penguins show a sizable m_t dependence in the range $m_t=(170\pm15)$ GeV. With increasing/decreasing m_t there is a relative variation of $\mathcal{O}(\pm19\%)$ and $\mathcal{O}(\pm10\%)$ for the absolute values of y_8 and $y_{9,10}$, respectively. This is illustrated further in

TABLE XVII. The NLO anomalous dimension matrix $\gamma_{se}^{(1)}$ for $N=3$ and NDR.

(i,j)	1	2	3	4	5
1	$\frac{194}{9}$	$-\frac{2}{3}$	$-\frac{88}{243}$	$\frac{88}{81}$	$-\frac{88}{243}$
2	$\frac{25}{3}$	$-\frac{49}{9}$	$-\frac{556}{729}$	$\frac{556}{243}$	$-\frac{556}{729}$
3	0	0	$\frac{1690}{729}-\frac{136(u-d/2)}{243}$	$-\frac{1690}{243}+\frac{136(u-d/2)}{81}$	$\frac{232}{729}-\frac{136(u-d/2)}{243}$
4	0	0	$-\frac{641}{243}-\frac{388u}{729}+\frac{32d}{729}$	$-\frac{655}{81}+\frac{388u}{243}-\frac{32d}{243}$	$\frac{88}{243}-\frac{388u}{729}+\frac{32d}{729}$
5	0	0	$\frac{-136(u-d/2)}{243}$	$\frac{136(u-d/2)}{81}$	$-2-\frac{136(u-d/2)}{243}$
6	0	0	$\frac{-748u}{729}+\frac{212d}{729}$	$\frac{748u}{243}-\frac{212d}{243}$	$3-\frac{748u}{729}+\frac{212d}{729}$
7	0	0	$\frac{-136(u+d/4)}{243}$	$\frac{136(u+d/4)}{81}$	$-\frac{116}{9}-\frac{136(u+d/4)}{243}$
8	0	0	$\frac{-748u}{729}-\frac{106d}{729}$	$\frac{748u}{243}+\frac{106d}{243}$	$-1-\frac{748u}{729}-\frac{106d}{729}$
9	0	0	$\frac{7012}{729}-\frac{136(u+d/4)}{243}$	$\frac{764}{243}+\frac{136(u+d/4)}{81}$	$-\frac{116}{729}-\frac{136(u+d/4)}{243}$
10	0	0	$\frac{1333}{243}-\frac{388u}{729}-\frac{16d}{729}$	$\frac{107}{81}+\frac{388u}{243}+\frac{16d}{243}$	$-\frac{44}{243}-\frac{388u}{729}-\frac{16d}{729}$

(i,j)	6	7	8	9	10
1	$\frac{88}{81}$	$\frac{152}{27}$	$\frac{40}{9}$	$\frac{136}{27}$	$\frac{56}{9}$
2	$\frac{556}{243}$	$-\frac{484}{729}$	$-\frac{124}{27}$	$-\frac{3148}{729}$	$\frac{172}{27}$
3	$-\frac{232}{243}+\frac{136(u-d/2)}{81}$	$\frac{3136}{729}+\frac{104(u-d/2)}{27}$	$\frac{64}{27}+\frac{88(u-d/2)}{9}$	$\frac{20272}{729}+\frac{184(u-d/2)}{27}$	$-\frac{112}{27}+\frac{8(u-d/2)}{9}$
4	$-\frac{88}{81}+\frac{388u}{243}-\frac{32d}{243}$	$-\frac{152}{27}+\frac{3140u}{729}+\frac{656d}{729}$	$-\frac{40}{9}-\frac{100u}{27}-\frac{16d}{27}$	$\frac{170}{27}+\frac{908u}{729}+\frac{1232d}{729}$	$-\frac{14}{3}+\frac{148u}{27}-\frac{80d}{27}$
5	$6+\frac{136(u-d/2)}{81}$	$-\frac{232}{9}+\frac{104(u-d/2)}{27}$	$\frac{40}{3}+\frac{88(u-d/2)}{9}$	$\frac{184(u-d/2)}{27}$	$\frac{8(u-d/2)}{9}$
6	$7+\frac{748u}{243}-\frac{212d}{243}$	$-2-\frac{5212u}{729}+\frac{4832d}{729}$	$\frac{182}{9}+\frac{188u}{27}-\frac{160d}{27}$	$\frac{-2260u}{729}+\frac{2816d}{729}$	$\frac{-140u}{27}+\frac{64d}{27}$
7	$\frac{20}{3}+\frac{136(u+d/4)}{81}$	$-\frac{134}{9}+\frac{104(u+d/4)}{27}$	$\frac{38}{3}+\frac{88(u+d/4)}{9}$	$\frac{184(u+d/4)}{27}$	$\frac{8(u+d/4)}{9}$
8	$\frac{91}{9}+\frac{748u}{243}+\frac{106d}{243}$	$2-\frac{5212u}{729}-\frac{2416d}{729}$	$\frac{154}{9}+\frac{188u}{27}+\frac{80d}{27}$	$\frac{-2260u}{729}-\frac{1408d}{729}$	$\frac{-140u}{27}-\frac{32d}{27}$
9	$\frac{116}{243}+\frac{136(u+d/4)}{81}$	$-\frac{1568}{729}+\frac{104(u+d/4)}{27}$	$-\frac{32}{27}+\frac{88(u+d/4)}{9}$	$\frac{5578}{729}+\frac{184(u+d/4)}{27}$	$\frac{38}{27}+\frac{8(u+d/4)}{9}$
10	$\frac{44}{81}+\frac{388u}{243}+\frac{16d}{243}$	$\frac{76}{27}+\frac{3140u}{729}-\frac{328d}{729}$	$\frac{20}{9}-\frac{100u}{27}+\frac{8d}{27}$	$\frac{140}{27}+\frac{908u}{729}-\frac{616d}{729}$	$-\frac{28}{9}+\frac{148u}{27}+\frac{40d}{27}$

TABLE XVIII. $\Delta S=1$ Wilson coefficients at $\mu=1$ GeV for $m_t=170$ GeV. $y_1=y_2\equiv 0$.

	$\Lambda^{(4)}_{\overline{\rm MS}}=215$ MeV			$\Lambda^{(4)}_{\overline{\rm MS}}=325$ MeV			$\Lambda^{(4)}_{\overline{\rm MS}}=435$ MeV		
Scheme	LO	NDR	HV	LO	NDR	HV	LO	NDR	HV
z_1	−0.607	−0.409	−0.494	−0.748	−0.509	−0.640	−0.907	−0.625	−0.841
z_2	1.333	1.212	1.267	1.433	1.278	1.371	1.552	1.361	1.525
z_3	0.003	0.008	0.004	0.004	0.013	0.007	0.006	0.023	0.015
z_4	−0.008	−0.022	−0.010	−0.012	−0.035	−0.017	−0.017	−0.058	−0.029
z_5	0.003	0.006	0.003	0.004	0.008	0.004	0.005	0.009	0.005
z_6	−0.009	−0.022	−0.009	−0.013	−0.035	−0.014	−0.018	−0.059	−0.025
z_7/α	0.004	0.003	−0.003	0.008	0.011	−0.002	0.011	0.021	−0.001
z_8/α	0	0.008	0.006	0.001	0.014	0.010	0.001	0.027	0.017
z_9/α	0.005	0.007	0	0.008	0.018	0.005	0.012	0.034	0.011
z_{10}/α	0	−0.005	−0.006	−0.001	−0.008	−0.010	−0.001	−0.014	−0.017
y_3	0.030	0.025	0.028	0.038	0.032	0.037	0.047	0.042	0.050
y_4	−0.052	−0.048	−0.050	−0.061	−0.058	−0.061	−0.071	−0.068	−0.074
y_5	0.012	0.005	0.013	0.013	−0.001	0.016	0.014	−0.013	0.021
y_6	−0.085	−0.078	−0.071	−0.113	−0.111	−0.097	−0.148	−0.169	−0.139
y_7/α	0.027	−0.033	−0.032	0.036	−0.032	−0.030	0.043	−0.031	−0.027
y_8/α	0.114	0.121	0.133	0.158	0.173	0.188	0.216	0.254	0.275
y_9/α	−1.491	−1.479	−1.480	−1.585	−1.576	−1.577	−1.700	−1.718	−1.722
y_{10}/α	0.650	0.540	0.547	0.800	0.690	0.699	0.968	0.892	0.906

TABLE XIX. $\Delta S=1$ Wilson coefficients at $\mu=m_c=1.3$ GeV for $m_t=170$ GeV and $f=3$ effective flavors. $|z_3|,\ldots,|z_{10}|$ are numerically irrelevant relative to $|z_{1,2}|$. $y_1=y_2\equiv 0$.

	$\Lambda^{(4)}_{\overline{\rm MS}}=215$ MeV			$\Lambda^{(4)}_{\overline{\rm MS}}=325$ MeV			$\Lambda^{(4)}_{\overline{\rm MS}}=435$ MeV		
Scheme	LO	NDR	HV	LO	NDR	HV	LO	NDR	HV
z_1	−0.521	−0.346	−0.413	−0.625	−0.415	−0.507	−0.732	−0.490	−0.617
z_2	1.275	1.172	1.214	1.345	1.216	1.276	1.420	1.265	1.354
y_3	0.027	0.023	0.025	0.034	0.029	0.033	0.041	0.036	0.042
y_4	−0.051	−0.048	−0.049	−0.061	−0.057	−0.060	−0.070	−0.068	−0.072
y_5	0.013	0.007	0.014	0.015	0.005	0.016	0.017	0.001	0.018
y_6	−0.076	−0.068	−0.063	−0.096	−0.089	−0.081	−0.120	−0.118	−0.103
y_7/α	0.030	−0.031	−0.031	0.039	−0.030	−0.028	0.048	−0.029	−0.026
y_8/α	0.092	0.103	0.112	0.121	0.136	0.145	0.155	0.179	0.189
y_9/α	−1.428	−1.423	−1.423	−1.490	−1.479	−1.479	−1.559	−1.548	−1.549
y_{10}/α	0.558	0.451	0.457	0.668	0.547	0.553	0.781	0.656	0.664

TABLE XX. $\Delta S=1$ Wilson coefficients at $\mu=2$ GeV for $m_t=170$ GeV. For $\mu>m_c$ the GIM mechanism gives $z_i\equiv 0$, $i=3,\ldots,10$. $y_1=y_2\equiv 0$.

	$\Lambda^{(4)}_{\overline{\rm MS}}=215$ MeV			$\Lambda^{(4)}_{\overline{\rm MS}}=325$ MeV			$\Lambda^{(4)}_{\overline{\rm MS}}=435$ MeV		
Scheme	LO	NDR	HV	LO	NDR	HV	LO	NDR	HV
z_1	−0.413	−0.268	−0.320	−0.480	−0.310	−0.376	−0.544	−0.352	−0.432
z_2	1.206	1.127	1.157	1.248	1.151	1.191	1.290	1.176	1.227
y_3	0.021	0.020	0.019	0.025	0.024	0.023	0.028	0.028	0.027
y_4	−0.041	−0.046	−0.040	−0.047	−0.055	−0.046	−0.053	−0.063	−0.053
y_5	0.011	0.010	0.012	0.012	0.011	0.013	0.014	0.011	0.015
y_6	−0.056	−0.058	−0.047	−0.068	−0.071	−0.057	−0.079	−0.086	−0.068
y_7/α	0.031	−0.023	−0.020	0.037	−0.019	−0.020	0.042	−0.016	−0.019
y_8/α	0.068	0.076	0.084	0.084	0.094	0.102	0.101	0.113	0.121
y_9/α	−1.357	−1.361	−1.357	−1.393	−1.389	−1.389	−1.430	−1.419	−1.423
y_{10}/α	0.442	0.356	0.360	0.513	0.414	0.419	0.581	0.472	0.477

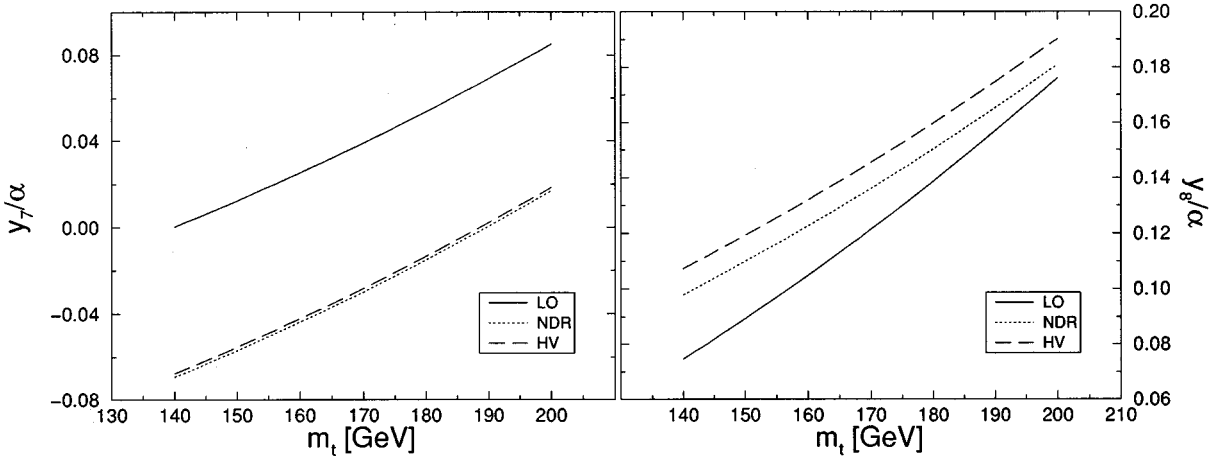

FIG. 5. Wilson coefficients $y_7(m_c)/\alpha$ and $y_8(m_c)/\alpha$ as functions of m_t for $\Lambda_{\overline{\rm MS}}^{(4)}=325$ MeV.

Figs. 5 and 6, where the m_t dependence of these coefficients is shown explicitly. This strong m_t dependence originates in the Z^0 penguin diagrams. The m_t dependence of y_9 and y_{10} can be conveniently parametrized by a linear function to an accuracy better than 0.5%. Details of this m_t parametrization can be found in Table XXI. Strictly speaking the m_t dependence is a NLO effect and could in principle be neglected when working at leading order. Here we have, however, chosen to keep this nontrivial m_t dependence in the Wilson-coefficient functions also at LO for the sake of comparison with the NLO results.

Finally, in Tables XVIII–XX one observes again the usual feature of decreasing Wilson coefficients with increasing scale μ.

F. The $\Delta B=1$ effective Hamiltonian including electroweak penguins

Finally we present the Wilson coefficient functions of the $\Delta B=1$, $\Delta C=0$ Hamiltonian, including the effects of electroweak penguin contributions (Buras *et al.*, 1993b). These effects play a role in certain penguin-induced B-meson decays as discussed by Fleischer (1994a,b), Deshpande *et al.* (1995), and Deshpande and He (1995).

The generalization of the $\Delta B=1$, $\Delta C=0$ Hamiltonian in pure QCD (Eq. 6.32) to incorporate electroweak penguin operators is straightforward. One obtains

$$\mathcal{H}_{\rm eff}(\Delta B=1)=\frac{G_F}{\sqrt{2}}\left\{\xi_c[C_1(\mu)Q_1^c(\mu)+C_2(\mu)Q_2^c(\mu)]+\xi_u[C_1(\mu)Q_1^u(\mu)+C_2(\mu)Q_2^u(\mu)]-\xi_t\sum_{i=3}^{10}C_i(\mu)Q_i(\mu)\right\},\tag{7.37}$$

where the operator basis now includes the electroweak penguin operators

$$Q_7=\frac{3}{2}(\bar{b}d)_{V-A}\sum_q e_q(\bar{q}q)_{V+A},\tag{7.38}$$

$$Q_8=\frac{3}{2}(\bar{b}_i d_j)_{V-A}\sum_q e_q(\bar{q}_j q_i)_{V+A},$$

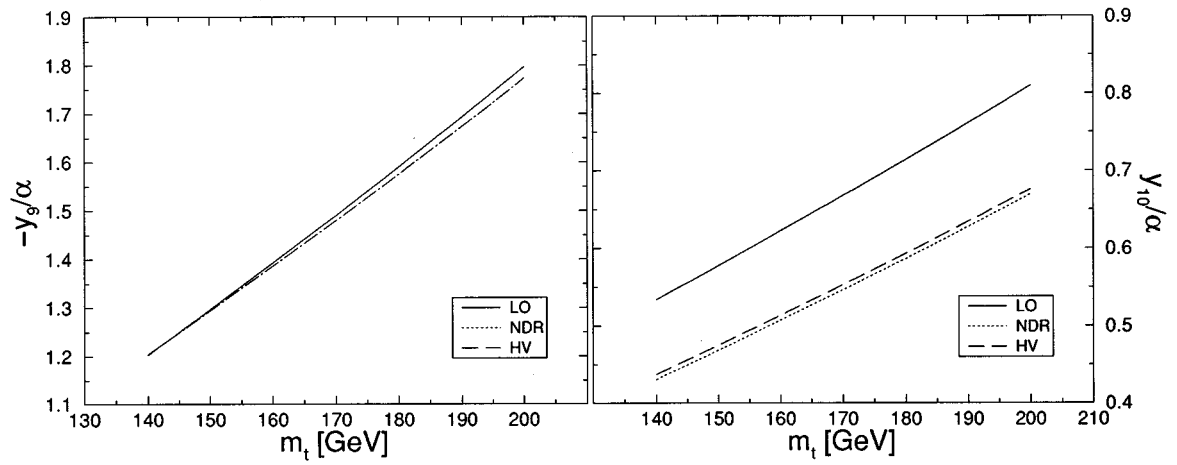

FIG. 6. Wilson coefficients $y_9(m_c)/\alpha$ and $y_{10}(m_c)/\alpha$ as a function of m_t for $\Lambda_{\overline{\rm MS}}^{(4)}=325$ MeV.

TABLE XXI. Coefficients in linear m_t parametrization $y_i/\alpha = a + b\cdot(m_t/170\ \text{GeV})$ of Wilson coefficients y_9/α and y_{10}/α at scale $\mu = m_c$ for $\Lambda^{(4)}_{\overline{\text{MS}}} = 325$ MeV.

	y_9/α		y_{10}/α	
	a	b	a	b
LO	0.189	−1.682	−0.111	0.780
NDR	0.129	−1.611	−0.128	0.676
HV	0.129	−1.611	−0.121	0.676

$$Q_9 = \frac{3}{2}(\bar{b}d)_{V-A}\sum_q e_q(\bar{q}q)_{V-A},$$

$$Q_{10} = \frac{3}{2}(\bar{b}_i d_j)_{V-A}\sum_q e_q(\bar{q}_j q_i)_{V-A}$$

in addition to Eq. (6.33). The Wilson coefficients at $\mu = m_b$ read

$$\vec{C}(m_b) = U_5(m_b, M_W, \alpha)\vec{C}(M_W), \tag{7.39}$$

where U_5 is the 10×10 evolution matrix of Eq. (7.22) for $f=5$ flavors. The $\vec{C}(M_W)$ are given in Eqs. (7.3)–(7.12) in the NDR scheme.

G. Numerical results for the $\Delta B = 1$ Wilson coefficients

Table XXII lists the $\Delta B=1$ Wilson coefficients for $Q_1^{u,c}, Q_2^{u,c}, Q_3, \ldots, Q_{10}$ in the mixed case of QCD and QED. Similar to the $\Delta S=1$ case, the coefficients for the current-current and QCD penguin operators $Q_1,\ldots,Q_6$ are only very weakly affected by the extension of the operator basis to the electroweak penguin operators $Q_7,\ldots,Q_{10}$. Therefore the discussion of $C_1,\ldots,C_6$ in connection with Table XIII is also valid for the present case. Here we therefore we restrict the discussion to the coefficients $C_7,\ldots,C_{10}$ of the operators $Q_7,\ldots,Q_{10}$ in the extended basis.

The coefficients $C_7,\ldots,C_{10}$ show a visible dependence on the scheme, $\Lambda_{\overline{\text{MS}}}$, and LO/NLO. However, this dependence is less pronounced for the coefficient C_9 than it is for $C_{7,8,10}$. This is noteworthy since in B-meson decays C_9 usually resides in the dominant electroweak-penguin contribution (Fleischer, 1994a,b; Deshpande *et al.*, 1995; Deshpande and He, 1995). In contrast to $C_1,\ldots,C_6$, the additional coefficients $C_7,\ldots,C_{10}$ show a nonnegligible m_t dependence in the range $m_t=(170\pm 15)$ GeV. With increasing/decreasing m_t there is, similar to the $\Delta S=1$ case, a relative variation of $\mathcal{O}(\pm 19\%)$ and $\mathcal{O}(\pm 10\%)$ for the absolute values of C_8 and $C_{9,10}$, respectively.

Since the coefficients C_9 and C_{10} play an important role in B decays, in Fig. 7 we show their m_t dependence explicitly. Again the m_t dependence can be parametrized by a linear function to an accuracy better than 0.5%. Details of the m_t parametrization are given in Table XXIII.

VIII. THE EFFECTIVE HAMILTONIAN FOR $K_L \to \pi^0 e^+ e^-$

The $\Delta S=1$ effective Hamiltonian for $K_L \to \pi^0 e^+ e^-$ at scales $\mu < m_c$ is given by

$$\mathcal{H}_{\text{eff}}(\Delta S=1) = \frac{G_F}{\sqrt{2}} V_{us}^* V_{ud}\left[\sum_{i=1}^{6,7V}(z_i(\mu)+\tau\, y_i(\mu))Q_i(\mu) + \tau\, y_{7A}(M_W)Q_{7A}(M_W)\right] \tag{8.1}$$

with

$$\tau = -\frac{V_{ts}^* V_{td}}{V_{us}^* V_{ud}}. \tag{8.2}$$

A. Operators

In Eq. (8.1) $Q_{1,2}$ denote the $\Delta S=1$ current-current and $Q_3,\ldots,Q_6$ the QCD penguin operators of Eq. (6.3). For scales $\mu > m_c$, again, the current-current operators $Q^c_{1,2}$ of Eq. (6.4) have to be taken into account.

The new operators specific to the decay $K_L \to \pi^0 e^+ e^-$ are

$$Q_{7V} = (\bar{s}d)_{V-A}(\bar{e}e)_V, \tag{8.3}$$

$$Q_{7A} = (\bar{s}d)_{V-A}(\bar{e}e)_A. \tag{8.4}$$

TABLE XXII. $\Delta B=1$ Wilson coefficients at $\mu = \bar{m}_b(m_b) = 4.40$ GeV for $m_t = 170$ GeV.

	$\Lambda^{(5)}_{\overline{\text{MS}}} = 140$ MeV			$\Lambda^{(5)}_{\overline{\text{MS}}} = 225$ MeV			$\Lambda^{(5)}_{\overline{\text{MS}}} = 310$ MeV		
Scheme	LO	NDR	HV	LO	NDR	HV	LO	NDR	HV
C_1	−0.273	−0.165	−0.202	−0.308	−0.185	−0.228	−0.339	−0.203	−0.251
C_2	1.125	1.072	1.091	1.144	1.082	1.105	1.161	1.092	1.117
C_3	0.013	0.013	0.012	0.014	0.014	0.013	0.016	0.016	0.015
C_4	−0.027	−0.031	−0.026	−0.030	−0.035	−0.029	−0.033	−0.039	−0.033
C_5	0.008	0.008	0.008	0.009	0.009	0.009	0.009	0.009	0.010
C_6	−0.033	−0.036	−0.029	−0.038	−0.041	−0.033	−0.043	−0.046	−0.037
C_7/α	0.042	−0.003	0.006	0.045	−0.002	0.005	0.047	−0.001	0.005
C_8/α	0.041	0.047	0.052	0.048	0.054	0.060	0.054	0.061	0.067
C_9/α	−1.264	−1.279	−1.269	−1.280	−1.292	−1.283	−1.294	−1.303	−1.296
C_{10}/α	0.291	0.234	0.237	0.328	0.263	0.266	0.360	0.288	0.291

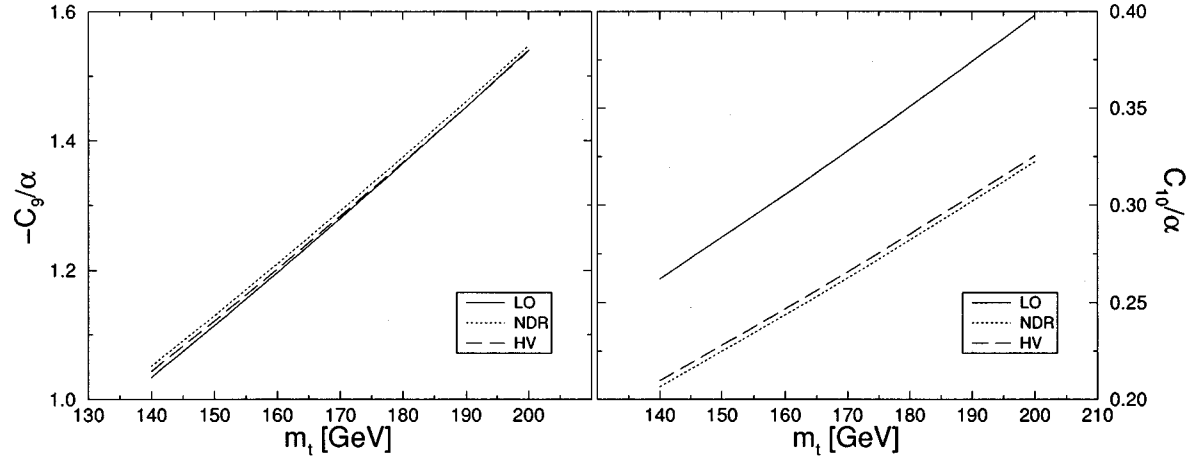

FIG. 7. Wilson coefficients C_9/α and C_{10}/α at $\mu=\bar{m}_b(m_b)=4.40$ GeV as a function of m_t for $\Lambda^{(5)}_{\overline{\rm MS}}=225$ MeV.

They originate through the γ and Z^0 penguin and box diagrams of Fig. 2.

It is convenient to introduce the auxiliary operator

$$Q'_{7V}=(\alpha/\alpha_s)(\bar{s}d)_{V-A}(\bar{e}e)_V \tag{8.5}$$

and to work in the basis $Q_1,\ldots,Q_6$, Q'_{7V} for the renormalization-group analysis. The factor α/α_s in the definition of Q'_{7V} implies that, in this new basis, the anomalous-dimension matrix γ will be a function of α_s alone. At the end of the renormalization-group analysis, this factor will be put back into the Wilson coefficient $C_{7V}(\mu)$ of the operator Q_{7V} in Eq. (8.3). There is no need to include a similar factor in Q_{7A}, as this operator does not mix under renormalization with the remaining operators. Since Q_{7A} has no anomalous dimension its Wilson coefficient is μ independent.

In principle one can think of including the electroweak four-quark penguin operators $Q_7,\ldots,Q_{10}$ of Eq. (7.2) in $\mathcal{H}_{\rm eff}$ of Eq. (8.1). However, their Wilson coefficients and matrix elements for the decay $K_L\to\pi^0e^+e^-$ are both of order $\mathcal{O}(\alpha)$, which implies that these operators eventually would enter the amplitude $A(K_L\to\pi^0e^+e^-)$ at $\mathcal{O}(\alpha^2)$. To the order considered here this contribution is thus negligible. This should be distinguished from the case of $K\to\pi\pi$ discussed in Sec. VII. There, in spite of being suppressed by α/α_s relative to QCD penguin operators, the electroweak penguin operators have to be included in the analysis because of the additional enhancement factor, ${\rm Re}A_0/{\rm Re}A_2\simeq 22$, present in the formula for ε'/ε (see Sec. XIX). Such an enhancement factor is not present in the $K_L\to\pi^0e^+e^-$ case, and the electroweak penguin operators can be safely neglected.

Through mixing under renormalization, the coefficients $C_3,\ldots,C_6$ at $\mathcal{O}(\alpha)$ and C_{7V} at $\mathcal{O}(\alpha^2)$ are affected by the electroweak four-quark penguin operators. Since the corresponding matrix elements are $\mathcal{O}(\alpha)$ and $\mathcal{O}(1)$, respectively, we again obtain a negligible $\mathcal{O}(\alpha^2)$ effect in $A(K_L\to\pi^0e^+e^-)$. In summary, the electroweak four-quark penguin operators $Q_7,\ldots,Q_{10}$ can safely be neglected in the following discussion of $\mathcal{H}_{\rm eff}(\Delta S=1)$ for $K_L\to\pi^0e^+e^-$.

We also neglect the "magnetic moment" operators. These operators, being of dimension five, do not influence the Wilson coefficients of the operators $Q_1,\ldots,Q_6$, Q_{7V}, Q_{7A}. Since their contributions to $K_L\to\pi^0e^+e^-$ are suppressed by an additional factor m_s, strictly speaking they appear at higher order in chiral perturbation theory. On the other hand, the magnetic-moment-type operators play a crucial role in $b\to s\gamma$ and $b\to d\gamma$ transitions, as discussed in Secs. IX and XXII. They also have to be kept in the decay $B\to X_se^+e^-$.

TABLE XXIII. Coefficients in linear m_t parametrization $C_i/\alpha=a+b$ $(m_t/170$ GeV) of Wilson coefficients C_9/α and C_{10}/α at scale $\mu=m_b=4.4$ GeV for $\Lambda^{(5)}_{\overline{\rm MS}}=225$ MeV.

	C_9/α		C_{10}/α	
	a	b	a	b
LO	0.152	−1.434	−0.056	0.385
NDR	0.109	−1.403	−0.065	0.328
HV	0.117	−1.403	−0.062	0.328

B. Wilson coefficients

Equations (6.6)–(6.8) remain valid in the case of $K_L\to\pi^0e^+e^-$ with $U_f(m_1,m_2)$ and $M(m_i)$ now denoting 7×7 matrices in the $Q_1,\ldots,Q_6,Q'_{7V}$ basis. The Wilson coefficients are given by seven-dimensional column vectors $\vec{z}(\mu)$ and $\vec{v}(\mu)$ having components $(z_1,\ldots,z_6,z'_{7V})$ and $(v_1,\ldots,v_6,v'_{7V})$, respectively. Here

$$v'_{7V}(\mu)=\frac{\alpha_s(\mu)}{\alpha}\,v_{7V}(\mu),\quad z'_{7V}(\mu)=\frac{\alpha_s(\mu)}{\alpha}\,z_{7V}(\mu) \tag{8.6}$$

are the rescaled Wilson coefficients of the auxiliary operator Q'_{7V} used in the renormalization-group evolution.

The initial conditions $C_1(M_W),\ldots,C_6(M_W)$, $z_1(M_W)$, $z_2(M_W)$ and $z_1(m_c),\ldots,z_6(m_c)$ for the four-quark operators $Q_1,\ldots,Q_6$ are readily obtained from Eqs. (6.9)–(6.14), (6.18), and (6.20).

The corresponding initial conditions for the remaining operators Q'_{7V} and Q_{7A} specific to $K_L\to\pi^0e^+e^-$ are then given in the NDR scheme by

$$C'_{7V}(M_W)=\frac{\alpha_s(M_W)}{2\pi}\left[\frac{C_0(x_t)-B_0(x_t)}{\sin^2\theta_W}-\tilde{D}_0(x_t)-4C_0(x_t)\right] \tag{8.7}$$

and

$$C_{7A}(M_W)=y_{7A}(M_W)=\frac{\alpha}{2\pi}\frac{B_0(x_t)-C_0(x_t)}{\sin^2\theta_W}. \tag{8.8}$$

In order to find $z'_{7V}(m_c)$, which results from the diagrams of Fig. 3, we simply have to rescale the NDR result for $z_7(m_c)$ in Eq. (7.17) by a factor of $-3\alpha_s/\alpha$. This yields

$$z'_{7V}(m_c)=-\frac{\alpha_s(m_c)}{2\pi}F_e(m_c). \tag{8.9}$$

C. Renormalization-group evolution and anomalous-dimension matrices

In the rescaled basis $Q_1,\ldots,Q_6,Q'_{7V}$, the anomalous-dimension matrix γ has, per construction, a pure $\mathcal{O}(\alpha_s)$ expansion

$$\gamma=\frac{\alpha_s}{4\pi}\gamma^{(0)}+\frac{\alpha_s^2}{(4\pi)^2}\gamma^{(1)}+\cdots, \tag{8.10}$$

where $\gamma^{(0)}$ and $\gamma^{(1)}$ are 7×7 matrices. The evolution matrices $U_f(m_1,m_2)$ in Eqs. (6.7) and (6.8) are, for the present case, simply given by Eqs. (6.24) and (3.94)–(3.98).

The 6×6 submatrix of $\gamma^{(0)}$ involving the operators $Q_1,\ldots,Q_6$ has already been given in Eq. (6.25). Here we only give the remaining entries of $\gamma^{(0)}$ related to the additional presence of the operator Q'_{7V}

$$\gamma^{(0)}_{17}=-\frac{16}{9}N,\quad \gamma^{(0)}_{27}=-\frac{16}{9},$$

$$\gamma^{(0)}_{37}=-\frac{16}{9}N\left(u-\frac{d}{2}-\frac{1}{N}\right),\quad \gamma^{(0)}_{47}=-\frac{16}{9}\left(u-\frac{d}{2}-N\right),$$

$$\gamma^{(0)}_{57}=-\frac{16}{9}N\left(u-\frac{d}{2}\right),\quad \gamma^{(0)}_{67}=-\frac{16}{9}\left(u-\frac{d}{2}\right),$$

$$\gamma^{(0)}_{77}=-2\beta_0=-\frac{22}{3}N+\frac{4}{3}f,\quad \gamma^{(0)}_{7i}=0\quad i=1,\ldots,6, \tag{8.11}$$

where N denotes the number of colors. These elements have been first calculated by Gilman and Wise (1980), except that $\gamma^{(0)}_{37}$ and $\gamma^{(0)}_{47}$ have been corrected by Eeg and Picek (1988) and Flynn and Randall (1989a).

The 6×6 submatrix of $\gamma^{(1)}$ involving the operators $Q_1,\ldots,Q_6$ has already been presented as $\gamma^{(1)}_s$ in Eq. (6.26), and the seventh column of $\gamma^{(1)}$ is given as follows in the NDR scheme (Buras *et al.*, 1994a),

$$\gamma^{(1)}_{17}=\frac{8}{3}(1-N^2), \tag{8.12}$$

$$\gamma^{(1)}_{27}=\frac{200}{81}\left(N-\frac{1}{N}\right),$$

$$\gamma^{(1)}_{37}=\frac{8}{3}\left(u-\frac{d}{2}\right)(1-N^2)+\frac{464}{81}\left(\frac{1}{N}-N\right),$$

$$\gamma^{(1)}_{47}=\left(u\,\frac{280}{81}+d\,\frac{64}{81}\right)\left(\frac{1}{N}-N\right)+\frac{8}{3}(N^2-1),$$

$$\gamma^{(1)}_{57}=\frac{8}{3}\left(u-\frac{d}{2}\right)(1-N^2),$$

$$\gamma^{(1)}_{67}=\left(u\,\frac{440}{81}-d\,\frac{424}{81}\right)\left(N-\frac{1}{N}\right),$$

$$\gamma^{(1)}_{77}=-2\beta_1=-\frac{68}{3}N^2+\frac{20}{3}Nf+4C_Ff,$$

$$\gamma^{(1)}_{7i}=0,\quad i=1,\ldots,6,$$

where $C_F=(N^2-1)/(2N)$. The corresponding results in the HV scheme are given by Buras *et al.* (1994a).

D. Quark-threshold matching matrix

For the case of $K_L\to\pi^0e^+e^-$ the matching matrix $M(m)$ in the basis $Q_1,\ldots,Q_6,Q'_{7V}$ has the form

$$M(m)=1+\frac{\alpha_s(m)}{4\pi}\delta r_s^T, \tag{8.13}$$

where 1 and δr_s^T are 7×7 matrices and m is the scale of the quark threshold.

The 6×6 submatrix of $M(m)$ involving $Q_1,\ldots,Q_6$ has been given in Eq. (6.28). The remaining entries of δr_s can be found from the matrix δr_e given in Eqs. (7.32) and (7.34) by making a simple rescaling by $-3\alpha_s/\alpha$, as in the case of $z_7(m_c)$.

In summary, for the quark threshold $m=m_b$, the matrix δr_s is

$$\delta r_s=\begin{pmatrix}
0 & 0 & 0 & 0 & 0 & 0 & 0\\
0 & 0 & 0 & 0 & 0 & 0 & 0\\
0 & 0 & 0 & 0 & 0 & 0 & -\frac{20}{9}\\
0 & 0 & \frac{5}{27} & -\frac{5}{9} & \frac{5}{27} & -\frac{5}{9} & -\frac{20}{27}\\
0 & 0 & 0 & 0 & 0 & 0 & -\frac{20}{9}\\
0 & 0 & \frac{5}{27} & -\frac{5}{9} & \frac{5}{27} & -\frac{5}{9} & -\frac{20}{27}\\
0 & 0 & 0 & 0 & 0 & 0 & 0
\end{pmatrix}. \tag{8.14}$$

TABLE XXIV. $K_L\to\pi^0e^+e^-$ Wilson coefficients for $Q_{7V,A}$ at μ=1 GeV for m_t=170 GeV. The corresponding coefficients for $Q_1,\ldots,Q_6$ can be found in Table X.

	$\Lambda^{(4)}_{\overline{\rm MS}}$=215 MeV			$\Lambda^{(4)}_{\overline{\rm MS}}$=325 MeV			$\Lambda^{(4)}_{\overline{\rm MS}}$=435 MeV		
Scheme	LO	NDR	HV	LO	NDR	HV	LO	NDR	HV
z_{7V}/α	–0.014	–0.015	0.005	–0.024	–0.046	–0.003	–0.035	–0.084	–0.011
y_{7V}/α	0.575	0.747	0.740	0.540	0.735	0.725	0.509	0.720	0.710
y_{7A}/α	–0.700	–0.700	–0.700	–0.700	–0.700	–0.700	–0.700	–0.700	–0.700

For $m=m_c$ the seventh column of δr_s in Eq. (8.14) has to be multiplied by –2.

E. Numerical results for the $K_L\to\pi^0e^+e^-$ Wilson coefficients

In the case of $K_L\to\pi^0e^+e^-$, for which $\gamma^{(0)}_{7i}=\gamma^{(1)}_{7i}=0$, i=1, . . . ,6, in Eqs. (8.11) and (8.12), respectively, the RG evolution of $Q_1,\ldots,Q_6$ is completely unaffected by the additional presence of the operator Q_{7V}. The $K_L\to\pi^0e^+e^-$ Wilson coefficients z_i and y_i, i=1, . . . ,6, with μ=1 GeV can therefore be found in Table X of Sec. VI.

The $K_L\to\pi^0e^+e^-$ Wilson coefficients for the remaining operators Q_{7V} and Q_{7A} are given in Table XXIV. Some insight into the analytic structure of y_{7V} will be gained by studying the analogous decay $B\to X_se^+e^-$ in Sec. X and also in Sec. XXI, where the phenomenology of $K_L\to\pi^0e^+e^-$ will be presented.

In Table XXV we show the μ dependence of z_{7V}/α and y_{7V}/α. We find a pronounced scheme dependence and μ dependence for z_{7V}. This signals that these dependences have to be carefully addressed in the calculation of the CP-conserving part in the $K_L\to\pi^0e^+e^-$ amplitude. On the other hand, the scheme and μ dependences for y_{7V} are below $\mathcal{O}$(1.5%). Similarly, z_{7V} shows a strong dependence on the choice of the QCD scale $\Lambda_{\overline{\rm MS}}$, while this dependence is small or absent for y_{7V} and y_{7A}, respectively.

Finally, as seen from Eq. (8.9), z_{7V} is independent of m_t. However, with increasing/decreasing m_t in the range m_t=(170±15) GeV, there is a relative variation of $\mathcal{O}(\pm3\%)$ and $\mathcal{O}(\pm14\%)$ for the absolute values of y_{7V} and y_{7A}, respectively. This is illustrated further in Fig. 8 and Table XXVI, where the m_t dependence of these coefficients is shown explicitly. Accidentally, for $m_t\approx175$ GeV one finds $|y_{7V}|\approx|y_{7A}|$. Most importantly, the impact of NLO corrections is to enhance the Wilson coefficient y_{7V} by roughly 25%. As we will see in Sec. XXI, this implies an enhancement of the direct CP violation in $K_L\to\pi^0e^+e^-$.

IX. THE EFFECTIVE HAMILTONIAN FOR $B\to X_s\gamma$

The effective Hamiltonian for $B\to X_s\gamma$ at scales $\mu=\mathcal{O}(m_b)$ is given by

$$\mathcal{H}_{\rm eff}(b\to s\gamma) = -\frac{G_F}{\sqrt{2}}V^*_{ts}V_{tb}\left[\sum_{i=1}^{6}C_i(\mu)Q_i(\mu)+C_{7\gamma}(\mu)Q_{7\gamma}(\mu)+C_{8G}(\mu)Q_{8G}(\mu)\right], \tag{9.1}$$

where, in view of $|V^*_{us}V_{ub}/V^*_{ts}V_{tb}|<0.02$, we have neglected the term proportional to $V^*_{us}V_{ub}$.

A. Operators

The complete list of operators is given as follows

$$Q_1=(\bar s_ic_j)_{V-A}(\bar c_jb_i)_{V-A}, \tag{9.2}$$
$$Q_2=(\bar sc)_{V-A}(\bar cb)_{V-A},$$

TABLE XXV. $K_L\to\pi^0e^+e^-$ Wilson coefficients z_{7V}/α and y_{7V}/α for m_t=170 GeV and various values of μ.

	$\Lambda^{(4)}_{\overline{\rm MS}}$=215 MeV			$\Lambda^{(4)}_{\overline{\rm MS}}$=325 MeV			$\Lambda^{(4)}_{\overline{\rm MS}}$=435 MeV		
Scheme	LO	NDR	HV	LO	NDR	HV	LO	NDR	HV
μ [GeV]					z_{7V}/α				
0.8	–0.031	–0.029	0.004	–0.053	–0.081	–0.012	–0.077	–0.149	–0.023
1.0	–0.014	–0.015	0.005	–0.024	–0.046	–0.003	–0.035	–0.084	–0.011
1.2	–0.004	–0.009	0.002	–0.006	–0.029	0	–0.009	–0.051	–0.002
μ [GeV]					y_{7V}/α				
0.8	0.578	0.751	0.744	0.545	0.739	0.730	0.514	0.722	0.712
1.0	0.575	0.747	0.740	0.540	0.735	0.725	0.509	0.720	0.710
1.2	0.571	0.744	0.736	0.537	0.731	0.721	0.505	0.716	0.706

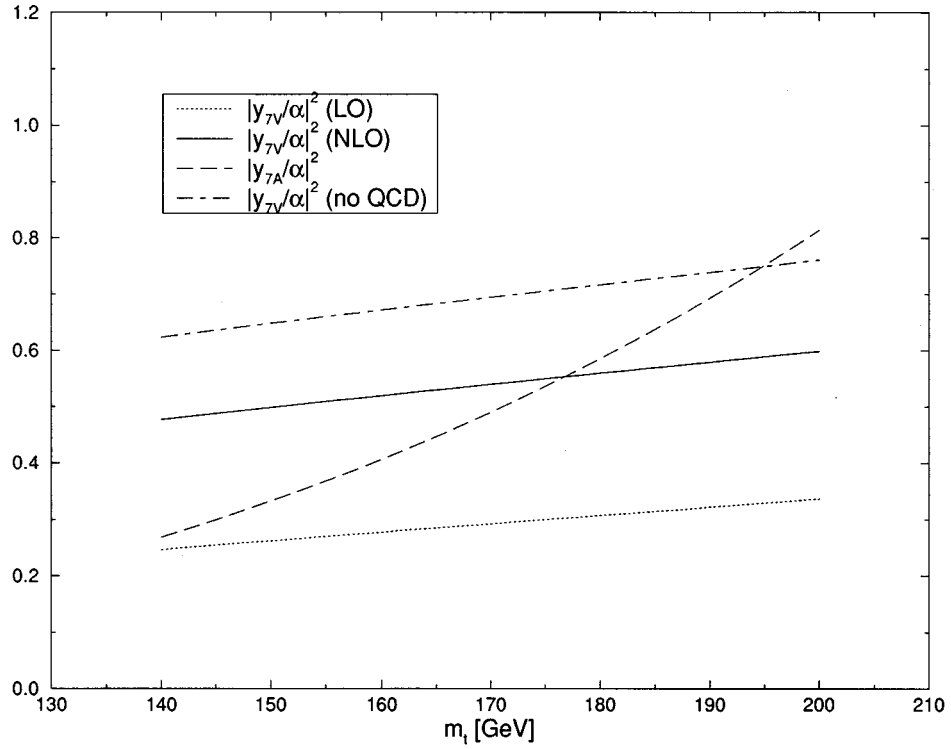

FIG. 8. Wilson coefficients $|y_{7V}/\alpha|^2$ and $|y_{7A}/\alpha|^2$ as a function of m_t for $\Lambda^{(4)}_{\overline{\rm MS}}=325$ MeV at scale $\mu=1.0$ GeV.

$$Q_3=(\bar{s}b)_{V-A}\sum_q (\bar{q}q)_{V-A},$$

$$Q_4=(\bar{s}_i b_j)_{V-A}\sum_q (\bar{q}_j q_i)_{V-A},$$

$$Q_5=(\bar{s}b)_{V-A}\sum_q (\bar{q}q)_{V+A},$$

$$Q_6=(\bar{s}_i b_j)_{V-A}\sum_q (\bar{q}_j q_i)_{V+A},$$

$$Q_{7\gamma}=\frac{e}{8\pi^2} m_b \bar{s}_i \sigma^{\mu\nu}(1+\gamma_5) b_i F_{\mu\nu},$$

$$Q_{8G}=\frac{g}{8\pi^2} m_b \bar{s}_i \sigma^{\mu\nu}(1+\gamma_5) T^a_{ij} b_j G^a_{\mu\nu}.$$

The current-current operators $Q_{1,2}$ and the QCD penguin operators $Q_3,\ldots,Q_6$ are already contained in the $\Delta B=1$ Hamiltonian presented in Sec. VI.F. The new operators $Q_{7\gamma}$ and Q_{8G}, specific for $b\to s\gamma$ and $b\to sg$ transitions, carry the name of magnetic penguin operators. They originate from the mass insertion on the external b-quark line in the QED and QCD penguin diagrams of Fig. 4(d), respectively. In view of $m_s \ll m_b$ we do not include the corresponding contributions from mass insertions on the external s-quark line.

B. Wilson coefficients

A very peculiar feature of the renormalization-group analysis of the set of operators in Eq. (9.2) is that the mixing under (infinite) renormalization between the set

TABLE XXVI. $K_L\to\pi^0 e^+ e^-$ Wilson coefficients y_{7V}/α and y_{7A}/α for $\mu=1.0$ GeV and various values of m_t.

	y_{7V}/α									
	$\Lambda^{(4)}_{\overline{\rm MS}}=215$ MeV			$\Lambda^{(4)}_{\overline{\rm MS}}=325$ MeV			$\Lambda^{(4)}_{\overline{\rm MS}}=435$ MeV			
m_t [GeV]	LO	NDR	HV	LO	NDR	HV	LO	NDR	HV	y_{7A}/α
150	0.546	0.719	0.711	0.512	0.706	0.697	0.481	0.692	0.681	–0.576
160	0.560	0.733	0.726	0.526	0.721	0.711	0.495	0.706	0.696	–0.637
170	0.575	0.747	0.740	0.540	0.735	0.725	0.509	0.720	0.710	–0.700
180	0.588	0.761	0.753	0.554	0.748	0.739	0.523	0.734	0.723	–0.765
190	0.601	0.774	0.766	0.567	0.761	0.752	0.536	0.747	0.736	–0.833
200	0.614	0.786	0.779	0.580	0.774	0.764	0.549	0.760	0.749	–0.902

$Q_1,\ldots,Q_6$ and the operators $Q_{7\gamma},Q_{8G}$ vanishes at the one-loop level. Consequently, in order to calculate the coefficients $C_{7\gamma}(\mu)$ and $C_{8G}(\mu)$ in the leading logarithmic approximation, two-loop calculations of $\mathcal{O}(eg_s^2)$ and $\mathcal{O}(g_s^3)$ are necessary. The corresponding NLO analysis requires the evaluation of the mixing in question at the three-loop level. In view of this new feature it is useful to include additional couplings in the definition of $Q_{7\gamma}$ and Q_{8G} as done in Eq. (9.2). In this manner the entries in the anomalous-dimension matrix representing the mixing between $Q_1,\ldots,Q_6$ and $Q_{7\gamma},Q_{8G}$ at the two-loop level are $\mathcal{O}(g_s^2)$ and enter the anomalous-dimension matrix $\gamma_s^{(0)}$. Correspondingly, the three-loop mixing between these two sets of operators enters the matrix $\gamma_s^{(1)}$. The mixing under renormalization in the sector $Q_{7\gamma},Q_{8G}$ proceeds in the usual manner, and the corresponding entries in $\gamma_s^{(0)}$ and $\gamma_s^{(1)}$ result from one-loop and two-loop calculations, respectively.

At present, the coefficients $C_{7\gamma}$ and C_{8G} are only known in the leading logarithmic approximation. Consequently, we are in the position to give here only their values in this approximation. The work on NLO corrections to $C_{7\gamma}$ and C_{8G} is in progress, and we will summarize below what is already known about these corrections.

Due to the peculiar features of this decay mentioned above, the first fully correct calculation of the leading anomalous-dimension matrix has been obtained only in 1993 (Ciuchini, Franco, Martinelli, Reina, and Silvestrini, 1993; Ciuchini, Franco, Reina, and Silvestrini 1994). It is instructive to clarify this right at the beginning. We follow here Buras, Misiak, Münz, and Pokorski (1994).

The point is that the mixing between the sets $Q_1,\ldots,Q_6$ and $Q_{7\gamma}$, Q_{8G} in $\gamma_s^{(0)}$ resulting from two-loop diagrams is generally regularization-scheme dependent. This is certainly disturbing because the matrix $\gamma_s^{(0)}$, being the first term in the expansion for γ_s, is usually scheme independent. There is a simple way to circumvent this difficulty (Buras, Misiak, Münz, and Pokorski, 1994).

As noticed by Ciuchini, Franco, Martinelli, Reina, and Silvestrini (1993) and Ciuchini, Franco, Reina, and Silvestrini (1994), the regularization-scheme dependence of $\gamma_s^{(0)}$ in the case of $b\to s\gamma$ and $b\to sg$ is signaled in the one-loop matrix elements of $Q_1,\ldots,Q_6$ for on-shell photons or gluons. They vanish in any four-dimensional regularization scheme and in the HV scheme, but some of them are nonzero in the NDR scheme. One has

$$\langle Q_i\rangle^{\gamma}_{\text{one loop}}=y_i\langle Q_{7\gamma}\rangle_{\text{tree}},\quad i=1,\ldots,6, \tag{9.3}$$

and

$$\langle Q_i\rangle^{G}_{\text{one loop}}=z_i\langle Q_{8G}\rangle_{\text{tree}},\quad i=1,\ldots,6. \tag{9.4}$$

In the HV scheme all the y_i's and z_i's vanish, while in the NDR scheme $\vec{y}=(0,0,0,0,-\frac{1}{3},-1)$ and $\vec{z}=(0,0,0,0,1,0)$. This regularization-scheme dependence is canceled by a corresponding regularization-scheme dependence in $\gamma_s^{(0)}$, as first demonstrated by Ciuchini, Franco, Martinelli, Reina, and Silvestrini (1993) and Ciuchini, Franco, Reina, and Silvestrini (1994). It should be stressed that the numbers y_i and z_i come from divergent, i.e., purely short-distance, parts of the one-loop integrals. So no reference to the spectator model or to any other model for the matrix elements is necessary here.

In view of all this it is convenient in the leading order to introduce the so-called "effective coefficients" (Buras, Misiak, Münz, and Pokorski, 1994) for the operators $Q_{7\gamma}$ and Q_{8G}, which are regularization-scheme independent. They are given as follows:

$$C_{7\gamma}^{(0)\text{eff}}(\mu)=C_{7\gamma}^{(0)}(\mu)+\sum_{i=1}^{6} y_i C_i^{(0)}(\mu), \tag{9.5}$$

and

$$C_{8G}^{(0)\text{eff}}(\mu)=C_{8G}^{(0)}(\mu)+\sum_{i=1}^{6} z_i C_i^{(0)}(\mu). \tag{9.6}$$

One can then introduce a scheme-independent vector

$$\vec{C}^{(0)\text{eff}}(\mu)=(C_1^{(0)}(\mu),\ldots,C_6^{(0)}(\mu),C_{7\gamma}^{(0)\text{eff}}(\mu),C_{8G}^{(0)\text{eff}}(\mu)). \tag{9.7}$$

From the renormalization-group equations (RGE) for $\vec{C}^{(0)}(\mu)$, it is straightforward to derive the RGE for $\vec{C}^{(0)\text{eff}}(\mu)$. It has the form

$$\mu\frac{d}{d\mu}C_i^{(0)\text{eff}}(\mu)=\frac{\alpha_s}{4\pi}\gamma_{ji}^{(0)\text{eff}}C_j^{(0)\text{eff}}(\mu), \tag{9.8}$$

where

$$\gamma_{ji}^{(0)\text{eff}}=\begin{cases}\gamma_{j7}^{(0)}+\sum_{k=1}^{6} y_k\gamma_{jk}^{(0)}-y_j\gamma_{77}^{(0)}-z_j\gamma_{87}^{(0)}, & i=7,\ j=1,\ldots,6\\ \gamma_{j8}^{(0)}+\sum_{k=1}^{6} z_k\gamma_{jk}^{(0)}-z_j\gamma_{88}^{(0)}, & i=8,\ j=1,\ldots6\\ \gamma_{ji}^{(0)}, & \text{otherwise.}\end{cases} \tag{9.9}$$

The matrix $\gamma^{(0)\text{eff}}$ is a scheme-independent quantity. It equals the matrix that one would obtain directly from two-loop diagrams in the HV scheme. In order to simplify the notation we will omit the label "eff" in the expressions for the elements of this effective one-loop anomalous-dimension matrix given below and keep it only in the Wilson coefficients of the operators $Q_{7\gamma}$ and Q_{8G}.

This discussion clarifies why it took so long to find the correct leading anomalous-dimension matrix for the $b\to s\gamma$ decay (Ciuchini, Franco, Martinelli, Reina, and Silvestrini, 1993; Ciuchini, Franco, Reina, and Silvestrini, 1994). All previous calculations (Cella *et al.*, 1990; Grinstein *et al.*, 1990; Adel and Yao, 1993, 1994; Misiak 1993) of the leading-order QCD corrections to $b\to s\gamma$ used the NDR scheme but unfortunately set z_i and y_i to zero, or did not include all operators or made other mistakes. The discrepancy between the calculation of Grigjanis *et al.* (1988) (DRED scheme) and Grinstein *et al.* (1990) (NDR scheme) has been clarified by Misiak (1994).

C. Renormalization-group evolution and anomalous-dimension matrices

The coefficients $C_i(\mu)$ in Eq. (9.1) can be calculated by using

$$\vec{C}(\mu)=U_5(\mu,M_W)\vec{C}(M_W). \tag{9.10}$$

Here $U_5(\mu,M_W)$ is the 8×8 evolution matrix, which is given in general terms in Eq. (3.93), with γ being the 8×8 anomalous-dimension matrix. In the leading order $U_5(\mu,M_W)$ is to be replaced by $U_5^{(0)}(\mu,M_W)$ and the initial conditions by $\vec{C}^{(0)}(M_W)$, given by Grinstein *et al.* (1990)

$$C_2^{(0)}(M_W)=1, \tag{9.11}$$

$$C_{7\gamma}^{(0)}(M_W)=\frac{3x_t^3-2x_t^2}{4(x_t-1)^4}\ln x_t+\frac{-8x_t^3-5x_t^2+7x_t}{24(x_t-1)^3} \equiv -\frac{1}{2}D_0'(x_t), \tag{9.12}$$

$$C_{8G}^{(0)}(M_W)=\frac{-3x_t^2}{4(x_t-1)^4}\ln x_t+\frac{-x_t^3+5x_t^2+2x_t}{8(x_t-1)^3} \equiv -\frac{1}{2}E_0'(x_t) \tag{9.13}$$

with all remaining coefficients being zero at $\mu=M_W$. The functions $D_0'(x_t)$ and $E_0'(x_t)$ are sometimes used in the literature. The 6×6 submatrix of $\gamma_s^{(0)}$ involving the operators $Q_1,\ldots,Q_6$ is given in Eq. (6.25). Here we only give the remaining nonvanishing entries of $\gamma_s^{(0)}$ (Ciuchini, Franco, Martinelli, Reina, and Silvestrini, 1993; Ciuchini, Franco, Reina, and Silvestrini, 1994).

For simplicity we define the notation $\gamma_{ij}\equiv(\gamma_s)_{ij}$. Then the elements $\gamma_{i7}^{(0)}$ with $i=1,\ldots,6$ are

$$\gamma_{17}^{(0)}=0,\quad \gamma_{27}^{(0)}=\frac{104}{27}C_F, \tag{9.14}$$

$$\gamma_{37}^{(0)}=-\frac{116}{27}C_F,\quad \gamma_{47}^{(0)}=\left(\frac{104}{27}u-\frac{58}{27}d\right)C_F, \tag{9.15}$$

$$\gamma_{57}^{(0)}=\frac{8}{3}C_F,\quad \gamma_{67}^{(0)}=\left(\frac{50}{27}d-\frac{112}{27}u\right)C_F. \tag{9.16}$$

The elements $\gamma_{i8}^{(0)}$ with $i=1,\ldots,6$ are

$$\gamma_{18}^{(0)}=3,\quad \gamma_{28}^{(0)}=\frac{11}{9}N-\frac{29}{9}\frac{1}{N}, \tag{9.17}$$

$$\gamma_{38}^{(0)}=\frac{22}{9}N-\frac{58}{9}\frac{1}{N}+3f,\quad \gamma_{48}^{(0)}=6+\left(\frac{11}{9}N-\frac{29}{9}\frac{1}{N}\right)f, \tag{9.18}$$

$$\gamma_{58}^{(0)}=-2N+\frac{4}{N}-3f,\quad \gamma_{68}^{(0)}=-4-\left(\frac{16}{9}N-\frac{25}{9}\frac{1}{N}\right)f. \tag{9.19}$$

Finally, the 2×2 one-loop anomalous-dimension matrix in the sector $Q_{7\gamma},Q_{8G}$ is given by (Grinstein *et al.*, 1990)

$$\gamma_{77}^{(0)}=8C_F,\quad \gamma_{78}^{(0)}=0,$$

$$\gamma_{87}^{(0)}=-\frac{8}{3}C_F,\quad \gamma_{88}^{(0)}=16C_F-4N. \tag{9.20}$$

As we discussed above, the first correct calculation of the two-loop mixing between $Q_1,\ldots,Q_6$ and $Q_{7\gamma},Q_{8G}$ has been presented by Ciuchini, Franco, Martinelli, Reina, and Silvestrini (1993) and Ciuchini, Franco, Reina, and Silvestrini (1994) and confirmed subsequently by Cella *et al.* (1994a, 1994b) and Misiak (1995). In order to extend these calculations beyond the leading order one would have to calculate $\gamma_s^{(1)}$ [see Eq. (3.92)] and $O(\alpha_s)$ corrections to the initial conditions in Eqs. (9.12) and (9.13). We summarize below the present status of this NLO calculation.

The 6×6 two-loop submatrix of $\gamma_s^{(1)}$ involving the operators $Q_1,\ldots,Q_6$ is given in Eq. (6.26). The two-loop generalization of Eq. (9.20) has been calculated only last year (Misiak and Münz, 1995). It is given for both NDR and HV schemes as follows:

$$\gamma_{77}^{(1)}=C_F\left(\frac{548}{9}N-16C_F-\frac{56}{9}f\right),$$

$$\gamma_{78}^{(1)}=0,$$

$$\gamma_{87}^{(1)}=C_F\left(-\frac{404}{27}N+\frac{32}{3}C_F+\frac{56}{27}f\right),$$

$$\gamma_{88}^{(1)}=-\frac{458}{9}-\frac{12}{N^2}+\frac{214}{9}N^2+\frac{56}{9}\frac{f}{N}-\frac{13}{9}fN. \tag{9.21}$$

The generalization of Eqs. (9.14)–(9.19) to next to leading order requires three-loop calculations, which have not been done yet. The $O(\alpha_s)$ corrections to $C_{7\gamma}(M_W)$ and $C_{8G}(M_W)$ have been considered by Adel and Yao (1993).

TABLE XXVII. Numerical constants in the expansion of $C_j^{(0)}(\mu)$, $C_{7\gamma}^{(0)}(M_W)$, and $C_{8G}^{(0)}(M_W)$.

i	1	2	3	4	5	6	7	8
a_i	$\frac{14}{23}$	$\frac{16}{23}$	$\frac{6}{23}$	$-\frac{12}{23}$	0.4086	−0.4230	−0.8994	0.1456
k_{1i}	0	0	$\frac{1}{2}$	$-\frac{1}{2}$	0	0	0	0
k_{2i}	0	0	$\frac{1}{2}$	$\frac{1}{2}$	0	0	0	0
k_{3i}	0	0	$-\frac{1}{14}$	$\frac{1}{6}$	0.0510	−0.1403	−0.0113	0.0054
k_{4i}	0	0	$-\frac{1}{14}$	$-\frac{1}{6}$	0.0984	0.1214	0.0156	0.0026
k_{5i}	0	0	0	0	−0.0397	0.0117	−0.0025	0.0304
k_{6i}	0	0	0	0	0.0335	0.0239	−0.0462	−0.0112
h_i	2.2996	−1.0880	$-\frac{3}{7}$	$-\frac{1}{14}$	−0.6494	−0.0380	−0.0185	−0.0057
$\bar{h}_i$	0.8623	0	0	0	−0.9135	0.0873	−0.0571	0.0209

D. Results for the Wilson coefficients

The leading-order results for the Wilson coefficients of all operators entering the effective Hamiltonian in Eq. (9.1) can be written in an analytic form. They are (Buras, Misiak, Münz, and Pokorski, 1994)

$$C_j^{(0)}(\mu)=\sum_{i=1}^{8} k_{ji}\eta^{a_i} \quad (j=1,\ldots,6), \tag{9.22}$$

$$C_{7\gamma}^{(0)\mathrm{eff}}(\mu)=\eta^{16/23}C_{7\gamma}^{(0)}(M_W)+\frac{8}{3}(\eta^{14/23}-\eta^{16/23}) \times C_{8G}^{(0)}(M_W)+C_2^{(0)}(M_W)\sum_{i=1}^{8} h_i\eta^{a_i}, \tag{9.23}$$

$$C_{8G}^{(0)\mathrm{eff}}(\mu)=\eta^{14/23}C_{8G}^{(0)}(M_W)+C_2^{(0)}(M_W)\sum_{i=1}^{8} \bar{h}_i\eta^{a_i}, \tag{9.24}$$

with

$$\eta=\frac{\alpha_s(M_W)}{\alpha_s(\mu)}, \tag{9.25}$$

and $C_{7\gamma}^{(0)}(M_W)$ and $C_{8G}^{(0)}(M_W)$ given in Eqs. (9.12) and (9.13), respectively. The numbers a_i, k_{ji}, h_i, and $\bar{h}_i$ are given in Table XXVII.

E. Numerical analysis

The decay $B\to X_s\gamma$ is the only decay in this review for which the complete NLO corrections are not available. In presenting the numerical values for the Wilson coefficients a few remarks on the choice of α_s should therefore be made. In the leading order, the leading-order expression for α_s should be used. The question then is what to use for Λ_{QCD} in this expression. In other decays for which NLO corrections were available, this was not important because LO results were secondary. We have therefore simply inserted our standard $\Lambda_{\overline{\mathrm{MS}}}$ values into the LO formula for α_s. This procedure gives $\alpha_s^{(5)}(M_Z)$=0.126, 0.136, and 0.144 for $\Lambda_{\overline{\mathrm{MS}}}^{(5)}$ = 140 MeV, 225 MeV, and 310 MeV, respectively. In view of these high values of $\alpha_s^{(5)}(M_Z)$ we will here proceed differently. Following Buras, Misiak, Münz, and Pokorski (1994), we will use $\alpha_s^{(5)}(M_Z)$=0.110, 0.117, and 0.124 as in the NLO calculations, but we will evolve $\alpha_s(\mu)$ to $\mu\approx\mathcal{O}(m_b)$ using the leading-order expressions. In short, we will use

$$\alpha_s(\mu)=\frac{\alpha_s(M_Z)}{1-\beta_0\alpha_s(M_Z)/2\pi\,\ln(M_Z/\mu)}. \tag{9.26}$$

This discussion shows again the importance of the complete NLO calculation for this decay.

Before starting the discussion of the numerical values for the coefficients $C_{7\gamma}^{(0)\mathrm{eff}}$ and $C_{8G}^{(0)\mathrm{eff}}$, let us illustrate the relative numerical importance of the three terms in Eq. (9.23) for $C_{7\gamma}^{(0)\mathrm{eff}}$.

For instance, for m_t=170 GeV, μ=5 GeV, and $\alpha_s^{(5)}(M_Z)$=0.117, one obtains

$$\begin{aligned} C_{7\gamma}^{(0)\mathrm{eff}}(\mu)&=0.698C_{7\gamma}^{(0)}(M_W)+0.086C_{8G}^{(0)}(M_W) \\ &\quad -0.156C_2^{(0)}(M_W) \\ &=0.698(-0.193)+0.086(-0.096)-0.156 \\ &=-0.299. \end{aligned} \tag{9.27}$$

In the absence of QCD we would have $C_{7\gamma}^{(0)\mathrm{eff}}(\mu)=C_{7\gamma}^{(0)}(M_W)$ (in that case one has η=1). Therefore the dominant term in the above expression [the one proportional to $C_2^{(0)}(M_W)$] is the additive QCD correction that causes the enormous QCD enhancement of the $b\to s\gamma$ rate (Bertolini *et al.*, 1987; Deshpande *et al.*, 1987). It originates solely from the two-loop diagrams. On the

TABLE XXVIII. Wilson coefficients $C_{7\gamma}^{(0)\text{eff}}$ and $C_{8G}^{(0)\text{eff}}$ for m_t=170 GeV and various values of $\alpha_s^{(5)}(M_Z)$ and μ.

	$\alpha_s^{(5)}(M_Z)$=0.110		$\alpha_s^{(5)}(M_Z)$=0.117		$\alpha_s^{(5)}(M_Z)$=0.124	
μ [GeV]	$C_{7\gamma}^{(0)\text{eff}}$	$C_{8G}^{(0)\text{eff}}$	$C_{7\gamma}^{(0)\text{eff}}$	$C_{8G}^{(0)\text{eff}}$	$C_{7\gamma}^{(0)\text{eff}}$	$C_{8G}^{(0)\text{eff}}$
2.5	–0.323	–0.153	–0.334	–0.157	–0.346	–0.162
5.0	–0.291	–0.140	–0.299	–0.143	–0.307	–0.147
7.5	–0.275	–0.133	–0.281	–0.136	–0.287	–0.139
10.0	–0.263	–0.129	–0.268	–0.131	–0.274	–0.133

other hand, the multiplicative QCD correction (the factor 0.698 above) tends to suppress the rate but fails in the competition with the additive contributions.

In the case of $C_{8G}^{(0)\text{eff}}$ a similar enhancement is observed,

$$C_{8G}^{(0)\text{eff}}(\mu)=0.730C_{8G}^{(0)}(M_W)-0.073C_2^{(0)}(M_W)$$
$$=0.730(-0.096)-0.073=-0.143. \quad (9.28)$$

In Table XXVIII we give the values of $C_{7\gamma}^{(0)\text{eff}}$ and $C_{8G}^{(0)\text{eff}}$ for different values of μ and $\alpha_s^{(5)}(M_Z)$. To this end Eq. (9.26) has been used. A strong μ dependence of both coefficients is observed. We will return to this dependence in Sec. XXII.

X. THE EFFECTIVE HAMILTONIAN FOR $B\to X_s e^+e^-$

The effective Hamiltonian for $B\to X_s e^+e^-$ at scales $\mu=\mathcal{O}(m_b)$ is given by

$$\mathcal{H}_{\text{eff}}(b\to se^+e^-)=\mathcal{H}_{\text{eff}}(b\to s\gamma)$$
$$-\frac{G_F}{\sqrt{2}}V_{ts}^*V_{tb}[C_{9V}(\mu)Q_{9V}(\mu)$$
$$+C_{10A}(\mu)Q_{10A}(\mu)], \quad (10.1)$$

where again we have neglected the term proportional to $V_{us}^*V_{ub}$ and $\mathcal{H}_{\text{eff}}(b\to s\gamma)$ is given in Eq. (9.1).

A. Operators

In addition to the operators relevant for $B\to X_s\gamma$, there are two new operators

$$Q_{9V}=(\bar{s}b)_{V-A}(\bar{e}e)_V, \quad Q_{10A}=(\bar{s}b)_{V-A}(\bar{e}e)_A, \quad (10.2)$$

where V and A refer to γ_μ and $\gamma_\mu\gamma_5$, respectively.

They originate in the Z^0 and γ penguin diagrams with the external $\bar{e}e$ of Fig. 4(f) and the corresponding box diagrams.

B. Wilson coefficients

The coefficient $C_{10A}(\mu)$ is given by

$$C_{10A}(M_W)=\frac{\alpha}{2\pi}\tilde{C}_{10}(M_W), \quad \tilde{C}_{10}(M_W)=-\frac{Y_0(x_t)}{\sin^2\Theta_W} \quad (10.3)$$

with $Y_0(x)$ given in Eq. (10.8). Since Q_{10A} does not renormalize under QCD, its coefficient does not depend on $\mu\approx\mathcal{O}(m_b)$. The only renormalization-scale dependence in Eq. (10.3) enters through the definition of the top-quark mass. We will return to this issue in Sec. XXIII.C.

The coefficient $C_{9V}(\mu)$ has been calculated with increasing precision by several groups (Grinstein *et al.*, 1989; Grigjanis *et al.*, 1989; Cella *et al.*, 1991; Misiak, 1993), culminating in two complete next-to-leading-order QCD calculations (Buras and Münz, 1995; Misiak, 1995) that agree with each other.

In order to calculate the coefficient C_{9V} including next-to-leading-order corrections, we have to perform, in principle, a two-loop renormalization-group analysis for the full set of operators contributing to Eq. (10.1). However, Q_{10A} is not renormalized, and the dimension-five operators $Q_{7\gamma}$ and Q_{8G} have no impact on C_{9V}. Consequently, only a set of seven operators, $Q_1,\ldots,Q_6$ and Q_{9V}, has to be considered. This is precisely the case of the decay $K_L\to\pi^0e^+e^-$ discussed by Buras, Lautenbacher, Misiak, and Münz (1994) and in Sec. VIII, except for an appropriate change of quark flavors and that now $\mu\approx\mathcal{O}(m_b)$ instead of $\mu\approx\mathcal{O}(1\text{ GeV})$. Since the NLO analysis of $K_L\to\pi^0e^+e^-$ has already been presented in

TABLE XXIX. Numerical constants in the expansion of P_0 and P_E.

i	1	2	3	4	5	6	7	8
p_i	0	0	$-\frac{80}{203}$	$\frac{8}{33}$	0.0433	0.1384	0.1648	–0.0073
r_i^{NDR}	0	0	0.8966	–0.1960	–0.2011	0.1328	–0.0292	–0.1858
s_i	0	0	–0.2009	–0.3579	0.0490	–0.3616	–0.3554	0.0072
q_i	0	0	0	0	0.0318	0.0918	–0.2700	0.0059
r_i^{HV}	0	0	–0.1193	0.1003	–0.0473	0.2323	–0.0133	–0.1799

TABLE XXX. The coefficient P_0 of $\tilde{C}_9$ for various values of $\Lambda_{\overline{\rm MS}}^{(5)}$ and μ.

	$\Lambda_{\overline{\rm MS}}^{(5)}=140$ MeV			$\Lambda_{\overline{\rm MS}}^{(5)}=225$ MeV			$\Lambda_{\overline{\rm MS}}^{(5)}=310$ MeV		
μ [GeV]	LO	NDR	HV	LO	NDR	HV	LO	NDR	HV
2.5	2.053	2.928	2.797	1.933	2.846	2.759	1.835	2.775	2.727
5.0	1.852	2.625	2.404	1.788	2.591	2.395	1.736	2.562	2.388
7.5	1.675	2.391	2.127	1.632	2.373	2.127	1.597	2.358	2.128
10.0	1.526	2.204	1.912	1.494	2.194	1.917	1.469	2.185	1.921

Sec. VIII, we will only give the final result for $C_{9V}(\mu)$. Because there is a one-step evolution from $\mu=M_W$ down to $\mu=m_b$ without any thresholds in between, it is possible to find an analytic formula for $C_{9V}(\mu)$. Defining $\tilde{C}_9$ by

$$C_{9V}(\mu)=\frac{\alpha}{2\pi}\,\tilde{C}_9(\mu), \tag{10.4}$$

one finds (Buras and Münz, 1995) in the NDR scheme

$$\tilde{C}_9^{\rm NDR}(\mu)=P_0^{\rm NDR}+\frac{Y_0(x_t)}{\sin^2\Theta_W}-4Z_0(x_t)+P_E E_0(x_t) \tag{10.5}$$

with

$$P_0^{\rm NDR}=\frac{\pi}{\alpha_s(M_W)}\left(-0.1875+\sum_{i=1}^{8} p_i\eta^{a_i+1}\right)+1.2468 +\sum_{i=1}^{8}\eta^{a_i}[r_i^{\rm NDR}+s_i\eta], \tag{10.6}$$

$$P_E=0.1405+\sum_{i=1}^{8} q_i\eta^{a_i+1}. \tag{10.7}$$

The functions $Y_0(x)$ and $Z_0(x)$ are defined by

$$Y_0(x)=C_0(x)-B_0(x),\quad Z_0(x)=C_0(x)+\tfrac{1}{4}D_0(x) \tag{10.8}$$

with $B_0(x)$, $C_0(x)$, and $D_0(x)$ given in Eqs. (7.13), (7.14), and (7.15), respectively. $E_0(x)$ is given in Eq. (6.15). The powers a_i are the same as in Table XXVII. The coefficients p_i, $r_i^{\rm NDR}$, s_i, and q_i can be found in Table XXIX. P_E is $\mathcal{O}(10^{-2})$, and consequently the last term in Eq. (10.5) can be neglected, although we keep it in the numerical analysis. These results agree with Misiak (1995).

In the HV scheme, only the coefficients r_i are changed. They are given on the last line of Table XXIX. Equivalently, we can write

$$P_0^k=P_0^{\rm NDR}+\xi_k\,\tfrac{4}{9}(3C_1^{(0)}+C_2^{(0)}-C_3^{(0)}-3C_4^{(0)}) \tag{10.9}$$

with

$$\xi_k=\begin{cases}0 & k={\rm NDR}\\ -1 & k={\rm HV}.\end{cases} \tag{10.10}$$

We note that

$$\sum_{i=1}^{8} p_i=0.1875,\quad \sum_{i=1}^{8} q_i=-0.1405, \tag{10.11}$$

$$\sum_{i=1}^{8}(r_i^k+s_i)=-1.2468+\frac{4}{9}(1+\xi_k),$$

$$\sum_{i=1}^{8} p_i(a_i+1)=-\frac{16}{69}. \tag{10.12}$$

In this way for $\eta=1$, one finds $P_E=0$, $P_0^{\rm NDR}=4/9$, and $P_0^{\rm HV}=0$, in accordance with the initial conditions at $\mu=M_W$. Moreover, the second relation in Eq. (10.12) assures the correct large logarithm in $P_0^{\rm NDR}$, i.e., $\frac{8}{9}\ln(M_W/\mu)$.

The special feature of $C_{9V}(\mu)$ compared to the coefficients of the remaining operators contributing to $B\to X_s e^+e^-$ is the large logarithm represented by $1/\alpha_s$ in P_0 in Eq. (10.6). Consequently, the renormalization-group improved perturbation theory for C_{9V} has the structure $\mathcal{O}(1/\alpha_s)+\mathcal{O}(1)+\mathcal{O}(\alpha_s)+\cdots$, whereas the corresponding series for the remaining coefficients is $\mathcal{O}(1)+\mathcal{O}(\alpha_s)+\cdots$. Therefore, in order to find the next-to-leading $\mathcal{O}(1)$ term in the branching ratio for $B\to X_s e^+e^-$, the full two-loop renormalization-group analysis has to be performed in order to find C_{9V}, but the coefficients of the remaining operators should be taken in the leading logarithmic approximation. This is gratifying because the coefficient of the magnetic operator $Q_{7\gamma}$ is known only in the leading logarithmic approximation.

TABLE XXXI. Wilson coefficient $\tilde{C}_9$ for $m_t=170$ GeV and various values of $\Lambda_{\overline{\rm MS}}^{(5)}$ and μ.

	$\Lambda_{\overline{\rm MS}}^{(5)}=140$ MeV			$\Lambda_{\overline{\rm MS}}^{(5)}=225$ MeV			$\Lambda_{\overline{\rm MS}}^{(5)}=310$ MeV		
μ [GeV]	LO	NDR	HV	LO	NDR	HV	LO	NDR	HV
2.5	2.053	4.493	4.361	1.933	4.410	4.323	1.835	4.338	4.290
5.0	1.852	4.191	3.970	1.788	4.156	3.961	1.736	4.127	3.954
7.5	1.675	3.958	3.694	1.632	3.940	3.694	1.597	3.924	3.695
10.0	1.526	3.772	3.480	1.494	3.761	3.485	1.469	3.752	3.488

C. Numerical results

In the numerical analysis we will use the two-loop expression for α_s and the parameters collected in the Appendix. Our presentation follows closely the one given by Buras and Münz (1995).

In Table XXX we show the constant P_0 in Eq. (10.6) for different μ and $\Lambda_{\overline{\rm MS}}$ in the leading order, corresponding to the first term in Eq. (10.6), and for the NDR and HV schemes as given by Eqs. (10.6) and (10.9), respectively. In Table XXXI we show the corresponding values for $\tilde{C}_9(\mu)$. To this end we set m_t=170 GeV.

We observe

(i) The NLO corrections to P_0 enhance this constant relative to the LO result by roughly 45% and 35% in the NDR and HV schemes, respectively. This enhancement is analogous to the one found in the case of $K_L\to\pi^0e^+e^-$.

(ii) In calculating P_0 in the LO we have used $\alpha_s(\mu)$ at one-loop level. Had we used the two-loop expression for $\alpha_s(\mu)$, we would find, for μ=5 GeV and $\Lambda_{\overline{\rm MS}}^{(5)}=225$ MeV, $P_0^{\rm LO}\approx 1.98$. Consequently, the NLO corrections would have smaller impact. Grinstein *et al.* (1989), including the next-to-leading term 4/9, would find P_0 roughly 20% smaller than the $P_0^{\rm NDR}$ given in Table XXX.

(iii) It is tempting to compare P_0 in Table XXX with that found in the absence of QCD corrections. In the limit $\alpha_s\to 0$ we find $P_0^{\rm NDR}=\frac{8}{9}\ln(M_W/\mu)+4/9$ and $P_0^{\rm HV}=\frac{8}{9}\ln(M_W/\mu)$, which, for μ=5 GeV, give $P_0^{\rm NDR}$=2.91 and $P_0^{\rm HV}$=2.46. Comparing these values with Table XXX, we conclude that the QCD suppression of P_0 present in the leading-order approximation is considerably weakened in the NDR treatment of γ_5 after the inclusion of NLO corrections. It is essentially removed for $\mu>5$ GeV in the HV scheme.

(iv) The NLO corrections to $\tilde{C}_9$, which also include the m_t-dependent contributions, are large as seen in Table XXXI. The results in HV and NDR schemes are more than a factor of two larger than the leading-order result $\tilde{C}_9=P_0^{\rm LO}$, which should not include m_t contributions. This demonstrates very clearly the necessity of NLO calculations that allow a consistent inclusion of the important m_t contributions. For the same set of parameters, Grinstein *et al.* (1989) would find $\tilde{C}_9$ to be smaller than $\tilde{C}_9^{\rm NDR}$ by 10–15%.

(v) The $\Lambda_{\overline{\rm MS}}$ dependence of $\tilde{C}_9$ is rather weak. On the other hand, its μ dependence is sizable ($\sim$15% in the range of μ considered), although smaller than that of the coefficients $C_{7\gamma}$ and C_{8G} given in Table XXVIII. We also find that the m_t dependence of $\tilde{C}_9$ is rather weak. Varying m_t between 150 GeV and 190 GeV changes $\tilde{C}_9$ by at most 10%. This weak m_t dependence of $\tilde{C}_9$ originates in the partial cancellation of m_t dependences between $Y_0(x_t)$ and $Z_0(x_t)$ in Eq. (10.5), as already seen in the case of $K_L\to\pi^0e^+e^-$ in Fig. 8. Finally, the difference between $\tilde{C}_9^{\rm NDR}$ and $\tilde{C}_9^{\rm HV}$ is small and amounts to roughly 5%.

(vi) The dominant m_t dependence in this decay originates from the m_t dependence of $\tilde{C}_{10}(M_W)$. In fact, as can be seen in Sec. VIII, $\tilde{C}_{10}(M_W)=2\pi y_{7A}/\alpha$, with y_{7a} present in $K_L\to\pi^0e^+e^-$. The m_t dependence of y_{7A} is shown in Fig. 8.

XI. EFFECTIVE HAMILTONIANS FOR RARE *K* AND *B* DECAYS

A. Overview

In the present section we will summarize the effective Hamiltonians valid at next to leading logarithmic accuracy in QCD, which describe the semileptonic, rare flavor changing neutral current (FCNC) transitions $K^+\to\pi^+\nu\bar{\nu}$, $(K_L\to\mu^+\mu^-)_{\rm SD}$, $K_L\to\pi^0\nu\bar{\nu}$, $B\to X_{s,d}\nu\bar{\nu}$, and $B\to l^+l^-$. These decay modes all are very similar in their structure, and it is natural to discuss them together. On the other hand, they differ from the decays $K\to\pi\pi$, $K\to\pi e^+e^-$, $B\to X_s\gamma$, and $B\to X_se^+e^-$ discussed in previous sections. Before giving the detailed formulas, it will be useful to recall the most important general features of this class of processes first. In addition, characteristic differences between the specific modes will also become apparent from the presentation.

(i) Within the standard model all the decays listed above are loop-induced semileptonic FCNC processes determined by Z^0 penguin and box diagrams [Figs. 2(d) and 2(e)].

In particular, a distinguishing feature of the present class of decays is the absence of a photon penguin contribution. For the decay modes with neutrinos in the final state this is obvious, since the photon does not couple to neutrinos. For the mesons decaying into a charged lepton pair the photon penguin amplitude vanishes due to vector current conservation.

An important consequence is that the decays considered here exhibit a hard Glashow-Iliopoulos-Maiani (GIM) suppression, quadratic in (small) internal quark masses, which is a property of the Z^0 penguin and box graphs. By contrast, the GIM suppression resulting from photon penguin contributions is logarithmic. Decays where the photon penguin contributes are, for example, $K_L\to\pi^0e^+e^-$ and $B\to X_se^+e^-$. The differences in the basic structure of these processes, resulting from the different pattern of GIM suppression, are the reason why we have discussed $K_L\to\pi^0e^+e^-$ and $B\to X_se^+e^-$ in a separate context.

(ii) The investigation of low-energy rare-decay processes allows one to probe, albeit indirectly, high-energy scales of the theory. Of particular interest is the sensitivity to properties of the top quark: its mass m_t and its CKM couplings V_{ts} and V_{td}.

(iii) A particular and very important advantage of the processes under discussion is that theoretically clean predictions can be obtained. The reasons for this are

(a) The low-energy hadronic matrix elements required are just the matrix elements of quark currents between hadron states, which can be extracted from the leading (nonrare) semileptonic decays. Other long-distance contributions are negligibly small.

An exception is the decay $K_L\to\mu^+\mu^-$, which has important contributions from the two-photon intermediate state, which are difficult to calculate reliably. However, the short-distance part $(K_L\to\mu^+\mu^-)_{\rm SD}$ alone, which we shall discuss here, is on the same footing as the other modes. The essential difficulty for phenomenological applications then is to separate the short-distance from the long-distance piece in the measured rate.

(b) According to the comments just made, the processes at hand are short-distance processes, calculable within a perturbative framework, possibly including renormalization-group improvement. The necessary separation of the short-distance dynamics from the low-energy matrix elements is achieved by means of an operator product expansion. The scale ambiguities, inherent to perturbative QCD, essentially constitute the only theoretical uncertainties present in the analysis. These uncertainties are well under control, as they may be systematically reduced through calculations beyond leading order.

(iv) The points made above emphasize that the short-distance-dominated loop-induced FCNC decays provide highly promising possibilities to investigate flavor dynamics at the quantum level. However, the very fact that these processes are based on higher-order electroweak effects, which makes them interesting theoretically, implies that the branching ratios will be very small and not easy to access experimentally.

The effective Hamiltonians governing the decays $K^+\to\pi^+\nu\bar\nu$, $(K_L\to\mu^+\mu^-)_{\rm SD}$, $K_L\to\pi^0\nu\bar\nu$, $B\to X_{s,d}\nu\bar\nu$, and $B\to l^+l^-$, resulting from the Z^0-penguin and box-type contributions, can all be written down in the following general form

$$\mathcal{H}_{\rm eff}=\frac{G_F}{\sqrt{2}}\frac{\alpha}{2\pi\,\sin^2\Theta_W}[\lambda_c F(x_c)+\lambda_t F(x_t)]\times(\bar n n')_{V-A}(\bar r r)_{V-A}\,, \tag{11.1}$$

where n,n' denote down-type quarks ($n,n'=d,s,b$ but $n\neq n'$) and r leptons, $r=l,\nu_l$ ($l=e,\mu,\tau$). The λ_i are products of CKM elements, in the general case $\lambda_i=V_{in}^*V_{in'}$. Furthermore, $x_i=m_i^2/M_W^2$.

The functions $F(x_i)$ describe the dependence on the internal up-type quark masses m_i (and on lepton masses if necessary) and are understood to include QCD corrections. They are increasing functions of the quark masses, a property that is particularly important for the top contribution.

Crucial features of the structure of the Hamiltonian are furthermore determined by the hard GIM suppression characteristic for this class of decays. First we note that the dependence of the Hamiltonian on the internal quarks comes in the form

$$\sum_{i=u,c,t}\lambda_i F(x_i)=\lambda_c(F(x_c)-F(x_u))+\lambda_t(F(x_t)-F(x_u)), \tag{11.2}$$

where we have used the unitarity of the CKM matrix. Now, hard GIM suppression means that for $x\ll 1$ F behaves quadratically in the quark masses. In the present case we have

TABLE XXXII. Order of magnitude of CKM parameters relevant for the various decays, expressed in powers of the Wolfenstein parameter $\lambda=0.22$. In the case of $K_L\to\pi^0\nu\bar\nu$, which is CP violating, only the imaginary parts of $\lambda_{c,t}$ contribute.

	$K^+\to\pi^+\nu\bar\nu$ $(K_L\to\mu^+\mu^-)_{\rm SD}$	$K_L\to\pi^0\nu\bar\nu$	$B\to X_s\nu\bar\nu$ $B_s\to l^+l^-$	$B\to X_d\nu\bar\nu$ $B_d\to l^+l^-$
λ_c	$\sim\lambda$	$({\rm Im}\lambda_c\sim\lambda^5)$	$\sim\lambda^2$	$\sim\lambda^3$
λ_t	$\sim\lambda^5$	$({\rm Im}\lambda_t\sim\lambda^5)$	$\sim\lambda^2$	$\sim\lambda^3$

$$F(x)\sim x\,\ln x,\quad \text{for } x\ll 1. \tag{11.3}$$

The first important consequence is that $F(x_u)\approx 0$ can be neglected. The Hamiltonian acquires the form anticipated in Eq. (11.1). It effectively consists of a charm and a top contribution. Therefore the relevant energy scales are M_W or m_t and, at least, m_c, which are large compared to $\Lambda_{\rm QCD}$. This fact indicates the short-distance nature of these processes.

A second consequence of Eq. (11.3) is that $F(x_c)/F(x_t)\approx\mathcal{O}(10^{-3})\ll 1$. Together with the weighting introduced by the CKM factors, this relation determines the relative importance of the charm versus the top contribution in Eq. (11.1). As seen in Table XXXII a simple pattern emerges if one writes down the order of magnitude of λ_c and λ_t in terms of powers of the Wolfenstein expansion parameter λ.

For the CP-violating decay $K_L\to\pi^0\nu\bar\nu$ and the B decays, the CKM factors λ_c and λ_t have the same order of magnitude. In view of $F(x_c)\ll F(x_t)$ the charm contribution is therefore negligible, and these decays are entirely determined by the top sector. For $K^+\to\pi^+\nu\bar\nu$ and $(K_L\to\mu^+\mu^-)_{\rm SD}$ on the other hand, λ_t is suppressed compared to λ_c by a factor of $\mathcal{O}(\lambda^4)\approx\mathcal{O}(10^{-3})$, which roughly compensates for the $\mathcal{O}(10^3)$ enhancement of $F(x_t)$ over $F(x_c)$. Hence the top and charm contributions have the same order of magnitude and must both be taken into account.

In principle, as far as flavordynamics is concerned, the top and the charm sector have the same structure. The only difference comes from the quark masses. However, this difference has striking implications for the detailed formalism necessary to treat the strong interaction corrections. We have $m_t/M_W=\mathcal{O}(1)$ and $m_c/M_W\ll 1$. Correspondingly, the QCD coupling α_s is also somewhat smaller at m_t than at m_c. For the charm contribution this implies that one can work to lowest order in the mass ratio m_c/M_W. On the other hand, for the same reason, logarithmic QCD corrections $\sim\alpha_s\ln M_W/m_c$ are large and have to be resummed to all orders in perturbation theory by renormalization-group methods. On the contrary, no large logarithms are present in the top sector, so that ordinary perturbation theory is applicable, but all orders in m_t/M_W have to be taken into account. In fact we see, from the point of view of QCD corrections, the charm and top contributions are quite ''complementary'' to each other, representing in a sense opposite limiting cases.

TABLE XXXIII. The functions $X^e_{\rm NL}$ and $X^\tau_{\rm NL}$ for various $\Lambda^{(4)}_{\overline{\rm MS}}$ and m_c.

	$X^e_{\rm NL}/10^{-4}$			$X^\tau_{\rm NL}/10^{-4}$		
$\Lambda^{(4)}_{\overline{\rm MS}}$ [MeV]\$m_c$ [GeV]	1.25	1.30	1.35	1.25	1.30	1.35
215	10.55	11.40	12.28	7.16	7.86	8.59
325	9.71	10.55	11.41	6.32	7.01	7.72
435	8.75	9.59	10.45	5.37	6.05	6.76

We are now ready to list the explicit expressions for the effective Hamiltonians.

B. The decay $K^+\to\pi^+\nu\bar\nu$

1. The next-to-leading-order effective Hamiltonian

The final result for the effective Hamiltonian inducing $K^+\to\pi^+\nu\bar\nu$ can be written as

$$\mathcal{H}_{\rm eff}=\frac{G_F}{\sqrt{2}}\frac{\alpha}{2\pi\sin^2\Theta_W}\sum_{l=e,\mu,\tau}[V^*_{cs}V_{cd}X^l_{NL}+V^*_{ts}V_{td}X(x_t)](\bar s d)_{V-A}(\bar\nu_l\nu_l)_{V-A}. \tag{11.4}$$

The index $l=e,\mu,\tau$ denotes the lepton flavor. The dependence on the charged lepton mass, resulting from the box graph, is negligible for the top contribution. In the charm sector this is the case only for the electron and the muon, but not for the τ lepton.

The function $X(x)$, relevant for the top part, is to $\mathcal{O}(\alpha_s)$ and to all orders in $x=m^2/M_W^2$

$$X(x)=X_0(x)+\frac{\alpha_s}{4\pi}X_1(x) \tag{11.5}$$

with (Inami and Lim, 1981)

$$X_0(x)=\frac{x}{8}\left[-\frac{2+x}{1-x}+\frac{3x-6}{(1-x)^2}\ln x\right] \tag{11.6}$$

and the QCD correction (Buchalla and Buras, 1993a)

$$X_1(x)=-\frac{23x+5x^2-4x^3}{3(1-x)^2}+\frac{x-11x^2+x^3+x^4}{(1-x)^3}\ln x+\frac{8x+4x^2+x^3-x^4}{2(1-x)^3}\ln^2 x-\frac{4x-x^3}{(1-x)^2}L_2(1-x)+8x\frac{\partial X_0(x)}{\partial x}\ln x_\mu, \tag{11.7}$$

where $x_\mu=\mu^2/M_W^2$ with $\mu=\mathcal{O}(m_t)$ and

$$L_2(1-x)=\int_1^x dt\,\frac{\ln t}{1-t}. \tag{11.8}$$

The μ dependence in the last term in Eq. (11.7) cancels to the order considered the μ dependence of the leading term $X_0(x(\mu))$.

The expression corresponding to $X(x_t)$ in the charm sector is the function $X^l_{\rm NL}$. It results from the RG calculation in NLLA and is given by

$$X^l_{\rm NL}=C_{\rm NL}-4B^{(1/2)}_{\rm NL}. \tag{11.9}$$

$C_{\rm NL}$ and $B^{(1/2)}_{\rm NL}$ correspond to the Z^0-penguin and the box-type contribution, respectively. One has (Buchalla and Buras, 1994a)

$$C_{\rm NL}=\frac{x(m)}{32}K_c^{24/25}\left[\left(\frac{48}{7}K_+ +\frac{24}{11}K_- -\frac{696}{77}K_{33}\right)\times\left(\frac{4\pi}{\alpha_s(\mu)}+\frac{15212}{1875}(1-K_c^{-1})\right)+\left(1-\ln\frac{\mu^2}{m^2}\right)\times(16K_+-8K_-)-\frac{1176244}{13125}K_+-\frac{2302}{6875}K_-+\frac{3529184}{48125}K_{33}+K\left(\frac{56248}{4375}K_+-\frac{81448}{6875}K_-+\frac{4563698}{144375}K_{33}\right)\right], \tag{11.10}$$

where

$$K=\frac{\alpha_s(M_W)}{\alpha_s(\mu)},\quad K_c=\frac{\alpha_s(\mu)}{\alpha_s(m)}, \tag{11.11}$$

$$K_+=K^{6/25},\quad K_-=K^{-12/25},\quad K_{33}=K^{-1/25}, \tag{11.12}$$

$$B^{(1/2)}_{\rm NL}=\frac{x(m)}{4}K_c^{24/25}\left[3(1-K_2)\left(\frac{4\pi}{\alpha_s(\mu)}+\frac{15212}{1875}\times(1-K_c^{-1})\right)-\ln\frac{\mu^2}{m^2}-\frac{r\ln r}{1-r}-\frac{305}{12}+\frac{15212}{625}K_2+\frac{15581}{7500}KK_2\right]. \tag{11.13}$$

Here $K_2=K^{-1/25}$, $m=m_c$, $r=m_l^2/m_c^2(\mu)$, and m_l is the lepton mass. We will at times omit the index l of X^l_{NL}. In Eqs. (11.10)–(11.13) the scale is $\mu=\mathcal{O}(m_c)$. The two-loop expression for $\alpha_s(\mu)$ is given in Eq. (3.19). Again, to the considered order, the explicit $\ln(\mu^2/m^2)$ terms in Eqs. (11.10) and (11.13) cancel the μ dependence of the leading terms.

These formulas give the complete next-to-leading-order effective Hamiltonian for $K^+\to\pi^+\nu\bar\nu$. The leading-order expressions (Novikov *et al.*, 1977; Ellis and Hagelin, 1983; Buchalla *et al.*, 1991; Dib *et al.*, 1991) are obtained by replacing $X(x_t)\to X_0(x_t)$ and $X^l_{\rm NL}\to X_L$, with X_L found from Eqs. (11.10) and (11.13) by retaining only the $1/\alpha_s(\mu)$ terms. In LLA the one-loop expression should be used for α_s. This amounts to setting $\beta_1=0$ in Eq. (3.19). The numerical values for $X_{\rm NL}$ for $\mu=m_c$ and several values of $\Lambda^{(4)}_{\overline{\rm MS}}$ and m_c are given in Table XXXIII. The μ dependence will be discussed fur-

ther in the phenomenological sections.

2. Z^0-penguin and box contribution in the top sector

For completeness we also give the expressions for the Z^0-penguin function $C(x)$ and the box function $B(x,1/2)$ separately, which contribute to $X(x)$ in Eq. (11.5) according to

$$X(x)=C(x)-4B(x,1/2). \tag{11.14}$$

The functions C and B depend on the gauge of the W boson. In 't Hooft–Feynman gauge (ξ=1) they are

$$C(x)=C_0(x)+\frac{\alpha_s}{4\pi}C_1(x), \tag{11.15}$$

where (Inami and Lim, 1981)

$$C_0(x)=\frac{x}{8}\left[\frac{6-x}{1-x}+\frac{3x+2}{(1-x)^2}\ln x\right] \tag{11.16}$$

and (Buchalla and Buras, 1993b)

$$\begin{aligned}C_1(x)=&\frac{29x+7x^2+4x^3}{3(1-x)^2}-\frac{x-35x^2-3x^3-3x^4}{3(1-x)^3}\ln x\\&-\frac{20x^2-x^3+x^4}{2(1-x)^3}\ln^2 x+\frac{4x+x^3}{(1-x)^2}L_2(1-x)\\&+8x\frac{\partial C_0(x)}{\partial x}\ln x_\mu .\end{aligned} \tag{11.17}$$

Similarly,

$$B(x,1/2)=B_0(x)+\frac{\alpha_s}{4\pi}B_1(x,1/2) \tag{11.18}$$

with the one-loop function (Inami and Lim, 1981)

$$B_0(x)=\frac{1}{4}\left[\frac{x}{1-x}+\frac{x}{(1-x)^2}\ln x\right] \tag{11.19}$$

and (Buchalla and Buras, 1993a)

$$\begin{aligned}B_1(x,1/2)=&\frac{13x+3x^2}{3(1-x)^2}-\frac{x-17x^2}{3(1-x)^3}\ln x-\frac{x+3x^2}{(1-x)^3}\ln^2 x\\&+\frac{2x}{(1-x)^2}L_2(1-x)+8x\frac{\partial B_0(x)}{\partial x}\ln x_\mu .\end{aligned} \tag{11.20}$$

The gauge dependence of C and B is cancelled in the combination X [Eq. (11.14)]. The second argument in $B(x,1/2)$ indicates the weak isospin of the external leptons (the neutrinos in this case).

3. The Z^0-penguin contribution in the charm sector

In the next two paragraphs we would like to summarize the essential ingredients of the RG calculation for the charm sector leading to Eqs. (11.10) and (11.13). In particular we present the operators involved, the initial values for the RG evolution of the Wilson coefficients, and the required two-loop anomalous dimensions. We will first treat the Z^0-penguin contribution [Eq. (11.10)] and discuss the box part [Eq. (11.13)] subsequently. Further details can be found in Buchalla and Buras (1994a).

At renormalization scales of the order $\mathcal{O}(M_W)$, after integrating out the W and Z bosons, the effective Hamiltonian responsible for the Z^0-penguin contribution of the charm sector is given by

$$\begin{aligned}\mathcal{H}_{\mathrm{eff},c}^{(Z)}=&\frac{G_F}{\sqrt{2}}\frac{\alpha}{2\pi\sin^2\Theta_W}\lambda_c\frac{\pi^2}{2M_W^2}\\&\times(v_+O_++v_-O_-+v_3Q),\end{aligned} \tag{11.21}$$

where the operator basis is

$$\begin{aligned}O_1=&-i\int d^4x\ T\{(\bar{s}_ic_j)_{V-A}(\bar{c}_jd_i)_{V-A}\}(x)\\&\times\{(\bar{c}_kc_k)_{V-A}(\bar{\nu}\nu)_{V-A}\}(0)-\{c\to u\},\end{aligned} \tag{11.22}$$

$$\begin{aligned}O_2=&-i\int d^4x\ T\{(\bar{s}_ic_i)_{V-A}(\bar{c}_jd_j)_{V-A}\}(x)\\&\times\{(\bar{c}_kc_k)_{V-A}(\bar{\nu}\nu)_{V-A}\}(0)-\{c\to u\},\end{aligned} \tag{11.23}$$

$$O_\pm=\frac{1}{2}(O_2\pm O_1), \tag{11.24}$$

$$Q=\frac{m^2}{g^2}(\bar{s}d)_{V-A}(\bar{\nu}\nu)_{V-A}. \tag{11.25}$$

The Wilson coefficients at $\mu=M_W$ are [$\vec{v}^T\equiv(v_+,v_-,v_3)$]

$$\vec{v}(M_W)=\vec{v}^{(0)}+\frac{\alpha_s(M_W)}{4\pi}\vec{v}^{(1)}, \tag{11.26}$$

$$\vec{v}^{(0)T}=(1,1,0), \tag{11.27}$$

$$\vec{v}^{(1)T}=(B_+,B_-,B_3), \tag{11.28}$$

where in the NDR scheme ($\overline{\mathrm{MS}}$, anticommuting γ_5 in $D\neq4$ dimensions)

$$B_\pm=\pm11\frac{N\mp1}{2N},\quad B_3=16 \tag{11.29}$$

with N denoting the number of colors.

In the basis of operators $\{O_+,O_-,Q\}$ the matrix of anomalous dimensions has the form

$$\gamma=\begin{pmatrix}\gamma_+ & 0 & \gamma_{+3}\\ 0 & \gamma_- & \gamma_{-3}\\ 0 & 0 & \gamma_{33}\end{pmatrix} \tag{11.30}$$

with the perturbative expansion

$$\gamma(\alpha_s)=\frac{\alpha_s}{4\pi}\gamma^{(0)}+\left(\frac{\alpha_s}{4\pi}\right)^2\gamma^{(1)}. \tag{11.31}$$

The nonvanishing entries of the anomalous dimension matrix are

$$\gamma_{33}^{(0)}=2(\gamma_{m0}-\beta_0),\quad \gamma_{33}^{(1)}=2(\gamma_{m1}-\beta_1),$$

$$\gamma_\pm^{(0)}=\pm6\frac{N\mp1}{N},$$

$$\gamma_\pm^{(1)}=\frac{N\mp1}{2N}\left(-21\pm\frac{57}{N}\mp\frac{19}{3}N\pm\frac{4}{3}f\right),$$

$$\gamma_{\pm 3}^{(0)}=\pm 8(N\pm 1), \quad \gamma_{\pm 3}^{(1)}=C_F(\pm 88N-48), \tag{11.32}$$

where γ_{m0}, γ_{m1}, and β_0, β_1 can be found in Eqs. (3.17) and (3.16), respectively. The expressions $\gamma^{(1)}$ refer to the NDR scheme, consistent with the scheme chosen for $\vec{v}(M_W)$. Following the general method for the solution of the RG equations explained in Sec. III.F.1, we can compute the Wilson coefficients $\vec{v}(\mu)$ at a scale $\mu=\mathcal{O}(m_c)$. It is convenient to work in an effective four-flavor theory (f=4) in the full range of the RG evolution from M_W down to μ. The possible inclusion of a b-quark threshold would change the result for X_{NL} by not more than 0.1% and can therefore be safely neglected.

After integrating out the charm quark at the scale $\mu=\mathcal{O}(m_c)$, the Z^0-penguin part of the charm contribution to the effective Hamiltonian becomes

$$\mathcal{H}_{\mathrm{eff},c}^{(Z)}=\frac{G_F}{\sqrt{2}}\frac{\alpha}{2\pi\ \sin^2\Theta_W}\lambda_c C_{NL}(\bar{s}d)_{V-A}(\bar{\nu}\nu)_{V-A}, \tag{11.33}$$

$$C_{\mathrm{NL}}=\frac{x(\mu)}{32}\left[\frac{1}{2}\left(1-\ln\frac{\mu^2}{m^2}\right)(\gamma_{+3}^{(0)}K_+ +\gamma_{-3}^{(0)}K_-) + \frac{4\pi}{\alpha_s(\mu)}v_3(\mu)\right]. \tag{11.34}$$

The explicit expression for $v_3(\mu)$ as obtained from solving the RG equation is given by Buchalla and Buras (1994a). Inserting this expression in Eq. (11.34), expressing the charm quark mass $m(\mu)$ in terms of $m(m)$ and setting N=3, f=4, we finally end up with Eq. (11.10).

4. The box contribution in the charm sector

The RG analysis for the box contribution proceeds in analogy to the Z^0-penguin case. The box part is even somewhat simpler. When the W boson is integrated out, the Hamiltonian based on the box diagram is

$$\mathcal{H}_{\mathrm{eff},c}^{(B)}=-\frac{G_F}{\sqrt{2}}\frac{\alpha}{2\pi\ \sin^2\Theta_W}\lambda_c\left(-\frac{\pi^2}{M_W^2}\right)(c_1 O+c_2 Q), \tag{11.35}$$

$$O=-i\int d^4x\ T\{(\bar{s}c)_{V-A}(\bar{\nu}l)_{V-A}\}(x) \times\{(\bar{l}\nu)_{V-A}(\bar{c}d)_{V-A}\}(0)-\{c\to u\} \tag{11.36}$$

with Q already given in Eq. (11.25). The Wilson coefficients at M_W in the NDR scheme are given by

$$\vec{c}^{\,T}(M_W)\equiv\{c_1(M_W),c_2(M_W)\} =(1,0)+\frac{\alpha_s(M_W)}{4\pi}(0,B_2), \quad B_2=-36. \tag{11.37}$$

In the operator basis $\{O,Q\}$ the anomalous-dimension matrix has the form

$$\gamma=\begin{pmatrix}0 & \gamma_{12}\\ 0 & \gamma_{22}\end{pmatrix}. \tag{11.38}$$

When expanded as

$$\gamma=\frac{\alpha_s}{4\pi}\gamma^{(0)}+\left(\frac{\alpha_s}{4\pi}\right)^2\gamma^{(1)}, \tag{11.39}$$

the nonzero elements are (NDR scheme for $\gamma^{(1)}$)

$$\gamma_{22}^{(0)}=2(\gamma_{m0}-\beta_0), \quad \gamma_{22}^{(1)}=2(\gamma_{m1}-\beta_1),$$
$$\gamma_{12}^{(0)}=-32, \quad \gamma_{12}^{(1)}=80C_F. \tag{11.40}$$

Finally, after integrating out charm at $\mu=\mathcal{O}(m_c)$,

$$\mathcal{H}_{\mathrm{eff},c}^{(B)}=-\frac{G_F}{\sqrt{2}}\frac{\alpha}{2\pi\ \sin^2\Theta_W}\lambda_c 4B_{NL}^{(1/2)} \times(\bar{s}d)_{V-A}(\bar{\nu}_l\nu_l)_{V-A}, \tag{11.41}$$

$$B_{\mathrm{NL}}^{(1/2)}=-\frac{x(\mu)}{64}\left[16\left(\ln\frac{\mu^2}{m^2}+\frac{5}{4}+\frac{r\ \ln r}{1-r}\right) +\frac{4\pi}{\alpha_s(\mu)}c_2(\mu)\right]. \tag{11.42}$$

Equation (11.41) is written here for one neutrino flavor. The index (1/2) refers to the weak isospin of the final-state leptons. From this result Eq. (11.13) can be derived (N=3, f=4). The explicit expression for $c_2(\mu)$ is given by Buchalla and Buras (1994a).

Although Wilson coefficients and anomalous dimensions depend on the renormalization scheme, the final results in Eqs. (11.10) and (11.13) are free from this dependence. The argument proceeds as in the general case presented in Sec. III.F.3.

5. Discussion

It is instructive to consider the function $X(x)$ in the limiting case of small masses ($x\ll 1$), where we keep only terms linear in x and include $\mathcal{O}(\alpha_s)$ corrections,

$$X(x)\doteq-\frac{3}{4}x\ \ln x-\frac{1}{4}x+\frac{\alpha_s}{4\pi}\left(-2x\ \ln^2 x-7x\ \ln x -\frac{23+2\pi^2}{3}x\right). \tag{11.43}$$

This simple and transparent expression can be regarded as a common limiting case of the top and the charm contribution: on the one hand it follows from keeping only terms linear in x in the top function [Eq. (11.5)], and on the other hand it can be obtained [up to the last term in Eq. (11.43), which is $\mathcal{O}(\alpha_s x)$ and goes beyond the NLLA] from expanding X_{NL} (Eq. 11.9) (for m_l=0) to first order in α_s.

This exercise provides one with a nice cross-check between the rather different looking functions X_{NL} and $X(x_t)$ of the charm and the top sector. Viewed the other way around, Eq. (11.43) may serve to further illustrate the complementary character of the calculations necessary in each of the two sectors. $X(x_t)$ is the generalization of Eq. (11.43) that includes all the higher-order mass terms. X_{NL}, on the other hand, generalizes Eq. (11.43) to include all the leading-logarithmic,

TABLE XXXIV. Residual scale ambiguity in the top and charm sector in LLA and NLLA.

	Top sector $[\mu_t=\mathcal{O}(m_t)]$	Charm sector $[\mu_c=\mathcal{O}(m_c)]$
LLA	$\mathcal{O}(\alpha_s)$	$\mathcal{O}(x_c)$
NLLA	$\mathcal{O}(\alpha_s^2)$	$\mathcal{O}(\alpha_s x_c)$

$\mathcal{O}(x\alpha_s^n \ln^{n+1}x)$, as well as the next-to-leading-logarithmic, $\mathcal{O}(x\alpha_s^n \ln^n x)$, corrections, to all orders n in α_s. Of these, only the terms with $n=0$ and $n=1$ are contained in Eq. (11.43). Applying this approximation to the charm part directly, one can convince oneself that the $\mathcal{O}(\alpha_s)$ correction term would amount to more than 50% of the lowest order result. This observation illustrates very clearly the necessity to go beyond straightforward perturbation theory and to employ the RG summation technique. The importance of also going to next-to-leading-order accuracy in the RG calculation is suggested by the relatively large size of the $\mathcal{O}(x\alpha_s \ln x)$ term. Note also that formally the nonlogarithmic mass term $(-x/4)$ in Eq. (11.43) is a next-to-leading-order effect in the framework of RG-improved perturbation theory. The same is true for the dependence on the charged lepton mass, which can be taken into account consistently only in NLLA.

A crucial issue is the residual dependence of the functions $X_{\rm NL}$ and $X(x_t)$ on the corresponding renormalization scales μ_c and μ_t. Since the quark current operator in Eq. (11.1) has no anomalous dimension, its matrix elements do not depend on the renormalization scale. The same must then hold for the coefficient functions $X_{\rm NL}$ and $X(x_t)$. However, in practice this is only true up to terms of the neglected order in perturbation theory. The resulting scale ambiguities represent the theoretical uncertainties present in the calculation of the short-distance-dominated processes under discussion. They can be systematically reduced by going to higher orders in the analysis. In Table XXXIV we compare the order of the residual scale dependence in LLA and in NLLA for the top and the charm contribution.

For numerical investigations we shall use 1 GeV$\leq\mu_c\leq$3 GeV for the renormalization scale $\mu_c=\mathcal{O}(m_c)$ in the charm sector. Similarly, in the case of the top contribution we choose $\mu_t=\mathcal{O}(m_t)$ in the range 100 GeV$\leq\mu_t\leq$300 GeV for m_t=170 GeV. Then, comparing LLA and NLLA, the theoretical uncertainty due to scale ambiguity is typically reduced from $\mathcal{O}(10\%)$ to $\mathcal{O}(1\%)$ in the top sector and from more than 50% to less than 20% in the charm sector. Here the quoted percentages refer to the total variation $(X_{\rm max}-X_{\rm min})/X_{\rm central}$ of the functions $X(x_t)$ or $X_{\rm NL}$ within the range of scales considered. Phenomenological implications of this gain in accuracy will be discussed in Sec. XXIV.

C. The decay $(K_L\to\mu^+\mu^-)_{\rm SD}$

1. The next-to-leading-order effective Hamiltonian

The analysis of $(K_L\to\mu^+\mu^-)_{\rm SD}$ proceeds in essentially the same manner as for $K^+\to\pi^+\nu\bar{\nu}$. The only difference is introduced through the reversed lepton line in the box contribution. In particular there is no lepton mass dependence, since only massless neutrinos appear as virtual leptons in the box diagram.

The effective Hamiltonian in next to leading order can be written as follows,

$$\mathcal{H}_{\rm eff}=-\frac{G_F}{\sqrt{2}}\frac{\alpha}{2\pi\sin^2\Theta_W}[V_{cs}^*V_{cd}Y_{\rm NL}+V_{ts}^*V_{td}Y(x_t)]\times(\bar{s}d)_{V-A}(\bar{\mu}\mu)_{V-A}+\text{H.c.}, \tag{11.44}$$

where H.c. stands for the Hermitian conjugate. The function $Y(x)$ is given by

$$Y(x)=Y_0(x)+\frac{\alpha_s}{4\pi}Y_1(x), \tag{11.45}$$

where (Inami and Lim, 1981)

$$Y_0(x)=\frac{x}{8}\left[\frac{4-x}{1-x}+\frac{3x}{(1-x)^2}\ln x\right] \tag{11.46}$$

and (Buchalla and Buras, 1993a)

$$Y_1(x)=\frac{4x+16x^2+4x^3}{3(1-x)^2}-\frac{4x-10x^2-x^3-x^4}{(1-x)^3}\ln x+\frac{2x-14x^2+x^3-x^4}{2(1-x)^3}\ln^2 x+\frac{2x+x^3}{(1-x)^2}\times L_2(1-x)+8x\frac{\partial Y_0(x)}{\partial x}\ln x_\mu. \tag{11.47}$$

The RG expression $Y_{\rm NL}$ representing the charm contribution is

$$Y_{\rm NL}=C_{\rm NL}-B_{\rm NL}^{(-1/2)}, \tag{11.48}$$

where $C_{\rm NL}$ is the Z^0-penguin part given in Eq. (11.10) and $B_{\rm NL}^{(1/2)}$ is the box contribution in the charm sector, relevant for the case of final-state leptons with weak isospin T_3=−1/2. One has (Buchalla and Buras, 1994a),

$$B_{\rm NL}^{(-1/2)}=\frac{x(m)}{4}K_c^{24/25}\left[3(1-K_2)\left(\frac{4\pi}{\alpha_s(\mu)}+\frac{15212}{1875}\times(1-K_c^{-1})\right)-\ln\frac{\mu^2}{m^2}-\frac{329}{12}+\frac{15212}{625}K_2+\frac{30581}{7500}KK_2\right]. \tag{11.49}$$

Note the simple relation to $B_{\rm NL}^{(1/2)}$ in Eq. (11.13) (for r=0)

$$B_{\rm NL}^{(-1/2)}-B_{\rm NL}^{(1/2)}=\frac{x(m)}{2}K_c^{24/25}(KK_2-1). \tag{11.50}$$

More details on the RG analysis in this case may be found in Buchalla and Buras (1994a).

2. Discussion

The gauge-independent function Y can be decomposed into the Z^0-penguin and the box contribution

TABLE XXXV. The function $Y_{\rm NL}$ for various $\Lambda^{(4)}_{\overline{\rm MS}}$ and m_c.

	$Y_{\rm NL}/10^{-4}$		
$\Lambda^{(4)}_{\overline{\rm MS}}$ [MeV]\$m_c$ [GeV]	1.25	1.30	1.35
215	3.09	3.31	3.53
325	3.27	3.50	3.73
435	3.40	3.64	3.89

$$Y(x)=C(x)-B(x,-1/2). \tag{11.51}$$

In Feynman-gauge for the W boson, $C(x)$ is given in Eq. (11.15). In the same gauge the box contribution is

$$B(x,-1/2)=B_0(x)+\frac{\alpha_s}{4\pi}B_1(x,-1/2) \tag{11.52}$$

with $B_0(x)$ from Eq. (11.19) and

$$\begin{aligned}B_1(x,-1/2)=&\frac{25x-9x^2}{3(1-x)^2}+\frac{11x+5x^2}{3(1-x)^3}\ln x\\&-\frac{x+3x^2}{(1-x)^3}\ln^2 x+\frac{2x}{(1-x)^2}L_2(1-x)\\&+8x\frac{\partial B_0(x)}{\partial x}\ln x_\mu .\end{aligned} \tag{11.53}$$

The equality $B(x,1/2)=B(x,-1/2)$ at the one-loop level is a particular property of the Feynman-gauge. It is violated by $\mathcal{O}(\alpha_s)$ corrections. There is, however, a very simple relation between $B_1(x,1/2)$ and $B_1(x,-1/2)$,

$$B_1(x,-1/2)-B_1(x,1/2)=16B_0(x). \tag{11.54}$$

We add a few comments on the most important differences between $Y_{\rm NL}$ and $X_{\rm NL}$. Expanding $Y_{\rm NL}$ to first order in α_s, we find

$$Y_{NL}\doteq\frac{1}{2}x+\frac{\alpha_s}{4\pi}x\ln^2 x+\mathcal{O}(\alpha_s x). \tag{11.55}$$

In contrast to $X_{\rm NL}$ both the terms of $\mathcal{O}(x\ln x)$ and of $\mathcal{O}(\alpha_s x\ln x)$ are absent in $Y_{\rm NL}$. The cancellation of the leading $\mathcal{O}(x\ln x)$ terms between Z^0-penguin and box contribution implies that the nonleading $\mathcal{O}(x)$ term plays a much bigger role for $Y_{\rm NL}$. A second consequence is the increased importance of QCD effects and the related larger sensitivity to μ_c, resulting in a bigger theoretical uncertainty for $Y_{\rm NL}$ than was the case for $X_{\rm NL}$. In addition, whereas $X(x_c)$ is suppressed by ~30% through QCD effects, the zeroth-order expression for Y is enhanced by as much as a factor of 2.5. Nevertheless, QCD corrections included, $X_{\rm NL}$ still exceeds Y_{NL} by a factor of 4, so that $Y_{\rm NL}$ is less important for $(K_L\to\mu^+\mu^-)_{\rm SD}$ than $X_{\rm NL}$ is for $K^+\to\pi^+\nu\bar\nu$. Although the impact of the bigger uncertainties in Y_{NL} is thus somewhat reduced in the complete result for $(K_L\to\mu^+\mu^-)_{\rm SD}$, the remaining theoretical uncertainty due to scale ambiguity is still larger than for $K^+\to\pi^+\nu\bar\nu$. This will be investigated numerically in Sec. XXV. The numerical values for $Y_{\rm NL}$ for $\mu=m_c$ and several values of $\Lambda^{(4)}_{\overline{\rm MS}}$ and m_c are given in Table XXXV.

D. The decays $K_L\to\pi^0\nu\bar\nu$, $B\to X_{s,d}\nu\bar\nu$, and $B_{s,d}\to l^+l^-$

After the above discussion it is easy to write down the effective Hamiltonians for $K_L\to\pi^0\nu\bar\nu$, $B\to X_{s,d}\nu\bar\nu$, and $B_{s,d}\to l^+l^-$. As we have seen, only the top contribution is important in these cases, and we can write

$$\begin{aligned}\mathcal{H}_{\rm eff}=&\frac{G_F}{\sqrt{2}}\frac{\alpha}{2\pi\sin^2\Theta_W}V^*_{tn'}V_{tn'}X(x_t)\\&\times(\bar n n')_{V-A}(\bar\nu\nu)_{V-A}+\text{H.c.}\end{aligned} \tag{11.56}$$

for the decays $K_L\to\pi^0\nu\bar\nu$, $B\to X_s\nu\bar\nu$, and $B\to X_d\nu\bar\nu$, with $(\bar n n')=(\bar s d)$, $(\bar b s)$, and $(\bar b d)$, respectively. Similarly,

$$\begin{aligned}\mathcal{H}_{\rm eff}=&-\frac{G_F}{\sqrt{2}}\frac{\alpha}{2\pi\sin^2\Theta_W}V^*_{tn'}V_{tn'}Y(x_t)\\&\times(\bar n n')_{V-A}(\bar l l)_{V-A}+\text{H.c.}\end{aligned} \tag{11.57}$$

for $B_s\to l^+l^-$ and $B_d\to l^+l^-$, with $(\bar n n')=(\bar b s)$ and $(\bar b d)$. The functions X and Y are given in Eqs. (11.5) and (11.45).

XII. THE EFFECTIVE HAMILTONIAN FOR K^0-$\bar K^0$ MIXING

A. General structure

The following section is devoted to the presentation of the effective Hamiltonian for $\Delta S=2$ transitions. This Hamiltonian incorporates the short-distance physics contributing to K^0-$\bar K^0$ mixing and is essential for the description of CP violation in the neutral K-meson system.

Being a FCNC process, K^0-$\bar K^0$ mixing can only occur at the loop level within the standard model. To lowest order it is induced through the box diagrams in Fig. 4(e). With QCD corrections included, the effective low-energy Hamiltonian derived from these diagrams can be written as follows ($\lambda_i=V^*_{is}V_{id}$),

$$\begin{aligned}\mathcal{H}^{\Delta S=2}_{\rm eff}=&\frac{G_F^2}{16\pi^2}M_W^2[\lambda_c^2\eta_1 S_0(x_c)+\lambda_t^2\eta_2 S_0(x_t)\\&+2\lambda_c\lambda_t\eta_3 S_0(x_c,x_t)][\alpha_s(\mu)]^{-2/9}\\&\times\left[1+\frac{\alpha_s(\mu)}{4\pi}J_3\right]Q+\text{H.c.}\end{aligned} \tag{12.1}$$

This equation, together with Eqs. (12.31), (12.10), and (12.68), for η_1, η_2, and η_3, respectively, represents the complete next-to-leading-order short-distance Hamiltonian for $\Delta S=2$ transitions. Equation (12.1) is valid for scales μ below the charm threshold $\mu_c=\mathcal{O}(m_c)$. In this case $\mathcal{H}^{\Delta S=2}_{\rm eff}$ consists of a single four-quark operator

$$Q=(\bar s d)_{V-A}(\bar s d)_{V-A}, \tag{12.2}$$

which is multiplied by the corresponding coefficient function. It is useful and customary to decompose this function into a charm, a top, and a mixed charm-top contribution, as displayed in Eq. (12.1). This form is obtained upon eliminating λ_u by means of CKM matrix

unitarity and setting $x_u=0$. The basic electroweak loop contributions without QCD correction are then expressed through the functions S_0, which read (Inami and Lim, 1981)

$$S_0(x_c)\doteq x_c, \tag{12.3}$$

$$S_0(x_t)=\frac{4x_t-11x_t^2+x_t^3}{4(1-x_t)^2}-\frac{3x_t^3\ln x_t}{2(1-x_t)^3}, \tag{12.4}$$

$$S_0(x_c,x_t)=x_c\left[\ln\frac{x_t}{x_c}-\frac{3x_t}{4(1-x_t)}-\frac{3x_t^2\ln x_t}{4(1-x_t)^2}\right]. \tag{12.5}$$

Here again we keep only linear terms in $x_c\ll 1$, but of course all orders in x_t.

Short-distance QCD effects are described through the correction factors η_1, η_2, η_3, and the explicitly α_s-dependent terms in Eq. (12.1). The discussion of these corrections will be the subject of the following sections.

Without QCD, i.e., in the limit $\alpha_s\to 0$, one has $\eta_i[\alpha_s]^{-2/9}\to 1$. In general, the complete coefficient function multiplying Q in Eq. (12.1) contains the QCD effects at high energies, $\mu_W=\mathcal{O}(M_W)$, $\mu_t=\mathcal{O}(m_t)$, together with their RG evolution down to the scale $\mu=\mathcal{O}(1\text{ GeV})$. A common ingredient for the three different contributions in Eq. (12.1) is the anomalous dimension of the operator Q and the corresponding evolution of its coefficient. The Fierz symmetric flavor structure of Q implies that it acquires the same anomalous dimension as the Fierz symmetric operator $Q_+=(Q_2+Q_1)/2$ (see Sec. V), explicitly,

$$\gamma=\frac{\alpha_s}{4\pi}\,\gamma^{(0)}+\left(\frac{\alpha_s}{4\pi}\right)^2\gamma^{(1)}, \tag{12.6}$$

$$\begin{aligned}\gamma^{(0)}&=6\,\frac{N-1}{N},\\ \gamma^{(1)}&=\frac{N-1}{2N}\left[-21+\frac{57}{N}-\frac{19}{3}N+\frac{4}{3}f\right]\ \text{(NDR)}.\end{aligned} \tag{12.7}$$

The resulting evolution of the coefficient of Q between general scales μ_1 and μ is then given by

$$C_Q(\mu)=\left[1+\frac{\alpha_s(\mu)-\alpha_s(\mu_1)}{4\pi}J_f\right]\left[\frac{\alpha_s(\mu_1)}{\alpha_s(\mu)}\right]^{d_f}C_Q(\mu_1), \tag{12.8}$$

where

$$d_f=\frac{\gamma^{(0)}}{2\beta_0},\quad J_f=\frac{d_f}{\beta_0}\,\beta_1-\frac{\gamma^{(1)}}{2\beta_0} \tag{12.9}$$

depend on the number of active flavors f. At the lower end of the evolution $f=3$. The terms in Eq. (12.8) that depend on $\alpha_s(\mu)$ are factored out explicitly in Eq. (12.1) to exhibit the μ dependence of the coefficient function in the $f=3$ regime, which has to cancel the corresponding μ dependence of the hadronic matrix element of Q between meson states in physical applications. A similar comment applies to the scheme dependence entering J_f in Eq. (12.9) through the scheme dependence of $\gamma^{(1)}$. Splitting off the μ dependence in Eq. (12.1) is of course not unique. The way it is done belongs to the *definition* of the η_i factors. Let us finally compare the structure of Eq. (12.1) with the effective Hamiltonians for rare decays discussed in Sec. XI. Common features of both types of processes include

(i) Both are generated to lowest order via electroweak FCNC loop transitions involving heavy quarks.

(ii) They contain a charm and a top contribution.

(iii) The Hamiltonian consists of a single dimension-six operator.

Aside from these similarities, however, there are also a few important differences, which have their root in the fact that the $\Delta S=2$ box diagrams involve two distinct quark lines, as compared to the single quark line in semileptonic rare decays,

(i) The CKM parameter combinations λ_i appear quadratically in Eq. (12.1) instead of only linearly.

(ii) Equation (12.1) in addition receives contributions from a mixed top-charm sector. This part turns out to have the most involved structure of the three contributions.

(iii) The operator Q has a nonvanishing QCD anomalous dimension, resulting in a nontrivial scale and scheme dependence of the Wilson coefficient.

(iv) The hadronic matrix element of the four-quark operator Q is a considerably more complicated object than the quark-current matrix elements in semileptonic rare decays.

We will now present the complete next-to-leading-order results for η_2, η_1, and η_3 in turn and discuss their most important theoretical features. The first leading-logarithmic-order calculations of η_1 have been presented by Vainshtein *et al.* (1976) and Novikov *et al.* (1977) and of η_2 by Vysotskij (1980). The complete leading-logarithmic-order calculation, which also includes η_3, was first performed by Gilman and Wise (1983). Leading-order calculations in the presence of a heavy top can be found in work by Kaufman *et al.* (1989), Datta *et al.* (1990, 1995), and Flynn (1990).

B. The top contribution—η_2

The basic structure of the top-quark sector in $\mathcal{H}_{\text{eff}}^{\Delta S=2}$ is easy to understand. First the top quark is integrated out, along with the W, at a matching scale $\mu_t=\mathcal{O}(m_t)$, leaving a m_t-dependent coefficient normalized at μ_t, which multiplies the single operator Q. Subsequently, the coefficient is simply renormalized down to scales $\mu=\mathcal{O}(1\text{ GeV})$ by means of Eq. (12.8). Including NLO corrections, the resulting QCD factor η_2 from Eq. (12.1) may be written (in $\overline{\text{MS}}$) as follows (Buras *et al.*, 1990),

$$\eta_2=[\alpha_s(m_c)]^{6/27}\left[\frac{\alpha_s(m_b)}{\alpha_s(m_c)}\right]^{6/25}\left[\frac{\alpha_s(\mu_t)}{\alpha_s(m_b)}\right]^{6/23}$$
$$\times\left[1+\frac{\alpha_s(m_c)}{4\pi}(J_4-J_3)+\frac{\alpha_s(m_b)}{4\pi}(J_5-J_4)\right.$$
$$+\frac{\alpha_s(\mu_t)}{4\pi}\left(\frac{S_1(x_t)}{S_0(x_t)}+B_t-J_5+\frac{\gamma^{(0)}}{2}\ln\frac{\mu_t^2}{M_W^2}\right.$$
$$\left.\left.+\gamma_{m0}\frac{\partial\ln S_0(x_t)}{\partial\ln x_t}\ln\frac{\mu_t^2}{M_W^2}\right)\right], \tag{12.10}$$

where $\gamma_{m0}=6C_F$,

$$B_t=5\frac{N-1}{2N}+3\frac{N^2-1}{2N}\quad(\text{NDR}), \tag{12.11}$$

and

$$S_1(x)=\frac{N-1}{2N}S_1^{(8)}(x)+\frac{N^2-1}{2N}S_1^{(1)}(x), \tag{12.12}$$

$$S_1^{(8)}(x)=-\frac{64-68x-17x^2+11x^3}{4(1-x)^2}$$
$$+\frac{32-68x+32x^2-28x^3+3x^4}{2(1-x)^3}\ln x$$
$$+\frac{x^2(4-7x+7x^2-2x^3)}{2(1-x)^4}\ln^2 x$$
$$+\frac{2x(4-7x-7x^2+x^3)}{(1-x)^3}L_2(1-x)$$
$$+\frac{16}{x}\left(\frac{\pi^2}{6}-L_2(1-x)\right), \tag{12.13}$$

$$S_1^{(1)}(x)=-\frac{x(4-39x+168x^2+11x^3)}{4(1-x)^3}$$
$$-\frac{3x(4-24x+36x^2+7x^3+x^4)}{2(1-x)^4}\ln x$$
$$+\frac{3x^3(13+4x+x^2)}{2(1-x)^4}\ln^2 x$$
$$-\frac{3x^3(5+x)}{(1-x)^3}L_2(1-x), \tag{12.14}$$

where the dilogarithm L_2 is defined in Eq. (11.8).

In Eq. (12.10) we have taken into account the heavy-quark thresholds at m_b and m_c in the RG evolution. As it must be, the dependence on the threshold scales is of the neglected order $\mathcal{O}(\alpha_s^2)$. In fact the threshold ambiguity here is also of $\mathcal{O}(\alpha_s^2)$ in LLA, since $\gamma^{(0)}$ is flavor independent. It turns out that this dependence is also very weak numerically, and we therefore set $\mu_c=m_c$ and $\mu_b=m_b$. Furthermore, it is a good approximation to neglect the b threshold completely using an effective four-flavor theory from μ_t down to m_c. This can be achieved by simply substituting $m_b\to\mu_t$ in Eq. (12.10).

The leading-order expression for η_2 is given by the first three factors on the rhs of Eq. (12.10). The fourth factor represents the next-to-leading-order generalization. Let us discuss now the most interesting and important features of the NLO result for η_2 exhibited in Eq. (12.10).

(i) η_2 is proportional to the initial value of the Wilson coefficient function at $\mu_t=M_W$

$$S(x)=S_0(x)+\frac{\alpha_s}{4\pi}[S_1(x)+B_tS_0(x)], \tag{12.15}$$

which has to be extracted from the box graphs in Fig. 4(e) and the corresponding gluon correction diagrams after a proper factorization of long- and short-distance contributions.

(ii) $S(x)$ in Eq. (12.15) is similar to the functions $X(x)$ and $Y(x)$ in Secs. XI.B.1 and XI.C.1, except that $S(x)$ is scheme dependent due to the renormalization that is required for the operator Q. This scheme dependence enters Eq. (12.15) through the scheme-dependent constant B_t, given in the NDR scheme in Eq. (12.11). This scheme dependence is cancelled in the combination B_t-J_5 by the two-loop anomalous dimension contained in J_5. Likewise, the scheme dependence of J_f cancels in the differences (J_f-J_{f-1}), as is evident from the discussion of Sec. III.F.3.

(iii) A very important point is the dependence on the high-energy matching scale μ_t. This dependence enters the NLO $\alpha_s(\mu_t)$ correction in Eq. (12.10) in two distinct ways: first as a term proportional to $\gamma^{(0)}$, and, secondly, in conjunction with γ_{m0}. The first of these terms cancels, to $\mathcal{O}(\alpha_s)$, the μ_t dependence present in the leading term $[\alpha_s(\mu_t)]^{6/23}$. The second, on the other hand, leads to an $\mathcal{O}(\alpha_s)\mu_t$ dependence of η_2. This is just the dependence needed to cancel the μ_t ambiguity of the leading function $S_0(x_t(\mu_t))$ in the product $\eta_2S_0(x_t)$, such that the physical results become independent of μ_t to $\mathcal{O}(\alpha_s)$. From these observations it is obvious that one may interpret μ_t in the first case as the initial scale of the RG evolution and in the second case as the scale at which the top-quark mass is defined. These two scales need not necessarily have the same value. The important point is that, to leading logarithmic accuracy, the μ_t dependence of both $\eta_2^{LO}(\mu_t)$ and $S_0(x_t(\mu_t))$ remains uncompensated, leaving a disturbingly large uncertainty in the short-distance calculation.

(iv) It is interesting to note that, in the limit $m_t\gg M_W$, the dependence on μ_t enters η_2 as $\ln\mu_t/m_t$, rather than $\ln\mu_t/M_W$. This feature provides a formal justification for choosing $\mu_t=\mathcal{O}(m_t)$ instead of $\mu_t=\mathcal{O}(M_W)$. An explicit expression for the large-m_t limit in the similar case of η_{2B} may be found in Sec. XIII.

(v) Although at NLO the product $\eta_2S_0(x_t)$ depends only very weakly on the precise value of μ_t as long as it is of $\mathcal{O}(m_t)$, the choice $\mu_t=m_t$ is again convenient. With this choice η_2 becomes almost independent of the top quark mass m_t. By contrast, for $\mu_t=M_W$, say, η_2 would decrease with rising m_t in order to compensate for the increase of $S_0(x_t(M_W))$ due to the use of a, for high m_t, ''unnaturally'' low scale M_W.

(vi) As mentioned above the dependence of the Wilson coefficient on the low-energy scale μ and the re-

maining scheme dependence (J_3) has been factored out explicitly in Eq. (12.1). Therefore the QCD correction factor η_2 is *by definition* scale and scheme independent on the lower end of the RG evolution.

C. The charm contribution—η_1

The calculation of η_1 beyond leading logarithmic order has been presented in great detail by Herrlich and Nierste (1994) and Herrlich (1994). Our task here will be to briefly describe the basic procedure and to summarize the main results.

In principle the charm contribution is similar in structure to the top contribution. However, since the quark mass $m_c \ll M_W$, the charm degrees of freedom can no longer be integrated out simultaneously with the W boson, which would introduce large logarithmic corrections $\sim\alpha_s \ln M_W/m_c$. To resum these logarithms one first constructs an effective theory at a scale $\mathcal{O}(M_W)$, where the W boson is removed. The relevant operators are subsequently renormalized down to scales $\mu_c=\mathcal{O}(m_c)$, where the charm quark is then integrated out. After this step only the operator Q [Eq. (12.2)] remains, and η_1 is finally obtained as discussed in Sec. XII.A.

Let us briefly outline the procedure for the case at hand. After integrating out the W, the effective Hamiltonian to first order in weak interactions, which is needed for the charm contribution, can be written as

$$\mathcal{H}_c^{(1)}=\frac{G_F}{\sqrt{2}}\sum_{q,q'=u,c} V_{q's}^* V_{qd}(C_+ Q_+^{q'q}+C_- Q_-^{q'q}), \tag{12.16}$$

where we have introduced the familiar $\Delta S=1$ four-quark operators in the multiplicatively renormalizable basis

$$Q_\pm^{q'q}=\tfrac{1}{2}[(\bar{s}_i q_i')_{V-A}(\bar{q}_j d_j)_{V-A} \pm(\bar{s}_i q_j')_{V-A}(\bar{q}_j d_i)_{V-A}]. \tag{12.17}$$

We remark that no penguin operators appear in the present case due to GIM cancellation between charm-quark and up-quark contributions.

$\Delta S=2$ transitions occur to second order in the effective interaction [Eq. (12.16)]. The $\Delta S=2$ effective Hamiltonian is therefore given by

$$\mathcal{H}_{\mathrm{eff},c}^{\Delta S=2}=-\frac{i}{2}\int d^4x\ T(\mathcal{H}_c^{(1)}(x)\mathcal{H}_c^{(1)}(0)). \tag{12.18}$$

Inserting Eq. (12.16) into Eq. (12.18), keeping only pieces that can contribute to the charm box diagrams and taking the GIM constraints into account, one obtains

$$\mathcal{H}_{\mathrm{eff},c}^{\Delta S=2}=\frac{G_F^2}{2}\lambda_c^2\sum_{i,j=+,-} C_i C_j O_{ij}, \tag{12.19}$$

where

$$O_{ij}=-\frac{i}{2}\int d^4x\ T[Q_i^{cc}(x)Q_j^{cc}(0)-Q_i^{uc}(x)Q_j^{cu}(0) -Q_i^{cu}(x)Q_j^{uc}(0)+Q_i^{uu}(x)Q_j^{uu}(0)]. \tag{12.20}$$

From the derivation of Eq. (12.19) it is evident that the Wilson coefficients of the bilocal operators O_{ij} are simply given by the product C_iC_j of the coefficients pertaining to the local operators Q_i, Q_j. The evolution of the C_i from M_W down to μ_c proceeds in the standard fashion and is described by equations of the type shown in Eq. (12.8) with the appropriate anomalous dimensions inserted. In the following we list the required ingredients. The Wilson coefficients at scale $\mu=M_W$ are

$$C_\pm(M_W)=1+\frac{\alpha_s(M_W)}{4\pi}B_\pm, \tag{12.21}$$

$$B_\pm=\pm 11\frac{N\mp 1}{2N}\quad(\mathrm{NDR}). \tag{12.22}$$

The two-loop anomalous dimensions are

$$\gamma_\pm=\frac{\alpha_s}{4\pi}\gamma_\pm^{(0)}+\left(\frac{\alpha_s}{4\pi}\right)^2\gamma_\pm^{(1)}, \tag{12.23}$$

$$\gamma_\pm^{(0)}=\pm 6\frac{N\mp 1}{N},$$

$$\gamma_\pm^{(1)}=\frac{N\mp 1}{2N}\left[-21\pm\frac{57}{N}\mp\frac{19}{3}N\pm\frac{4}{3}f\right].\quad(\mathrm{NDR}) \tag{12.24}$$

For $i,j=+,-$ we introduce

$$d_i^{(f)}=\frac{\gamma_i^{(0)}}{2\beta_0},\quad J_i^{(f)}=\frac{d_i^{(f)}}{\beta_0}\beta_1-\frac{\gamma_i^{(1)}}{2\beta_0} \tag{12.25}$$

and

$$d_{ij}^{(f)}=d_i^{(f)}+d_j^{(f)},\quad J_{ij}^{(f)}=J_i^{(f)}+J_j^{(f)}. \tag{12.26}$$

The essential step consists in matching Eq. (12.19) onto an effective theory without charm, which will contain the single operator $Q=(\bar{s}d)_{V-A}(\bar{s}d)_{V-A}$. In NLO this matching has to be performed to $\mathcal{O}(\alpha_s)$. At a normalization scale μ_c it reads explicitly, expressed in terms of operator matrix elements ($i,j=+,-$),

$$\langle O_{ij}\rangle=\frac{m_c^2(\mu_c)}{8\pi^2}\left[\tau_{ij}+\frac{\alpha_s(\mu_c)}{4\pi}\left(\kappa_{ij}\ln\frac{\mu_c^2}{m_c^2}+\beta_{ij}\right)\right]\langle Q\rangle, \tag{12.27}$$

$$\tau_{++}=\frac{N+3}{4},\quad \tau_{+-}=\tau_{-+}=-\frac{N-1}{4},\quad \tau_{--}=\frac{N-1}{4}, \tag{12.28}$$

$$\kappa_{++}=3(N-1)\tau_{++},\quad \kappa_{+-}=\kappa_{-+}=3(N+1)\tau_{+-},$$

$$\kappa_{--}=3(N+3)\tau_{--}. \tag{12.29}$$

The β_{ij} are scheme dependent. In the NDR scheme they are given by (Herrlich and Nierste, 1994)

$$\beta_{++}=(1-N)\left(\frac{N^2-6}{12N}\,\pi^2+3\,\frac{-N^2+2N+13}{4N}\right),$$
$$\beta_{+-}=\beta_{-+}=(1-N)\left(\frac{-N^2+2N-2}{12N}\,\pi^2+\frac{3N^2+13}{4N}\right),$$
$$\beta_{--}=(1-N)\left(\frac{N^2-4N+2}{12N}\,\pi^2-\frac{3N^2+10N+13}{4N}\right). \tag{12.30}$$

Now, starting from Eq. (12.19), evolving C_i from M_W down to μ_c, integrating out charm at μ_c with the help of Eq. (12.27), evolving the resulting coefficient according to Eq. (12.8), and recalling the definition of η_1 in Eq. (12.1), one finally obtains

$$\eta_1=[\alpha_s(\mu_c)]^{d_3}\sum_{i,j=+,-}\left(\frac{\alpha_s(m_b)}{\alpha_s(\mu_c)}\right)^{d_{ij}^{(4)}}\left(\frac{\alpha_s(M_W)}{\alpha_s(m_b)}\right)^{d_{ij}^{(5)}}$$
$$\times\left[\tau_{ij}+\frac{\alpha_s(\mu_c)}{4\pi}\left(\kappa_{ij}\ln\frac{\mu_c^2}{m_c^2}+\tau_{ij}(J_{ij}^{(4)}-J_3)+\beta_{ij}\right)\right.$$
$$+\tau_{ij}\left(\frac{\alpha_s(m_b)}{4\pi}\,(J_{ij}^{(5)}-J_{ij}^{(4)})+\frac{\alpha_s(M_W)}{4\pi}\right.$$
$$\left.\left.\times(B_i+B_j-J_{ij}^{(5)})\right)\right]. \tag{12.31}$$

We conclude this section with a discussion of a few important issues concerning the structure of this formula.

(i) Equation (12.31), as first obtained by Herrlich and Nierste (1994), represents the next-to-leading-order generalization of the leading-logarithmic-order expression for η_1 given by Gilman and Wise (1983). The latter follows as a special case of Eq. (12.31) when the $\mathcal{O}(\alpha_s)$ correction terms are put to zero.

(ii) Equation (12.31) is independent of the renormalization scheme up to terms of the neglected order $\mathcal{O}(\alpha_s^2)$. We have written η_1 in a form in which this scheme independence becomes manifest. While the various J terms, B_i, and β_{ij} in Eq. (12.31) all depend on the renormalization scheme when considered separately, the combinations $\tau_{ij}(J_{ij}^{(4)}-J_3)+\beta_{ij}$, $J_{ij}^{(5)}-J_{ij}^{(4)}$, and $B_i+B_j-J_{ij}^{(5)}$ are scheme invariant.

(iii) The product $\eta_1(\mu_c)x_c(\mu_c)$ is independent of μ_c to the considered order,

$$\frac{d}{d\,\ln\mu_c}\,\eta_1(\mu_c)x_c(\mu_c)=\mathcal{O}(\alpha_s^2), \tag{12.32}$$

in accordance with the requirements of renormalization-group invariance. The cancellation of the μ_c dependence to $\mathcal{O}(\alpha_s)$ is related to the presence of an explicitly μ_c-dependent term at NLO in Eq. (12.31) and is guaranteed through the identity

$$\kappa_{ij}=\tau_{ij}\left(\gamma_{m0}+\frac{\gamma^{(0)}}{2}-\frac{\gamma_i^{(0)}+\gamma_j^{(0)}}{2}\right), \tag{12.33}$$

which is easily verified using Eqs. (3.17), (12.7), (12.24), (12.28), and (12.29).

(iv) Also the ambiguity in the scale μ_W, at which W is integrated out, is reduced from $\mathcal{O}(\alpha_s)$ to $\mathcal{O}(\alpha_s^2)$ when going from leading to next to leading order. As mentioned above the dependence on the b-threshold scale μ_b is $\mathcal{O}(\alpha_s^2)$ in NLLA as well as in LLA. Numerically the dependence on μ_b is very small. Also the variation of the result with the high-energy matching scale μ_W is considerably weaker than the residual dependence on μ_c. Therefore we have set $\mu_b=m_b$ and $\mu_W=M_W$ in Eq. (12.31). In numerical analyses we will take the dominant μ_c dependence as representative for the short-distance scale ambiguity of η_1. The generalization to the case $\mu_W\neq M_W$ is discussed by Herrlich and Nierste (1994). The more general case $\mu_b\neq m_b$ is trivially obtained by substituting $m_b\to\mu_b$ in Eq. (12.31).

(v) Note that, due to the GIM structure of O_{ij}, no mixing under infinite renormalization occurs between O_{ij} and the local operator Q. This is related to the absence of the logarithm in the function $S_0(x_c)$ in Eq. (12.3).

It is instructive to compare the results obtained for η_1 and η_2. Expanding Eq. (12.31) to first order in α_s, in this way "switching off" the RG summations, we find

$$[\alpha_s(\mu)]^{-2/9}\left(1+\frac{\alpha_s(\mu)}{4\pi}\,J_3\right)\eta_1$$
$$\doteq 1+\frac{\alpha_s}{4\pi}\left[\frac{\gamma^{(0)}}{2}\left(\ln\frac{\mu^2}{M_W^2}+\ln\frac{m^2}{M_W^2}-1+\frac{2}{9}\,\pi^2\right)\right.$$
$$\left.+\gamma_{m0}\left(\ln\frac{\mu^2}{m^2}+\frac{1}{3}\right)\right], \tag{12.34}$$

where we have replaced $\mu_c\to\mu$ and $m_c\to m$. In deriving Eq. (12.34) besides (12.33) the following identities are useful

$$\sum_{i,j=+,-}\tau_{ij}=1,\quad \sum_{i,j=+,-}\tau_{ij}\,\frac{\gamma_i^{(0)}+\gamma_j^{(0)}}{2}=\gamma^{(0)}, \tag{12.35}$$

$$\sum_{i,j=+,-}\tau_{ij}(B_i+B_j)=2B_+. \tag{12.36}$$

The same result [Eq. (12.34)] is obtained from η_2 as well if we set $m_c=m_b=\mu_t=\mu$, $m_t=m$ in Eq. (12.10), and expand for $m\ll M_W$. This exercise yields a useful cross-check between the calculations for η_1 and η_2. In addition it gives some further insight into the structure of the QCD corrections to $\Delta S=2$ box diagrams, establishing η_1 and η_2 as two different generalizations of the same asymptotic limit [Eq. (12.34)].

D. The top-charm contribution—η_3

To complete the description of the $K^0-\bar{K}^0$ effective Hamiltonian we now turn to the mixed top-charm component, defined by the contribution $\sim\lambda_c\lambda_t$ in Eq. (12.1), and the associated QCD correction factor η_3. The short-distance QCD effects have first been obtained within the LLA by Gilman and Wise (1983). The calculation of η_3 at next to leading order is due to the work of Herrlich and Nierste (1995a, 1996) and Nierste (1995). As already mentioned, the renormalization-group analysis neces-

sary for η_3 is more involved than in the cases of η_1 and η_2. The characteristic differences will become clear from the following presentation.

We begin by writing down the relevant $\Delta S=1$ Hamiltonian, obtained after integrating out W and top, which provides the basis for the construction of the $\Delta S=2$ effective Hamiltonian we want to derive. It is given by

$$\mathcal{H}_{ct}^{(1)}=\frac{G_F}{\sqrt{2}}\left(\sum_{q,q'=u,c} V_{q's}^* V_{qd} \sum_{i=1,2} C_i Q_i^{q'q} - \lambda_t \sum_{i=3}^{6} C_i Q_i\right) \tag{12.37}$$

with

$$Q_1^{q'q}=(\bar{s}_i q_j')_{V-A}(\bar{q}_j d_i)_{V-A},$$
$$Q_2^{q'q}=(\bar{s}_i q_i')_{V-A}(\bar{q}_j d_j)_{V-A} \tag{12.38}$$

and corresponds to the Hamiltonian [Eq. (6.5)] discussed in Sec. VI, except that we have included the $\Delta C=1$ components Q_i^{uc}, Q_i^{cu}, which contribute in the analysis of η_3. In contrast to the simpler case of η_1 presented in the previous section, now also the penguin operators Q_i, $i=3,...,6$ [Eq. (6.3)] have to be considered. Being proportional to $\lambda_t = V_{ts}^* V_{td}$, they will contribute to the $\lambda_c\lambda_t$ part of Eq. (12.1). We remark in this context that, on the other hand, the penguin contribution to the λ_t^2 sector is entirely negligible. Since only light quarks are involved in $Q_3,\ldots,Q_6$, the double penguin diagrams, which would contribute to the λ_t^2 piece of the $\Delta S=2$ amplitude, are suppressed by at least a factor of m_b^2/m_t^2 compared with the dominant top-exchange effects discussed in Sec. XII.B.

At second order in Eq. (12.37) $\Delta S=2$ transitions are generated. Inserting Eq. (12.37) in an expression similar to Eq. (12.18), eliminating λ_u by means of $\lambda_u=-\lambda_c-\lambda_t$, and collecting the terms proportional to $\lambda_c\lambda_t$, we obtain the top-charm component of the effective $\Delta S=2$ Hamiltonian in the form

$$\mathcal{H}_{\text{eff},ct}^{\Delta S=2}=\frac{G_F^2}{2}\lambda_c\lambda_t \sum_{i=\pm}\left[\sum_{j=1}^{6} C_i C_j Q_{ij} + C_{7i} Q_7\right], \tag{12.39}$$

where

$$Q_{ij}=-\frac{i}{2}\int d^4x\ T[2Q_i^{uu}(x)Q_j^{uu}(0)-Q_i^{uc}(x)Q_j^{cu}(0) - Q_i^{cu}(x)Q_j^{uc}(0)] \tag{12.40}$$

for $j=1,2$ and

$$Q_{ij}=-\frac{i}{2}\int d^4x\ T\{[Q_i^{uu}(x)-Q_i^{cc}(x)]Q_j(0) + Q_j(x)[Q_i^{uu}(0)-Q_i^{cc}(0)]\} \tag{12.41}$$

for $j=3,\ldots,6$.

In defining these operators we have already omitted bilocal products with flavor structure such as $(\bar{s}u\bar{u}d)\cdot(\bar{s}c\bar{c}d)$, which cannot contribute to $\Delta S=2$ box diagrams. Furthermore, for the factor entering the bilocal operators with index i, we have changed the basis from $Q_{1,2}^{q'q}$ to $Q_{\pm}^{q'q}$ given in Eq. (12.17). In addition local counterterms proportional to the $\Delta S=2$ operator,

$$Q_7=\frac{m_c^2}{g^2}(\bar{s}d)_{V-A}(\bar{s}d)_{V-A}, \tag{12.42}$$

have been added to Eq. (12.39). These are necessary here because the bilocal operators can in general mix into Q_7 under infinite renormalization, a fact related to the logarithm present in the leading term, $-x_c\ln x_c$, entering $S_0(x_c,x_t)$ in Eq. (12.5). This behavior is in contrast to the charm contribution, where the corresponding function $S_0(x_c)=x_c$ does not contain a logarithmic term, and consequently no local $\Delta S=2$ counterterm is necessary in Eq. (12.19). On the other hand, the situation here is analogous to the case of the charm contribution to the effective Hamiltonian for $K^+\to\pi^+\nu\bar{\nu}$ in Sec. XI.B, which similarly behaves as $x_c\ln x_c$ in lowest order and correspondingly requires a counterterm, as displayed in Eqs. (11.21) and (11.35).

After integrating out top and W at the high-energy matching scale $\mu_W=\mathcal{O}(M_W)$, the Wilson coefficients C_j, $j=1,\ldots,6$ of Eqs. (12.37) and (12.39) are given in the NDR scheme by (see Sec. VI)

$$\vec{C}^T(\mu_W)=(0,1,0,0,0,0)+\frac{\alpha_s(\mu_W)}{4\pi}\left(6,-2,-\frac{2}{9},\frac{2}{3},-\frac{2}{9},\frac{2}{3}\right)\ln\frac{\mu_W}{M_W}+\frac{\alpha_s(\mu_W)}{4\pi} \times\left(\frac{11}{2},-\frac{11}{6},-\frac{1}{6}\tilde{E}_0(x_t),\frac{1}{2}\tilde{E}_0(x_t),-\frac{1}{6}\tilde{E}_0(x_t),\frac{1}{2}\tilde{E}_0(x_t)\right), \tag{12.43}$$

and $C_\pm=C_2\pm C_1$. $\tilde{E}_0(x_t)$ can be found in Eq. (6.16). The coefficient of Q_7 is obtained through matching the $\Delta S=2$ matrix element of the effective theory [Eq. (12.39)] to the corresponding full-theory matrix element, which, in the required approximation ($x_c\ll 1$), is given by [compare to Eq. (12.1)]

$$A_{\text{full},ct}=\frac{G_F^2}{16\pi^2}M_W^2 2\lambda_c\lambda_t S_0(x_c,x_t)\langle Q\rangle. \tag{12.44}$$

At next to leading order this matching has to be done to one loop, including finite parts. Note that here the loop effect is due to electroweak interactions and QCD does not contribute explicitly in this step. The matching condition determines the sum $C_7\equiv C_{7+}+C_{7-}$, which, in the NDR scheme and with the conventional definition of evanescent operators (Buras and Weisz, 1990) [see also (Herrlich and Nierste, 1995a, 1996; Nierste, 1995)], is given by

$$C_7(\mu_W)=\frac{\alpha_s(\mu_W)}{4\pi}\left[-8\ln\frac{\mu_W}{M_W}+4\ln x_t-\frac{3x_t}{1-x_t}-\frac{3x_t^2\ln x_t}{(1-x_t)^2}+2\right] \tag{12.45}$$

at next to leading order. In LLA one simply would have $C_7(\mu_W)=0$. The distribution of C_7 among C_{7+} and C_{7-} is arbitrary and has no impact on the physics. For example, we may choose

$$C_{7+}=C_7, \quad C_{7-}=0. \tag{12.46}$$

Having determined the initial values of the Wilson coefficients

$$\vec{C}^{(\pm)T}\equiv(C_\pm C_1,\ldots,C_\pm C_6,C_{7\pm}) \tag{12.47}$$

at a scale μ_W, $\vec{C}^{(\pm)}(\mu_W)$, the next step consists in solving the RG equations to determine $\vec{C}^{(\pm)}(\mu_c)$ at the charm mass scale $\mu_c=\mathcal{O}(m_c)$. The renormalization-group evolution of $\vec{C}^{(\pm)}$ is given by

$$\frac{d}{d\ln\mu}\vec{C}^{(\pm)}(\mu)=\gamma_{ct}^{(\pm)T}\vec{C}^{(\pm)}(\mu), \tag{12.48}$$

$$\gamma_{ct}^{(\pm)}=\begin{pmatrix}\gamma_s+\gamma_\pm\cdot 1 & \vec{\gamma}_{\pm 7}\\ \vec{0}^{\,T} & \gamma_{77}\end{pmatrix}. \tag{12.49}$$

Here γ_s is the standard 6×6 anomalous-dimension matrix for the $\Delta S=1$ effective Hamiltonian including QCD penguins from Eqs. (6.23), (6.25), and (6.26) (NDR scheme). Similarly, $\gamma_\pm$ are the anomalous dimensions of the current-current operators. They can be obtained as $\gamma_\pm=\gamma_{s,11}\pm\gamma_{s,12}$ and are also given in Sec. V. γ_{77} represents the anomalous dimension of Q_7 [Eq. (12.42)] and reads

$$\gamma_{77}=\gamma_+ +2\gamma_m+2\beta(g)/g=\frac{\alpha_s}{4\pi}\gamma_{77}^{(0)}+\left(\frac{\alpha_s}{4\pi}\right)^2\gamma_{77}^{(1)}. \tag{12.50}$$

For $N=3$ and in NDR

$$\gamma_{77}^{(0)}=-2+\frac{4}{3}f, \quad \gamma_{77}^{(1)}=\frac{175}{3}+\frac{152}{9}f. \tag{12.51}$$

Finally $\vec{\gamma}_{\pm 7}$, the vector of anomalous dimensions expressing the mixing of the bilocal operators $Q_{\pm i}$ ($i=1,\ldots,6$) into Q_7, is given by

$$\vec{\gamma}_{\pm 7}=\frac{\alpha_s}{4\pi}\vec{\gamma}_{\pm 7}^{(0)}+\left(\frac{\alpha_s}{4\pi}\right)^2\vec{\gamma}_{\pm 7}^{(1)}, \tag{12.52}$$

where

$$\vec{\gamma}_{+7}^{(0)T}=(-16,-8,-32,-16,32,16), \tag{12.53}$$

$$\vec{\gamma}_{-7}^{(0)T}=(8,0,16,0,-16,0), \tag{12.54}$$

$$\vec{\gamma}_{+7}^{(1)T}=\left(-212,-28,-424,-56,\frac{1064}{3},\frac{832}{3}\right), \tag{12.55}$$

$$\vec{\gamma}_{-7}^{(1)T}=\left(276,-92{,}552,-184,-\frac{1288}{3},0\right). \tag{12.56}$$

The scheme-dependent numbers in $\vec{\gamma}_{\pm 7}^{(1)}$ are given here in the NDR scheme with the conventional treatment of evanescent operators as described by Buras and Weisz (1990), Herrlich and Nierste (1995a), and Nierste (1995). In order to solve the RG equation (12.48) it is useful (Herrlich and Nierste, 1995a, 1996; Nierste, 1995) to define the eight-dimensional vector $[C^T=(C_1,\ldots,C_6)]$

$$\vec{D}^T=(\vec{C}^T,C_{7+}/C_+,C_{7-}/C_-), \tag{12.57}$$

which obeys

$$\frac{d}{d\ln\mu}\vec{D}=\gamma_{ct}^T\vec{D}, \tag{12.58}$$

where

$$\gamma_{ct}=\begin{pmatrix}\gamma_s & \vec{\gamma}_{+7} & \vec{\gamma}_{-7}\\ \vec{0}^T & \gamma_{77}-\gamma_+ & 0\\ \vec{0}^T & 0 & \gamma_{77}-\gamma_-\end{pmatrix}. \tag{12.59}$$

The solution of Eq. (12.58) proceeds in the standard fashion as described in Sec. III.F.1 and has the form

$$\vec{D}(\mu_c)=U_4(\mu_c,\mu_b)M(\mu_b)U_5(\mu_b,\mu_W)\vec{D}(\mu_W), \tag{12.60}$$

similar to Eq. (3.105). The b-quark-threshold matching matrix $M(\mu_b)$ is an 8×8 matrix whose 6×6 submatrix M_{ij}, $i,j=1,\ldots,6$ is identical to the matrix M described in Sec. VI.D. The remaining elements are $M_{77}=M_{88}=1$ and zero otherwise. From Eq. (12.60) the Wilson coefficients $C_i(\mu_c)$ are obtained as

$$C_i(\mu_c)=D_i(\mu_c), \quad i=1,\ldots,6,$$

$$C_7(\mu_c)=C_+(\mu_c)D_7(\mu_c)+C_-(\mu_c)D_8(\mu_c). \tag{12.61}$$

The final step in the calculation of η_3 consists of removing the charm degrees of freedom from the effective theory. Without charm the effective short-distance Hamiltonian corresponding to Eq. (12.39) can be written as

$$\mathcal{H}_{\mathrm{eff},ct}^{\Delta S=2}=\frac{G_F^2}{2}\lambda_c\lambda_t C_{ct}Q. \tag{12.62}$$

The matching condition is obtained by equating the matrix elements of Eqs. (12.39) and (12.62), evaluated at a scale $\mu_c=\mathcal{O}(m_c)$. At next to leading order one needs the finite parts of the matrix elements of Q_{ij}, which can be written in the form

$$\langle Q_{ij}(\mu_c)\rangle=\frac{m_c^2(\mu_c)}{8\pi^2}r_{ij}(\mu_c)\langle Q\rangle, \tag{12.63}$$

where, in the renormalization scheme described after Eq. (12.56), the r_{ij} are given by

$$r_{ij}(\mu_c)=\begin{cases}(4\ln(\mu_c/m_c)-1)\tau_{ij}, & j=1,2,\\ (8\ln(\mu_c/m_c)-4)\tau_{ij}, & j=3,4,\\ (-8\ln(\mu_c/m_c)+4)\tau_{ij}, & j=5,6,\end{cases} \tag{12.64}$$

$$\tau_{\pm 1}=\tau_{\pm 3}=\tau_{\pm 5}=(1\pm 3)/2, \tag{12.65}$$

$$\tau_{+j}=1, \quad \tau_{-j}=0, \quad j \text{ even}. \tag{12.66}$$

Using Eq. (12.63), the matching condition at μ_c between Eqs. (12.39) and (12.62) implies

$$C_{ct}(\mu_c)=\sum_{i=\pm}\sum_{j=1}^{6} C_i(\mu_c)C_j(\mu_c)\,\frac{m_c^2(\mu_c)}{8\pi^2}\,r_{ij}(\mu_c) + C_7(\mu_c)\,\frac{m_c^2(\mu_c)}{4\pi\alpha_s(\mu_c)}. \tag{12.67}$$

Evolving C_{ct} from μ_c to $\mu<\mu_c$ in a three-flavor theory, using Eq. (12.8), and comparing Eqs. (12.62) and (12.1), we obtain the final result

$$\eta_3=\frac{x_c(\mu_c)}{S_0(x_c(\mu_c),x_t(\mu_W))}\,\alpha_s(\mu_c)^{2/9} \times\left[\frac{\pi}{\alpha_s(\mu_c)}\,C_7(\mu_c)\left(1-\frac{\alpha_s(\mu_c)}{4\pi}\,J_3\right) +\frac{1}{2}\sum_{i=\pm}\sum_{j=1}^{6} C_i(\mu_c)C_j(\mu_c)r_{ij}(\mu_c)\right]. \tag{12.68}$$

One may convince oneself that $\eta_3 S_0(x_c,x_t)$ is independent of the renormalization scales, in particular of μ_c, up to terms of $\mathcal{O}(x_c\alpha_s^{2/9}\alpha_s)$.

Furthermore, using the formulas given in this section, it is easy to see from the explicit expression [Eq. (12.68)] that $\eta_3\alpha_s^{-2/9}\to 1$ in the limit $\alpha_s\to 0$, as should indeed be the case. The next-to-leading-order formula [Eq. (12.68)] for η_3, first calculated by Herrlich and Nierste (1995a, 1996) and Nierste (1995), provides the generalization of the leading-logarithmic-order result obtained by Gilman and Wise (1983). It is instructive to compare Eq. (12.68) with the leading-order approximation, which can be written as

$$\eta_3^{\mathrm{LO}}=\alpha_s(\mu_c)^{2/9}\,\frac{-\pi C_7^{\mathrm{LO}}(\mu_c)}{\alpha_s(\mu_c)\ln x_c}, \tag{12.69}$$

using the notation of Eq. (12.68). C_7^{LO} denotes the coefficient C_7, restricted to the leading logarithmic approximation. Equation (12.69), derived here as a special case of Eq. (12.68), is equivalent to the result obtained by Gilman and Wise (1983).

If penguin operators and the b-quark threshold in the RG evolution are neglected, it is possible to write down in closed form a relatively simple, explicit expression for η_3. Using a four-flavor effective theory for the evolution from the W scale down to the charm scale, we find in this approximation

$$\eta_3=\frac{x_c(\mu_c)}{S_0(x_c(\mu_c),x_t)}\,\alpha_s(\mu_c)^{2/9}\left[\frac{\pi}{\alpha_s(\mu_c)}\left(-\frac{18}{7}\,K_{++} -\frac{12}{11}\,K_{+-}+\frac{6}{29}\,K_{--}+\frac{7716}{2233}\,K_7\right) \times\left(1-\frac{\alpha_s(\mu_c)}{4\pi}\,\frac{307}{162}\right)+\left(\ln\frac{\mu_c}{m_c}-\frac{1}{4}\right) \times(3K_{++}-2K_{+-}+K_{--})+\frac{262497}{35000}\,K_{++} -\frac{123}{625}\,K_{+-}+\frac{1108657}{1305000}\,K_{--}-\frac{277133}{50750}\,K_7+K \times\left(-\frac{21093}{8750}\,K_{++}+\frac{13331}{13750}\,K_{+-}-\frac{10181}{18125}\,K_{--} -\frac{1731104}{2512125}\,K_7\right) +\left(\ln x_t-\frac{3x_t}{4(1-x_t)}-\frac{3x_t^2\ln x_t}{4(1-x_t)^2}+\frac{1}{2}\right)KK_7\Bigg], \tag{12.70}$$

where

$$K_{++}=K^{12/25},\quad K_{+-}=K^{-6/25},\quad K_{--}=K^{-24/25}, \tag{12.71}$$

$$K_7=K^{1/5},\quad K=\frac{\alpha_s(M_W)}{\alpha_s(\mu_c)}. \tag{12.72}$$

Here we have set $\mu_W=M_W$. Equation (12.70) represents the next-to-leading-order generalization of an approximate formula for the leading log η_3, also omitting gluon penguins, that has been first given by Gilman and Wise (1983). The analytical expression for η_3 in Eq. (12.70) provides an excellent approximation, deviating generally by less than 1% from the full result.

E. Numerical results

1. General remarks

After presenting the theoretical aspects of the short-distance QCD factors η_1, η_2, and η_3 in the previous sections, we shall now turn to a discussion of their numerical values. However, before considering explicit numbers, we would like to make a few general remarks. First of all, it is important to recall that in the matrix element $\langle\bar K^0|\mathcal{H}_{\mathrm{eff}}^{\Delta S=2}|K^0\rangle$ [see Eq. (12.1)], only the complete products

$$S_{0i}\cdot\eta_i[\alpha_s(\mu)]^{-2/9}\left[1+\frac{\alpha_s(\mu)}{4\pi}\,J_3\right]\langle\bar K^0|Q(\mu)|K^0\rangle \equiv C_i(\mu)\langle\bar K^0|Q(\mu)|K^0\rangle \tag{12.73}$$

are physically relevant. Here S_{0i} denote the appropriate quark-mass-dependent functions S_0 for the three contributions (i=1,2,3) in Eq. (12.1). None of the factors in Eq. (12.73) is physically meaningful by itself. In particular, there is some arbitrariness in splitting the product [Eq. (12.73)] into the short-distance part and the matrix element of Q [Eq. (12.2)] containing long-distance contributions. This arbitrariness has, of course, no impact on the physical result. However, it is essential to employ a definition for the operator matrix element that is consistent with the short-distance QCD factor used. Conventionally, the matrix element $\langle\bar K^0|Q|K^0\rangle$ is expressed in terms of the so-called bag parameter $B_K(\mu)$ defined through

$$\langle\bar K^0|Q(\mu)|K^0\rangle\equiv\frac{8}{3}\,F_K^2m_K^2B_K(\mu), \tag{12.74}$$

where m_K is the kaon mass and F_K=160 MeV is the kaon decay constant. In principle, one could just use the scale- and scheme-dependent bag factor $B_K(\mu)$ along with the coefficient functions $C_i(\mu)$ as defined by Eq. (12.73), evaluated at the same scale and in the same renormalization scheme. However, it has become customary to define the short-distance QCD correction factors η_i by splitting off from the Wilson coefficient $C_i(\mu)$ the factor $[\alpha_s(\mu)]^{-2/9}[1+\alpha_s(\mu)/(4\pi)J_3]$, which carries the dependence on the renormalization scheme and the scale μ. This factor is then attributed to the matrix element of Q, formally cancelling its scale and scheme dependence. Accordingly, one defines a renormalization scale and scheme-invariant bag parameter B_K [cf. Eqs. (12.73) and (12.74)]

$$B_K \equiv [\alpha_s(\mu)]^{-2/9}\left[1+\frac{\alpha_s(\mu)}{4\pi}J_3\right]B_K(\mu). \tag{12.75}$$

If the η_i as described in this review are employed to describe the short-distance QCD corrections, Eq. (12.75) is the consistent definition to be used for the kaon bag parameter.

Eventually the quantity $B_K(\mu)$ should be calculated within lattice QCD. At present, the analysis of Sharpe (1994), for example, gives a central value of $B_K(2\text{ GeV})_{\text{NDR}}$=0.616, with a still sizable uncertainty. For a recent review see also Soni (1995). This result already incorporates the lattice-continuum theory matching and refers to the usual NDR scheme. It is clear that the NLO calculation of short-distance QCD effects is essential for consistency with this matching and for a proper treatment of the scheme dependence. Both require $\mathcal{O}(\alpha_s)$ corrections, which go beyond the LLA.

To convert to the scheme-invariant parameter B_K, one uses Eq. (12.75) with the NDR-scheme value for J_3=307/162 to obtain B_K=0.84. Note that the factor involving J_3, which appears at NLO, increases the rhs by ≈4.5%. The leading factor $\alpha_s^{-2/9}$ is about 1.31. Of course, the fact that presently there is still a rather large uncertainty in the calculation of the hadronic matrix element is somewhat forgiving, regarding the precise definition of B_K. However, as the lattice calculations improve further and the errors decrease, the issue of a consistent definition of the η_i and B_K will become crucial, and it is important to keep Eq. (12.75) in mind.

Let us next add a side remark concerning the separation of the full amplitude into the formally RG-invariant factors η_i and B_K. This separation is essentially unique, up to trivial constant factors, if the evolution from the charm scale μ_c down to a "hadronic" scale $\mu<\mu_c$ is written in the resummed form as shown in Eq. (12.8) and one requires that all factors depending on the scale μ are absorbed into the matrix element. On the other hand, the hadronic scale $\mu=\mathcal{O}(1\text{ GeV})$ is not really much different from the charm scale $\mu_c=\mathcal{O}(m_c)$, so that the logarithms $\ln\mu/\mu_c$ are not very large. Therefore one could argue that it is not necessary to resum those logarithms. In this case the first two factors on the rhs of Eq. (12.8) could be expanded to first order in α_s and the amplitude [Eq. (12.73)] would be

$$C_i(\mu_c)\left(1+\frac{\alpha_s}{\pi}\ln\frac{\mu}{\mu_c}\right)\langle\bar{K}^0|Q(\mu)|K^0\rangle. \tag{12.76}$$

From this expression it is obvious that the separation of the physical amplitude into scheme-invariant short-distance factors and a scheme-invariant matrix element is in general not unique. This illustrates once more the ambiguity existing for theoretical concepts such as operator matrix elements or QCD correction factors, which only cancels in physical quantities.

For definiteness, we will stick to the RG improved form for the evolution between μ_c and μ and the definitions for η_i and B_K that we have discussed in detail above.

2. Results for η_1, η_2, and η_3

We are now ready to quote numerical results for the short-distance QCD corrections η_i at next to leading order and to compare them with the leading-order approximation. The factors η_1 and η_3 have been analyzed in detail by Herrlich and Nierste (1994) and Nierste (1995). Here we summarize briefly their main results. Using the central parameter values $m_c(m_c)$=1.3 GeV, $\Lambda^{(4)}_{\overline{\text{MS}}}$=0.325 GeV, $m_t(m_t)$=170 GeV, and fixing the scales as $\mu_c=m_c$ and $\mu_W=M_W$ for η_1, μ_W=130 GeV for η_3, one obtains at NLO

$$\eta_1=1.38, \quad \eta_3=0.47. \tag{12.77}$$

This is to be compared with the LO values corresponding to the same input, η_1^{LO}=1.12 and η_3^{LO}=0.35. We note that the next-to-leading-order corrections are sizable, typically 20%–30%, but still perturbative. The numbers above may be compared with the leading-logarithmic-order values η_1^{LO}=0.85 and η_3^{LO}=0.36 that have been previously used in the literature, based on the choice m_c=1.4 GeV, Λ_{QCD}=0.2 GeV, and $\mu_W=M_W$. The considerable difference between the two LO values for η_1 mainly reflects the large dependence of η_1 on Λ_{QCD}.

In fact, when the QCD scale is allowed to vary within $\Lambda^{(4)}_{\overline{\text{MS}}}$=(0.325±0.110) GeV, the value for η_1 (NLO) changes by ∼±35%. The leading-order result η_1^{LO} appears to be slightly less sensitive to Λ_{QCD}. However, in this approximation the relation of Λ_{QCD} to $\Lambda^{(4)}_{\overline{\text{MS}}}$ is not well defined, which introduces an additional source of uncertainty when working to leading logarithmic accuracy.

The situation is much more favorable in the case of η_3, where the sensitivity to $\Lambda^{(4)}_{\overline{\text{MS}}}$ is quite small, ∼±3%. Likewise the dependence on the charm-quark mass is very small for both η_1 and η_3. Using m_c=(1.3±0.05) GeV and the central value for $\Lambda^{(4)}_{\overline{\text{MS}}}$, it is about ±4% for η_1 and entirely negligible for η_3.

Finally, there are the purely theoretical uncertainties due to the renormalization scales. They are dominated by the ambiguity related to μ_c. The products $S_0(x_c(\mu_c))\cdot\eta_1(\mu_c)$ and $S_0(x_c(\mu_c),x_t)\cdot\eta_3(\mu_c)$ are independent of μ_c up to terms of the neglected order in RG-improved perturbation theory. In the case of $S_0(x_c(\mu_c))\cdot\eta_1(\mu_c)$ $[S_0(x_c(\mu_c), x_t)\cdot\eta_3(\mu_c)]$ the remaining

sensitivity to μ_c typically amounts to $\pm 15\%$ [$\pm 7\%$] at NLO. These scale dependences are somewhat reduced compared to the leading-order calculation, where the corresponding uncertainty is around $\pm 30\%$ [$\pm 10\%$].

To summarize, sizable uncertainties are still associated with the number for the QCD factor η_1, whose central value is found to be $\eta_1=1.38$ (Herrlich and Nierste, 1994). On the other hand, the prediction for η_3 appears to be quite stable and can be reliably determined as $\eta_3=0.47\pm 0.03$ (Herrlich and Nierste, 1995a, Nierste, 1995). One should emphasize, however, that these conclusions have their firm basis only within the framework of a complete NLO analysis, as the one performed by Herrlich and Nierste (1994) and Nierste (1995). Fortunately the quantity η_1, for which a high precision seems difficult to achieve, plays a less important role in the phenomenology of indirect CP violation.

Finally, we turn to a brief discussion of η_2 (Buras *et al.*, 1990), representing the short-distance QCD effects of the top-quark contribution. For central parameter values, in particular $\Lambda^{(4)}_{\overline{\rm MS}}=0.325$ GeV and $m_t(m_t)=170$ GeV, and for $\mu_t=m_t(m_t)$, the numerical value is

$$\eta_2=0.574. \tag{12.78}$$

Varying the QCD scale within $\Lambda^{(4)}_{\overline{\rm MS}}=(0.325\pm 0.110)$ GeV results in a $\pm 0.5\%$ change in η_2.

The dependence on $m_t(m_t)$ is even smaller, only $\pm 0.3\%$ for $m_t(m_t)=(170\pm 15)$ GeV. It is worthwhile to compare the NLO results with the LLA. Using the same input as before yields a central value of $\eta_2^{\rm LO}=0.612$, about 7% larger than the NLO result [Eq. (12.78)]. However, what is even more important than the difference in central values, is the quite striking reduction of scale uncertainty when going from the LLA to the full NLO treatment. Recall that the μ_t dependence in η_2 has to cancel the scale dependence of the function $S_0(x_t(\mu_t))$. Allowing for a typical variation of the renormalization scale $\mu_t=\mathcal{O}(m_t)$ from 100 GeV to 300 GeV results in a sizable change in $S_0(x_t(\mu_t))\eta_2^{\rm LO}$ of $\pm 9\%$. In fact, in leading order, the μ_t dependence of η_2 even has the wrong sign, reinforcing the scale dependence present in $S_0(x_t(\mu_t))$ instead of reducing it. The large sensitivity to the unphysical parameter μ_t is essentially eliminated (to $\pm 0.4\%$) for $\eta_2 S_0(x_t)$ at NLO, a quite remarkable improvement of the theoretical accuracy. The situation here is similar to the case of the top-quark-dominated rare K and B decays discussed in Secs. XI, XXIV, and XXVI. For a further illustration of the reduction in scale uncertainty, see the discussion of the analogous case of η_{2B} in Sec. XIII.B.

The dependence of η_2 on the charm and bottom threshold scales, $\mu_c=\mathcal{O}(m_c)$ and $\mu_b=\mathcal{O}(m_b)$, is also extremely weak. Taking 1 GeV$\leq\mu_c\leq$3 GeV and 3 GeV$\leq\mu_b\leq$9 GeV results in a variation of η_2 by merely $\pm 0.26\%$ and $\pm 0.06\%$, respectively.

In summary, the NLO result for $\eta_2 S_0(x_t)$ is, by contrast to the LLA, essentially free from theoretical uncertainties. Furthermore, η_2 is also rather insensitive to the input parameters $\Lambda_{\overline{\rm MS}}$ and m_t. The top contribution plays the dominant role for indirect CP violation in the neutral kaon system. The considerable improvement in the theoretical analysis of the short-distance QCD factor η_2 brought about by the next-to-leading-order calculation is therefore particularly satisfying.

XIII. THE EFFECTIVE HAMILTONIAN FOR B^0-$\bar{B}^0$ MIXING

A. General structure

Due to the particular hierarchy of the CKM matrix elements, only the top sector can contribute significantly to B^0-$\bar{B}^0$ mixing. The charm sector and the mixed top-charm contributions are entirely negligible here, in contrast to the K^0-$\bar{K}^0$ case, which considerably simplifies the analysis.

Referring to the earlier presentation of the top sector for $\Delta S=2$ transitions in Sec. XII.B, we can immediately write down the only effective $\Delta B=2$ Hamiltonian. Performing the RG evolution down to scales $\mu_b=\mathcal{O}(m_b)$ and making the necessary replacements $(s\to b)$, we get, in analogy to Eq. (12.1) (Buras *et al.*, 1990)

$$\mathcal{H}_{\rm eff}^{\Delta B=2}=\frac{G_F^2}{16\pi^2}M_W^2(V_{tb}^*V_{td})^2\eta_{2B}S_0(x_t) \times[\alpha_s(\mu_b)]^{-6/23}\left[1+\frac{\alpha_s(\mu_b)}{4\pi}J_5\right]Q+\text{H.c.}, \tag{13.1}$$

where here

$$Q=(\bar{b}d)_{V-A}(\bar{b}d)_{V-A} \tag{13.2}$$

and

$$\eta_{2B}=[\alpha_s(\mu_t)]^{6/23}\left[1+\frac{\alpha_s(\mu_t)}{4\pi}\left(\frac{S_1(x_t)}{S_0(x_t)}+B_t-J_5+\frac{\gamma^{(0)}}{2}\ln\frac{\mu_t^2}{M_W^2}+\gamma_{m0}\frac{\partial\ln S_0(x_t)}{\partial\ln x_t}\ln\frac{\mu_t^2}{M_W^2}\right)\right]. \tag{13.3}$$

The definitions of the various quantities in Eq. (13.3) can be found in Sec. XII.B. Several important aspects of η_2 in the kaon system have also been discussed in this section. Similar comments apply to the present case of η_{2B}. Here we would still like to supplement this discussion by writing down the formula for η_{2B} in the limiting case $m_t\gg M_W$,

$$\eta_{2B}=[\alpha_s(\mu_t)]^{6/23}\left\{1+\frac{\alpha_s(\mu_t)}{4\pi}\left[\frac{\gamma^{(0)}}{2}\ln\frac{\mu_t^2}{m_t^2}+\gamma_{m0}\ln\frac{\mu_t^2}{m_t^2}+11-\frac{20}{9}\pi^2+B_t-J_5+\mathcal{O}\left(\frac{M_W^2}{m_t^2}\right)\right]\right\}. \tag{13.4}$$

This expression clarifies the structure of the RG evolution in the limit $m_t\gg M_W$. It also suggests that the renormalization scale is most naturally taken to be $\mu_t=\mathcal{O}(m_t)$ rather than $\mu_t=\mathcal{O}(M_W)$ both in the definition of the top-quark mass and as the initial scale of the RG evolution.

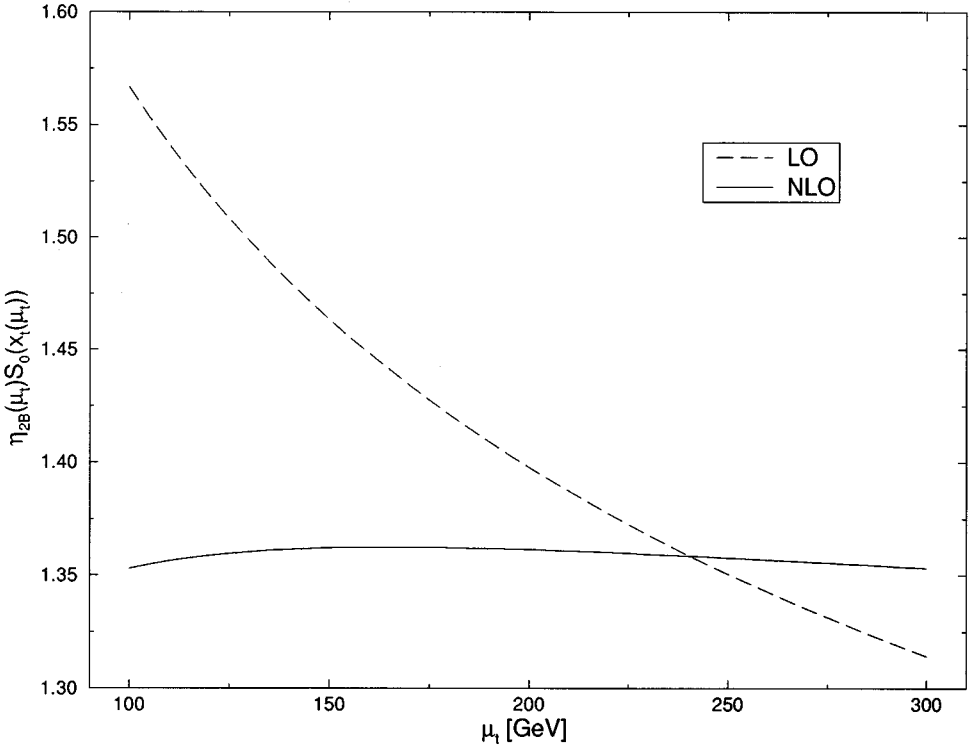

FIG. 9. Scale μ_t dependence of $\eta_{2B}(\mu_t)S_0(x_t(\mu_t))$ in leading order and next to leading order. The quantity $\eta_{2B}(\mu_t)S_0(x_t(\mu_t))$ enters the theoretical expression for Δm_B, describing B^0-$\bar{B}^0$ mixing. It is independent of the precise value of the renormalization scale μ_t up to terms of the neglected order in α_s. The remaining sensitivity represents an unavoidable theoretical uncertainty. This ambiguity is shown here for the leading-order (dashed) and the next-to-leading-order calculation (solid).

Equation (13.4) also holds, with obvious modifications, for the η_2 factor in the kaon system, which has been discussed in Sec. XII.B.

We finally mention that in the literature the μ_b-dependent factors in Eq. (13.1) are sometimes not attributed to the matrix elements of Q, as implied by Eq. (13.1), but absorbed into the definition of the QCD correction factor

$$\bar{\eta}_{2B}=\eta_{2B}[\alpha_s(\mu_b)]^{-6/23}\left[1+\frac{\alpha_s(\mu_b)}{4\pi}J_5\right]. \tag{13.5}$$

Whichever definition is employed, it is important to remember this difference and to evaluate the hadronic matrix element consistently. Note that, in contrast to η_{2B}, $\bar{\eta}_{2B}$ is scale and scheme dependent.

B. Numerical results

The correction factor η_{2B} describes the short-distance QCD effects in the theoretical expression for B^0-$\bar{B}^0$ mixing. Due to the arbitrariness that exists in dividing the physical amplitude into a short-distance contribution and a hadronic matrix element, the short-distance QCD factor is strictly speaking an unphysical quantity and hence definition dependent. The B factor, parametrizing the hadronic matrix element, has to match the convention used for η_{2B}. With the definition of η_{2B} employed in this article and given explicitly in the previous section, the appropriate B factor to be used is the so-called scheme-independent bag parameter B_B as defined in Eq. (18.18), where $\mu=\mu_b=\mathcal{O}(m_b)$. We remark that the factor η_{2B} is identical for B_d-$\bar{B}_d$ and B_s-$\bar{B}_s$ mixing. The effects of SU(3) symmetry breaking enter only the hadronic matrix elements. This feature is a consequence of the factorization of short-distance and long-distance contributions inherent to the operator product expansion. For further comments, see also the discussion of the analogous case of short-distance QCD factors in the neutral kaon system in Sec. XII.E.1.

In the following we summarize the main results of a numerical analysis of η_{2B}. The factor η_{2B} is analogous to η_2, which enters the top contribution to K^0-$\bar{K}^0$ mixing, and both quantities share many important features.

The value of η_{2B} for $\Lambda^{(4)}_{\overline{\rm MS}}$=0.325 GeV, $m_t(m_t)$=170 GeV, and with μ_t set equal to $m_t(m_t)$ is, at NLO,

$$\eta_{2B}=0.551. \tag{13.6}$$

This can be compared with $\eta_{2B}^{\rm LO}=0.580$, obtained with the same input in the leading logarithmic approximation. In the latter case the product $\eta_{2B}^{\rm LO}(\mu_t)\cdot S(x_t(\mu_t))$ is, however, affected by a residual scale ambiguity of $\pm 9\%$ (for 100 GeV$\leqslant\mu_t\leqslant$300 GeV). This uncertainty is reduced to the negligible amount of $\pm 0.3\%$ in the complete NLO expression of $\eta_{2B}(\mu_t)\cdot S(x_t(\mu_t))$, corresponding to an increase in accuracy by a factor of 25. The sensitivity to the unphysical scale μ_t in leading and next to leading order is illustrated in Fig. 9.

In addition η_{2B} is also very stable against changes in

the input parameters. With $\Lambda^{(4)}_{\overline{\rm MS}}=(0.325\pm0.110)$ GeV and $m_t(m_t)=(170\pm15)$ GeV η_{2B} varies by $\pm1.3\%$ and $\pm0.3\%$, respectively.

It is clear from this discussion that the short-distance QCD effects in B^0-$\bar{B}^0$ mixing are very well under control, once NLO corrections have been properly included, and the remaining uncertainties are extremely small. The effective Hamiltonian given in Eq. (13.1) therefore provides a solid foundation for the incorporation of nonperturbative effects, to be determined from lattice gauge theory, and for further phenomenological investigations related to B^0-$\bar{B}^0$ mixing phenomena.

XIV. PENGUIN BOX EXPANSION FOR FLAVOR CHANGING NEUTRAL CURRENT PROCESSES

An important virtue of OPE and RG is that, with $m_t>M_W$, the dependence of weak decays on the top-quark mass is very elegantly isolated. It resides only in the initial conditions for the Wilson coefficients at scale $\mu\approx M_W$, i.e., in $C_i(M_W)$. A quick look at the initial conditions in the previous sections reveals the important fact that the leading m_t dependence in all decays considered is represented universally by the m_t-dependent functions that result from exact calculations of the relevant penguin and box diagrams with internal top-quark exchanges. These are the functions

$$S_0(x_t),\quad B_0(x_t),\quad C_0(x_t),\quad D_0(x_t),$$
$$E_0(x_t),\quad D_0'(x_t),\quad E_0'(x_t), \tag{14.1}$$

for which explicit expressions are given in Eqs. (12.4), (7.13)–(7.15), (6.15), (9.12), and (9.13), respectively. In certain decays some of these functions do not appear because the corresponding penguin or box diagram does not contribute to the initial conditions. However, the function $C_0(x_t)$ resulting from the Z^0 penguin diagram enters all $\Delta F=1$ decays except $B\to X_s\gamma$. Having a quadratic dependence on m_t, this function is responsible for the dominant m_t dependence of these decays. Since the nonleading m_t dependence of $C_0(x_t)$ is gauge dependent, $C_0(x_t)$ is always accompanied by $B_0(x_t)$ or $D_0(x_t)$ in such a way that this dependence cancels. For this reason it is useful to replace the gauge-dependent functions $B_0(x_t)$, $C_0(x_t)$, and $D_0(x_t)$ by the gauge-independent set (Buchalla *et al.*, 1991)

$$X_0(x_t)=C_0(x_t)-4B_0(x_t),$$
$$Y_0(x_t)=C_0(x_t)-B_0(x_t),$$
$$Z_0(x_t)=C_0(x_t)+\frac{1}{4}D_0(x_t), \tag{14.2}$$

as we have already done at various places in this review. The inclusion of NLO QCD corrections to B^0-$\bar{B}^0$, K^0-$\bar{K}^0$ mixing, and the rare K and B decays of Sec. XI requires the calculation of QCD corrections to penguin and box diagrams in the full theory. This results in the functions $\tilde{S}(x_t)=\eta_2 S_0(x_t)$, $X(x_t)$, and $Y(x_t)$, with the latter two given in Eqs. (11.5) and (11.45), respectively.

It turns out, however, that, if the top quark mass is defined as $m_t\equiv\bar{m}_t(m_t)$, one has

$$\tilde{S}(x_t)=\eta_2 S_0(x_t),\quad X(x_t)=\eta_X X_0(x_t),$$
$$Y(x_t)=\eta_Y Y_0(x_t) \tag{14.3}$$

with η_2, η_X, and η_Y almost independent of m_t. Numerical values of η_X and η_Y are given in the phenomenological sections.

With this definition of m_t the basic m_t-dependent functions listed in Eqs. (14.1) and (14.2) represent the m_t dependence of weak decays at the NLO level to a good approximation. It should be remarked that the QCD corrections to D_0, E_0, D_0', and E_0' have not been calculated yet. They would, however, only be required for even higher-order corrections (NNLO) in the RG-improved perturbation theory as far as D_0 and E_0 are concerned. On the other hand, in the case of D_0' and E_0', which are relevant for the $b\to s\gamma$ decay, these corrections are necessary.

An inspection of the effective Hamiltonians derived in the previous sections shows that, for B^0-$\bar{B}^0$ mixing, K^0-K^0 mixing, and the rare decays of Sec. XI, the m_t dependence of the effective Hamiltonian is explicitly given in terms of the basic functions listed above. Due to the one-step evolution from μ_t to μ_b, we have also presented the explicit m_t dependence for $B\to X_s\gamma$ and $B\to X_s e^+e^-$ decays. On the other hand, for $K\to\pi\pi$ and $K_L\to\pi^0e^+e^-$, where the renormalization-group evolution is very complicated, the m_t dependence of a given box or penguin diagram is distributed among various Wilson coefficient functions. In other words the m_t dependence acquired at scale $\mu\approx\mathcal{O}(M_W)$ is hidden in a complicated numerical evaluation of $U(\mu,M_W)$.

For phenomenological applications it is more elegant and more convenient to have a formalism in which the final formulas for all amplitudes are given explicitly in terms of the basic m_t-dependent functions discussed above.

Buchalla *et al.* (1991) presented an approach that accomplishes this task. It gives the decay amplitudes as linear combinations of the basic, universal, process-independent but m_t-dependent functions $F_r(x_t)$ of Eq. (14.1) with corresponding coefficients P_r characteristic for the decay under consideration. This approach, termed "penguin box expansion" (PBE), has the following general form

$$A(\text{decay})=P_0(\text{decay})+\sum_r P_r(\text{decay})F_r(x_t), \tag{14.4}$$

where the sum runs over all possible functions contributing to a given amplitude. In Eq. (14.4) we have separated a m_t-independent term P_0 that summarizes contributions stemming from internal quarks other than the top, in particular the charm quark.

Many examples of PBE appear in this review. Several decays or transitions depend on only a single function out of the complete set of Eq. (14.1). For completeness we give here the correspondence between various processes and the basic functions

B^0-$\bar{B}^0$ mixing	$S_0(x_t)$
$K\to\pi\nu\bar{\nu}, B\to K\nu\bar{\nu}$, $B\to\pi\nu\bar{\nu}$	$X_0(x_t)$
$K\to\mu\bar{\mu}$, $B\to l\bar{l}$	$Y_0(x_t)$
$K_L\to\pi^0 e^+e^-$	$Y_0(x_t)$, $Z_0(x_t)$, $E_0(x_t)$
ε'	$X_0(x_t)$, $Y_0(x_t)$, $Z_0(x_t)$, $E_0(x_t)$
$B\to X_s\gamma$	$D'_0(x_t)$, $E'_0(x_t)$
$B\to X_s e^+e^-$	$Y_0(x_t)$, $Z_0(x_t)$, $E_0(x_t)$, $D'_0(x_t)$, $E'_0(x_t)$

In Buchalla *et al.* (1991) an explicit transformation from OPE to PBE has been made. This transformation and the relation between these two expansions can be very clearly seen on the basis of

$$A(P\to F)=\sum_{i,k}\langle F|O_k(\mu)|P\rangle U_{kj}(\mu,M_W)C_j(M_W), \tag{14.5}$$

where $U_{kj}(\mu,M_W)$ represents the renormalization-group transformation from M_W down to μ. As we have seen, OPE puts the last two factors in this formula together, in this way mixing the physics around M_W with all physical contributions down to very low energy scales. On the other hand the PBE is realized by putting the first two factors together and rewriting $C_j(M_W)$ in terms of Eq. (14.1). This results in the expansion of Eq. (14.4). Further technical details and the methods for the evaluation of the coefficients P_r can be found in Buchalla *et al.* (1991), where further virtues of PBE are discussed.

Finally, we give approximate formulas having power-like dependence on x_t for the basic, gauge-independent functions of PBE

$$\begin{aligned}
&S_0(x_t)=0.784\,x_t^{0.76}, \quad X_0(x_t)=0.660\,x_t^{0.575},\\
&Y_0(x_t)=0.315\,x_t^{0.78}, \quad Z_0(x_t)=0.175\,x_t^{0.93},\\
&E_0(x_t)=0.564\,x_t^{-0.51}, \quad D'_0(x_t)=0.244\,x_t^{0.30},\\
&E'_0(x_t)=0.145\,x_t^{0.19}.
\end{aligned} \tag{14.6}$$

In the range $150\ \text{GeV}\leqslant m_t\leqslant 200\ \text{GeV}$ these approximations reproduce the exact expressions to an accuracy better than 1%.

XV. HEAVY-QUARK EFFECTIVE THEORY BEYOND LEADING LOGARITHMIC ORDER

A. General remarks

Since its advent in 1989, heavy-quark effective theory (HQET) has developed into an elaborate and well-established formalism, which provides a systematic framework for the treatment of hadrons containing a heavy quark. HQET represents a static approximation for the heavy quark, covariantly formulated in the language of an effective field theory. It allows one to extract the dependence of hadronic matrix elements on the heavy-quark mass and to exploit the simplifications that arise in QCD in the static limit.

There are several excellent reviews on this subject (Georgi, 1991; Grinstein, 1991; Isgur and Wise, 1992; Mannel, 1993; Neubert, 1994c) and we do not attempt here to cover the details of this extended field. However, we would like to emphasize the close parallels in the general formalism employed to calculate perturbative QCD effects for the effective weak Hamiltonians we have been discussing in this review and in the context of HQET. In particular we will concentrate on results that have been obtained in HQET beyond the leading logarithmic approximation in QCD perturbation theory. Such calculations have been done mainly for bilinear current operators involving heavy-quark fields, which have important applications in semileptonic decays of heavy hadrons. For the purpose of illustration we will focus on the simplest case of heavy-light currents. Furthermore, while existing reviews concentrate on semileptonic decays and current operators, we will also include results obtained for nonleptonic transitions and summarize the calculation of NLO QCD corrections to B^0-$\bar{B}^0$ mixing in HQET (Flynn *et al.*, 1991; Giménez, 1993). These latter papers generalize the leading logarithmic order results first obtained by Voloshin and Shifman (1987) and Politzer and Wise (1988a, 1988b).

Throughout this section we will restrict ourselves to the leading order in HQET and not address the question of $1/m$ corrections. For a discussion of this topic we refer the reader to the literature, in particular the above-mentioned review articles.

B. Basic concepts

Let us briefly recall the most important basic concepts underlying the idea of HQET. The Lagrangian describing a quark field Ψ with mass m and its QCD interactions with gluons is given by

$$\mathcal{L}=\bar{\Psi}i\not{D}\Psi-m\bar{\Psi}\Psi, \tag{15.1}$$

where $D_\mu=\partial_\mu-igT^aA^a_\mu$ is the gauge-covariant derivative. If Ψ is a heavy quark, i.e., its mass is large compared to the QCD scale, $\Lambda_{\rm QCD}/m\ll 1$, it acts approximately like a static color source, and its QCD interactions are simplified. A heavy quark inside a hadron moving with velocity v has approximately the same velocity. Thus its momentum can be written as $p=mv+k$, where k is a small residual momentum of the order of $\Lambda_{\rm QCD}$ and subject to changes of the same order through soft QCD interactions. To implement this approximation, the quark field Ψ is decomposed into

$$\Psi(x)=e^{-imv\cdot x}[h_v(x)+H_v(x)] \tag{15.2}$$

with h_v and H_v defined by

$$h_v(x)=e^{imv\cdot x}\frac{1+\not{v}}{2}\Psi(x), \tag{15.3}$$

$$H_v(x)=e^{imv\cdot x}\frac{1-\not{v}}{2}\Psi(x). \tag{15.4}$$

To be specific we consider here the case of a hadron containing a heavy quark, as opposed to a heavy anti-

quark. In order to describe a heavy antiquark, the definitions given in Eqs. (15.3) and (15.4) are replaced by

$$h_v^{(-)}(x)=e^{-imv\cdot x}\,\frac{1-\not{v}}{2}\,\Psi(x), \tag{15.5}$$

$$H_v^{(-)}(x)=e^{-imv\cdot x}\,\frac{1+\not{v}}{2}\,\Psi(x). \tag{15.6}$$

Consequently, for a heavy antiquark, one only needs to substitute $v\to -v$ in the expressions given below.

In the rest frame of the heavy quark, h_v and H_v correspond to the upper and lower components of Ψ, respectively. In general, for $m\to\infty$, h_v and H_v represent the "large" and "small" components of Ψ. In fact, the equations of motion of QCD imply that H_v is suppressed by a factor $\Lambda_{\rm QCD}/m$ in comparison to h_v. The inclusion of an explicit exponential factor $\exp(-imv\cdot x)$ in Eq. (15.2) ensures that the momentum associated with the field h_v is only a small residual momentum of order $\Lambda_{\rm QCD}$.

Now an effective theory for h_v is constructed by eliminating the small component field H_v from explicitly appearing in the description of the heavy quark. On the classical level this can be done by using the equations of motion or, equivalently, by directly integrating out the H_v degrees of freedom in the context of a path-integral formulation (Mannel *et al.*, 1992). The effective Lagrangian one obtains from Eq. (15.1) along these lines is given by ($D_\perp^\mu=D^\mu-v^\mu v\cdot D$)

$$\mathcal{L}_{\rm eff,tot}=\bar h_v iv\cdot D h_v+\bar h_v i\not{D}_\perp\,\frac{1}{iv\cdot D+2m-i\varepsilon}\,i\not{D}_\perp h_v\,. \tag{15.7}$$

The first term in Eq. (15.7)

$$\mathcal{L}_{\rm eff}=\bar h_v(iv^\mu\partial_\mu+gv^\mu T^a A_\mu^a)h_v \tag{15.8}$$

represents the Lagrangian of HQET to lowest order in $1/m$ and will be sufficient for the present purposes. The second, nonlocal contribution in Eq. (15.7) can be expanded into a series of local, higher-dimension operators carrying coefficients with increasing powers of $1/m$. To first order it yields the correction due to the residual heavy-quark kinetic energy and the chromomagnetic interaction term, which couples the heavy-quark spin to the gluon field.

From Eq. (15.8) one can obtain the Feynman rules of HQET, the propagator of the effective field h_v

$$\frac{i}{v\cdot k}\,\frac{1+\not{v}}{2} \tag{15.9}$$

and the $\bar h_v$-h_v-gluon vertex, $igv^\mu T^a$. The explicit factor $(1+\not{v})/2$ in Eq. (15.9) arises because the effective field h_v is a constrained spinor, satisfying $\not{v}h_v\equiv h_v$, as is obvious from Eq. (15.3). The velocity v_μ is a constant in the effective theory and plays the role of a label for the effective field h_v. In principle, a different field h_v has to be considered for every velocity v. The Lagrangian in Eq. (15.8) exhibits the crucial features of HQET: the quark-gluon coupling is independent of the quark's spin degrees of freedom, and the Lagrangian is independent of the heavy-quark flavor, since the heavy quark mass has been eliminated. This observation forms the basis for the spin-flavor symmetry of HQET (Isgur and Wise, 1989, 1990), which gives rise to important simplifications in the strong interactions of heavy quarks and allows one to establish relations among the form factors of different heavy-hadron matrix elements. The heavy-quark symmetries are broken by $1/m$ contributions as well as radiative corrections.

So far the discussion has been limited to the QCD interactions of the heavy quark. Weak interactions introduce new operators into the theory, which may be current operators, bilinear in quark fields, or four-quark operators, which are relevant for semileptonic and nonleptonic transitions, respectively. Such operators form the basic ingredients to be studied in weak decay phenomenology. They can as well be expanded in powers of $1/m$ and incorporated into the framework of HQET. For example, a heavy-light current operator $\bar q\Gamma\Psi$ (evaluated at the origin, $x=0$) can be written, using Eq. (15.2), as

$$\bar q\Gamma\Psi=\bar q\Gamma h_v+\mathcal{O}(1/m) \tag{15.10}$$

to lowest order in HQET.

Up to now we have restricted the discussion to the classical level. In addition, of course, quantum radiative corrections have to be included. They will, for example, modify relations such as Eq. (15.10). Technically their effects are taken into account by performing the appropriate matching calculations, which relate operators in the effective theory to the corresponding operators in the full theory to the required order in renormalization-group improved QCD perturbation theory. The procedure is very similar to the calculation of the usual effective Hamiltonians for weak decays. The basic difference consists in the heavy degrees of freedom that are being integrated out in the matching process. In the general case of effective weak Hamiltonians, the heavy field to be removed as a dynamical variable is the W boson, whereas it is the lower-component heavy-quark field H_v in the case of HQET. This similarity will become obvious from the presentation below.

At this point some comment might be in order concerning the relationship of the HQET formalism to the general weak effective Hamiltonians discussed in this review, in particular those relevant for b physics. The effective Hamiltonians for $\Delta B=1,2$ nonleptonic transitions are the relevant Hamiltonians for scales $\mu=\mathcal{O}(m_b)$, which are appropriate for B hadron decays, and their Wilson coefficients incorporate the QCD short-distance dynamics between scales of $\mathcal{O}(M_W)$ and $\mathcal{O}(m_b)$. As already mentioned at the end of Sec. V, it is therefore not necessary to invoke HQET. The physics below $\mu=\mathcal{O}(m_b)$ is completely contained within the relevant hadronic matrix elements. On the other hand, HQET may be useful in certain cases, like B^0-$\bar B^0$ mixing, to gain additional insight into the structure of the hadronic matrix elements for scales below m_b, but still large compared to $\Lambda_{\rm QCD}$. These scales are still perturbative, and the related contributions can be extracted analytically

within HQET. In particular, this procedure makes the dependence of the matrix element on the heavy-quark mass explicit, as we will see in examples below. Furthermore, this approach can be useful, e.g., in connection with lattice calculations of hadronic matrix elements, which are easier to perform in the static limit for b quarks, i.e., employing HQET (Sachrajda, 1992). However, the simplifications obtained are at the expense of the approximation due to the expansion in $1/m$.

The most important application of HQET has been to the analysis of exclusive semileptonic transitions involving heavy quarks, where this formalism allows one to exploit the consequences of heavy-quark symmetry to relate form factors and provides a basis for systematic corrections to the $m\to\infty$ limit. This area of weak decay phenomenology has already been reviewed in detail (Georgi, 1991; Grinstein, 1991; Isgur and Wise, 1992; Mannel, 1993; Neubert, 1994c) and will not be covered in the present article.

C. Heavy-light currents

As an example of a next-to-leading-order QCD calculation within the context of HQET, we will now discuss the case of a weak current composed of one heavy-and one light-quark field, to leading order in the $1/m$ expansion. For definiteness we consider the axial vector heavy-light current, whose matrix elements determine the decay constants of pseudoscalar mesons containing a single heavy quark, like f_B and f_D.

The axial-vector current operator in the full theory is given by

$$A=\bar{q}\,\gamma_\mu\gamma_5\Psi, \tag{15.11}$$

where Ψ is the heavy- and q the light-quark field. In HQET this operator can be expanded in the following way,

$$A=C_1(\mu)\tilde{A}_1+C_2(\mu)\tilde{A}_2+\mathcal{O}(1/m), \tag{15.12}$$

where the operator basis in the effective theory is

$$\tilde{A}_1=\bar{q}\,\gamma_\mu\gamma_5 h_v, \quad \tilde{A}_2=\bar{q}v_\mu\gamma_5 h_v, \tag{15.13}$$

with the heavy-quark effective field h_v defined in Eq. (15.3). The use of the expansion [Eq. (15.12)] is to make the dependence of the matrix elements of A on the heavy-quark mass m explicit. The dependence on this mass is twofold. First, there is a power dependence that is manifest in the heavy-quark expansion in powers of $1/m$. From this series the lowest order term is shown in Eq. (15.12). Second, there is a logarithmic dependence on m due to QCD radiative corrections, which can be calculated in perturbation theory. This dependence is factorized into the coefficient functions C_1 and C_2 in much the same way as the logarithmic dependence of nonleptonic weak decay amplitudes on the W-boson mass is factorized into the Wilson coefficients of the usual weak Hamiltonians. Since the dynamics of HQET is, by construction, independent of m, no further m dependence is present in the matrix elements of the effective theory operators $\tilde{A}_{1,2}$, except for trivial factors of m related to the normalization of meson states. Consequently the m dependence of Eq. (15.12) is determined explicitly.

We remark that, in general, the meson states in HQET to be used for the rhs of Eq. (15.12) differ from the meson states in the full theory that are used to sandwich the operator A on the lhs. For the leading order in $1/m$ we are working in, this distinction is irrelevant, however. An important point is that the operators $\tilde{A}_{1,2}$ in the effective theory have anomalous dimensions, although the operator A in the full theory, being an axial-vector current operator, does not. As a consequence matrix elements of $\tilde{A}_{1,2}$ will depend on the renormalization scale and scheme. This dependence is cancelled, however, through a corresponding dependence of the coefficients, so that the physical matrix elements of A will be scale and scheme independent as they must be. The existence of anomalous dimensions for the effective-theory operators merely reflects the logarithmic dependence on the heavy-quark mass m due to QCD effects. This dependence results in logarithmic divergences in the limit $m\to\infty$, corresponding to the effective theory, which require additional infinite renormalizations not present in full QCD. Obviously the situation is completely analogous to the case of constructing effective weak Hamiltonians through integrating out the W boson, which we have described in detail in Sec. III. In fact, the extraction of the coefficient functions by factorizing long- and short-distance contributions to quark-level amplitudes and the renormalization-group treatment follow exactly the same principles.

The Wilson coefficients at the high matching scale $\mu_h=\mathcal{O}(m)$, the initial condition to the RG evolution, can be calculated in ordinary perturbation theory with the result (NDR scheme)

$$C_1(\mu_h)=1+\frac{\alpha_s}{4\pi}\left(\gamma_{hl}^{(0)}\ln\frac{\mu_h}{m}+B_1\right), \tag{15.14}$$

$$C_2(\mu_h)=\frac{\alpha_s}{4\pi}B_2, \tag{15.15}$$

with

$$B_1=-4C_F, \quad B_2=-2C_F, \tag{15.16}$$

and $\gamma_{hl}^{(0)}$ given in Eq. (15.18) below. C_F is the QCD color factor $(N^2-1)/(2N)$. We remark that the coefficient of the new operator $\tilde{A}_2$, generated at $\mathcal{O}(\alpha_s)$, is finite without requiring renormalization. As a consequence no explicit scale dependence appears in Eq. (15.15), and B_2 is a scheme-independent constant. For the same reason $\tilde{A}_1$ and $\tilde{A}_2$ do not mix under renormalization, but renormalize only multiplicatively. The anomalous dimension of the effective heavy-quark currents is independent of the Dirac structure. It is the same for $\tilde{A}_1$ and $\tilde{A}_2$ and, at two-loop order, is given by

$$\gamma_{hl}=\gamma_{hl}^{(0)}\frac{\alpha_s}{4\pi}+\gamma_{hl}^{(1)}\left(\frac{\alpha_s}{4\pi}\right)^2, \tag{15.17}$$

where

$$\gamma_{hl}^{(0)} = -3C_F, \tag{15.18}$$

$$\gamma_{hl}^{(1)} = \left(-\frac{49}{6}+\frac{2}{3}\pi^2\right)NC_F+\left(\frac{5}{2}-\frac{8}{3}\pi^2\right)C_F^2+\frac{5}{3}C_F f$$
$$= -\frac{254}{9}-\frac{56}{27}\pi^2+\frac{20}{9}f \quad \text{(NDR)}, \tag{15.19}$$

and $N(f)$ denotes the number of colors (flavors). The anomalous dimension $\gamma_{hl}^{(0)}$ has been first calculated by Voloshin and Shifman (1987) and Politzer and Wise (1988a, 1988b). The generalization to next to leading order has been performed by Ji and Musolf (1991) and Broadhurst and Grozin (1991).

The RG equations are readily solved to obtain the coefficients at a lower but still perturbative scale μ, where, formally, $\mu \ll \mu_h = \mathcal{O}(m)$. Using the results of Sec. III.F, we have

$$C_1(\mu) = \left(1+\frac{\alpha_s(\mu)}{4\pi}J_{hl}\right)\left[\frac{\alpha_s(\mu_h)}{\alpha_s(\mu)}\right]^{d_{hl}}\left(1+\frac{\alpha_s(\mu_h)}{4\pi}\right.$$
$$\left.\times\left[\gamma_{hl}^{(0)}\ln\frac{\mu_h}{m}+B_1-J_{hl}\right]\right), \tag{15.20}$$

$$C_2(\mu) = \left[\frac{\alpha_s(\mu_h)}{\alpha_s(\mu)}\right]^{d_{hl}}\frac{\alpha_s(\mu_h)}{4\pi}B_2 \tag{15.21}$$

with

$$d_{hl} = \frac{\gamma_{hl}^{(0)}}{2\beta_0}, \quad J_{hl} = \frac{d_{hl}}{\beta_0}\beta_1 - \frac{\gamma_{hl}^{(1)}}{2\beta_0}. \tag{15.22}$$

We remark that the corresponding formulae for the vector current can be simply obtained from the above expressions by letting $\gamma_5 \to 1$ and changing the sign of B_2.

In addition to the case of heavy-light currents considered here, the NLO corrections have also been calculated for flavor-conserving and flavor-changing heavy-heavy currents of the type $\bar{\Psi}\Gamma\Psi$ and $\bar{\Psi}_1\Gamma\Psi_2$, respectively, where Ψ, $\Psi_{1,2}$ are heavy quark fields ($\Gamma = \gamma_\mu, \gamma_\mu\gamma_5$). In these cases the anomalous dimensions become velocity dependent. Additional complications arise in the analysis of flavor-changing heavy-heavy currents due to the presence of two distinct heavy-mass scales. For a detailed presentation see Neubert (1994c) and references cited therein.

D. The pseudoscalar decay constant in the static limit

An important application of the results summarized in the last section is the calculation of the short-distance QCD effects, from scales between $\mu_h = \mathcal{O}(m)$ and $\mu = \mathcal{O}(1\ \text{GeV})$, for the decay constants f_P of pseudoscalar heavy mesons. Using only the leading term in the expansion [Eq. (15.12)], omitting all $1/m$ power corrections, corresponds to the static limit for f_P, which plays some role in lattice studies. As already mentioned we will restrict ourselves to this limit. We should remark, however, that nonnegligible power corrections are known to exist for the realistic case of B- or D-meson decay constants (Sachrajda, 1992). The decay constant f_P is defined through

$$\langle 0|A|P\rangle = -if_P m_P v_\mu, \tag{15.23}$$

where the pseudoscalar meson state $|P\rangle$ is normalized in the conventional way ($\langle P|P\rangle = 2EV$). The matrix elements of $\tilde{A}_{1,2}$ are related via heavy-quark symmetry and are given by

$$\langle 0|\tilde{A}_1|P\rangle = -\langle 0|\tilde{A}_2|P\rangle = -i\tilde{f}(\mu)\sqrt{m_P}v_\mu. \tag{15.24}$$

Apart from the explicit mass factor $\sqrt{m_P}$, which is merely due to the normalization of $|P\rangle$, these matrix elements are independent of the heavy-quark mass. The "reduced" decay constant $\tilde{f}(\mu)$ is therefore m independent. It does, however, depend on the renormalization scale and scheme chosen. The computation of $\tilde{f}(\mu)$ is a nonperturbative problem involving strong dynamics below scale μ. Using Eqs. (15.12), (15.20), (15.21), (15.23), and (15.24), we obtain

$$f_P = \frac{\tilde{f}(\mu)}{\sqrt{m_P}}\left(1+\frac{\alpha_s(\mu)}{4\pi}J_{hl}\right)\left[\frac{\alpha_s(\mu_h)}{\alpha_s(\mu)}\right]^{d_{hl}}\left(1+\frac{\alpha_s(\mu_h)}{4\pi}\right.$$
$$\left.\times\left[\gamma_{hl}^{(0)}\ln\frac{\mu_h}{m}+B_1-J_{hl}-B_2\right]\right). \tag{15.25}$$

The dependence of the coefficient function on the renormalization scheme through J_{hl} in the second factor in Eq. (15.25) and its dependence on μ cancel the corresponding dependences in the hadronic quantity $\tilde{f}(\mu)$ to the considered order in α_s. The last factor in Eq. (15.25) is scheme independent. Furthermore, the cancellation of the dependence on μ_h to the required order can be seen explicitly. Note also the leading scaling behavior $f_P \sim 1/\sqrt{m_P}$, which is manifest in Eq. (15.25).

Although $\tilde{f}(\mu)$ cannot be calculated without nonperturbative input, its independence from the heavy-quark mass m implies that $\tilde{f}$ will drop out in the ratio of f_B over f_D, if charm is treated as a heavy quark. One thus obtains

$$\frac{f_B}{f_D} = \sqrt{\frac{m_D}{m_B}}\left[\frac{\alpha_s(\mu_b)}{\alpha_s(\mu_c)}\right]^{d_{hl}}\left(1+\frac{\alpha_s(\mu_b)-\alpha_s(\mu_c)}{4\pi}\right.$$
$$\times(B_1-J_{hl}-B_2)+\frac{\alpha_s(\mu_b)}{4\pi}\gamma_{hl}^{(0)}\ln\frac{\mu_b}{m_b}$$
$$\left.-\frac{\alpha_s(\mu_c)}{4\pi}\gamma_{hl}^{(0)}\ln\frac{\mu_c}{m_c}\right). \tag{15.26}$$

The QCD factor on the right-hand side of Eq. (15.26) amounts to 1.14 for $m_b = 4.8$ GeV, $m_c = 1.4$ GeV, and $\Lambda_{\overline{\text{MS}}} = 0.2$ GeV if we set $\mu_i = m_i$, $i = b, c$. If we allow for a variation of the renormalization scales, $2/3 \leqslant \mu_i/m_i \leqslant 2$, this factor lies within a range of 1.12 to 1.16. This is to be compared with the leading logarithmic approximation, where the central value is 1.12 with a variation from 1.10 to 1.15. Note that, due to cancellations in the ratio f_B/f_D, the scale ambiguity is not much larger in LLA

than in NLLA. However, the next-to-leading-order QCD effects further enhance f_B/f_D independently of the renormalization scheme.

E. $\Delta B=2$ transitions in the static limit

In Sec. XIII we have described the effective Hamiltonian for B^0-$\bar{B}^0$ mixing. The calculation of the mixing amplitude requires the evaluation of the matrix element $\langle \bar{B}^0|Q|B^0\rangle \equiv \langle Q\rangle$ of the operator

$$Q=(\bar{b}d)_{V-A}(\bar{b}d)_{V-A} \tag{15.27}$$

in addition to the short-distance Wilson coefficient. Coefficient function and operator matrix element are to be evaluated at a common renormalization scale, $\mu_b=\mathcal{O}(m_b)$, say. In contrast to the determination of the Wilson coefficient, the computation of the hadronic matrix element involves nonperturbative long-distance contributions. Ultimately this problem should be solved using lattice QCD. However, the b quark is rather heavy, and it is therefore difficult to incorporate it as a fully dynamical field in the context of a lattice-regularization approach. On the other hand, QCD effects from scales below $\mu_b=\mathcal{O}(m_b)$ down to $\sim$1 GeV are still accessible to a perturbative treatment. HQET provides the tool to calculate these contributions. At the same time it allows one to extract the dependence of $\langle \bar{B}^0|Q|B^0\rangle$ on the bottom mass m_b explicitly, albeit at the price of the further approximation introduced by the expansion in inverse powers of m_b.

In a first step the operator Q in Eq. (15.27) is expressed as a linear combination of HQET operators by matching the full to the effective theory at a scale $\mu_b=\mathcal{O}(m_b)$

$$\langle Q(\mu_b)\rangle=\left(1+\frac{\alpha_s(\mu_b)}{4\pi}\left[(\tilde{\gamma}^{(0)}-\gamma^{(0)})\ln\frac{\mu_b}{m_b}+\tilde{B}-B\right]\right)\times\langle\tilde{Q}(\mu_b)\rangle+\frac{\alpha_s(\mu_b)}{4\pi}\,\tilde{B}_s\langle\tilde{Q}_s(\mu_b)\rangle. \tag{15.28}$$

Here

$$\tilde{Q}=2(\bar{h}d)_{V-A}(\bar{h}^{(-)}d)_{V-A},\qquad \tilde{Q}_s=2(\bar{h}d)_{S-P}(\bar{h}^{(-)}d)_{S-P}, \tag{15.29}$$

with $(\bar{h}d)_{S-P}\equiv\bar{h}(1-\gamma_5)d$ are the necessary operators in HQET relevant for the case of a $B^0\to\bar{B}^0$ transition. The field $\bar{h}$ creates a heavy quark, while $\bar{h}^{(-)}$ annihilates a heavy antiquark. Since the effective-theory field $\bar{h}$ ($\bar{h}^{(-)}$) cannot, unlike the full-theory field $\bar{b}$ in Q, at the same time annihilate (create) the heavy antiquark (quark), explicit factors of two have to appear in Eq. (15.29). Similar to the case of the heavy-light current discussed in the previous section, a new operator $\tilde{Q}_s$ with scalar-pseudoscalar structure is generated. Its coefficient is finite, and hence no operator mixing under infinite renormalization occurs between $\tilde{Q}$ and $\tilde{Q}_s$.

In a second step, the matrix element $\langle\tilde{Q}(\mu_b)\rangle$ at the high scale μ_b has to be expressed through the matrix element of $\tilde{Q}$ evaluated at a lower scale $\mu\sim1$ GeV, which is relevant for a nonperturbative calculation, for example, using lattice gauge theory. This relation can be obtained through the usual renormalization-group evolution and reads in NLLA

$$\langle\tilde{Q}(\mu_b)\rangle=\left[\frac{\alpha_s(\mu_b)}{\alpha_s(\mu)}\right]^{\tilde{d}}\left(1+\frac{\alpha_s(\mu)-\alpha_s(\mu_b)}{4\pi}\,\tilde{J}\right)\langle\tilde{Q}(\mu)\rangle, \tag{15.30}$$

where

$$\tilde{d}=\frac{\tilde{\gamma}^{(0)}}{2\beta_0},\quad \tilde{J}=\frac{\tilde{d}}{\beta_0}\,\beta_1-\frac{\tilde{\gamma}^{(1)}}{2\beta_0}, \tag{15.31}$$

with the beta-function coefficients β_0 and β_1 given in Eq. (3.16). The calculation of the one-loop anomalous dimension $\tilde{\gamma}^{(0)}$ of the HQET operator $\tilde{Q}$, required for the leading logarithmic approximation to Eq. (15.30), has been first performed by Voloshin and Shifman (1987) and Politzer and Wise (1998a, 1988b). The computation of the two-loop anomalous dimension $\tilde{\gamma}^{(1)}$ is due to Giménez (1993). Finally, the next-to-leading-order matching condition [Eq. (15.28)] has been determined by Flynn *et al.* (1991). In the following we summarize the results obtained in these papers.

The scheme-dependent next-to-leading-order quantities B, $\tilde{B}$, and $\tilde{\gamma}^{(1)}$ refer to the NDR scheme with anticommuting γ_5 and the usual subtraction of evanescent terms as defined by Buras and Weisz (1990). For $N=3$ colors we then have

$$\tilde{\gamma}^{(0)}=-8,\quad \gamma^{(0)}=4, \tag{15.32}$$

$$\tilde{B}-B=-14,\quad B=\frac{11}{3},\quad \tilde{B}_s=-8, \tag{15.33}$$

$$\tilde{\gamma}^{(1)}=-\frac{808}{9}-\frac{52}{27}\,\pi^2+\frac{64}{9}\,f, \tag{15.34}$$

where f is the number of active flavors.

At this point we would like to make the following comments.

(i) The logarithmic term in Eq. (15.28) reflects the $\mathcal{O}(\alpha_s)$ scale dependence of the matrix elements of Q and $\tilde{Q}$. Accordingly, its coefficient is given by the difference in the one-loop anomalous dimensions of these operators, $\gamma^{(0)}$ and $\tilde{\gamma}^{(0)}$.

(ii) The one-loop anomalous dimension of the effective-theory operator $\tilde{Q}$, $\tilde{\gamma}^{(0)}$, is exactly twice as large as the one-loop anomalous dimension of the heavy-light current discussed in Sec. XV.C [see Eq. (15.18)]. Therefore the scale dependence of $\langle\tilde{Q}\rangle$ below μ_b is entirely contained in the scale dependence of the decay constant squared $\tilde{f}^2(\mu)$. This implies the well-known result that in LLA the parameter B_B has no perturbative scale dependence in the static theory below μ_b. As the result of Giménez (1993) for $\tilde{\gamma}^{(1)}$ shows, this somewhat accidental cancellation is not valid beyond the one-loop level.

(iii) The matching condition of Eq. (15.28) contains a scheme-dependent constant term in the relation be-

tween $\langle Q\rangle$ and $\langle\tilde{Q}\rangle$. We have written this coefficient in the form $\tilde{B}$-B in order to make the cancellation of scheme dependences, to be discussed below, more transparent. Here B is identical to B_+ introduced in Eq. (5.8) and characterizes the scheme dependence of $\langle Q\rangle$ (see also Secs. XII and XIII).

(iv) The quantity $\tilde{\gamma}^{(1)}$ has been originally calculated by Giménez (1993) using dimensional reduction (DRED) instead of NDR as the renormalization scheme. However, $\tilde{B}$ turns out to be the same in DRED and NDR, implying that $\tilde{\gamma}^{(1)}$ also coincides in these schemes (Giménez, 1993).

Finally we may put together Eqs. (15.28) and (15.30), omitting for the moment the scheme-independent, constant correction due to $\tilde{Q}_s$, to obtain

$$\langle Q(\mu_b)\rangle=\left[\frac{\alpha_s(\mu_b)}{\alpha_s(\mu)}\right]^{\tilde{d}}\left(1+\frac{\alpha_s(\mu_b)}{4\pi}\left[(\tilde{\gamma}^{(0)}-\gamma^{(0)})\ln\frac{\mu_b}{m_b}+\tilde{B}-B-\tilde{J}\right]+\frac{\alpha_s(\mu)}{4\pi}\tilde{J}\right)\langle\tilde{Q}(\mu)\rangle. \quad (15.35)$$

This relation serves to express the B^0-$\bar{B}^0$ matrix element of the operator Q, evaluated at a scale $\mu_b=\mathcal{O}(m_b)$ relevant for the effective Hamiltonian of Sec. XIII, in terms of the static theory matrix element $\langle\tilde{Q}(\mu)\rangle$ normalized at a low scale $\mu\sim 1$ GeV. The latter is more readily accessible to a nonperturbative lattice calculation than the full-theory matrix element $\langle Q(\mu_b)\rangle$. Note that Eq. (15.35) as it stands is valid in the continuum theory. In order to use lattice results, one still has to perform an $\mathcal{O}(\alpha_s)$ matching of $\tilde{Q}$ to its lattice counterpart. This step, however, does not require any further renormalization-group improvement, since by means of Eq. (15.35) $\tilde{Q}$ is already normalized at the appropriate low scale μ. The continuum-lattice theory matching was determined by Flynn *et al.* (1991) and is also discussed by Giménez (1993).

Of course, the right-hand side in Eq. (15.35) gives only the leading contribution in the $1/m$ expansion of the full matrix element $\langle Q(\mu_b)\rangle$ (apart from $\tilde{Q}_s$). Going beyond this approximation would require the consideration of several new operators, which appear at the next order in $1/m$. These contributions have been studied by Kilian and Mannel (1993) in the leading logarithmic approximation. On the other hand Eq. (15.35), while restricted to the static limit, includes and resums all leading and next to leading logarithmic corrections between the scales $\mu_b=\mathcal{O}(m_b)$ and $\mu\sim 1$ GeV in the relation between Q and $\tilde{Q}$. It is interesting to consider the scale and scheme dependences present in Eq. (15.35). The dependence on μ in the first factor on the rhs of Eq. (15.35) is canceled by the μ dependence of $\langle\tilde{Q}(\mu)\rangle$. The dependence on μ_b of this factor is canceled by the explicit $\ln\mu_b$ term proportional to $\tilde{\gamma}^{(0)}$. Hence the only scale dependence remaining on the rhs, to the considered order $\mathcal{O}(\alpha_s)$, is the one $\sim\alpha_s(\mu_b)\gamma^{(0)}\ln\mu_b$. This is precisely the scale dependence of the full-theory matrix element on the lhs, which is required to cancel the corresponding dependence of the Wilson coefficient. Similarly, the term $\sim\alpha_s(\mu_b)B$ represents the correct scheme dependence of $\langle Q(\mu_b)\rangle$, while the scheme dependence of $\alpha_s(\mu)\tilde{J}$ cancels with the scheme dependence of $\langle\tilde{Q}(\mu)\rangle$ and the difference $\tilde{B}$-$\tilde{J}$ is scheme independent by itself. This discussion demonstrates explicitly that the transition from full QCD to HQET can be made at an arbitrary scale $\mu_b=\mathcal{O}(m_b)$, as we have already emphasized above.

Finally, we would like to remark that, since the logarithm $\ln\mu_b/\mu$ is not really very large in the present case, one might take the attitude of neglecting higher-order resummations of logarithmic terms altogether and restrict oneself to the $\mathcal{O}(\alpha_s)$ corrections alone. Then Eq. (15.28) would already be the final result, as it was used by Flynn *et al.* (1991). This approximation is fully consistent from a theoretical point of view. Yet it is useful to have the more complete expression Eq. (15.35) at hand. Of course, as indicated above, the finite $\mathcal{O}(\alpha_s)$ correction due to the matrix element of $\tilde{Q}_s$ in Eq. (15.28) must still be added to the rhs of Eq. (15.35). However, to complete the NLO renormalization-group calculation, also the leading logarithmic corrections related to the operator $\tilde{Q}_s$ should then be resummed. This part of the analysis has been performed only recently and is discussed in Ciuchini, Franco, and Giménez (1996) and Buchalla (1996).

XVI. COMMENTS ON INPUT PARAMETERS

The phenomenology of weak decays depends sensitively on a number of input parameters. We have collected the numerical values of these parameters in the Appendix. To this end we have frequently used the values quoted by the Particle Data Group (1994). The basis for our choice of the numerical values for various nonperturbative parameters, such as B_K or F_B, will be given in the course of the presentation. In certain cases, like the B-meson lifetimes and the size of the B^0_d-$\bar{B}^0_d$ mixing, for which the experimental averages change constantly, we have chosen values that are in the ballpark of those presented at various conferences and workshops during the summer of 1995. Here we would like to comment briefly on three important parameters, $|V_{cb}|$, $|V_{ub}/V_{cb}|$, and m_t. The importance of these parameters lies in the fact that many branching ratios and also the CP violation in the standard model depend sensitively on them.

A. Cabibbo-Kobayashi-Maskawa matrix element $|V_{cb}|$

During the last two years there has been considerable progress made by experimentalists (Patterson, 1995) and theorists in the extraction of $|V_{cb}|$ from the exclusive and inclusive B decays. In these investigations the HQET in the case of exclusive decays and the heavy quark expansions for inclusive decays played a considerable role (Ball *et al.*, 1995a; Neubert, 1994a; Shifman *et al.*, 1995). From these treatments, one arrives at

$$|V_{cb}|=0.040\pm 0.003 \Rightarrow A=0.82\pm 0.06. \quad (16.1)$$

This should be compared with an error of ± 0.006 for $|V_{cb}|$ quoted in 1993. The corresponding reduction of

the error in A by a factor of 2 has important consequences for the phenomenology of weak decays.

B. Cabibbo-Kobayashi-Maskawa matrix element ratio $|V_{ub}/V_{cb}|$

The accuracy of this ratio is much worse, with the value

$$\left|\frac{V_{ub}}{V_{cb}}\right| = 0.08 \pm 0.02 \tag{16.2}$$

quoted by the Particle Data Group (1994) still the accepted one. It is important to emphasize that the theoretical status of $|V_{ub}/V_{cb}|$ is considerably less mature than it is for $|V_{cb}|$ and some model dependence is unfortunately still present in Eq. (16.2). In the following we shall adopt this estimate for definiteness, keeping the associated problems in mind. There is a hope that the error can be reduced in the future both due to progress in lattice calculations (Simone, 1996) and the recent CLEO measurements of the exclusive semileptonic decays $B \to (\pi,\rho) l \nu_l$ (Thorndike, 1995). An interesting theoretical approach, based on the construction of a constrained dispersive model for $B \to \pi$ form factors, has recently been discussed by Burdman and Kambor (1996).

C. Top-quark mass m_t

Next it is important to stress that the discovery of the top quark (Abe *et al.*, 1994a, 1994b, 1994c; Abachi *et al.*, 1995) and its mass measurement had an important impact on the field of rare decays and CP violation, considerably reducing one potential uncertainty. It is, however, important to keep in mind that the parameter m_t used in weak decays is not equal to the one used in the electroweak precision studies at LEP or SLD. In the latter investigations the so-called pole mass is used, whereas in all the NLO calculations listed in Table I and used in this review, m_t refers to the running current top-quark mass normalized at $\mu = m_t$: $\bar{m}_t(m_t)$. One has

$$m_t^{(\mathrm{pole})} = \bar{m}_t(m_t)\left[1 + \frac{4}{3}\frac{\alpha_s(m_t)}{\pi}\right] \tag{16.3}$$

so that for $m_t = \mathcal{O}(170\ \mathrm{GeV})$, $\bar{m}_t(m_t)$ is typically 8 GeV smaller than $m_t^{(\mathrm{Pole})}$.

In principle any definition $\bar{m}_t(\mu_t)$ with $\mu_t = \mathcal{O}(m_t)$ could be used. In the leading order this arbitrariness in the choice of μ_t introduces a potential theoretical uncertainty in those branching ratios that depend sensitively on the top-quark mass. The inclusion of NLO corrections reduces this uncertainty considerably, so that the resulting branching ratios remain essentially independent of the choice of μ_t. We have discussed this point already in previous sections. Numerical examples will be given in this part below. The choice $\mu_t = m_t$ turns out to be convenient and will be adopted in what follows.

Using the $m_t^{(\mathrm{pole})}$ quoted by CDF (Abe *et al.*, 1994a, 1994b, 1994c) together with Eq. (16.3) we find roughly

$$m_t \equiv \bar{m}_t(m_t) = (170 \pm 15)\ \mathrm{GeV}, \tag{16.4}$$

which we will use in the phenomenological applications. In principle an error of ± 11 GeV could be used, but we prefer to be conservative.

XVII. INCLUSIVE B DECAYS

A. General remarks

Inclusive decays of B mesons constitute an important testing ground for our understanding of strong-interaction dynamics in its interplay with the weak forces. At the same time inclusive semileptonic modes provide useful information on $|V_{cb}|$.

Due to quark-hadron duality, inclusive decays of heavy mesons can, in general, be calculated more reliably than corresponding exclusive modes. During recent years a systematic formulation for the treatment of inclusive heavy-meson decays has been developed. It is based on operator product and heavy-quark expansion, which are applied to the B-meson inclusive width, expressed as the absorptive part of the B forward-scattering amplitude

$$\Gamma(B \to X) = \frac{1}{2m_B}\,\mathrm{Im}\left(i\int d^4x \langle B|T\mathcal{H}_{\mathrm{eff}}^{(X)}(x)\mathcal{H}_{\mathrm{eff}}^{(X)}(0)|B\rangle\right). \tag{17.1}$$

Here $\mathcal{H}_{\mathrm{eff}}^{(X)}$ is the part of the complete $\Delta B=1$ effective Hamiltonian that contributes to the particular inclusive final state X under consideration. For example, for inclusive semileptonic decays

$$\mathcal{H}_{\mathrm{eff},\Delta B=1}^{(SL)} = \frac{G_F}{\sqrt{2}} V_{cb}(\bar{c}b)_{V-A} \sum_{l=e,\mu,\tau} (\bar{l}\nu_l)_{V-A} + \mathrm{H.c.}. \tag{17.2}$$

For nonleptonic modes the relevant expression is the $\Delta B=1$ short-distance effective Hamiltonian given in Eq. (6.32). It has been shown (Chay *et al.*, 1990; Bigi *et al.*, 1992, 1993; Bjorken *et al.*, 1992; Bigi, Blok, Shifman, Uraltsev, and Vainshtein, 1994; Blok *et al.* 1994; Falk *et al.*, 1994; Mannel, 1994; Manohar and Wise, 1994) that the leading term in a systematic expansion of Eq. (17.1) in $1/m_b$ is determined by the decay width of a free b quark calculated in the parton picture. Furthermore, for total integrated rates the nonperturbative corrections to this perturbative result start at order $(\Lambda/m_b)^2$, where Λ is a hadronic scale ~ 1 GeV, and are quite small in the case of B decays (Bigi *et al.*, 1992). In the light of this formulation it becomes apparent that the perturbative, partonic description of heavy-hadron decay is thus promoted from the status of a model calculation to the leading contribution in a systematic expansion based on QCD. We will still comment on the $(\Lambda/m_b)^2$ corrections below. In the following we will, however, concentrate on the leading quark-level analysis of inclusive B decays. As we shall see, the treatment of short-distance QCD effects at the next-to-leading-order level, at least for the dominant modes, is of crucial importance for a proper understanding of these processes.

The calculation of b-quark decay starts from the effective $\Delta B=1$ Hamiltonian containing the relevant four-fermion operators multiplied by Wilson coefficients. To obtain the decay rate, the matrix elements (squared) of these operators have to be calculated perturbatively to the required order in α_s. While in LLA a zeroth-order evaluation is sufficient; $\mathcal{O}(\alpha_s)$ virtual gluon effects (along with real gluon bremsstrahlung contributions for the proper cancellation of infrared divergences in the inclusive rate) have to be taken into account at NLO. In this way the renormalization scale and scheme dependence present in the coefficient functions is canceled to the considered order $[\mathcal{O}(\alpha_s)]$ in the decay rate. Thus, by contrast to low-energy decays, in the case of inclusive heavy-quark decay, a physical final result can be obtained within perturbation theory alone.

Our goal will be to review the present status of the theoretical prediction for the B-meson semileptonic branching ratio $B_{\rm SL}$. This quantity has received some attention in recent years since theoretical calculations (Altarelli and Petrarca, 1991; Tanimoto, 1992; Palmer and Stech, 1993; Bigi, Blok, Shifman and Vainshtein, 1994; Falk *et al.*, 1995) tended to yield values around 12.5–13.5%, above the experimental figure $B_{\rm SL}=(10.4\pm0.4)\%$ (Particle Data Group, 1994). However, these earlier analyses have not been complete in regard to the inclusion of final-state mass effects and NLO QCD corrections in the nonleptonic widths. More precisely, these calculations took into account mass effects appropriate for the leading order in QCD along with NLO QCD corrections obtained for massless final-state quarks. Recently the most important of these, so far lacking, mass effects have been properly included in the NLO QCD calculation through the work of Bagan *et al.*, (1994), Bagan, Ball, Braun, and Gosdzinsky (1995), and Bagan, Ball, Fiol, and Gosdzinsky (1995). These $\mathcal{O}(\alpha_s)$ mass effects tend to decrease $B_{\rm SL}$ and, according to the analysis of these authors, essentially bring it, within theoretical uncertainties, into agreement with the experimental number. Before further discussing these issues, it is appropriate to start with a short overview summarizing the possible b-quark decay modes and classifying their relative importance.

B. b-quark decay modes

First of all, a b quark can decay *semileptonically* to the final states $cl\bar{\nu}_l$ and $ul\bar{\nu}_l$ with $l=e,\mu,\tau$. In the case of nonleptonic final states we may distinguish three classes: decays induced through current-current operators alone (Class I), decays induced by both current-current and penguin operators (Class II), and pure penguin transitions (Class III). The classes have the following allowed final states:

Class I $c\bar{u}d,\ c\bar{u}s,\ u\bar{c}s,\ u\bar{c}d$

Class II $c\bar{c}s,\ c\bar{c}d,\ u\bar{u}d,\ u\bar{u}s$

Class III $d\bar{d}d,\ d\bar{d}s,\ s\bar{s}d,\ s\bar{s}s.$

Clearly there is a rich structure of possible decay modes even at the quark level, and a complete treatment would be quite complicated. However, not all of these final states are equally important. In order to perform the analysis of b-quark decay, in particular in view of the calculation of $B_{\rm SL}$, it is useful to identify the most important channels and to introduce appropriate approximations in dealing with less prominent decays. To organize the procedure, we make the following observations.

(i) The dominant, i.e., CKM-allowed and tree-level-induced, decays are $b\to cl\nu$, $b\to c\bar{u}d$, and $b\to c\bar{c}s$. For these a complete NLO calculation including final-state mass effects is necessary.

(ii) The channels $c\bar{u}s$, $c\bar{c}d$, $u\bar{c}d$, and $u\bar{u}s$ may be incorporated with excellent accuracy into the modes $c\bar{u}d$, $c\bar{c}s$, $u\bar{c}s$, and $u\bar{u}d$, respectively, by using the approximate CKM unitarity in the first two generations. The error thus introduced through the $s-d$ mass difference is entirely negligible.

(iii) Penguin transitions are generally suppressed by the smallness of their Wilson coefficient functions, which are typically of the order of a few percent. For this reason, one may neglect the pure penguin decays of class III altogether, as their decay rates involve penguin coefficients squared.

(iv) Furthermore we may neglect the penguin contributions to the CKM-suppressed $b\to u$ transitions of class II.

(v) In addition one may treat the remaining smaller effects, namely $b\to u$ transitions and the interference of penguins with the leading current-current contribution in $b\to c\bar{c}s$, within LLA.

(vi) Finally, rare, flavor-changing neutral-current b-decay modes are negligible in the present context as well.

Next we will write down expressions for the relevant decay-rate contributions we have discussed.

For the dominant modes $b\to cl\nu$, $b\to c\bar{u}d$, and $b\to c\bar{c}s$ (without penguin effects) one has at next-to-leading order

$$\Gamma(b\to cl\nu)=\Gamma_0 P(x_c,x_l,0)\left[1+\frac{2\alpha_s(\mu)}{3\pi}\,g(x_c,x_l,0)\right], \tag{17.3}$$

$$\begin{aligned}\Gamma(b\to c\bar{u}d)=\Gamma_0 P(x_c,0,0)\Bigg\{&2L_+^2+L_-^2\\&+\frac{\alpha_s(M_W)-\alpha_s(\mu)}{2\pi}\,(2L_+^2R_++L_-^2R_-)\\&+\frac{2\alpha_s(\mu)}{3\pi}\Bigg[\frac{3}{4}\,(L_+-L_-)^2 g_{11}(x_c)\\&+\frac{3}{4}\,(L_++L_-)^2 g_{22}(x_c)+\frac{1}{2}\,(L_+^2-L_-^2)\\&\times\left(g_{12}(x_c)-12\ln\frac{\mu}{m_b}\right)\Bigg]\Bigg\},\end{aligned} \tag{17.4}$$

TABLE XXXVI. Typical values for the ratio of NLO to LO results for dominant b-decay channels with (I) and without (II) including finite charm-mass effects in the NLO correction terms. The leading-order final-state mass effects (through the function P) are taken into account in all cases.

	$b\to ce\nu$	$b\to c\tau\nu$	$b\to c\bar{u}d$	$b\to c\bar{c}s$
I	0.85	0.88	1.06	1.32
II	0.79	0.80	1.01	1.02

$$\Gamma(b\to c\bar{c}s)=\Gamma_0 P(x_c,x_c,x_s)\Bigg\{2L_+^2+L_-^2 + \frac{\alpha_s(M_W)-\alpha_s(\mu)}{2\pi}(2L_+^2R_+ + L_-^2R_-) + \frac{2\alpha_s(\mu)}{3\pi}\Bigg[\frac{3}{4}(L_+-L_-)^2 h_{11}(x_c) + \frac{3}{4}(L_++L_-)^2 h_{22}(x_c) + \frac{1}{2}(L_+^2-L_-^2) \times\left(h_{12}(x_c)-12\ln\frac{\mu}{m_b}\right)\Bigg]\Bigg\}. \tag{17.5}$$

Equation (17.5) neglects small strange-quark mass effects in the NLO terms, which have been included in the numerical analysis by Bagan, Ball, Fiol, and Gosdzinsky (1995). In the equations above $\Gamma_0=G_F^2 m_b^5|V_{cb}|^2/(192\pi^3)$, and $P(x_1,x_2,x_3)$ is the leading-order phase-space factor given, for arbitrary masses $x_i=m_i/m_b$, by

$$P(x_1,x_2,x_3)=12\int_{(x_2+x_3)^2}^{(1-x_1)^2}\frac{ds}{s}(s-x_2^2-x_3^2) \times(1+x_1^2-s)w(s,x_2^2,x_3^2)w(s,x_1^2,1) \tag{17.6}$$

$$w(a,b,c)=(a^2+b^2+c^2-2ab-2ac-2bc)^{1/2}. \tag{17.7}$$

P is a completely symmetric function of its arguments.

Furthermore,

$$L_\pm=L_\pm(\mu)=\left[\frac{\alpha_s(M_W)}{\alpha_s(\mu)}\right]^{d_\pm} \tag{17.8}$$

with $d_+=6/23$, $d_-=-12/23$ [see Eq. (5.10)], and $\mu=\mathcal{O}(m_b)$. The scheme-independent $R_\pm$ come from the NLO renormalization-group evolution and are given by $R_\pm=B_\pm-J_\pm$ [see Eq. (5.9)]. For $f=5$ flavors $R_+=6473/3174$ and $R_-=-9371/1587$. Note that the leading dependence of $L_\pm$ on the renormalization scale μ is canceled to $\mathcal{O}(\alpha_s)$ by the explicit μ dependence in the α_s correction terms. Virtual gluon and bremsstrahlung corrections to the matrix elements of four-fermion operators are contained in the mass-dependent functions g, g_{ij}, and h_{ij}.

The function $g(x_1,x_2,x_3)$ is available for arbitrary x_1, x_2, and x_3 from Hokim and Pham (1983, 1984). The special case $g(x_1,0,0)$ has been analyzed also by Cabibbo and Maiani (1978). Analytical expressions have been given by Nir (1989) for $g(x_1,0,0)$ and by Bagan *et al.* (1994) for $g(0,x_2,0)$. The functions $g_{11}(x)$, $g_{12}(x)$, and $g_{22}(x)$ are calculated analytically by Bagan *et al.* (1994). Furthermore, as discussed by Bagan *et al.* (1994), $h_{11}(x)$ and $h_{22}(x)$ can be obtained from the work of Hokim and Pham (1983, 1984). Finally, $h_{12}(x)$ has been determined by Bagan, Ball, Fiol, and Gosdzinsky (1995). For the full mass dependence of these functions we refer the reader to the cited literature. Here we quote the results obtained in the massless limit. These have been computed by Altarelli *et al.* (1981) and Buchalla (1993) for g_{ij}, h_{ij} $[g_{ij}(0)=h_{ij}(0)]$

$$g_{11}(0)=g_{22}(0)=\frac{31}{4}-\pi^2,\quad g_{12}(0)=g_{11}(0)-\frac{19}{2}. \tag{17.9}$$

Furthermore,

$$g(0,0,0)=\frac{25}{4}-\pi^2. \tag{17.10}$$

In Table XXXVI we have listed some typical numbers extracted from Bagan, Ball, Braun, and Gosdzinsky (1995) and Bagan, Ball, Fiol, and Gosdzinsky (1995), which illustrate the impact of charm-mass effects (for $x_c=0.3$) in the NLO correction terms by giving the enhancement factor of the NLO over the LO results. There are of course various ambiguities involved in this comparison. The numbers in Table XXXVI are therefore merely intended to show the general trend. Note the sizable enhancement through NLO mass effects in the nonleptonic channels, in particular $b\to c\bar{c}s$. A large QCD enhancement in the latter case has also been reported by Voloshin (1995). In principle the validity of the heavy-quark expansion might be questioned for $b\to c\bar{c}s$, since in this case the energy release is relatively small. On the other hand, the direct partonic NLO calculation of $B(b\to c\bar{c}s)$ is in agreement with an indirect determination of this quantity that does not require theoretical input for $b\to c\bar{c}s$. The latter determination is possible by combining experimental information on the semileptonic branching ratio $B(B\to Xe\nu)$ with the NLO calculation of $\Gamma(b\to c\bar{u}d)/\Gamma(b\to ce\nu)$ and has been described by Buchalla *et al.* (1995). A discussion of the implications for the charm yield in B decays can also be found in this paper.

To complete the presentation of b decay modes we next write down expressions for the CKM-suppressed channels $b\to ul\nu$, $b\to u\bar{c}s$, and $b\to u\bar{u}d$ (without penguins) as well as the contribution to the $b\to c\bar{c}s$ rate due to interference of the leading, current-current-type transitions with penguin operators. Restricting ourselves to the LLA for these small contributions, we obtain

$$\Gamma\left(b\to u\sum_l l\nu\right)=\Gamma_0\left|\frac{V_{ub}}{V_{cb}}\right|^2\sum_l P(0,x_l,0), \tag{17.11}$$

$$\Gamma(b\to u\bar{c}s)=\Gamma_0\left|\frac{V_{ub}}{V_{cb}}\right|^2 P(0,x_c,x_s)[2L_+^2+L_-^2], \tag{17.12}$$

$$\Gamma(b\to u\bar{u}d)=\Gamma_0\left|\frac{V_{ub}}{V_{cb}}\right|^2[2L_+^2+L_-^2], \tag{17.13}$$

$$\Delta\Gamma_{\text{penguin}}(b\to c\bar{c}s)$$
$$=6\Gamma_0 P(x_c,x_c,x_s)\left\{c_1\left[c_3+\frac{1}{3}c_4+F\left(c_5+\frac{1}{3}c_6\right)\right]\right.$$
$$\left.+c_2\left[\frac{1}{3}c_3+c_4+F\left(\frac{1}{3}c_5+c_6\right)\right]\right\}, \tag{17.14}$$

where $c_1,\ldots,c_6$ are the leading-order Wilson coefficients and

$$F=\frac{6x_c^2}{P(x_c,x_c,x_s)}\int_{(x_c+x_s)^2}^{(1-x_c)^2}\frac{ds}{s^2}(s+x_s^2-x_c^2)(1+s-x_c^2)$$
$$\times w(s,x_c^2,x_s^2)w(1,s,x_c^2). \tag{17.15}$$

Numerically we have, for $|V_{ub}/V_{cb}|=0.1$,

$$\Gamma\left(b\to u\sum_l l\nu\right)\approx 0.024\Gamma_0,\quad \Gamma(b\to u\bar{c}s)\approx 0.017\Gamma_0, \tag{17.16}$$

$$\Gamma(b\to u\bar{u}d)\approx 0.034\Gamma_0,$$

$$\Delta\Gamma_{\text{penguin}}(b\to c\bar{c}s)\approx -0.041\Gamma_0. \tag{17.17}$$

Note that the contribution due to the interference with penguin transitions in $b\to c\bar{c}s$ is negative. Hence, in addition to being small, the effects in Eqs. (17.16) and (17.17) tend to cancel each other in the total nonleptonic width.

Finally one may also incorporate nonperturbative corrections. These have been derived by Bigi *et al.* (1992) and are also discussed by Bagan *et al.* (1994). As mentioned above, nonperturbative effects are suppressed by two powers of the heavy b-quark mass and amount typically to a few percent. For details we refer the reader to the cited articles.

C. The *B*-meson semileptonic branching ratio

An important application of the results described in the previous section is the theoretical prediction for the inclusive semileptonic branching ratio of B mesons

$$B_{\text{SL}}=\frac{\Gamma(B\to Xe\nu)}{\Gamma_{\text{tot}}(B)}. \tag{17.18}$$

On the parton level, $\Gamma(B\to Xe\nu)\simeq\Gamma(b\to ce\nu)$, and

$$\Gamma_{\text{tot}}(B)\simeq\sum_{l=e,\mu,\tau}\Gamma(b\to cl\nu)+\Gamma(b\to c\bar{u}d)$$
$$+\Gamma(b\to c\bar{c}s)+\Delta\Gamma_{\text{penguin}}(b\to c\bar{c}s)$$
$$+\Gamma(b\to u). \tag{17.19}$$

Here we have applied the approximations discussed above. $\Gamma(b\to u)$ summarizes the $b\to u$ transitions.

Based on a similar treatment of the partonic rates, including next-to-leading-order QCD corrections for the dominant channels and also incorporating nonperturbative corrections, Bagan, Ball, Braun, and Gosdzinsky (1995) and Bagan, Ball, Fiol, and Gosdzinsky (1995) have carried out an analysis of B_{SL} and estimated the theoretical uncertainties. The mass difference m_b-m_c is rather accurately constrained by charm and beauty hadron masses using heavy-quark effective theory. To reduce uncertainties from quark masses, this relationship was employed in their prediction. They obtain (Bagan, Ball, Fiol, and Gosdzinsky, 1995; Bagan, Ball, Braun, and Gosdzinsky, 1996)

$$B_{\text{SL}}=(12.0\pm 1.4)\% \quad\text{and}\quad B_{\text{SL}}=(11.3\pm 1.7)\%, \tag{17.20}$$

using pole and $\overline{\text{MS}}$ masses, respectively. The error is dominated in both cases by the renormalization-scale uncertainty ($m_b/2<\mu<2m_b$). Note also the sizable scheme ambiguity. Within existing uncertainties, the theoretical prediction does not disagree significantly with the experimental value $B_{\text{SL,exp}}=(10.4\pm 0.4)\%$ (Particle Data Group, 1994), although it seems to lie somewhat on the high side.

It is amusing to note that the naive mode-counting estimate for B_{SL}, neglecting QCD and final-state mass effects completely, yields $B_{\text{SL}}=1/9=11.1\%$ in good agreement with experiment. Including the final-state masses, still neglecting QCD, enhances this number to $B_{\text{SL}}=15.8\%$. Incorporating QCD effects at the leading-logarithmic-order *increases* the hadronic modes, thus leading to a *decrease* in B_{SL}, which results typically in $B_{\text{SL}}=14.7\%$. A substantial further decrease is finally brought about through the NLO QCD corrections, which both further enhance hadronic channels, in particular $b\to c\bar{c}s$, and simultaneously reduce $b\to ce\nu$. As pointed out by Bagan, Ball, Braun, and Gosdzinsky (1995) and Bagan, Ball, Fiol, and Gosdzinsky (1995) and illustrated in Table XXXVI, final-state mass effects in the NLO correction terms play a non-negligible role for this enhancement of hadronic decays. The nonperturbative effects also lead to a slight decrease of B_{SL}.

In short, leading final-state mass effects and QCD corrections, acting in opposite directions on B_{SL}, tend to cancel each other, resulting in a number for B_{SL} not too different from the simple mode-counting guess.

We finally mention that, besides a calculation of B_{SL}, the partonic treatment of heavy-meson decay has further important applications, such as the determination of $|V_{cb}|$ from inclusive semileptonic B decay, $B\to X_c e\nu$. Analyses of this type have been presented by Ball and Nierste (1994), Bigi and Uraltsev (1994), Luke and Savage (1994), and Shifman *et al.* (1995).

Exact results beyond the presently known NLO accuracy seem extremely difficult to obtain, even for relatively simple quantities like the semileptonic b-quark decay rate. There exist, however, calculations in the literature devoted to the investigation of these higher-order perturbative effects. Due to the severe technical difficulties, those calculations require additional assumptions. For instance, in an interesting study Ball *et al.* (1995a) have investigated the effects of the running of α_s on the semileptonic b-quark decay rate to all orders in perturbation theory. This calculation is equivalent to a resummation of all terms of the form $\alpha_s(\beta_0\alpha_s)^n$, which are related to one-gluon exchange diagrams containing

an arbitrary number n of fermion bubbles. The work of Ball *et al.* (1995a) applies the renormalon techniques developed by Ball *et al.* (1995b) and Beneke and Braun (1995) [see also (Beneke and Braun, 1994) and (Bigi *et al.*, 1994b)] and generalizes the $\mathcal{O}(\beta_0\alpha_s^2)$ results computed by Luke *et al.* (1995). The underlying idea is similar in spirit to the BLM approach (Brodsky *et al.*, 1983). An important application of the result is the extraction of $|V_{cb}|$ (Ball *et al.*, 1995a). The formalism has also been used to study higher-order QCD corrections to the τ-lepton hadronic width (Ball *et al.*, 1995b). Irrespective of the ultimate reliability of the approximation, these investigations are useful from a conceptual point of view, as they help to illustrate important features of the higher-order behavior of the perturbative expansion.

In principle the discussion we have given for b decays may of course, with appropriate modifications, be applied to the case of charm as well. However, here the nonperturbative corrections to the parton picture, which scale like $1/m_Q^2$ with the heavy-quark mass m_Q, are an order of magnitude larger than for B mesons, and accurate theoretical predictions are much more difficult to obtain (Blok and Shifman, 1993).

XVIII. ε_K, B^0-$\bar{B}^0$ MIXING, AND THE UNITARITY TRIANGLE

A. Basic formula for ε_K

The indirect CP violation in $K\to\pi\pi$ is described by the well-known parameter ε_K. The general formula for ε_K is given as follows:

$$\varepsilon_K=\frac{\exp(i\pi/4)}{\sqrt{2}\Delta M_K}\,(\mathrm{Im}M_{12}+2\xi\ \mathrm{Re}M_{12}), \tag{18.1}$$

where

$$\xi=\frac{\mathrm{Im}A_0}{\mathrm{Re}A_0} \tag{18.2}$$

with $A_0\equiv A(K\to(\pi\pi)_{I=0})$ and ΔM_K the K_L-K_S mass difference. The off-diagonal element M_{12} in the neutral K-meson mass matrix represents the K^0-$\bar{K}^0$ mixing. It is given by

$$2m_K M_{12}^*=\langle\bar{K}^0|\mathcal{H}_{\mathrm{eff}}(\Delta S=2)|K^0\rangle, \tag{18.3}$$

where $\mathcal{H}_{\mathrm{eff}}(\Delta S=2)$ is the effective Hamiltonian of Eq. (12.1). Defining the renormalization-group-invariant parameter B_K by

$$B_K=B_K(\mu)[\alpha_s^{(3)}(\mu)]^{-2/9}\left[1+\frac{\alpha_s^{(3)}(\mu)}{4\pi}J_3\right], \tag{18.4}$$

$$\langle\bar{K}^0|(\bar{s}d)_{V-A}(\bar{s}d)_{V-A}|K^0\rangle\equiv\frac{8}{3}B_K(\mu)F_K^2m_K^2 \tag{18.5}$$

and, using Eq. (12.1), we find

$$M_{12}=\frac{G_F^2}{12\pi^2}F_K^2B_Km_KM_W^2[\lambda_c^{*2}\eta_1S_0(x_c)+\lambda_t^{*2}\eta_2S_0(x_t)+2\lambda_c^*\lambda_t^*\eta_3S_0(x_c,x_t)], \tag{18.6}$$

where the functions $S_0(x_i)$ and $S_0(x_i,x_j)$ are those of Eqs. (12.3)–(12.5). F_K is the K-meson decay constant and m_K the K-meson mass. The coefficient J_3 is given in Eq. (12.9) and the QCD factors η_i have been discussed in Sec. XII. Their numerical values are

$$\eta_1=1.38,\quad \eta_2=0.57,\ \text{and}\ \ \eta_3=0.47. \tag{18.7}$$

The last term in Eq. (18.1) constitutes at most a 2% correction to ε_K and consequently can be neglected in view of other uncertainties, in particular those connected with B_K. Inserting Eq. (18.6) into Eq. (18.1), we find

$$\varepsilon_K=C_\varepsilon B_K\mathrm{Im}\lambda_t\{\mathrm{Re}\lambda_c[\eta_1S_0(x_c)-\eta_3S_0(x_c,x_t)]-\mathrm{Re}\lambda_t\eta_2S_0(x_t)\}\exp(i\pi/4), \tag{18.8}$$

where we have used the unitarity relation $\mathrm{Im}\lambda_c^*=\mathrm{Im}\lambda_t$ and neglected $\mathrm{Re}\lambda_t/\mathrm{Re}\lambda_c=\mathcal{O}(\lambda^4)$ in evaluating $\mathrm{Im}(\lambda_c^*\lambda_t^*)$. The numerical constant C_ε is given by

$$C_\varepsilon=\frac{G_F^2F_K^2m_KM_W^2}{6\sqrt{2}\pi^2\Delta M_K}=3.78\times10^4. \tag{18.9}$$

Using the standard parametrization of Eq. (2.13) to evaluate $\mathrm{Im}\lambda_i$ and $\mathrm{Re}\lambda_i$, setting the values for s_{12}, s_{13}, s_{23}, and m_t in accordance with the Appendix, and taking a value for B_K (see below), one can determine the phase δ by comparing Eq. (18.8) with the experimental value for ε_K.

Once δ has been determined in this manner, one can find the corresponding point $(\bar{\varrho},\bar{\eta})$ by using Eqs. (2.19) and (2.22). Actually, for a given set $(s_{12},s_{13},s_{23},m_t,B_K)$ there are two solutions for δ and consequently two solutions for $(\bar{\varrho},\bar{\eta})$. In order to see this clearly it is useful to use the Wolfenstein parametrization in which $\mathrm{Im}\lambda_t$, $\mathrm{Re}\lambda_c$, and $\mathrm{Re}\lambda_t$ are given to a very good approximation by Eqs. (2.23)–(2.25). We then find that Eq. (18.8) and the experimental value for ε_K specify a hyperbola in the $(\bar{\varrho},\bar{\eta})$ plane given by

$$\bar{\eta}\{(1-\bar{\varrho})A^2\eta_2S_0(x_t)+P_0(\varepsilon)\}A^2B_K=0.226, \tag{18.10}$$

where

$$P_0(\varepsilon)=[\eta_3S_0(x_c,x_t)-\eta_1x_c]\frac{1}{\lambda^4}. \tag{18.11}$$

The hyperbola [Eq. (18.10)] intersects the circle given by Eq. (2.32) in two points, which correspond to the two solutions for δ mentioned earlier.

The position of the hyperbola in the $(\bar{\varrho},\bar{\eta})$ plane depends on m_t, $|V_{cb}|=A\lambda^2$, and B_K. With decreasing m_t, $|V_{cb}|$, and B_K the ε_K hyperbola moves away from the origin of the $(\bar{\varrho},\bar{\eta})$ plane. When the hyperbola and the circle touch each other, lower bounds consistent with $\varepsilon_K^{\mathrm{exp}}$ for m_t, $|V_{cb}|$, $|V_{ub}/V_{cb}|$, and B_K can be found. The lower bound on m_t is discussed by Buras (1993). Corre-

TABLE XXXVII. Predictions for various quantities using present and future input parameter ranges given in the Appendix. Imλ_t and $|V_{td}|$ are given in units of 10^{-4} and 10^{-3}, respectively, δ is in degrees.

	No x_d constraint		With x_d constraint	
	Present	Future	Present	Future
δ	37.7–160.0	57.4–144.9	37.7–140.2	58.5–93.3
Imλ_t	0.64–1.75	0.82–1.50	0.87–1.75	1.12–1.50
$\lvert V_{td}\rvert$	6.7–13.5	7.7–12.1	6.7–11.9	7.8–9.3
x_s			11.1–47.0	19.6–29.6
$\sin(2\alpha)$	–0.86–1.00	–0.323–1.00	–0.86–1.00	–0.30–0.73
$\sin(2\beta)$	0.21–0.80	0.34–0.73	0.34–0.80	0.57–0.73
$\sin\gamma$	0.34–1.00	0.58–1.00	0.61–1.00	0.85–1.00

sponding results for $|V_{ub}/V_{cb}|$ and B_K are shown in Figs. 11 and 12, respectively. They will be discussed below.

Moreover, approximate analytic expressions for these bounds can be derived. One has

$$(m_t)_{\min}=M_W\left[\frac{1}{2A^2}\left(\frac{1}{A^2B_KR_b}-1.4\right)\right]^{0.658}, \tag{18.12}$$

$$|V_{ub}/V_{cb}|_{\min}=\frac{\lambda}{1-\lambda^2/2}\,[A^2B_K(2x_t^{0.76}A^2+1.4)]^{-1}, \tag{18.13}$$

$$(B_K)_{\min}=[A^2R_b(2x_t^{0.76}A^2+1.4)]^{-1}. \tag{18.14}$$

Concerning the parameter B_K, the analyses of Sharpe (1994) and Ishizuka (1993) (B_K=0.83±0.03) using the lattice method and of Bijnens and Prades (1995), using a somewhat modified form of the $1/N$ approach of Bardeen *et al.* (1988) and Gérard (1990) give results in the ballpark of the original $1/N$ result, B_K=0.70±0.10. In particular the analysis of Bijnens and Prades (1995) seems to have explained the difference between these values for B_K and the lower values obtained using the QCD Hadronic Duality approach (Pich and de Rafael, 1985; Prades *et al.*, 1991) (B_K=0.39±0.10) or using SU(3) symmetry and PCAC (B_K=1/3) (Donoghue *et al.*, 1982). These higher values of B_K are also found in the most recent lattice analysis (Crisafulli *et al.*, 1996) (B_K=0.86±0.15) and in the lattice calculations of Bernard and Soni (1991) (B_K=0.78±0.11) and the JLQCD group (B_K=0.67±0.07) with the quoted values obtained on the basis of the review by Soni (1995). In the numerical analysis we will use

$$B_K=0.75\pm0.15. \tag{18.15}$$

B. Basic formula for B^0-$\bar{B}^0$ mixing

The B^0-$\bar{B}^0$ mixing is usually described by

$$x_{d,s}\equiv\frac{(\Delta M)_{B_{d,s}}}{\Gamma_{B_{d,s}}}=\frac{2|M_{12}|_{B_{d,s}}}{\Gamma_{B_{d,s}}}, \tag{18.16}$$

where $(\Delta M)_{B_{d,s}}$ is the mass difference between the mass eigenstates in the B^0_d-$\bar{B}^0_d$ system and the B^0_s-$\bar{B}^0_s$ system, respectively, and $\Gamma_{B_{d,s}}=1/\tau_{B_{d,s}}$ with $\tau_{B_{d,s}}$ being the corresponding lifetimes. The off-diagonal term M_{12} in Eq. (18.16) is given by

$$2m_B|M_{12}|=|\langle\bar{B}^0|\mathcal{H}_{\rm eff}(\Delta B=2)|B^0\rangle|, \tag{18.17}$$

where $\mathcal{H}_{\rm eff}(\Delta B=2)$ is the effective Hamiltonian of Eq. (13.1). Defining the renormalization-group-invariant parameter B_B by

$$B_B=B_B(\mu)[\alpha_s^{(5)}(\mu)]^{-6/23}\left[1+\frac{\alpha_s^{(5)}(\mu)}{4\pi}J_5\right], \tag{18.18}$$

$$\langle\bar{B}^0|(\bar{b}d)_{V-A}(\bar{b}d)_{V-A}|B^0\rangle\equiv\frac{8}{3}\,B_B(\mu)F_B^2m_B^2 \tag{18.19}$$

and using Eq. (13.1), we find

$$x_{d,s}=\tau_{B_{d,s}}\frac{G_F^2}{6\pi^2}\,\eta_Bm_{B_{d,s}}(B_{B_{d,s}}F^2_{B_{d,s}})M_W^2S_0(x_t)|V_{t(d,s)}|^2 \tag{18.20}$$

with the QCD factor η_B discussed in Sec. XIII and given by η_B=0.55.

The measurement of B^0_d-$\bar{B}^0_d$ mixing allows one to determine $|V_{td}|$ or R_t of Eq. (2.33):

$$|V_{td}|=A\lambda^3R_t,\quad R_t=1.52\,\frac{R_0}{\sqrt{S_0(x_t)}}, \tag{18.21}$$

where

$$R_0=\left[\frac{0.040}{|V_{cb}|}\right]\left[\frac{200\ \text{MeV}}{\sqrt{B_{B_d}}F_{B_d}}\right]\left[\frac{x_d}{0.75}\right]^{0.5}\left[\frac{1.6ps}{\tau_B}\right]^{0.5}\left[\frac{0.55}{\eta_B}\right]^{0.5}, \tag{18.22}$$

which gives, setting η_B=0.55,

$$|V_{td}|=8.56\cdot10^{-3}\left[\frac{170\ \text{GeV}}{\bar{m}_t(m_t)}\right]^{0.76}\left[\frac{200\ \text{MeV}}{\sqrt{B_{B_d}}F_{B_d}}\right]\times\left[\frac{x_d}{0.75}\right]^{0.5}\left[\frac{1.6ps}{\tau_B}\right]^{0.5}. \tag{18.23}$$

There is a vast literature on the lattice calculations of F_B. The most recent results are somewhat lower than those quoted a few years ago. Based on a review by Sachrajda (1994), the recent extensive study by Duncan

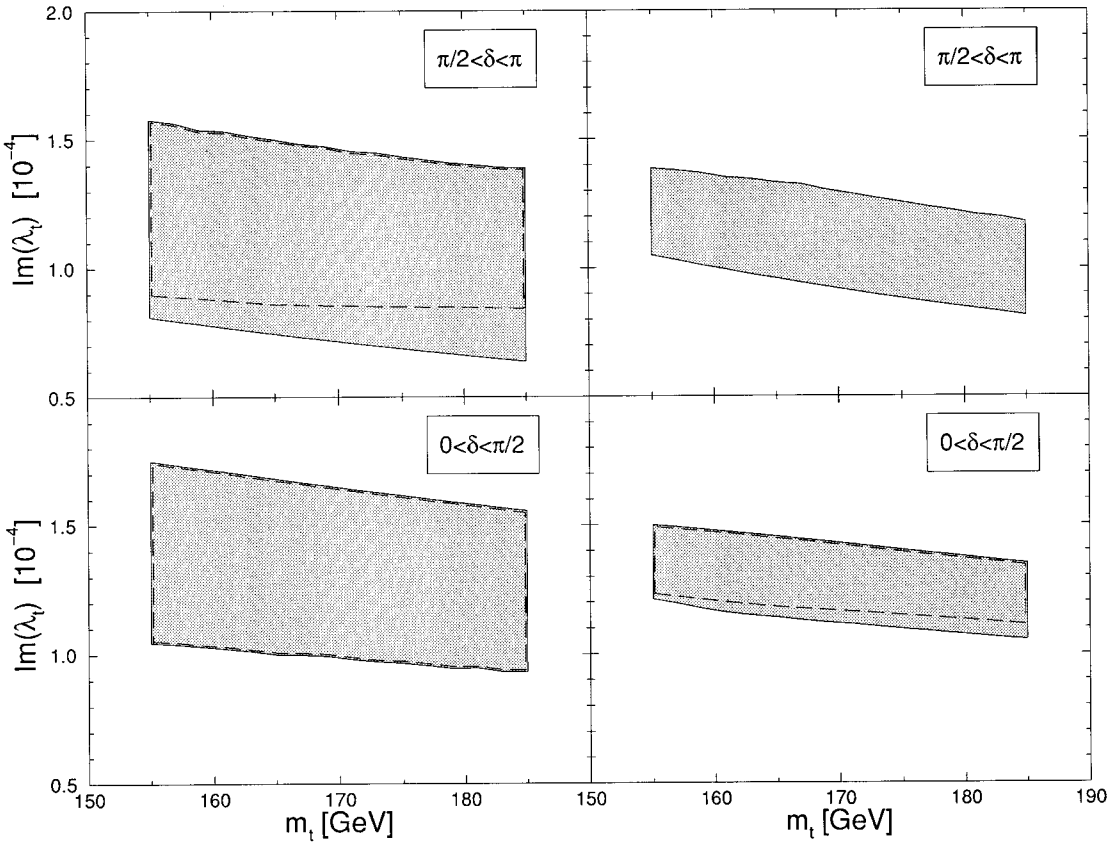

FIG. 10. Present (left) and future (right) allowed ranges for $\mathrm{Im}(\lambda_t)$. The ranges have been obtained by fitting ε_K in Eq. (18.8) to the experimental value. Input parameter ranges are given in the Appendix. The impact of the additional constraint coming from x_d is illustrated by the dashed lines. With the x_d constraint imposed the solution $\pi/2<\delta<\pi$ is completely eliminated for the future scenario.

et al. (1995) and the analyses by Bernard *et al.* (1994) and Draper and McNeile (1994), we conclude that $F_{B_d} = (180 \pm 40)$ MeV. This together with the earlier result of the European Collaboration (Abada *et al.*, 1992) for B_B, gives $F_{B_d}\sqrt{B_{B_d}} = 194 \pm 45$ MeV. A reduction of the error in this important quantity is desirable. These results for F_B are compatible with the results obtained using QCD sum rules [e.g., Bagan *et al.* (1992) and Neubert (1992)]. An interesting upper bound $F_{B_d} < 195$ MeV using QCD dispersion relations has also recently been obtained (Boyd *et al.*, 1995). In the numerical analysis we will use

$$\sqrt{B_{B_d}}F_{B_d} = (200 \pm 40) \ \text{MeV}. \tag{18.24}$$

The accuracy of the determination of R_t can be considerably improved by measuring simultaneously the B_s^0-$\bar{B}_s^0$ mixing described by x_s. We have

$$R_t = \frac{1}{\sqrt{R_{ds}}}\sqrt{\frac{x_d}{x_s}}\frac{1}{\lambda}\sqrt{1-\lambda^2(1-2\varrho)},$$

$$R_{ds} = \frac{\tau_{B_d}}{\tau_{B_s}}\frac{m_{B_d}}{m_{B_s}}\left[\frac{F_{B_d}\sqrt{B_{B_d}}}{F_{B_s}\sqrt{B_{B_s}}}\right]^2. \tag{18.25}$$

Note that m_t and $|V_{cb}|$ have been eliminated in this way and that R_{ds} depends only on SU(3) flavor-breaking effects, which contain much smaller theoretical uncertainties than the hadronic matrix elements in x_d and x_s separately. Provided x_d/x_s has been accurately measured, a determination of R_t within $\pm 10\%$ should be possible. Indeed the most recent lattice results (Baxter *et al.*, 1994; Duncan *et al.*, 1995) give $F_{B_s}/F_{B_d} = 1.22 \pm 0.04$. A similar result $F_{B_s}/F_{B_d} = 1.16 \pm 0.05$ has been obtained using QCD sum rules (Narison, 1994). It would be useful to know B_{B_s}/B_{B_d} with a similar precision. For $B_{B_s} = B_{B_d}$ we find, using the lattice result, R_{ds}=0.66±0.04.

C. sin 2β from ε_K and B^0-$\bar{B}^0$ mixing

Combining Eqs. (18.10) and (18.20), one can derive an analytic formula for $\sin(2\beta)$ (Buras, Lautenbacher, and Ostermaier, 1994)

$$\sin(2\beta) = \frac{1}{1.16A^2\eta_2 R_0^2}\left[\frac{0.226}{A^2 B_K} - \bar{\eta}P_0(\varepsilon)\right]. \tag{18.26}$$

$P_0(\varepsilon)$ is weakly dependent on m_t and, for 155 GeV$\leq m_t \leq$185 GeV, one has $P_0(\varepsilon)\approx 0.31\pm 0.02$. As $\bar{\eta}\leq 0.45$ for $|V_{ub}/V_{cb}|\leq 0.1$, the first term in parentheses is generally a factor of 2–3 larger than the second term.

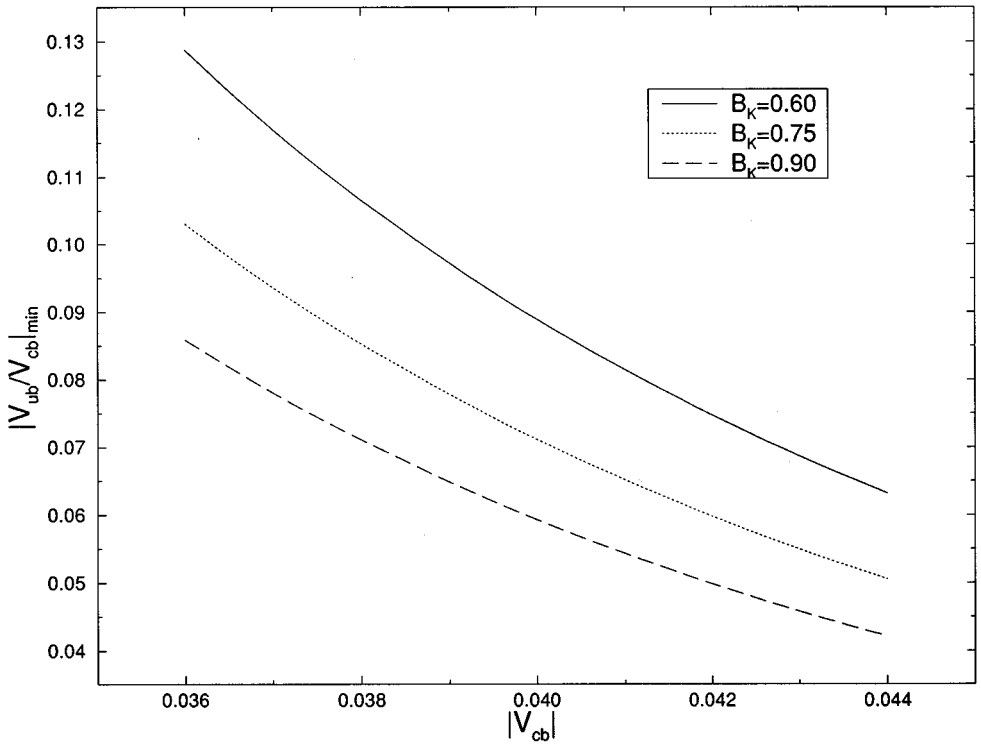

FIG. 11. $|V_{ub}/V_{cb}|_{\min}$ for $m_t \leq 185$ GeV and various choices of B_K.

Since this dominant term is independent of m_t, the values for $\sin(2\beta)$ extracted from ε_K and B^0-$\bar{B}^0$ mixing show only a weak dependence on m_t, as stressed in particular by Rosner (1992).

Since $A^2 R_0^2$ is independent of $|V_{cb}|$, the dominant uncertainty in this determination of $\sin(2\beta)$ resides in $A^2 B_K$, in the first term in the parentheses, and in $F_{B_d}\sqrt{B_{B_d}}$ contained in R_0^2.

D. Phenomenological analysis

We will now combine the analyses of ε_K and of B_d^0-$\bar{B}_d^0$ mixing to obtain allowed ranges for several quantities of interest. We consider two sets of input parameters, which are collected in the Appendix. The first set represents the present situation. The second set can be considered as a "future vision," in which the errors on various input parameters have been decreased. It is plausible that such errors will be achieved by the end of this decade, although one cannot guarantee that the central values will remain. In Table XXXVII we show the results for δ, $\mathrm{Im}\lambda_t$, $\sin 2\alpha$, $\sin 2\beta$, $\sin\gamma$, $|V_{td}|$, and x_s. They correspond to the two sets of parameters in question, with and without the constraint from B_d^0-$\bar{B}_d^0$ mixing. The results for $\mathrm{Im}\lambda_t$ and $|V_{td}|$ will play an important role in the phenomenology of rare decays and CP violation. For completeness we also show the expectations for $\sin 2\alpha$, $\sin 2\beta$, and $\sin\gamma$, which enter various CP asymmetries in B decays. As already discussed in detail by Buras, Lautenbacher, and Ostermaier (1994), $\sin 2\alpha$ cannot be predicted accurately this way. On the other hand, $\sin 2\beta$ and $\sin\gamma$ are more constrained, and the resulting ranges for these quantities indicate that large CP asymmetries should be observed in a variety of B decays.

In Fig. 10 we show $\mathrm{Im}\lambda_t$ as a function of m_t. In Fig. 11 the lower bound on $|V_{ub}/V_{cb}|$ resulting from the ε_K constraint is shown as a function of $|V_{cb}|$ for various values of B_K. To this end we have set m_t=185 GeV. For lower values of m_t the lower bound on $|V_{ub}/V_{cb}|$ is stronger. A similar analysis has been made by Herrlich and Nierste (1995a). The latter work and the plot in Fig. 11 demonstrate clearly the impact of the ε_K constraint on the allowed values of $|V_{ub}/V_{cb}|$ and $|V_{cb}|$. Simultaneously, small values of $|V_{ub}/V_{cb}|$ and $|V_{cb}|$, although still consistent with tree-level decays, are not allowed by the size of the indirect CP violation observed in $K \to \pi\pi$. Another representation of this behavior is shown in Fig. 12, where we plot the minimal value of B_K consistent with the experimental value of ε_K as a function of V_{cb} for different $|V_{ub}/V_{cb}|$ and m_t<185 GeV.

Finally in Fig. 13 we show the allowed ranges in the $(\bar{\rho}, \bar{\eta})$ plane obtained using the information from V_{cb}, $|V_{ub}/V_{cb}|$, ε_K, and B_d^0-$\bar{B}_d^0$ mixing. In this plot we also show the impact of a future measurement of B_s^0-$\bar{B}_s^0$ mixing with x_s=10, 15, 25, and 40, which, by means of the Eq. (18.25), gives an important measurement of the side R_t of the unitarity triangle. Whereas at present a broad range in the $(\bar{\rho}, \bar{\eta})$ plane is allowed, the situation might change in the future, allowing only the values of $0 \leq \bar{\rho} \leq 0.2$ and $0.30 \leq \bar{\eta} \leq 0.40$. This results in smaller ranges for various quantities of interest as explicitly seen in Table XXXVII.

Other analyses of the unitarity triangle can be found in works by Ali and London (1995), Ciuchini *et al.*

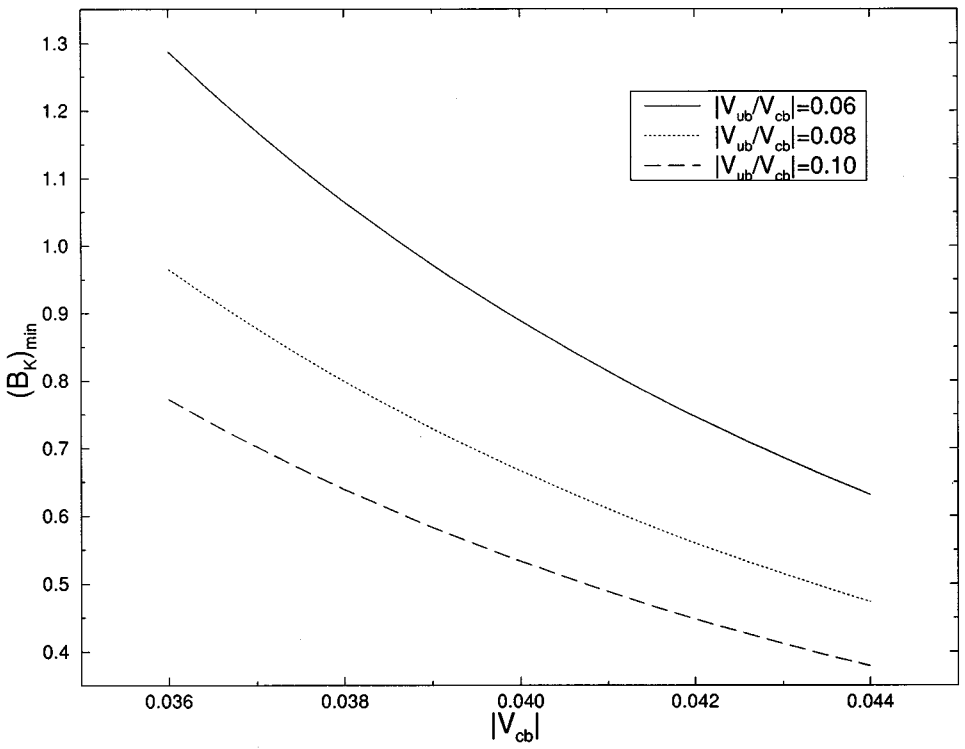

FIG. 12. $(B_K)_{\min}$ of Eq. (18.14) for $m_t \leqslant 185$ GeV and various choices of $|V_{ub}/V_{cb}|$.

(1995), Herrlich and Nierste (1995a), and Peccei and Wang (1995).

XIX. ε'/ε BEYOND LEADING LOGARITHMIC ORDER

A. Basic formulas

The direct CP violation in $K\to\pi\pi$ is described by ε'. The parameter ε' is given in terms of the amplitudes $A_0 \equiv A(K\to(\pi\pi)_{I=0})$ and $A_2 \equiv A(K\to(\pi\pi)_{I=2})$ as follows

$$\varepsilon' = -\frac{\omega}{\sqrt{2}}\,\xi(1-\Omega)\exp(i\Phi), \tag{19.1}$$

where

$$\xi = \frac{\mathrm{Im}A_0}{\mathrm{Re}A_0}, \quad \omega = \frac{\mathrm{Re}A_2}{\mathrm{Re}A_0}, \quad \Omega = \frac{1}{\omega}\frac{\mathrm{Im}A_2}{\mathrm{Im}A_0}, \tag{19.2}$$

and $\Phi = \pi/2 + \delta_2 - \delta_0 \approx \pi/4$.

When using Eqs. (19.1) and (19.2) in phenomenological applications, one usually takes $\mathrm{Re}A_0$ and ω from experiment, i.e.,

$$\begin{aligned} &\mathrm{Re}A_0 = 3.33\times10^{-7}\ \text{GeV}, \\ &\mathrm{Re}\,A_2 = 1.50\times10^{-8}\ \text{GeV}, \quad \omega = 0.045, \end{aligned} \tag{19.3}$$

where the last relation reflects the so-called $\Delta I = 1/2$ rule. The main reason for this strategy is the unpleasant fact that nobody has suceeded in fully explaining this rule, which to a large extent is believed to originate in the long-distance QCD contributions. We will be more specific about this in the next section. On the other hand the imaginary parts of the amplitudes in Eq. (19.2), being related to CP violation and the top-quark physics, should be dominated by short-distance contributions. Therefore $\mathrm{Im}A_0$ and $\mathrm{Im}A_2$ are usually calculated using the effective Hamiltonian given in Eq. (7.1). Using this Hamiltonian and the experimental values for ε, $\mathrm{Re}A_0$, and ω, we can write the ratio ε'/ε as

$$\varepsilon'/\varepsilon = \mathrm{Im}\lambda_t[P^{(1/2)} - P^{(3/2)}], \tag{19.4}$$

where

$$P^{(1/2)} = \sum P_i^{(1/2)} = r\sum y_i\langle Q_i\rangle_0(1-\Omega_{\eta+\eta'}), \tag{19.5}$$

$$P^{(3/2)} = \sum P_i^{(3/2)} = \frac{r}{\omega}\sum y_i\langle Q_i\rangle_2 \tag{19.6}$$

with

$$r = \frac{G_F\omega}{2|\varepsilon|\mathrm{Re}A_0}. \tag{19.7}$$

Here the hadronic matrix-element shorthand notation is

$$\langle Q_i\rangle_I \equiv \langle(\pi\pi)_I|Q_i|K\rangle, \tag{19.8}$$

and the sum in Eqs. (19.5) and (19.6) runs over all contributing operators. This means for $\mu > m_c$ contributions from operators $Q_{1,2}^c$ to $P^{(1/2)}$ and $P^{(3/2)}$ have to be taken into account. These are necessary for $P^{(1/2)}$ and $P^{(3/2)}$ to be independent of the renormalization scale μ. Next,

$$\Omega_{\eta+\eta'} = \frac{1}{\omega}\frac{(\mathrm{Im}A_2)_{\mathrm{IB}}}{\mathrm{Im}A_0} \tag{19.9}$$

represents the contribution stemming from isospin breaking (IB) in the quark masses ($m_u \neq m_d$). For $\Omega_{\eta+\eta'}$ we will take

$$\Omega_{\eta+\eta'} = 0.25 \pm 0.05, \tag{19.10}$$

which is in the ballpark of the values obtained in the $1/N_c$ approach (Buras and Gérard, 1987) and in chiral perturbation theory (Donoghue *et al.*, 1986; Lusignoli, 1989). $\Omega_{\eta+\eta'}$ is independent of m_t.

The numerical values of the Wilson coefficients y_i have been already given in Sec. VII.E. We therefore turn our attention to the hadronic matrix elements [Eq. (19.8)], which constitute the main source of uncertainty in the calculation of ε'/ε.

B. Hadronic matrix elements for $K \to \pi\pi$

The hadronic matrix elements $\langle Q_i \rangle_I$ depend generally on the renormalization scale μ and on the scheme used to renormalize the operators Q_i. These two dependences are canceled by those present in the Wilson coefficients $C_i(\mu)$ so that the resulting physical amplitudes do not depend on μ or the renormalization scheme of the operators. Unfortunately the accuracy of the present nonperturbative methods used to evaluate $\langle Q_i \rangle_I$, like lattice methods or $1/N_c$ expansion, is not sufficient to obtain the required μ and scheme dependences of $\langle Q_i \rangle_I$. For a review of the existing methods and their comparison, see Buras *et al.* (1993b) and Ciuchini *et al.* (1995). In view of this situation it has been suggested (Buras *et al.*, 1993b) that one determines as many matrix elements $\langle Q_i \rangle_I$ as possible from the leading CP-conserving $K \to \pi\pi$ decays for which the experimental data are summarized in Eq. (19.3). To this end it turned out to be very convenient to determine $\langle Q_i \rangle_I$ at a scale $\mu = m_c$. Using the renormalization-group evolution, one can then find $\langle Q_i \rangle_I$ at any other scale $\mu \neq m_c$ (Buras *et al.*, 1993b). Here we simply summarize the results of this work.

We first express the matrix elements $\langle Q_i \rangle_I$ in terms of the nonperturbative parameters $B_i^{(1/2)}$ and $B_i^{(3/2)}$ for $\langle Q_i \rangle_0$ and $\langle Q_i \rangle_2$, respectively. For $\mu \leqslant m_c$ we have (Buras *et al.*, 1993b)

$$\langle Q_1 \rangle_0 = -\tfrac{1}{9} X B_1^{(1/2)}, \tag{19.11}$$

$$\langle Q_2 \rangle_0 = \tfrac{5}{9} X B_2^{(1/2)}, \tag{19.12}$$

$$\langle Q_3 \rangle_0 = \tfrac{1}{3} X B_3^{(1/2)}, \tag{19.13}$$

$$\langle Q_4 \rangle_0 = \langle Q_3 \rangle_0 + \langle Q_2 \rangle_0 - \langle Q_1 \rangle_0, \tag{19.14}$$

$$\langle Q_5 \rangle_0 = \tfrac{1}{3} B_5^{(1/2)} \langle \overline{Q_6} \rangle_0, \tag{19.15}$$

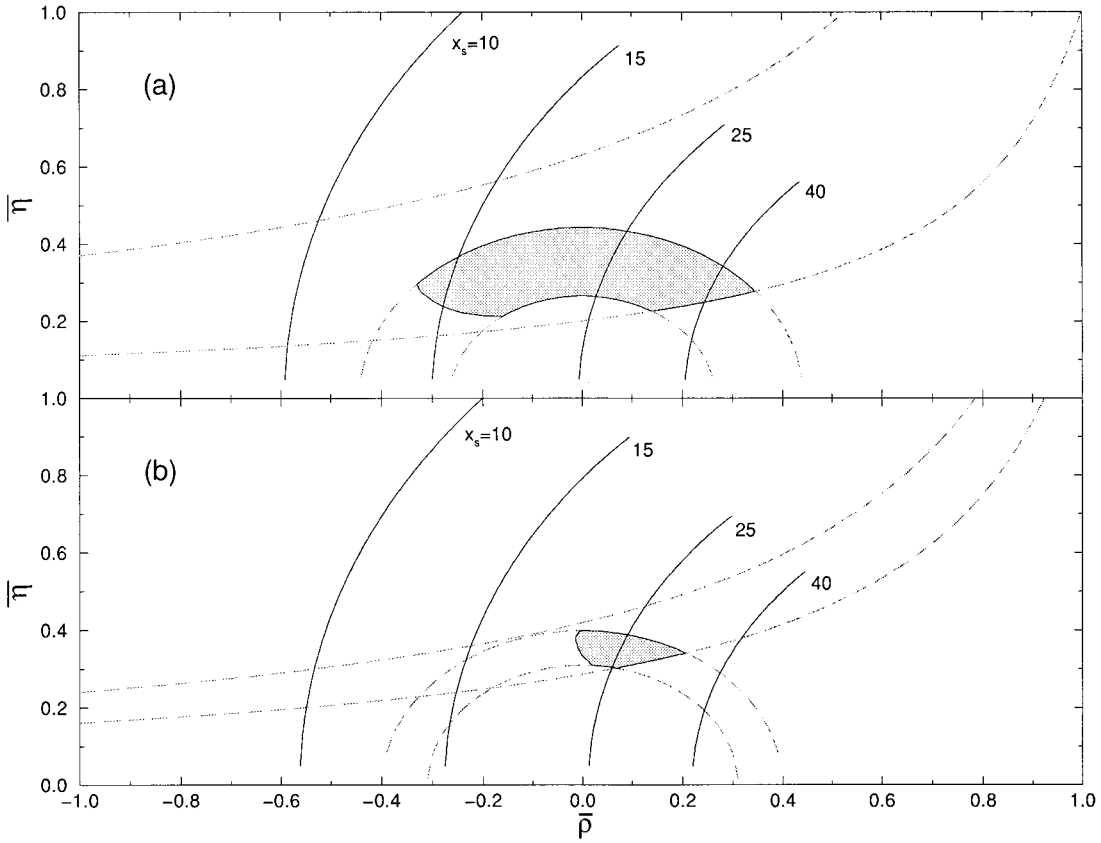

FIG. 13. Present (a) and future (b) allowed ranges for the upper corner A of the unitarity triangle using data from K^0-$\bar{K}^0$, B^0-$\bar{B}^0$ mixing, and tree-level B decays. Input parameter ranges are given in the Appendix. The solid lines correspond to $(R_t)_{\max}$ from Eq. (18.25) using R_{ds}=0.66 and $x_s \geqslant$10, 15, 25, and 40, respectively.

$$\langle Q_6\rangle_0 = -4\sqrt{\frac{3}{2}}\left[\frac{m_K^2}{m_s(\mu)+m_d(\mu)}\right]^2 \frac{F_\pi}{\kappa} B_6^{(1/2)}, \tag{19.16}$$

$$\langle Q_7\rangle_0 = -\left[\frac{1}{6}\langle\overline{Q_6}\rangle_0(\kappa+1) - \frac{X}{2}\right]B_7^{(1/2)}, \tag{19.17}$$

$$\langle Q_8\rangle_0 = -\left[\frac{1}{2}\langle\overline{Q_6}\rangle_0(\kappa+1) - \frac{X}{6}\right]B_8^{(1/2)}, \tag{19.18}$$

$$\langle Q_9\rangle_0 = \tfrac{3}{2}\langle Q_1\rangle_0 - \tfrac{1}{2}\langle Q_3\rangle_0, \tag{19.19}$$

$$\langle Q_{10}\rangle_0 = \langle Q_2\rangle_0 + \tfrac{1}{2}\langle Q_1\rangle_0 - \tfrac{1}{2}\langle Q_3\rangle_0, \tag{19.20}$$

$$\langle Q_1\rangle_2 = \langle Q_2\rangle_2 = \frac{4\sqrt{2}}{9} X B_1^{(3/2)}, \tag{19.21}$$

$$\langle Q_i\rangle_2 = 0, \quad i=3,\ldots,6, \tag{19.22}$$

$$\langle Q_7\rangle_2 = -\left[\frac{\kappa}{6\sqrt{2}}\langle\overline{Q_6}\rangle_0 + \frac{X}{\sqrt{2}}\right]B_7^{(3/2)}, \tag{19.23}$$

$$\langle Q_8\rangle_2 = -\left[\frac{\kappa}{2\sqrt{2}}\langle\overline{Q_6}\rangle_0 + \frac{\sqrt{2}}{6} X\right]B_8^{(3/2)}, \tag{19.24}$$

$$\langle Q_9\rangle_2 = \langle Q_{10}\rangle_2 = \tfrac{3}{2}\langle Q_1\rangle_2, \tag{19.25}$$

where

$$\kappa = \frac{\Lambda_\chi^2}{m_K^2 - m_\pi^2} = \frac{F_\pi}{F_K - F_\pi}, \tag{19.26}$$

$$X = \sqrt{\frac{3}{2}} F_\pi (m_K^2 - m_\pi^2), \tag{19.27}$$

and

$$\langle\overline{Q_6}\rangle_0 = \frac{\langle Q_6\rangle_0}{B_6^{(1/2)}}. \tag{19.28}$$

The actual numerical values used for m_K, m_π, F_K, and F_π are collected in the Appendix.

In the vacuum-insertion method B_i=1 independent of μ. In QCD, however, the hadronic parameters B_i generally depend on the renormalization scale μ and the renormalization scheme considered.

C. $\langle Q_i(\mu)\rangle_2$ for $(V-A)\otimes(V-A)$ operators

The matrix elements $\langle Q_1\rangle_2$, $\langle Q_2\rangle_2$, $\langle Q_9\rangle_2$, and $\langle Q_{10}\rangle_2$ can be determined to a very good approximation from $\mathrm{Re}A_2$ in Eq. (19.3) as functions of $\Lambda_{\overline{\mathrm{MS}}}$, μ, and the renormalization scheme considered. To this end it is useful to set α=0, as the $\mathcal{O}(\alpha)$ effects in CP-conserving amplitudes, such as the contributions of electroweak penguins, are very small. One then finds

$$\langle Q_1(\mu)\rangle_2 = \langle Q_2(\mu)\rangle_2 = \frac{10^6\ \mathrm{GeV}^2}{1.77}\frac{\mathrm{Re}A_2}{z_+(\mu)} = \frac{8.47\times10^{-3}\ \mathrm{GeV}^3}{z_+(\mu)}, \tag{19.29}$$

and, comparing with Eq. (19.21),

$$B_1^{(3/2)}(\mu) = \frac{0.363}{z_+(\mu)} \tag{19.30}$$

with $z_+ = z_1 + z_2$. Since $z_+(\mu)$ depends on the scale μ and the renormalization scheme used, Eq. (19.30) gives automatically the scheme and μ dependence of $B_1^{(3/2)}$ and of the related matrix elements $\langle Q_1\rangle_2$, $\langle Q_2\rangle_2$, $\langle Q_9\rangle_2$, and $\langle Q_{10}\rangle_2$. The impact of $\mathcal{O}(\alpha)$ corrections on this result has been analyzed by Buras *et al.* (1993b). It amounts to only a few percent, as expected. These corrections are included in the numerical analysis presented in the above reference and here as well. Using $\mu=m_c$=1.3 GeV, $\Lambda_{\overline{\mathrm{MS}}}^{(4)}$ = 325 MeV, and $z_+(m_c)$ from Table XIX, we find, according to Eq. (19.30),

$$B_{1,\mathrm{NDR}}^{(3/2)}(m_c) = 0.453, \quad B_{1,\mathrm{HV}}^{(3/2)}(m_c) = 0.472. \tag{19.31}$$

The following comments should be made:

(i) $B_1^{(3/2)}(\mu)$ decreases with increasing μ.

(ii) The extracted value for $B_1^{(3/2)}$; is more than a factor of 2 smaller than the vacuum-insertion estimate.

(iii) It is compatible with the $1/N_c$ value $B_1^{(3/2)}(1\ \mathrm{GeV}) \approx 0.55$ (Bardeen *et al.*, 1987a) and somewhat smaller than the lattice result $B_1^{(3/2)}(2\ \mathrm{GeV}) \approx 0.6$ (Ciuchini *et al.*, 1995).

D. $\langle Q_i(\mu)\rangle_0$ for $(V-A)\otimes(V-A)$ operators

The determination of $\langle Q_i(\mu)\rangle_0$ matrix elements is more involved because several operators may contribute to $\mathrm{Re}A_0$. The main idea of Buras *et al.* (1993b) is then to set $\mu=m_c$, as at this scale only Q_1 and Q_2 operators contribute to $\mathrm{Re}A_0$ in the HV scheme. One then finds $\langle Q_1(m_c)\rangle_0$ as a function of $\langle Q_2(m_c)\rangle_0$

$$\langle Q_1(m_c)\rangle_0 = \frac{10^6\ \mathrm{GeV}^2}{1.77}\frac{\mathrm{Re}A_0}{z_1(m_c)} - \frac{z_2(m_c)}{z_1(m_c)}\langle Q_2(m_c)\rangle_0, \tag{19.32}$$

where the reference in $\langle Q_{1,2}(m_c)\rangle_0$ to the HV scheme has been suppressed for convenience. Using Eqs. (19.14), (19.19), and (19.20) one is able to obtain $\langle Q_4(m_c)\rangle_0$, $\langle Q_9(m_c)\rangle_0$, and $\langle Q_{10}(m_c)\rangle_0$ as functions of $\langle Q_2(m_c)\rangle_0$ and $\langle Q_3(m_c)\rangle_0$. Because $\langle Q_3(m_c)\rangle_0$ is color suppressed, it is less essential for this analysis than $\langle Q_2(m_c)\rangle_0$. Moreover, its Wilson coefficient is small and, similar to $\langle Q_9(m_c)\rangle_0$ and $\langle Q_{10}(m_c)\rangle_0$, $\langle Q_3(m_c)\rangle_0$ has only a small impact on ε'/ε. On the other hand, the coefficient y_4 is substantial, and consequently $\langle Q_4(m_c)\rangle_0$ plays a considerable role in the analysis of ε'/ε. The matrix element $\langle Q_3(m_c)\rangle_0$ then has an indirect impact on ε'/ε through Eq. (19.14). For numerical evaluation, $\langle Q_3(m_c)\rangle_0$ of Eq. (19.13) with $B_3^{(1/2)}$=1 can be used, keeping in mind that this may introduce a small uncertainty in the final analysis. This uncertainty has been investigated by Buras *et al.* (1993b).

Once the matrix elements in question have been determined as functions of $\langle Q_2(m_c)\rangle_0$ in the HV scheme,

TABLE XXXVIII. B_i expansion coefficients for $P^{(1/2)}$.

		LO		NDR		HV	
$\Lambda_{\overline{\rm MS}}^{(4)}$ [MeV]	m_t [GeV]	$a_0^{(1/2)}$	$a_6^{(1/2)}$	$a_0^{(1/2)}$	$a_6^{(1/2)}$	$a_0^{(1/2)}$	$a_6^{(1/2)}$
	155	–2.138	5.110	–2.251	4.676	–2.215	4.159
215	170	–2.070	5.138	–2.187	4.698	–2.150	4.181
	185	–1.996	5.162	–2.117	4.716	–2.081	4.200
	155	–2.231	6.540	–2.414	6.255	–2.362	5.389
325	170	–2.161	6.576	–2.350	6.282	–2.298	5.416
	185	–2.085	6.606	–2.281	6.306	–2.229	5.439
	155	–2.288	8.171	–2.549	8.417	–2.473	6.972
435	170	–2.212	8.214	–2.482	8.451	–2.406	7.005
	185	–2.130	8.251	–2.409	8.480	–2.333	7.035

they can be found by a finite renormalization in any other scheme (Buras *et al.*, 1993b).

If one also makes the very plausible assumption, valid in all known nonperturbative approaches, that $\langle Q_-(m_c)\rangle_0 \geqslant \langle Q_+(m_c)\rangle_0 \geqslant 0$, the experimental value of $\mathrm{Re}A_0$ in Eq. (19.3) together with Eq. (19.32) and Table XIX implies, for $\Lambda_{\overline{\rm MS}}^{(4)} = 325$ MeV,

$$B_{2,\rm LO}^{(1/2)}(m_c)=5.7\pm1.1, \quad B_{2,\rm NDR}^{(1/2)}(m_c)=6.6\pm1.0,$$
$$B_{2,\rm HV}^{(1/2)}(m_c)=6.2\pm1.0. \tag{19.33}$$

The extraction of $B_1^{(1/2)}(m_c)$ and an analogous parameter $B_4^{(1/2)}(m_c)$ are presented in detail by Buras *et al.* (1993b). $B_1^{(1/2)}(m_c)$ depends very sensitively on $B_2^{(1/2)}(m_c)$, and its central value is as high as 15. $B_4^{(1/2)}(m_c)$ is less sensitive and typically (10–15)% lower than $B_2^{(1/2)}(m_c)$. In any case this analysis shows very large departures from the results of the vacuum-insertion method.

E. $\langle Q_i(\mu)\rangle_{0,2}$ for $(V-A)\otimes(V+A)$ operators

The matrix elements of the $(V-A)\otimes(V+A)$ operators Q_5-Q_8 cannot be constrained by CP-conserving data, and one has to rely on existing nonperturbative methods to calculate them. Fortunately, there are some indications that the existing nonperturbative estimates of $\langle Q_i(\mu)\rangle_{0,2}$, $i=5,\ldots,8$ are more reliable than the corresponding calculations for $(V-A)\otimes(V-A)$ operators.

First of all, the parameters $B_{5,6}^{(1/2)}$ (Kilcup, 1991; Sharpe, 1991) and $B_{7,8}^{(3/2)}$ (Franco *et al.*, 1989; Bernard and Soni, 1991; Kilcup, 1991; Sharpe, 1991) calculated in the lattice approach,

$$B_{5,6}^{(1/2)}=1.0\pm0.2, \quad B_{7,8}^{(3/2)}=1.0\pm0.2, \tag{19.34}$$

agree well with the vacuum-insertion values ($B_i=1$) and in the case of $B_6^{(1/2)}$ and $B_8^{(3/2)}$ with the $1/N_c$ approach ($B_6^{(1/2)}=B_8^{(3/2)}=1$) (Bardeen *et al.*, 1987b; Buras and Gérard, 1987).

We note next that, with fixed values for $B_{5,6}^{(1/2)}$ and $B_{7,8}^{(3/2)}$, the μ dependence of $\langle Q_{5,6}\rangle_0$ and $\langle Q_{7,8}\rangle_2$ is governed by the μ dependence of $m_s(\mu)$. For $\langle Q_6\rangle_0$ and $\langle Q_8\rangle_2$ this property has first been found in the $1/N_c$ approach (Buras and Gérard, 1987): in the large-N_c limit the anomalous dimensions of Q_6 and Q_8 are simply twice the anomalous dimension of the mass operator, leading to $\sim 1/m_s^2(\mu)$ for the corresponding matrix elements. Another support comes from a renormalization study by Buras *et al.* (1993b). In this analysis the B_i factors in Eq. (19.34) have been set to unity at $\mu=m_c$. Subsequently the evolution of the matrix elements in the range 1 GeV$\leqslant\mu\leqslant$4 GeV has been calculated, showing that, for the NDR scheme, $B_{5,6}^{(1/2)}$ and $B_{7,8}^{(3/2)}$ were μ independent within an accuracy of (2–3)%. The μ dependence in the HV scheme has been found to be stronger but still below 10%.

Concerning $B_{7,8}^{(1/2)}$, one can simply set $B_{7,8}^{(1/2)}=1$, as the matrix elements $\langle Q_{7,8}\rangle_0$ play only a minor role in the ε'/ε analysis.

In summary, the present treatment of $\langle Q_i\rangle_{0,2}$, $i=5,\ldots,8$ follows the one used by Buras *et al.* (1993b). We will set

$$B_{7,8}^{(1/2)}(m_c)=1, \quad B_5^{(1/2)}(m_c)=B_6^{(1/2)}(m_c),$$
$$B_7^{(3/2)}(m_c)=B_8^{(3/2)}(m_c), \tag{19.35}$$

and we will treat $B_6^{(1/2)}(m_c)$ and $B_8^{(3/2)}(m_c)$ as free parameters in the neighborhood of the values given in Eq. (19.34). Then the main uncertainty in the values of $\langle Q_i\rangle_{0,2}$, $i=5,\ldots,8$ results from the value of the strange-quark mass $m_s(m_c)$. The present estimates give

$$m_s(m_c)=(170\pm20)\ \text{MeV} \tag{19.36}$$

with the lower values coming from recent lattice calculations (Allton *et al.*, 1994) and the higher ones from QCD sum rules (Chetyrkin *et al.*, 1995; Jamin and Münz, 1995).

F. The four dominant contributions to ε'/ε

$P^{(1/2)}$ and $P^{(3/2)}$ in Eq. (19.4) can be written as linear combinations of two independent hadronic parameters $B_6^{(1/2)}$ and $B_8^{(3/2)}$ (Buras *et al.*, 1993b). This B_i expansion is given by

$$P^{(1/2)}=a_0^{(1/2)}+\left[\frac{178\ \text{MeV}}{m_s(m_c)+m_d(m_c)}\right]^2 a_6^{(1/2)}B_6^{(1/2)}, \tag{19.37}$$

TABLE XXXIX. B_i expansion coefficients for $P^{(3/2)}$.

		LO		NDR		HV	
$\Lambda_{\overline{\rm MS}}^{(4)}$ [MeV]	m_t [GeV]	$a_0^{(3/2)}$	$a_8^{(3/2)}$	$a_0^{(3/2)}$	$a_8^{(3/2)}$	$a_0^{(3/2)}$	$a_8^{(3/2)}$
	155	–0.797	1.961	–0.819	1.887	–0.838	2.114
215	170	–0.880	2.602	–0.900	2.438	–0.919	2.666
	185	–0.965	3.296	–0.983	3.036	–1.002	3.263
	155	–0.788	2.645	–0.814	2.639	–0.837	2.894
325	170	–0.870	3.422	–0.895	3.305	–0.917	3.560
	185	–0.956	4.264	–0.978	4.027	–1.000	4.281
	155	–0.779	3.425	–0.809	3.622	–0.835	3.899
435	170	–0.861	4.360	–0.889	4.435	–0.915	4.712
	185	–0.947	5.372	–0.971	5.316	–0.998	5.593

$$P^{(3/2)}=a_0^{(3/2)}+\left[\frac{178\ \text{MeV}}{m_s(m_c)+m_d(m_c)}\right]^2 a_8^{(3/2)}B_8^{(3/2)}. \tag{19.38}$$

Here $a_0^{(1/2)}$ and $a_0^{(3/2)}$ effectively summarize all dependences other than $B_6^{(1/2)}$ and $B_8^{(3/2)}$, especially $B_2^{(1/2)}$ in the case of $a_0^{(1/2)}$. Note that, in contrast to Buras *et al.* (1993b), we have absorbed the dependence on $B_2^{(1/2)}$ into $a_0^{(1/2)}$ and have exhibited the dependence on m_s, which was not shown explicitly there. The residual m_s dependence present in $a_0^{(1/2)}$ and $a_0^{(3/2)}$ is negligible. Setting $\mu=m_c$ and using the strategy for hadronic matrix elements outlined above, one finds the coefficients $a_i^{(1/2)}$ and $a_i^{(3/2)}$ as functions of $\Lambda_{\overline{\rm MS}}$, m_t, and the renormalization scheme considered. These dependences are given in Tables XXXVIII and XXXIX. We should stress that $P^{(1/2)}$ and $P^{(3/2)}$ are independent of μ and the renormalization scheme considered.

Inspecting Eqs. (19.37) and (19.38) and Tables XXXVIII, XXXIX, we identify the following four contributions which govern the ratio ε'/ε at scales $\mu=\mathcal{O}(m_c)$:

(1) The contribution of $(V-A)\otimes(V-A)$ operators to $P^{(1/2)}$ is dominantly represented by $a_0^{(1/2)}$. This term is to a large extent fixed by the experimental value of A_0 and consequently is only very weakly dependent on $\Lambda_{\overline{\rm MS}}$ and the renormalization scheme considered. The weak dependence on m_t results from small contributions of electroweak penguin operators. Taking $\Lambda_{\overline{\rm MS}}^{(4)}=325$ MeV, $\mu=m_c$, and $m_t=170$ GeV, we have $a_0^{(1/2)}\approx -2.3$ for both schemes considered. We observe that the contribution of $(V-A)\otimes(V-A)$ operators, in particular Q_4, to ε'/ε is *negative*.

(2) The contribution of $(V-A)\otimes(V+A)$ QCD penguin operators to $P^{(1/2)}$ is given by the second term in Eq. (19.37). This contribution is large and *positive*. The coefficient $a_6^{(1/2)}$ depends sensitively on $\Lambda_{\overline{\rm MS}}$, which results from the strong dependence of y_6 on the QCD scale. The dependence on m_t is very weak on the other hand. Taking $\Lambda_{\overline{\rm MS}}^{(4)}=325$ MeV, $m_s(m_c)=170$ MeV, and $m_t=170$ GeV and setting $B_6^{(1/2)}=1$ in the NDR and HV schemes, we find a positive contribution to ε'/ε amounting to 6.3 and 5.4 in the NDR and HV schemes, respectively.

(3) The contribution of the $(V-A)\otimes(V-A)$ electroweak penguin operators Q_9 and Q_{10} to $P^{(3/2)}$ is represented by $a_0^{(3/2)}$. As in the case of the first contribution, the matrix elements contributing to $a_0^{(3/2)}$ are fixed by the CP-conserving data, this time by the amplitude A_2. Consequently, the scheme and the $\Lambda_{\overline{\rm MS}}$ dependence of $a_0^{(3/2)}$ is very weak. The sizable m_t dependence of $a_0^{(3/2)}$ results from the m_t dependence of y_9+y_{10}. $a_0^{(3/2)}$ contributes *positively* to ε'/ε. For $m_t=170$ GeV this contribution is roughly 0.9 for both renormalization schemes in the full range of $\Lambda_{\overline{\rm MS}}$ considered.

(4) The contribution of the $(V-A)\otimes(V+A)$ electroweak penguin operators Q_7 and Q_8 to $P^{(3/2)}$ is represented by the second term in Eq. (19.38). This contribution depends sensitively on m_t and $\Lambda_{\overline{\rm MS}}$, as could be expected on the basis of y_7 and y_8. Taking again $B_8^{(3/2)}=1$ in both renormalization schemes, we find for the central values of $\Lambda_{\overline{\rm MS}}^{(4)}$, m_t, and m_c a *negative* contribution to ε'/ε equal to –3.9 and –3.6 for the NDR and HV schemes, respectively.

Before analyzing ε'/ε numerically in more detail, let us set $\mathrm{Im}\lambda_t=1.3\times10^{-4}$ and $B_6^{(1/2)}=B_8^{(3/2)}=1$ in both schemes. Then, for the central values of the remaining parameters, one obtains $\varepsilon'/\varepsilon=2.0\times10^{-4}$ and $\varepsilon'/\varepsilon=0.6\times10^{-4}$ for the NDR and HV schemes, respectively. This strong scheme dependence can only be compensated for by having $B_6^{(1/2)}$ and $B_8^{(3/2)}$ different in the two schemes considered. As we will see below the strong cancellations between various contributions at $m_t\approx170$ GeV make the prediction for ε'/ε rather uncertain. One should also stress that the formulation presented here does not exhibit analytically the m_t dependence. As the coefficients $a_0^{(3/2)}$ and $a_8^{(3/2)}$ depend very sensitively on m_t, it is useful to display this dependence in an analytic form.

G. An analytic formula for ε'/ε

As shown by Buras and Lautenbacher (1993) it is possible to cast the above discussion into an analytic formula which exhibits the m_t dependence together with the dependence on m_s, $B_6^{(1/2)}$, and $B_8^{(3/2)}$. Such an analytic formula should be useful for those phenomenolo-

TABLE XL. $\Delta S=1$ PBE coefficients for various $\Lambda_{\overline{\rm MS}}$ in the NDR scheme.

	$\Lambda^{(4)}_{\overline{\rm MS}}=215$ MeV			$\Lambda^{(4)}_{\overline{\rm MS}}=325$ MeV			$\Lambda^{(4)}_{\overline{\rm MS}}=435$ MeV		
i	$r_i^{(0)}$	$r_i^{(6)}$	$r_i^{(8)}$	$r_i^{(0)}$	$r_i^{(6)}$	$r_i^{(8)}$	$r_i^{(0)}$	$r_i^{(6)}$	$r_i^{(8)}$
0	–2.644	4.784	0.876	–2.749	6.376	0.689	–2.845	8.547	0.436
X	0.555	0.008	0	0.521	0.012	0	0.495	0.017	0
Y	0.422	0.037	0	0.385	0.046	0	0.356	0.057	0
Z	0.074	–0.007	–4.798	0.149	–0.009	–5.789	0.237	–0.011	–7.064
E	0.209	–0.591	0.205	0.181	–0.727	0.265	0.152	–0.892	0.342

gists and experimentalists who are not interested in getting involved with the technicalities discussed in preceding sections.

In order to find an analytic expression for ε'/ε that exactly reproduces the results discussed above, one uses the PBE presented in Sec. XIV. The resulting analytic expression for ε'/ε is then given as follows,

$$\varepsilon'/\varepsilon = \mathrm{Im}\lambda_t F(x_t), \tag{19.39}$$

where

$$F(x_t)=P_0+P_X X_0(x_t)+P_Y Y_0(x_t)+P_Z Z_0(x_t) + P_E E_0(x_t) \tag{19.40}$$

with the m_t-dependent functions listed in Sec. XIV. The coefficients P_i are given in terms of $B_6^{(1/2)}\equiv B_6^{(1/2)}(m_c)$, $B_8^{(3/2)}\equiv B_8^{(3/2)}(m_c)$, and $m_s(m_c)$ as follows,

$$P_i=r_i^{(0)}+\left[\frac{178\ \text{MeV}}{m_s(m_c)+m_d(m_c)}\right]^2 (r_i^{(6)}B_6^{(1/2)}+r_i^{(8)}B_8^{(3/2)}). \tag{19.41}$$

The P_i are μ and renormalization-scheme independent. They depend, however, on $\Lambda_{\overline{\rm MS}}$. In Table XL we give the numerical values of $r_i^{(0)}$, $r_i^{(6)}$, and $r_i^{(8)}$ for different values of $\Lambda_{\overline{\rm MS}}$ at $\mu=m_c$ in the NDR renormalization scheme. Analogous results in the HV scheme are given in Table XLI. The coefficients $r_i^{(0)}$, $r_i^{(6)}$, and $r_i^{(8)}$ do not depend on $m_s(m_c)$, as this dependence has been factored out. $r_i^{(0)}$ does, however, depend on the particular choice for the parameter $B_2^{(1/2)}$ in the parametrization of the matrix element $\langle Q_2\rangle_0$. The values given in the tables correspond to the central values in Eq. (19.33). Variation of $B_2^{(1/2)}$ in the full allowed range introduces an uncertainty of at most 18% in the $r_i^{(0)}$ column of the tables. Since the parameters $r_i^{(0)}$ give only subdominant contributions to ε'/ε, keeping $B_2^{(1/2)}$ and $r_i^{(0)}$ at their central values is a very good approximation.

For different scales μ the numerical values in the tables change without modifying the values of the P_i's, as it should be. To this end $B_6^{(1/2)}$ and $B_8^{(3/2)}$ have to be modified, as they depend, albeit weakly, on μ.

Concerning the scheme dependence, we note that, whereas r_0 coefficients are scheme dependent, the coefficients r_i, $i=X,Y,Z,E$ do not show any scheme dependence. This is related to the fact that the m_t dependence in ε'/ε enters first at the NLO level and consequently all coefficients r_i in front of the m_t-dependent functions must be scheme independent. That this turns out to be the case is a nice check of our calculations.

Consequently, when changing the renormalization scheme, one is only obliged to change $B_6^{(1/2)}$ and $B_8^{(3/2)}$ in the formula for P_0 in order to obtain a scheme independence of ε'/ε. In calculating P_i, where $i\neq 0$, $B_6^{(1/2)}$ and $B_8^{(3/2)}$ can in fact remain unchanged because their variation in this part corresponds to higher-order contributions to ε'/ε, which would have to be taken into account in the next order of perturbation theory.

For similar reasons the NLO analysis of ε'/ε is still insensitive to the precise definition of m_t. In view of the fact that the NLO calculations of $\mathrm{Im}\lambda_t$ have been done with $m_t=\bar{m}_t(m_t)$, we will also use this definition in calculating $F(x_t)$.

The inspection of Tables XL and XLI shows that the terms involving $r_0^{(6)}$ and $r_Z^{(8)}$ dominate the ratio ε'/ε. The function $Z_0(x_t)$, representing a gauge-invariant combination of Z^0 and γ penguins, grows rapidly with m_t, and, due to $r_Z^{(8)}<0$, these contributions suppress ε'/ε strongly for large m_t (Flynn and Randall, 1989b; Buchalla *et al.*, 1990). These two dominant terms, $r_0^{(6)}$ and $r_Z^{(8)}$, correspond essentially to the second terms in Eqs. (19.37) and (19.38), respectively. The first term in Eq. (19.37) corresponds roughly to $r_0^{(0)}$ given here, while the first term in Eq. (19.38) is represented to a large extent by the posi-

TABLE XLI. $\Delta S=1$ PBE coefficients for various $\Lambda_{\overline{\rm MS}}$ in the HV scheme.

	$\Lambda^{(4)}_{\overline{\rm MS}}=215$ MeV			$\Lambda^{(4)}_{\overline{\rm MS}}=325$ MeV			$\Lambda^{(4)}_{\overline{\rm MS}}=435$ MeV		
i	$r_i^{(0)}$	$r_i^{(6)}$	$r_i^{(8)}$	$r_i^{(0)}$	$r_i^{(6)}$	$r_i^{(8)}$	$r_i^{(0)}$	$r_i^{(6)}$	$r_i^{(8)}$
0	–2.631	4.291	0.668	–2.735	5.548	0.457	–2.830	7.163	0.185
X	0.555	0.008	0	0.521	0.012	0	0.495	0.017	0
Y	0.422	0.037	0	0.385	0.046	0	0.356	0.057	0
Z	0.074	–0.007	–4.798	0.149	–0.009	–5.789	0.237	–0.011	–7.064
E	0.209	–0.591	0.205	0.181	–0.727	0.265	0.152	–0.892	0.342

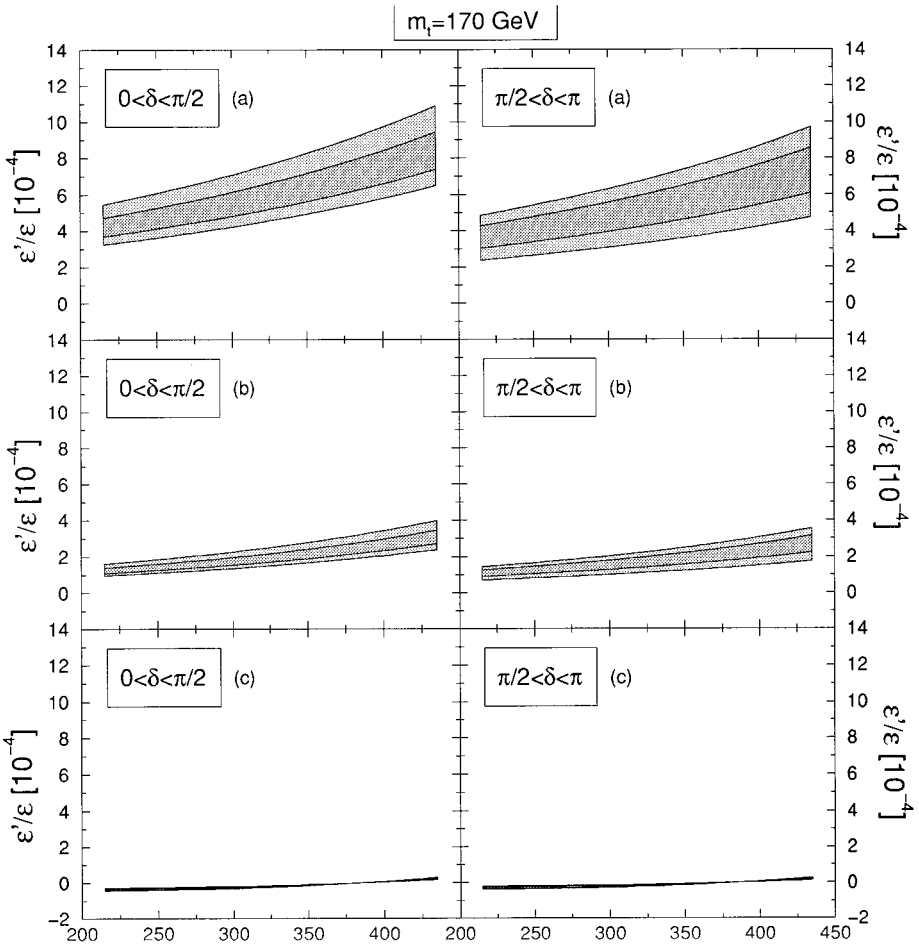

FIG. 14. The ranges of ε'/ε in the NDR scheme as a function of $\Lambda^{(4)}_{\overline{\rm MS}}$ for m_t=170 GeV and present (light grey) and future (dark grey) parameter ranges given in the Appendix. The three pairs of ε'/ε plots correspond to hadronic parameter sets (a) $[B_6^{(1/2)}(m_c)]_{\rm eff}$=1.5, $[B_8^{(3/2)}(m_c)]_{\rm eff}$=1.0, (b) $[B_6^{(1/2)}(m_c)]_{\rm eff}$=1.0, $[B_8^{(3/2)}(m_c)]_{\rm eff}$=1.0, and (c) $[B_6^{(1/2)}(m_c)]_{\rm eff}$=1.0, $[B_8^{(3/2)}(m_c)]_{\rm eff}$ =1.5, respectively.

tive contributions of $X_0(x_t)$ and $Y_0(x_t)$. The last term in Eq. (19.40), representing the residual m_t dependence of QCD penguins, plays only a minor role in the full analysis of ε'/ε.

H. Numerical results

Let us define two effective B factors:

$$(B_i^{(j)}(m_c))_{\rm eff}=\left[\frac{178\ \text{MeV}}{\bar m_s(m_c)+\bar m_d(m_c)}\right]^2 B_i^{(j)}(m_c). \qquad (19.42)$$

In Fig. 14 we show ε'/ε for m_t=170 GeV as a function of $\Lambda_{\overline{\rm MS}}$ for different choices of the effective B_i factors. We show here only the results in the NDR scheme. As discussed above ε'/ε is generally lower in the HV scheme, if the same values for $B_6^{(1/2)}$ and $B_8^{(3/2)}$ are used in both schemes. In view of the fact that the differences between NDR and HV schemes are smaller than the uncertainties in $B_6^{(1/2)}$ and $B_8^{(3/2)}$, we think it is sufficient to present only the results in the NDR scheme here. The results in the HV scheme can be found in work by Buras *et al.* (1993b) and Ciuchini *et al.* (1995).

Figure 14 shows a strong dependence of ε'/ε on $\Lambda_{\overline{\rm MS}}$. However, the main uncertainty originates in the poor knowledge of $(B_i)_{\rm eff}$. In Fig. 14(a), in which the QCD penguin contributions dominate, ε'/ε can reach values as high as 1×10^{-3}. However, in Fig. 14(c) the electroweak penguin contributions are large enough to essentially cancel the QCD penguin contributions completely. Consequently, in this case $|\varepsilon'/\varepsilon|<2\times10^{-5}$, and the standard model prediction of ε'/ε cannot be distinguished from a superweak theory. As shown in Fig. 15, higher values of ε'/ε can be obtained for m_t=155 GeV, although still $\varepsilon'/\varepsilon<13\times10^{-4}$.

For m_t=185 GeV the values of ε'/ε are correspondingly smaller, and in Fig. 14(c) small negative values are found for ε'/ε. In Figs. 14–16 the dark grey regions refer to the future ranges for $\mathrm{Im}\lambda_t$. Of course one should hope that the knowledge of $(B_i)_{\rm eff}$ and of $\Lambda^{(4)}_{\overline{\rm MS}}$ will be improved in the future so that a firmer prediction for ε'/ε can be obtained.

Finally, Fig. 17 shows the interrelated influence of m_t and the two most important hadronic matrix elements for penguin operators on the theoretical prediction of

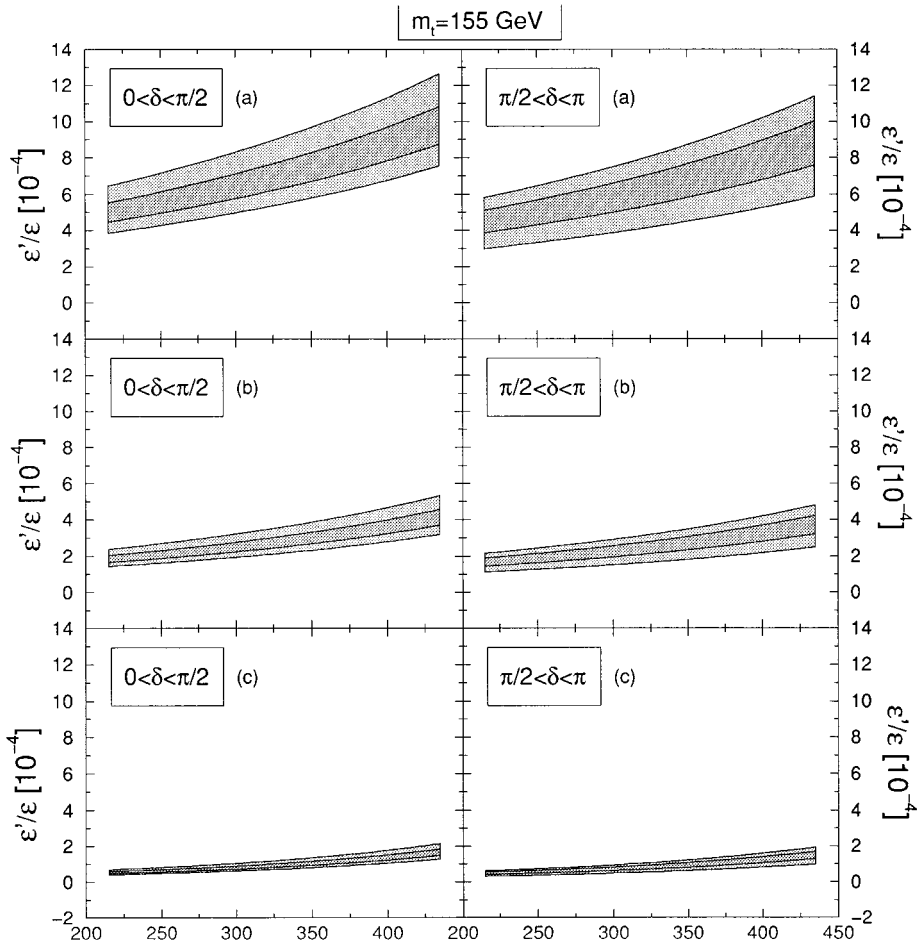

FIG. 15. Same as Fig. 14 but for m_t=155 GeV.

ε'/ε. For a dominant QCD penguin matrix element $\langle Q_6\rangle_0$, ε'/ε stays positive for all m_t values considered. $\varepsilon'/\varepsilon\approx 0$ becomes possible for equally weighted matrix elements $\langle Q_6\rangle_0$ and $\langle Q_8\rangle_2$ around m_t=205 GeV. A dominant electroweak penguin matrix element $\langle Q_8\rangle_2$ shifts the point $\varepsilon'/\varepsilon\approx 0$ to $m_t\approx 165$ GeV and even allows for a negative ε'/ε for higher values of m_t. The key issue to understand this behavior of ε'/ε is the observation that the Q_6 contribution to ε'/ε is positive and only weakly m_t dependent. On the other hand the contribution coming from Q_8 is negative and shows a strong m_t dependence.

The results in Fig. 14–17 use only the ε_K constraint. In order to complete the analysis we want to impose the x_d constraint and vary $m_s(m_c)$, $B_6^{(1/2)}$, and $B_8^{(3/2)}$ in the full ranges given in Eqs. (19.34) and (19.36).

This gives for the "present" scenario

$$-2.1\times 10^{-4}\leq \varepsilon'/\varepsilon\leq 13.2\times 10^{-4}, \tag{19.43}$$

to be compared with

$$-1.1\times 10^{-4}\leq \varepsilon'/\varepsilon\leq 10.4\times 10^{-4} \tag{19.44}$$

in the case of the "future" scenario. In both cases the x_d constraint has essentially no impact on the predicted range for ε'/ε.

Finally, extending the "future" scenario to $m_s(m_c)$=(170±10) MeV, $\Lambda_{\overline{\rm MS}}^{(4)}$=(325±50) MeV, and $B_6^{(1/2)}, B_8^{(3/2)}$=1.0±0.1 would give

$$0.3\cdot 10^{-4}\leq \varepsilon'/\varepsilon\leq 5.4\times 10^{-4}, \tag{19.45}$$

again with no impact from imposing the x_d constraint.

Allowing an additional variation $B_{2,\rm NDR}^{(1/2)}(m_c)$ =6.6±1.0, extends the ranges of Eqs. (19.43)–(19.45) to $-2.5\times 10^{-4}\leq\varepsilon'/\varepsilon\leq 13.7\times 10^{-4}$, $-1.5\times 10^{-4}\leq\varepsilon'/\varepsilon\leq 10.8\times 10^{-4}$, and $0.1\times 10^{-4}\leq\varepsilon'/\varepsilon\leq 5.8\times 10^{-4}$, respectively.

Next let us compare our results with the results of other analyses presented in the literature. A very detailed numerical analysis of ε'/ε has been presented by the Rome group (Ciuchini *et al.*, 1995). The analysis of the Wilson coefficients is the same as presented here. The values for the most important B_i parameters, $B_6^{(1/2)}$ and $B_8^{(3/2)}$, are taken from lattice calculations, and consequently this part of the analysis is rather similar to ours. For the remaining matrix elements the Rome group uses either existing lattice estimates or educated guesses that are discussed in their paper. In spite of the fact that the treatment of these remaining hadronic matrix elements differs from the one presented here, the final result of the Rome group, $\mathrm{Re}(\varepsilon'/\varepsilon)=(3.1\pm 2.5)\times 10^{-4}$, is compatible with our results.

The difference in the range for ε'/ε presented here and the Rome group is related to the different treatment of theoretical and experimental errors. Whereas we simply scan all parameters within one standard deviation,

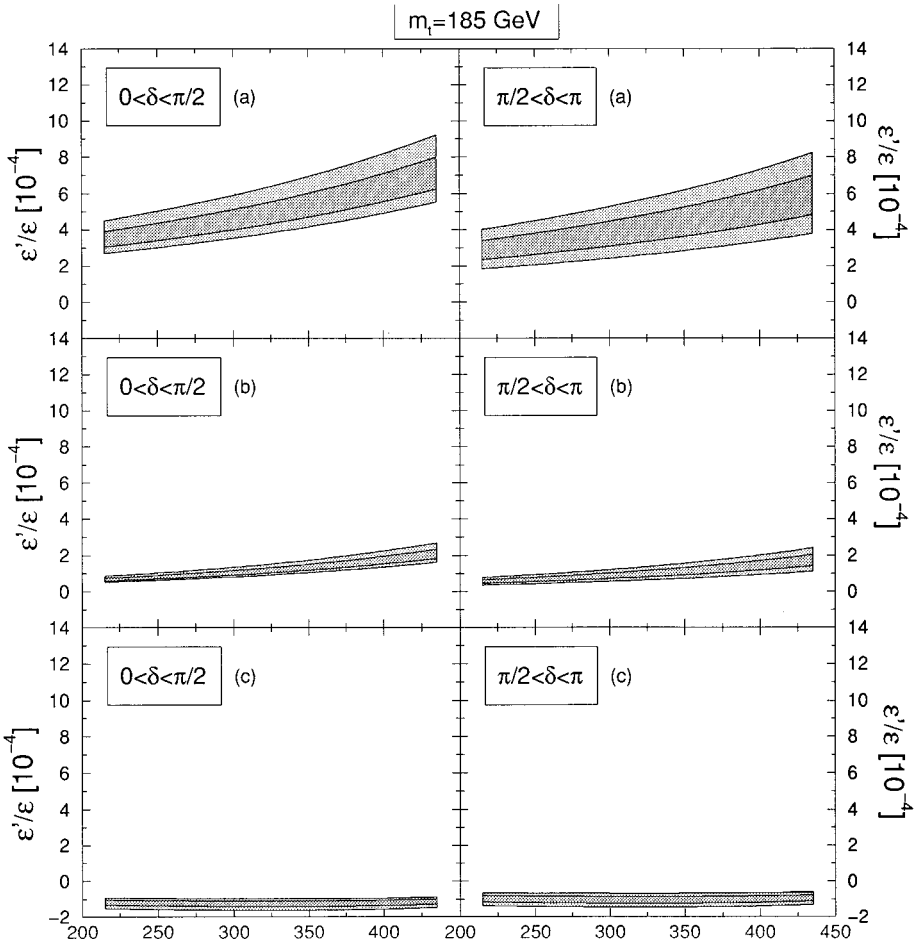

FIG. 16. Same as Fig. 14 but for m_t=185 GeV.

Ciuchini *et al.* (1995) use Gaussian distributions in treating the experimental errors. Consequently our procedure is more conservative. We agree with these authors that values for ε'/ε above 1×10^{-3}, although not excluded, are very improbable. This should be contrasted with the work of the Dortmund group (Fröhlich *et al.*, 1991; Heinrich *et al.*, 1992), which finds values for ε'/ε in the ballpark of $(1–2)\times10^{-3}$. We do not know of any consistent framework for hadronic matrix elements that would give such high values within the standard model.

(Bertolini *et al.* 1995a, 1995b), calculate the hadronic matrix elements relevant for ε'/ε within the chiral quark

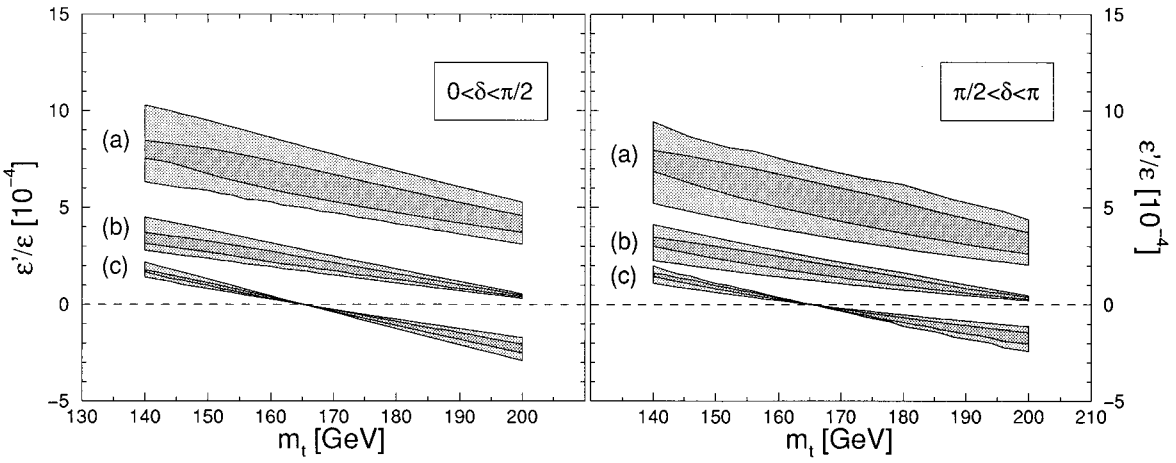

FIG. 17. The ranges of ε'/ε in the NDR scheme as a function of m_t for $\Lambda^{(4)}_{\overline{\rm MS}}=325$ MeV and present (light grey) and future (dark grey) parameter ranges given in the Appendix. The three bands correspond to hadronic parameter sets (a) $[B_6^{(1/2)}(m_c)]_{\rm eff}$=1.5, $[B_8^{(3/2)}(m_c)]_{\rm eff}$=1.0, (b) $[B_6^{(1/2)}(m_c)]_{\rm eff}$=1.0, $[B_8^{(3/2)}(m_c)]_{\rm eff}$=1.0, and (c) $[B_6^{(1/2)}(m_c)]_{\rm eff}$=1.0, $[B_8^{(3/2)}(m_c)]_{\rm eff}$=1.5, respectively.

TABLE XLII. The quantities R_c and R_p contributing to $\mathrm{Re}A_0/\mathrm{Re}A_2$ as described in the text, calculated using the vacuum-insertion estimate for the hadronic matrix elements. The Wilson-coefficient functions are evaluated for various $\Lambda_{\overline{\mathrm{MS}}}^{(4)}$ in the leading logarithmic approximation as well as in next to leading order in two different schemes (NDR and HV).

	$\Lambda_{\overline{\mathrm{MS}}}^{(4)}=215$ MeV			$\Lambda_{\overline{\mathrm{MS}}}^{(4)}=325$ MeV			$\Lambda_{\overline{\mathrm{MS}}}^{(4)}=435$ MeV		
Scheme	LO	NDR	HV	LO	NDR	HV	LO	NDR	HV
R_c	1.8	1.4	1.6	2.0	1.6	1.8	2.4	1.8	2.2
R_p	0.1	0.3	0.1	0.2	0.5	0.2	0.3	1.0	0.4

model. These authors find a rather large range $-50\times10^{-4}\leqslant\varepsilon'/\varepsilon\leqslant14\times10^{-4}$. In particular they find, in contrast to Buras *et al.* (1993b) and Ciuchini *et al.* (1995), and the present analysis, that negative values for ε'/ε as large as -5×10^{-3} are possible. This is related to the fact that, for certain model parameters in the chiral quark model, $B_6^{(1/2)}$ and $B_8^{(3/2)}$ can deviate considerably from unity and generally $B_6^{(1/2)}\leqslant B_8^{(3/2)}$. There remains an interesting question of how well the chiral quark model represents QCD.

It is obvious from this section that the status of hadronic matrix elements relevant for ε'/ε is very unsatisfactory. In particular the matching between Wilson coefficients and hadronic matrix elements with respect to the μ dependence and the renormalization-scheme dependence should be improved. Unfortunately the progress in this direction is rather slow.

The experimental situation on $\mathrm{Re}(\varepsilon'/\varepsilon)$ is unclear at present. While the result of the NA31 collaboration at CERN with $\mathrm{Re}(\varepsilon'/\varepsilon)=(23\pm7)\times10^{-4}$ (Barr *et al.*, 1993) clearly indicates direct CP violation, the value of E731 at Fermilab, $\mathrm{Re}(\varepsilon'/\varepsilon)=(7.4\pm5.9)\times10^{-4}$ (Gibbons *et al.*, 1993) is compatible with superweak theories (Wolfenstein, 1964) in which $\varepsilon'/\varepsilon=0$. The E731 result is in the ballpark of the theoretical estimates. The NA31 value appears a bit high compared to the range given in Eq. (19.43) above.

Hopefully, in about three years the experimental situation concerning ε'/ε will be clarified through the improved measurements by the two collaborations at the 10^{-4} level and by experiments at the Φ factory in Frascati. One should also hope that the theoretical situation of ε'/ε will improve by then as well.

XX. K_L-K_S MASS DIFFERENCE AND $\Delta I=1/2$ RULE

It is probably a good moment to make a few comments on the K_L-K_S mass difference given by

$$\Delta M=M(K_L)-M(K_S)=3.51\times10^{-15}\ \text{GeV} \tag{20.1}$$

and the approximate $\Delta I=1/2$ rule in $K\to\pi\pi$ decays. As we have already mentioned in the beginning of Sec. XIX.A, this empirical rule manifests itself in the dominance of $\Delta I=1/2$ over $\Delta I=3/2$ decay amplitudes. It can be expressed as

$$\frac{\mathrm{Re}A_0}{\mathrm{Re}A_2}=22.2, \tag{20.2}$$

using the notation of Sec. XIX.A.

A. $\Delta M(K_L-K_S)$

The K_L-K_S mass difference can be written as

$$\Delta M=2\ \mathrm{Re}M_{12}+(\Delta M)_{\mathrm{LD}} \tag{20.3}$$

with M_{12} given in Eq. (18.6) and $(\Delta M)_{\mathrm{LD}}$ representing long-distance contributions, corresponding, for instance, to the exchange of intermediate light pseudoscalar mesons (π^0,η). The first term in Eq. (20.3), the so-called short-distance contribution, is dominated by the first term in Eq. (18.6), so that

$$(\Delta M)_{\mathrm{SD}}=\frac{G_F^2}{6\pi^2}F_K^2B_Km_KM_W^2\left[\lambda_c^2\eta_1\frac{m_c^2}{M_W^2}+\Delta_{\mathrm{top}}\right], \tag{20.4}$$

where Δ_{top} represents the two top-dependent terms in Eq. (18.6). In writing Eq. (20.4) we are neglecting the tiny imaginary part in $\lambda_c=V_{cs}^*V_{cd}$. A very extensive numerical analysis of Eq. (20.4) has been presented by Herrlich and Nierste (1994), who calculated the NLO corrections to η_1 and also to η_3 (Herrlich and Nierste, 1995a), which enters Δ_{top}. The NLO calculation of the short-distance contributions improves the matching to the nonperturbative matrix element parametrized by B_K and clarifies the proper definition of B_K to be used along with the QCD factors η_i. In addition the NLO study reveals an enhancement of η_1 over its LO estimate by about 20%. Although sizable, this enhancement can still be considered being perturbative, as required by the consistency of the calculation. This increase in η_1, reinforced by updates in input parameters $(\Lambda_{\overline{\mathrm{MS}}})$, brings $(\Delta M)_{\mathrm{SD}}$ closer to the experimental value in Eq. (20.1). With $\Lambda_{\overline{\mathrm{MS}}}^{(4)}=325$ MeV and $m_c=1.3$ GeV, giving $\eta_1^{\mathrm{NLO}}=1.38$, one finds that typically 70% of ΔM can be described by the short-distance component. The exact value is still somewhat uncertain because η_1 is rather sensitive to $\Lambda_{\overline{\mathrm{MS}}}$. Further uncertainties are introduced by the error in B_K and the renormalization scale ambiguity, which is still quite pronounced even at NLO. The result is, however, certainly more reliable than previous LO estimates. Using the old value $\eta_1^{\mathrm{LO}}=0.85$, corre-

sponding to m_c=1.4 GeV and $\Lambda_{\rm QCD}$=200 MeV, $(\Delta M)_{\rm SD}/\Delta M$ would be below 50%, suggesting a dominance of long-distance contributions in ΔM. As discussed by Herrlich and Nierste (1994), such a situation would be "unnatural," since the long-distance component is formally suppressed by $\Lambda^2_{\rm QCD}/m_c^2$. Hence the short-distance dominance indicated by the NLO analysis is also gratifying in this respect. The long-distance contributions, to which one can attribute the remaining ~30% in ΔM not explained by the short-distance part, are nicely discussed by Bijnens *et al.* (1991).

In summary, the observed K_L-K_S mass difference can be roughly described within the standard model after the NLO corrections have been taken into account. However, the remaining theoretical uncertainties in the dominant part of Eq. (20.4) and the uncertainties in $(\Delta M)_{\rm LD}$ do not allow one to use ΔM as a constraint on the CKM parameters.

B. The ΔI=1/2 rule

Using the effective Hamiltonian in Eq. (7.1) and keeping only the dominant terms, one has

$$\frac{{\rm Re}A_0}{{\rm Re}A_2}\approx\frac{z_1(\mu)\langle Q_1(\mu)\rangle_0+z_2(\mu)\langle Q_2(\mu)\rangle_0+z_6(\mu)\langle Q_6(\mu)\rangle_0}{z_1(\mu)\langle Q_1(\mu)\rangle_2+z_2(\mu)\langle Q_2(\mu)\rangle_2}, \tag{20.5}$$

where $\langle Q_i\rangle_{0,2}$ are defined in Eq. (19.8). The coefficients $z_i(\mu)$ can be found in Table XVIII. For the hadronic matrix elements we use Eqs. (19.11), (19.12), (19.16), and (19.21), which have been discussed in Sec. XIX.B. We find then, separating current-current and penguin contributions

$$\frac{{\rm Re}A_0}{{\rm Re}A_2}=R_c+R_p, \tag{20.6}$$

$$R_c=\frac{5z_2(\mu)B_2^{(1/2)}-z_1(\mu)B_1^{(1/2)}}{4\sqrt{2}z_+(\mu)B_1^{(3/2)}},\quad z_+=z_1+z_2, \tag{20.7}$$

$$R_p=-11.9\,\frac{z_6(\mu)}{z_+(\mu)}\,\frac{B_6^{(1/2)}}{B_1^{(3/2)}}\left[\frac{178\ \text{MeV}}{m_s(\mu)+m_d(\mu)}\right]^2. \tag{20.8}$$

The factor 11.9 expresses the enhancement of the matrix elements of the penguin operator Q_6 over $\langle Q_{1,2}\rangle$ first pointed out by Vainshtein *et al.* (1977). It is instructive to calculate R_c and R_p using the vacuum-insertion estimate, for which $B_1^{(1/2)}=B_2^{(1/2)}=B_1^{(3/2)}=B_6^{(1/2)}=1$. Without QCD effects one finds R_c=0.9 and R_p=0 in complete disagreement with the data. In Table XLII we show the values of R_c and R_p at μ=1 GeV, using the results of Table XVIII. We have set m_s+m_d=178 MeV.

The inclusion of QCD effects enhances both R_c and R_p (Altarelli and Maiani, 1974; Gaillard and Lee, 1974a). However, even for the highest values of $\Lambda^{(4)}_{\overline{\rm MS}}$, the ratio ${\rm Re}A_0/{\rm Re}A_2$ is at least a factor of eight smaller than the experimental value in Eq. (20.2). Moreover, a considerable scheme dependence is observed. Lowering μ would improve the situation, but for μ<1 GeV the perturbative calculations of $z_i(\mu)$ can no longer be trusted. Similarly, lowering m_s down to 100 MeV would increase the penguin contribution. In view of the most recent estimates in Eq. (19.36), however, such a low value of m_s seems to be excluded. We conclude therefore, as already known for many years, that the vacuum-insertion estimate fails completely in explaining the ΔI=1/2 rule. As we have discussed in Sec. XIX the vacuum-insertion estimate $B_6^{(1/2)}$=1 is supported by the $1/N$ expansion approach and by lattice calculations. Consequently, the only solution to the ΔI=1/2 rule problem appears to be a change in the values of the remaining B_i factors. For instance, repeating the above calculation with $B_1^{(3/2)}$=0.48, $B_2^{(1/2)}$=5, and $B_1^{(1/2)}$=10 would give, in the NDR scheme, $R_c\approx$20, $R_p\approx$2, and ${\rm Re}A_0/{\rm Re}A_2\approx$22, in accordance with the experimental value.

There have been several attempts to explain the ΔI=1/2 rule, which basically use the effective Hamiltonian in Eq. (7.1) but employ different methods for the hadronic matrix elements. In particular we would like to mention the $1/N$ approach (Bardeen *et al.*, 1987a), the work of Pich and de Rafael (1991) based on an effective action for four-quark operators, the diquark approach of Neubert and Stech (1991), QCD sum rules (Jamin and Pich, 1994), chiral perturbation calculations (Kambor *et al.*, 1990, 1991), and very recently an analysis (Antonelli *et al.*, 1996) in the framework of the chiral quark model (Cohen and Manohar, 1984).

With these methods values for ${\rm Re}A_0/{\rm Re}A_2$ in the range 15–20 can be obtained. It is beyond the scope of this review to discuss the weak and strong points of each method, although at least one of us believes that the "meson evolution" picture advocated by Bardeen *et al.* (1987a) represents the main bulk of the physics behind the value of 22. In view of the uncertainties present in these approaches, we have not used them in the analysis of ε'/ε but have constrained the hadronic matrix elements so that they satisfy the ΔI=1/2 rule exactly.

XXI. THE DECAY $K_L\to\pi^0e^+e^-$

A. General remarks

Let us next move on to discuss the rare decay $K_L\to\pi^0e^+e^-$. Whereas in $K\to\pi\pi$ decays the CP-violating contribution is only a tiny part of the full amplitude and the direct CP violation, as we have just seen, is expected to be at least three orders of magnitude

smaller than the indirect CP violation, the corresponding hierarchies are very different for $K_L\to\pi^0e^+e^-$. At lowest order in electroweak interactions (one-loop photon penguin, Z^0 penguin and W box diagrams) this decay takes place only if CP symmetry is violated. The CP-conserving contribution to the amplitude comes from a two-photon exchange, which, although of higher order in α, could in principle be sizable. Extensive studies of several groups indicate, however, that the CP-conserving part is likely to be smaller than the CP-violating contributions. We will be more specific about this at the end of this section.

The CP-violating part can again be divided into a direct and an indirect part. The latter is given by the $K_S\to\pi^0e^+e^-$ amplitude multiplied by the CP-violating parameter ε_K. The amplitude $A(K_S\to\pi^0e^+e^-)$ can be written as

$$A(K_S\to\pi^0e^+e^-)=\langle\pi^0e^+e^-|\mathcal{H}_{\rm eff}|K_S\rangle, \tag{21.1}$$

where $\mathcal{H}_{\rm eff}$ can be found in Eq. (8.1) with the operators $Q_1,\ldots,Q_6$ defined in Eq. (6.3), the operators Q_{7V} and Q_{7A} given by

$$Q_{7V}=(\bar sd)_{V-A}(\bar ee)_V,\quad Q_{7A}=(\bar sd)_{V-A}(\bar ee)_A, \tag{21.2}$$

and the Wilson coefficients z_i and y_i calculated in Sec. VIII.

Let us next note that the coefficients of Q_{7V} and Q_{7A} are $\mathcal{O}(\alpha)$ but their matrix elements $\langle\pi^0e^+e^-|Q_{7V,A}|K_S\rangle$ are $\mathcal{O}(1)$. In the case of Q_i (i=1,...,6) the situation is reversed: the Wilson coefficients are $\mathcal{O}(1)$, but the matrix elements $\langle\pi^0e^+e^-|Q_i|K_S\rangle$ are $\mathcal{O}(\alpha)$. Consequently, at $\mathcal{O}(\alpha)$ all operators contribute to $A(K_S\to\pi^0e^+e^-)$. However, because $K_S\to\pi^0e^+e^-$ is CP conserving, the coefficients y_i multiplied by $\tau=\mathcal{O}(\lambda^4)$ can be fully neglected, and the operator Q_{7A} drops out in this approximation. Now, whereas $\langle\pi^0e^+e^-|Q_{7V}|K_S\rangle$ can be trivially calculated, this is not the case for $\langle\pi^0e^+e^-|Q_i|K_S\rangle$ with i=1,...,6, which can only be evaluated using nonperturbative methods. Moreover, it is clear from the short-distance analysis of Sec. VIII that the inclusion of Q_i in the estimate of $A(K_S\to\pi^0e^+e^-)$ cannot be avoided. Indeed, whereas $\langle\pi^0e^+e^-|Q_{7V}|K_S\rangle$ is independent of μ and the renormalization scheme, the coefficient z_{7V} shows very strong scheme and μ dependences. They can only be canceled by the contributions from the four-quark operators Q_i. All this demonstrates that the estimate of the indirect CP violation in $K_L\to\pi^0e^+e^-$ cannot be done very reliably at present. Some estimates in the framework of chiral perturbation theory will be discussed below. On the other hand, a much better assessment of the importance of indirect CP violation in $K_L\to\pi^0e^+e^-$ will become possible after a measurement of $B(K_S\to\pi^0e^+e^-)$.

Fortunately the directly CP-violating contribution can be fully calculated as a function of m_t, CKM parameters, and the QCD coupling constant α_s. There are practically no theoretical uncertainties related to hadronic matrix elements because $\langle\pi^0|(\bar sd)_{V-A}|K_L\rangle$ can be extracted using isospin symmetry from the well-measured decay $K^+\to\pi^0e^+\nu$. In what follows, we will concentrate on this contribution.

TABLE XLIII. PBE coefficient P_0 of y_{7V} for various values of $\Lambda^{(4)}_{\overline{\rm MS}}$ and μ. In the absence of QCD P_0=8/9 $\ln(M_W/m_c)$=3.664 holds universally.

		P_0		
$\Lambda^{(4)}_{\overline{\rm MS}}$ [MeV]	μ [GeV]	LO	NDR	HV
215	0.8	2.073	3.159	3.110
	1.0	2.048	3.133	3.084
	1.2	2.027	3.112	3.063
325	0.8	1.863	3.080	3.024
	1.0	1.834	3.053	2.996
	1.2	1.811	3.028	2.970
435	0.8	1.672	2.976	2.914
	1.0	1.640	2.965	2.899
	1.2	1.613	2.939	2.872

B. Analytic formula for $B(K_L\to\pi^0e^+e^-)_{\rm dir}$

The directly CP-violating contribution is governed by the coefficients y_i, and consequently only the penguin operators $Q_3,\ldots,Q_6$, Q_{7V}, and Q_{7A} have to be considered. Since $y_i=\mathcal{O}(\alpha_s)$ for i=3,...,6, the contribution of QCD penguins to $B(K_L\to\pi^0e^+e^-)_{\rm dir}$ is really $\mathcal{O}(\alpha\alpha_s)$, as compared to the $\mathcal{O}(\alpha)$ contributions of Q_{7V} and Q_{7A}. In deriving the final formula, we will therefore neglect the contributions of the operators $Q_3,\ldots,Q_6$, i.e., we will assume that

$$\sum_{i=3}^{6}y_i(\mu)\langle\pi^0e^+e^-|Q_i|K_L\rangle \ll y_{7V}(\mu)\langle\pi^0e^+e^-|Q_{7V}|K_L\rangle. \tag{21.3}$$

This assumption is supported by the corresponding relation for the quark-level matrix elements

$$\sum_{i=3}^{6}y_i(\mu)\langle de^+e^-|Q_i|s\rangle\ll y_{7V}(\mu)\langle de^+e^-|Q_{7V}|s\rangle, \tag{21.4}$$

which can be easily verified perturbatively.

The neglect of the QCD penguin operators is compatible with the scheme and μ independence of the resulting branching ratio. Indeed y_{7A} does not depend on μ and the renormalization scheme at all, and the corresponding dependences in y_{7V} are at the level of $\pm1\%$ as discussed in Sec. VIII.E. Introducing the numerical constant

$$\kappa_e=\frac{1}{V_{us}^2}\frac{\tau(K_L)}{\tau(K^+)}\left(\frac{\alpha}{2\pi}\right)^2B(K^+\to\pi^0e^+\nu)=6.3\times10^{-6}, \tag{21.5}$$

one then finds

$$B(K_L\to\pi^0e^+e^-)_{\rm dir}=\kappa_e({\rm Im}\lambda_t)^2(\tilde y_{7V}^2+\tilde y_{7A}^2), \tag{21.6}$$

where

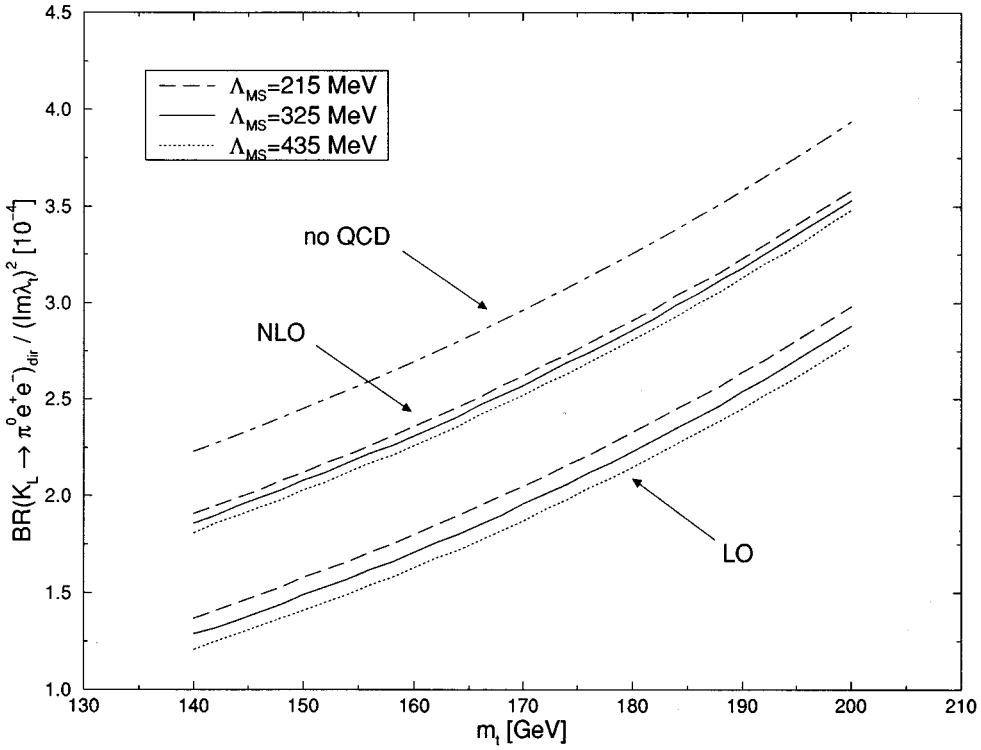

FIG. 18. $B(K_L \to \pi^0 e^+ e^-)_{\rm dir}/({\rm Im}\lambda_t)^2$ as a function of m_t for various values of $\Lambda^{(4)}_{\overline{\rm MS}}$ at scale μ=1.0 GeV.

$$y_i = \frac{\alpha}{2\pi}\,\tilde{y}_i\,. \tag{21.7}$$

Next, using the method of the penguin box expansion (Sec. XIV), we can write, similar to Eqs. (10.5) and (10.3),

$$\tilde{y}_{7V} = P_0 + \frac{Y_0(x_t)}{\sin^2\Theta_W} - 4Z_0(x_t) + P_E E_0(x_t), \tag{21.8}$$

$$\tilde{y}_{7A} = -\frac{1}{\sin^2\Theta_W}\,Y_0(x_t) \tag{21.9}$$

with Y_0, Z_0, and E_0 given in Eqs. (11.46), (14.2), and (6.15). P_E is $\mathcal{O}(10^{-2})$, and consequently the last term in Eq. (21.8) can be neglected. P_0 is given for different values of μ and $\Lambda_{\overline{\rm MS}}$ in Table XLIII. There we also show the leading-order results and the case without QCD corrections.

The analytic expressions in Eqs. (21.8) and (21.9) are useful as they display not only the explicit m_t dependence, but also isolate the impact of leading- and next-to-leading-order QCD effects. These effects modify only the constants P_0 and P_E. As anticipated from the results of Sec. VIII.E, P_0 is strongly enhanced relative to the LO result. This enhancement amounts roughly to a factor of 1.6±0.1. However, this enhancement is partially due to the fact that, for $\Lambda_{\rm LO}=\Lambda_{\overline{\rm MS}}$, the QCD coupling constant in the leading order is 20–30% larger than its next-to-leading-order value. Calculating P_0 in LO but with the full α_s of Eq. (3.19), we have found that the enhancement then amounts to a factor of 1.33±0.06. In any case the inclusion of NLO QCD effects and a meaningful use of $\Lambda_{\overline{\rm MS}}$ show that the next-to-leading-order effects weaken the QCD suppression of y_{7V}. As seen in Table XLIII, the suppression of P_0 by QCD corrections amounts to about 15% in the complete next-to-leading-order calculation.

C. Numerical analysis

In Fig. 8 of Sec. VIII.E we have found $|y_{7V}/\alpha|^2$ and $|y_{7A}/\alpha|^2$ as functions of m_t together with the leading-order result for $|y_{7V}/\alpha|^2$ and the case without QCD corrections. From there it is obvious that the dominant m_t dependence of $B(K_L \to \pi^0 e^+ e^-)_{\rm dir}$ originates from the coefficient of the operator Q_{7A}. Another noteworthy feature was that, accidentally for $m_t \approx 175$ GeV, one finds $y_{7V} \approx y_{7A}$.

In Fig. 18 the ratio $B(K_L \to \pi^0 e^+ e^-)_{\rm dir}/({\rm Im}\lambda_t)^2$ is shown as a function of m_t. The enhancement of the directly CP-violating contribution through NLO corrections relative to the LO estimate is clearly visible on this plot. As we will see below, due to large uncertainties present in ${\rm Im}\lambda_t$, this enhancement cannot yet be fully appreciated phenomenologically.

The very weak dependence on $\Lambda_{\overline{\rm MS}}$ should be contrasted with the very strong dependence found in the case of ε'/ε. Therefore, provided the other two contributions to $K_L \to \pi^0 e^+ e^-$ can be shown to be small or can be reliably calculated one day, the measurement of $B(K_L \to \pi^0 e^+ e^-)$ should offer a good determination of ${\rm Im}\lambda_t$.

Next we would like to comment on the possible uncertainties due to the definition of m_t. At the level of accuracy at which we work we cannot fully address this question yet. In order to be able to do so, one needs to know the perturbative QCD corrections to $Y_0(x_t)$ and $Z_0(x_t)$ and, for consistency, an additional order in the renormalization-group improved calculation of P_0. Since the m_t dependence of y_{7V} is rather moderate, the main concern here is the coefficient y_{7A}, whose m_t dependence is fully given by $Y(x_t)$. Fortunately the QCD-corrected function $Y(x_t)$ is known from the analysis of $K_L \to \mu^+\mu^-$ and can be directly used here. As we will discuss in Sec. XXV, for $m_t = m_t(m_t)$ the QCD corrections to $Y_0(x_t)$ are around 2%. On this basis we believe that, if $m_t = m_t(m_t)$ is chosen, the additional QCD corrections to $B(K_L \to \pi^0 e^+ e^-)_{\rm dir}$ should be small.

Finally we give the predictions for the present and future sets of input parameters as described in the Appendix. It should be emphasized that the uncertainties in these predictions result entirely from the CKM parameters. This situation will improve considerably in the era of dedicated B-physics experiments in the next decade, which allows a precise prediction for $B(K_L \to \pi^0 e^+ e^-)_{\rm dir}$.

We find

$$B(K_L \to \pi^0 e^+ e^-)_{\rm dir} = \begin{cases} (4.26 \pm 3.03) \times 10^{-12} & \text{no } x_d \text{ constraint} \\ (4.48 \pm 2.77) \times 10^{-12} & \text{with } x_d \text{ constraint,} \end{cases} \tag{21.10}$$

$$B(K_L \to \pi^0 e^+ e^-)_{\rm dir} = \begin{cases} (3.71 \pm 1.61) \times 10^{-12} & \text{no } x_d \text{ constraint} \\ (4.32 \pm 0.96) \times 10^{-12} & \text{with } x_d \text{ constraint.} \end{cases} \tag{21.11}$$

These results are compatible with those found by Buras, Lautenbacher, Misiak, and Münz (1994), Donoghue and Gabbiani (1995), and Köhler and Paschos (1995) with differences originating from different choices of CKM parameters.

D. The indirectly *CP*-violating and *CP*-conserving parts

Now we want to compare the results obtained for the direct CP-violating part with the estimates made for the indirect CP-violating contribution and the CP-conserving one. The most recent discussions have been presented by Cohen *et al.* (1993), Heiliger and Seghal (1993), Donoghue and Gabbiani (1995), and Köhler and Paschos (1995), where references to earlier papers can be found.

The indirect CP-violating amplitude is given by the $K_S \to \pi^0 e^+ e^-$ amplitude multiplied by the CP parameter ε_K. Once $B(K_S \to \pi^0 e^+ e^-)$ has been accurately measured, it will be possible to calculate this contribution precisely. Using chiral perturbation theory, it is, however, possible to get an estimate by relating $K_S \to \pi^0 e^+ e^-$ to the $K^+ \to \pi^+ e^+ e^-$ transition (Ecker *et al.*, 1987, 1988). To this end one can write

$$B(K_L \to \pi^0 e^+ e^-)_{\rm indir} = B(K^+ \to \pi^+ e^+ e^-) \frac{\tau(K_L)}{\tau(K^+)} \times |\varepsilon_K|^2 r^2, \tag{21.12}$$

where

$$r^2 = \frac{\Gamma(K_S \to \pi^0 e^+ e^-)}{\Gamma(K^+ \to \pi^+ e^+ e^-)}. \tag{21.13}$$

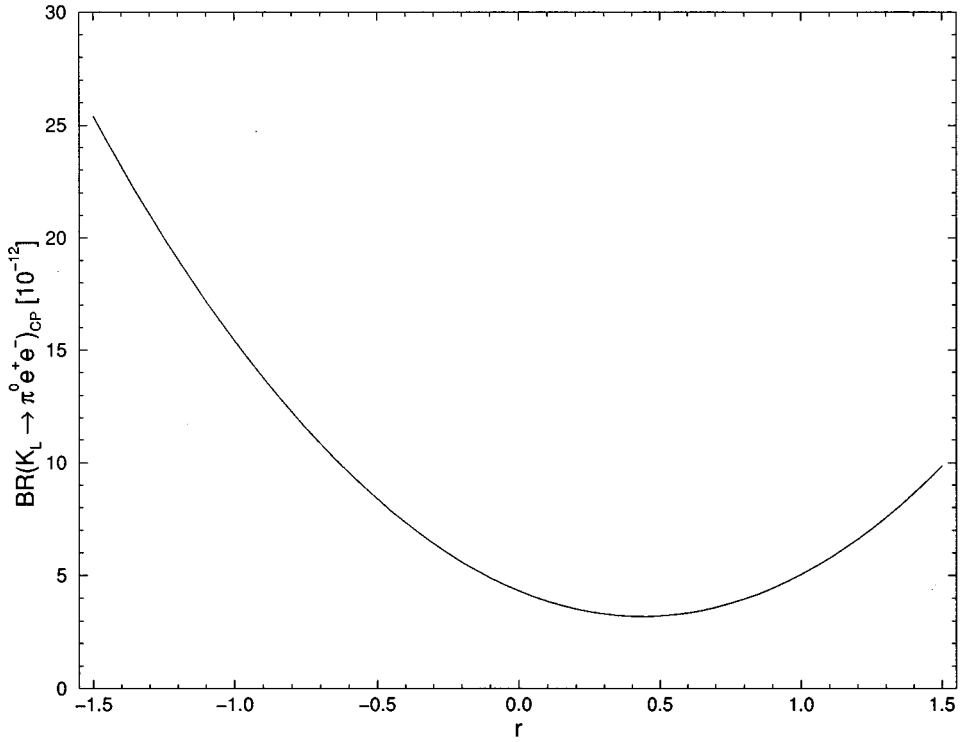

FIG. 19. $B(K_L \to \pi^0 e^+ e^-)_{CP}$ for $m_t = 170$ GeV, $\Lambda^{(4)}_{\overline{\rm MS}} = 325$ MeV, and $\mathrm{Im}\lambda_t = 1.3 \times 10^{-4}$ as a function of r.

With $B(K^+\to\pi^+e^+e^-)=(2.74\pm0.23)\times10^{-7}$ (Alliegro *et al.*, 1992) and the most recent chiral perturbation theory estimate $|r|\leq0.5$ (Ecker *et al.*, 1988; Bruno and Prades, 1993), one has

$$B(K_L\to\pi^0e^+e^-)_{\rm indir}=(5.9\pm0.5)\cdot10^{-12}r^2 \leq1.6\times10^{-12}, \tag{21.14}$$

i.e., a branching ratio more than a factor of 2 below the direct CP-violating contribution. Yet, as emphasized recently by Donoghue and Gabbiani (1995) and Heiliger and Seghal (1993), the knowledge of r is very uncertain at present. In particular, the estimate in Eq. (21.14) is based on a relation between two nonperturbative parameters, which is rather *ad hoc* and certainly not a consequence of chiral symmetry. As shown by Donoghue and Gabbiani (1995), a small deviation from this relation increases r to values above unity, so that $B(K_L\to\pi^0e^+e^-)_{\rm indir}$ could be comparable or even larger than $B(K_L\to\pi^0e^+e^-)_{\rm dir}$. It appears then that this enormous uncertainty in the indirectly CP-violating part can only be removed by measuring the rate of $K_S\to\pi^0e^+e^-$.

It should also be stressed that in reality the CP indirect amplitude may interfere with the vector part of the CP direct amplitude. The full CP-violating amplitude can then be written following Dib *et al.* (1989a, 1989b) as follows:

$$B(K_L\to\pi^0e^+e^-)_{CP}=|2.43\times10^{-6}re^{i\pi/4} -i\sqrt{\kappa_e}\,{\rm Im}\lambda_t\tilde{y}_{7V}|^2 +\kappa_e({\rm Im}\lambda_t)^2\tilde{y}_{7A}^2. \tag{21.15}$$

As an example, we show in Fig. 19 $B(K_L\to\pi^0e^+e^-)_{CP}$ for m_t=170 GeV, $\Lambda^{(4)}_{\overline{\rm MS}}$ = 325 MeV, and ${\rm Im}\lambda_t=1.3\times10^{-4}$, as a function of r. We observe that, whereas for $0\leq r\leq1$ the dependence of $B(K_L\to\pi^0e^+e^-)_{CP}$ on r is moderate, it is rather strong otherwise and already for $r<-0.6$ values as high as 10^{-11} are found.

The estimate of the CP-conserving contribution is also difficult. We refer the reader to works by Cohen *et al.* (1993), Heiliger and Seghal (1993), and Donoghue and Gabbiani (1995), where further references to an extensive literature on this subject can be found. The measurement of the branching ratio

$$B(K_L\to\pi^0\gamma\gamma)=\begin{cases}(1.7\pm0.3)\times10^{-6} & \text{(Barr } et\ al.,\ 1992)\\ (2.0\pm1.0)\times10^{-6} & \text{(Papadimitriou } et\ al.,\ 1991)\end{cases} \tag{21.16}$$

and of the shape of the $\gamma\gamma$ mass spectrum plays an important role in this estimate. The most recent analyses give

$$B(K_L\to\pi^0e^+e^-)_{\rm cons}\approx\begin{cases}(0.3\text{–}1.8)\times10^{-12} & \text{(Cohen } et\ al.,\ 1993)\\ 4.0\times10^{-12} & \text{(Heiliger and Seghal, 1993)}\\ (5\pm5)\times10^{-12} & \text{(Donoghue and Gabbiani, 1995),}\end{cases} \tag{21.17}$$

i.e., not necessarily below the CP-violating contribution. An improved estimate of this component is certainly desirable. It should be noted that there is no interference in the rate between the CP-conserving and CP-violating contributions so that the results in Fig. 19 and Eq. (21.17) can simply be added.

E. Outlook

The results discussed above indicate that, within the standard model, $B(K_L\to\pi^0e^+e^-)$ could be as high as 1×10^{-11}. Moreover, the direct CP-violating contribution is found to be important and could even be dominant. Unfortunately the large uncertainties in the remaining two contributions will probably not allow an easy identification of the direct CP violation by measuring the branching ratio only. The future measurements of $B(K_S\to\pi^0e^+e^-)$ and improvements in the estimate of the CP-conserving part may of course change this unsatisfactory situation. Alternatively, the measurements of the electron-energy asymmetry (Heiliger and Seghal, 1993; Donoghue and Gabbiani, 1995) and the study of the time evolution of $K^0\to\pi^0e^+e^-$ (Littenberg, 1989b; Donoghue and Gabbiani, 1995; Köhler and Paschos, 1995) could allow for a refined study of CP violation in this decay.

The present experimental bounds

$$B(K_L\to\pi^0e^+e^-) \leq\begin{cases}4.3\times10^{-9} & \text{(Harris } et\ al.,\ 1993)\\ 5.5\times10^{-9} & \text{(Ohl } et\ al.,\ 1990)\end{cases} \tag{21.18}$$

are still three orders of magnitude away from the theoretical expectations. Yet the prospects of getting the required sensitivity of order 10^{-11}–10^{-12} in five years are encouraging (Littenberg and Valencia, 1993; Ritchie and Wojcicki, 1993; Winstein and Wolfenstein, 1993).

XXII. THE DECAY $B\to X_s\gamma$

A. General remarks

The $B\to X_s\gamma$ decay is known to be extremely sensitive to the structure of fundamental interactions at the electroweak scale. As with any FCNC process, it does not arise at the tree level in the standard model. The one-loop W-exchange diagrams that generate this decay at

the lowest order in the standard model are small enough to be comparable to possible nonstandard contributions (charged scalar exchanges SUSY one-loop diagrams, W_R exchanges in the L-R symmetric models, etc.).

The $B\to X_s\gamma$ decay is particularly interesting because its rate is of order $G_F^2\alpha$, while most of the other FCNC processes involving leptons or photons are of order $G_F^2\alpha^2$. The long-range strong interactions are expected to play a minor role in the inclusive $B\to X_s\gamma$ decay. This is because the mass of the b quark is much larger than the QCD scale Λ. Moreover, the only relevant intermediate hadronic states ψX_s are expected to give very small contributions as long as we assume no interference between short- and long-distance terms in the inclusive rate. Therefore it has become quite common to use the following approximate equality to estimate the $B\to X_s\gamma$ rate,

$$\frac{\Gamma(B\to X_s\gamma)}{\Gamma(B\to X_c e\bar{\nu}_e)}\simeq\frac{\Gamma(b\to s\gamma)}{\Gamma(b\to ce\bar{\nu}_e)}\equiv R(m_t,\alpha_s,\xi), \quad (22.1)$$

where the quantities on the rhs are calculated in the spectator model corrected for short-distance QCD effects. The normalization to the semileptonic rate is usually introduced in order to cancel the uncertainties due to the Cabibbo-Kobayashi-Maskawa (CKM) matrix elements and factors of m_b^5 in the rhs of Eq. (22.1). Additional support for the approximation given above comes from the heavy-quark expansions. Indeed the spectator model has been shown to correspond to the leading-order approximation of an expansion in $1/m_b$. The first corrections appear at the $\mathcal{O}(1/m_b^2)$ level. The latter terms have been studied by several authors (Bigi *et al.*, 1992, 1993, 1994a; Bjorken *et al.*, 1992; Blok *et al.*, 1994; Falk *et al.*, 1994; Mannel, 1994; Manohar and Wise, 1994) with the result that they affect $B(B\to X_s\gamma)$ and $B(B\to X_c e\bar{\nu}_e)$ by only a few percent.

As indicated above, the ratio R depends only on m_t and α_s in the standard model. In extensions of the standard model, additional parameters are present, which have been commonly denoted by ξ. The main point to be stressed here is that R is a calculable function of its parameters in the framework of a renormalization-group improved perturbation theory. Consequently, the decay in question is particularly suited for tests of the standard model and its extensions.

One of the main difficulties in analyzing the inclusive $B\to X_s\gamma$ decay is calculating the short-distance QCD effects due to hard gluon exchanges between the quark lines of the leading one-loop electroweak diagrams. These effects are known (Bertolini *et al.*, 1987; Deshpande *et al.*, 1987; Grigjanis *et al.*, 1988, 1992; Grinstein *et al.*, 1990; Misiak, 1991) to enhance the $B\to X_s\gamma$ rate in the standard model by a factor of 2–3, depending on the top-quark mass. So the $B\to X_s\gamma$ decay appears to be the only known short-distance process in the standard model that is dominated by two-loop contributions.

The $B\to X_s\gamma$ decay has already been measured. In 1993 CLEO reported (Ammar *et al.*, 1993) the following branching ratio for the exclusive $B\to K^*\gamma$ decay,

$$B(B\to K^*\gamma)=(4.5\pm1.5\pm0.9)\times10^{-5}. \quad (22.2)$$

In 1994 a first measurement of the inclusive rate was presented (Alam *et al.*, 1995),

$$B(B\to X_s\gamma)=(2.32\pm0.57\pm0.35)\times10^{-4}, \quad (22.3)$$

where the first error is statistical and the second is systematic.

As we will see below these experimental findings are in the ballpark of the standard model expectations based on the leading logarithmic approximation.

In fact a complete leading order analysis of $B(B\to X_s\gamma)$ in the standard model was presented almost a year before the CLEO result, giving (Buras, Misiak, Münz, and Pokorski, 1994)

$$B(B\to X_s\gamma)_{TH}=(2.8\pm0.8)\times10^{-4}, \quad (22.4)$$

where the error is dominated by the uncertainty in the choice of the renormalization scale $m_b/2<\mu<2m_b$, as first stressed by Ali and Greub (1993). Since $B\to X_s\gamma$ is dominated by QCD effects, it is not surprising that this scale uncertainty in the leading order is particularly large. Such an uncertainty, inherent in any finite order of perturbation theory, can be reduced by including next-to-leading-order corrections. Unfortunately, it will take some time before the μ dependences present in $B\to X_s\gamma$ can be reduced in the same manner as was done for the other decays (Buras *et al.*, 1990; Buchalla and Buras, 1993a, 1994a; Herrlich and Nierste, 1994). As we already stated in Sec. IX.B, a full next-to-leading-order computation of $B\to X_s\gamma$ would require calculation of three-loop mixings between the operators $Q_1,\ldots,Q_6$ and the magnetic penguin operators $Q_{7\gamma},Q_{8G}$. Moreover, certain two-loop matrix elements of the relevant operators should be calculated in the spectator model. A formal analysis at the next-to-leading-order level (Buras, Misiak, Münz, and Pokorski, 1994) is, however, very encouraging and shows that the μ dependence can be considerably reduced once all the necessary calculations have been performed. We will return to this issue below.

B. The decay $B\to X_s\gamma$ in the leading logarithm approximation

The leading logarithmic calculations (Grinstein *et al.*, 1990), (Ali and Greub, 1993), (Misiak, 1993), (Buras, Misiak, Münz, and Pokorski, 1994), (Cella *et al.*, 1994a), (Ciuchini, Franco, Reina, and Silvestrini, 1994), (Misiak, 1995) can be summarized in a compact form, as follows:

$$R=\frac{\Gamma(b\to s\gamma)}{\Gamma(b\to ce\bar{\nu}_e)}=\frac{|V_{ts}^*V_{tb}|^2}{|V_{cb}|^2}\frac{6\alpha}{\pi f(z)}|C_{7\gamma}^{(0)\mathrm{eff}}(\mu)|^2, \quad (22.5)$$

where $C_{7\gamma}^{(0)\mathrm{eff}}(\mu)$ is the effective coefficient given in Eq. (9.23) and Table XXVIII, $z=m_c/m_b$, and

$$f(z)=1-8z^2+8z^6-z^8-24z^4\ln z \quad (22.6)$$

is the phase-space factor in the semileptonic b decay. Note that at this stage one should not include the $\mathcal{O}(\alpha_s)$ corrections to $\Gamma(b\to ce\bar{\nu})$, since they are part of the

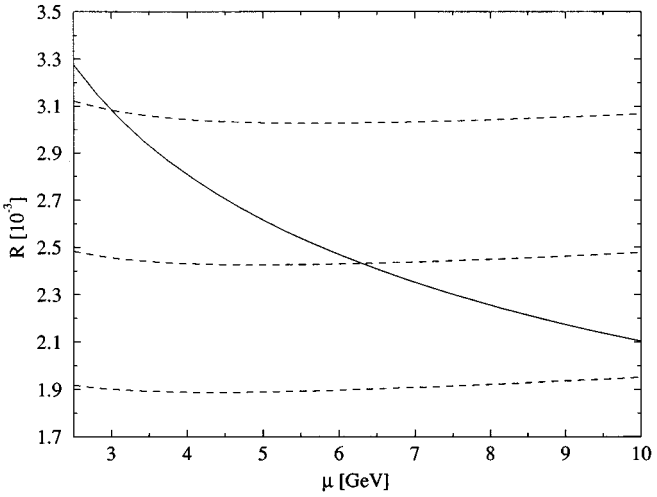

FIG. 20. μ dependence of the theoretical prediction for the ratio R for m_t=170 GeV and $\Lambda_{\overline{\rm MS}}^{(5)}$=225 MeV. The solid line corresponds to the leading-order prediction. The dashed lines describe possible next-to-leading-order results.

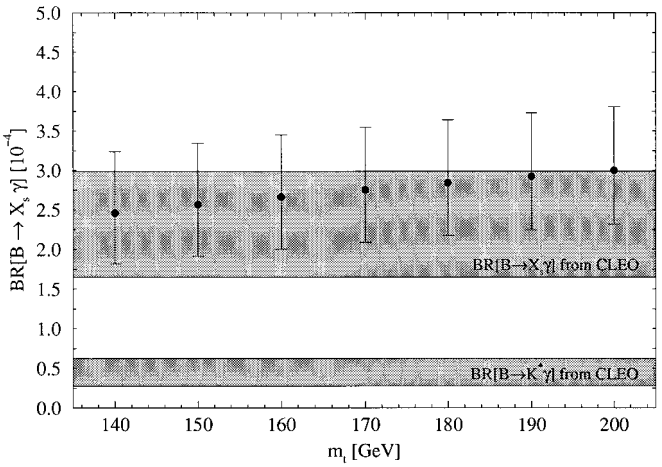

FIG. 21. Predictions for $B\to X_s\gamma$ in the SM as a function of the top-quark mass with the theoretical uncertainties taken into account.

next-to-leading-order effects. For the same reason we do not include the $\mathcal{O}(\alpha_s)$ QCD corrections to the matrix element of the operator $Q_{7\gamma}$ (the QCD bremsstrahlung $b\to s\gamma+g$ and the virtual corrections to $b\to s\gamma$), which are known (Ali and Greub, 1991a, 1991b; Pott, 1995) and will be a part of a future NLO analysis.

Equation (22.5) and the expression [Eq. (9.23)] for $C_{7\gamma}^{(0)\rm eff}(\mu)$ summarize the complete leading logarithmic approximation for the $B\to X_s\gamma$ rate in the standard model. Their important property is that they are exactly the same in many interesting extensions of the standard model, such as the two-Higgs-doublet model (2HDM) (Grinstein *et al.*, 1990; Barger *et al.*, 1993; Hayashi *et al.*, 1993; Hewett, 1993; Buras, Misiak, Münz, and Pokorski, 1994) or the minimal supersymmetric standard model (MSSM) (Bertolini *et al.*, 1991; Barbieri and Giudice, 1993; Borzumati, 1994). The only quantities that change are the coefficients $C_2^{(0)}(M_W)$, $C_{7\gamma}^{(0)}(M_W)$, and $C_{8G}^{(0)}(M_W)$. On the other hand, in a general $\mathrm{SU}(2)_L\times\mathrm{SU}(2)_R\times\mathrm{U}(1)$ model additional modifications are necessary because new operators enter (Cho and Misiak, 1994).

A critical analysis of theoretical and experimental uncertainties present in the prediction for $B(B\to X_s\gamma)$ based on the above formulae has been made (Buras, Misiak, Münz, and Pokorski, 1994). Here we just briefly list the main findings:

(i) First of all, Eq. (22.5) is based on the spectator model. As we have mentioned above, the heavy-quark expansion gives a strong support for this model in inclusive B decays. One can expect the error from using the spectator model in $B\to X_s\gamma$ to amount to at most $\pm10\%$. This number is understood to include the uncertainty due to long-distance contributions. These are dominated by intermediate $c\bar{c}$ resonances coupling to the final state photon and have been estimated to be rather small (Deshpande *et al.*, 1996). However, the calculation of long-distance effects is notoriously difficult, and the question of their impact on $B\to X_s\gamma$ is not yet completely settled at present (Soares, 1996).

(ii) The uncertainty coming from the ratio $z=m_c/m_b$ in the phase-space factor $f(z)$ for the semileptonic decay is estimated to be around 6%.

(iii) The error due to the ratio of the CKM parameters in Eq. (22.5) is small. Assuming unitarity of the 3×3 CKM matrix and imposing the constraints from the CP-violating parameter ε_K and B^0-$\bar{B}^0$ mixing, one finds

$$\frac{|V_{ts}^*V_{tb}|^2}{|V_{cb}|^2}=0.95\pm0.03. \tag{22.7}$$

(iv) There exists an uncertainty due to the determination of α_s. This uncertainty is not small because of the importance of QCD corrections in the considered decay. For instance, the difference between the ratios R of Eq. (22.5) obtained with the help of $\alpha_{\overline{\rm MS}}(M_Z)=0.11$ and 0.13, respectively, is roughly 20%.

(v) The dominant uncertainty in Eq. (22.5) comes from the unknown next-to-leading-order contributions. This uncertainty is best signaled by the strong μ dependence of the leading-order expression [Eq. (22.5)], which is shown by the solid line in Fig. 20, for the case m_t=170 GeV.

(vi) One can see that, when μ is varied by a factor of 2 in both directions around $m_b\simeq5$ GeV, the ratio [Eq. (22.5)] changes by around $\pm25\%$, i.e., the ratios R obtained for μ=2.5 GeV and μ=10 GeV differ by a factor of 1.6 (Ali and Greub, 1993).

(vii) The dashed lines in Fig. 20 show the expected μ dependence of the ratio [Eq. (22.5)] once a complete next-to-leading-order calculation is performed. The μ dependence is then much weaker, but, until one performs the calculation explicitly, one cannot say which of the dashed curves is the proper one. The way the dashed lines are obtained is described by (Buras, Misiak, Münz, and Pokorski, 1994).

(viii) Finally, there exists a $\pm2.4\%$ error in determin-

ing $B(B\to X_s\gamma)$ from Eq. (22.1), which is due to the error in the experimental measurement of $B(B\to X_c e\bar{\nu}_e)=(10.43\pm0.24)\%$ (Particle Data Group, 1994).

(ix) The uncertainty due to the value of m_t is small as is shown explicitly below.

Figure 21, based on the work of Buras, Misiak, Münz, and Pokorski, 1994, presents the standard model prediction for the inclusive $B\to X_s\gamma$ branching ratio including the errors listed above as a function of m_t and with the CLEO result.

We stress that the theoretical curves have been obtained prior to the experimental result. Since the theoretical error is dominated by scale ambiguities, a complete NLO analysis is very desirable.

C. Looking at $B\to X_s\gamma$ beyond leading logarithmic order

In this section we describe briefly a complete next-to-leading-order calculation of $B\to X_s\gamma$ in general terms. This section collects the most important findings of Sec. 4 of Buras, Misiak, Münz, and Pokorski (1994).

Let us first enumerate what has been already calculated in the literature and which calculations are still required in order to complete the next-to-leading-order calculation of $B(B\to X_s\gamma)$.

The present status is as follows,

(i) The 6×6 submatrix of $\gamma^{(1)}$ describing the two-loop mixing of $(Q_1,\ldots,Q_6)$ and the corresponding $\mathcal{O}(\alpha_s)$ corrections in $\vec{C}(M_W)$ have been already calculated. They are given in Sec. VI.

(ii) The two-loop mixing in the $(Q_{7\gamma},Q_{8G})$ sector of $\gamma^{(1)}$ is known (Misiak and Münz, 1995) and given in Sec. IX.C.

(iii) The $\mathcal{O}(\alpha_s)$ corrections to the matrix element of the operators $Q_{7\gamma}$ and Q_{8G} have been calculated (Ali and Greub, 1991a, 1991b). They have been recently confirmed by Pott (1996), who also presents the results for the matrix elements of the remaining operators.

The remaining ingredients of a next-to-leading-order analysis of $B(B\to X_s\gamma)$ are

(i) The three-loop mixing between the sectors $(Q_1,\ldots,Q_6)$ and $(Q_{7\gamma},Q_{8G})$, which, with our normalizations, contributes to $\gamma^{(1)}$.

(ii) The $\mathcal{O}(\alpha_s)$ corrections to $C_{7\gamma}(M_W)$ and $C_{8G}(M_W)$ in Eqs. (9.12) and (9.13). This requires evaluation of two-loop penguin diagrams with internal-W and top-quark masses and a proper matching with the effective five-quark theory. An attempt to calculate the necessary two-loop standard model diagrams has been made by Adel and Yao (1994).

(iii) The finite parts of the effective-theory two-loop diagrams with the insertions of the four-quark operators.

All these calculations are very involved, and the necessary three-loop calculation is a truly formidable task! Yet, as stressed by Buras, Misiak, Münz, and Pokorski (1994), all these calculations have to be done if we want to reduce the theoretical uncertainties in $b\to s\gamma$ to around 10%.

As shown in the above reference, the cancellation of the dominant μ dependence in the leading order can be achieved by calculating the relevant two-loop matrix element of the dominant four-quark operator Q_2. This matrix element is, however, renormalization-scheme dependent and, moreover, mixing with other operators takes place. This scheme dependence can only be canceled by calculating $\gamma^{(1)}$ in the same renormalization scheme. This point has been extensively discussed in this review, and we will not repeat this discussion here. However, it is clear from these remarks that, in order to address the μ dependence and the renormalization-scheme dependence as well as their cancellations, it is necessary to perform a complete next-to-leading-order analysis of $\vec{C}(\mu)$ and of the corresponding matrix elements.

In this context we would like to comment on an analysis of Ciuchini, Franco, Martinelli, Reina, and Silvestrini (1994), in which the known two-loop mixing of $Q_1,\ldots,Q_6$ has been added to the leading-order analysis of $B\to X_s\gamma$. Strong renormalization-scheme dependence of the resulting branching ratio has been found, giving the branching ratio $(1.7\pm0.2)\times10^{-4}$ and $(2.3\pm0.2)\times10^{-4}$ at $\mu=5$ GeV for HV and NDR schemes, respectively. It has also been observed that, whereas in the HV scheme the μ dependence has been weakened, it is still strong in the NDR scheme. In our opinion this partial cancellation of the μ dependence in the HV scheme is rather accidental and has nothing to do with the cancellation of the μ dependence discussed above. The latter requires the evaluation of finite parts in two-loop matrix elements of the four-quark operators $Q_1,\ldots,Q_6$. On the other hand the strong scheme-dependence in the partial NLO analysis presented by Ciuchini, Franco, Martinelli, Reina, and Silvestrini (1994), demonstrates very clearly the need for a full analysis. In view of this discussion we think that the decrease of the branching ratio for $B\to X_s\gamma$ relative to the LO prediction of Ciuchini, Franco, Martinelli, Reina, and Silvestrini (1994), given by $B(B\to X_s\gamma)=(1.9\pm0.2\pm0.5)\times10^{-4}$, is still premature and one should wait until the full NLO analysis has been done.

Our discussion has been restricted to $B(B\to X_s\gamma)$. Also the photon spectrum has been the subject of several papers. We just refer to the most recent articles (Bigi *et al.*, 1994a; Neubert, 1994b; Ali and Greub, 1995; Dikeman *et al.*, 1996; Kapustin *et al.*, 1995; Kapustin and Ligeti, 1995; Pott, 1996), where further references can be found.

XXIII. THE DECAY $B\to X_s e^+e^-$

A. General remarks

The rare decay $B\to X_s e^+e^-$ has been the subject of many theoretical studies in the framework of the standard model and its extensions such as the Two-Higgs-Doublet models and models involving supersymmetry (Hou *et al.*, 1987; Grinstein *et al.*, 1989; Jaus and Wyler, 1990; Ali *et al.*, 1991, 1995; Deshpande *et al.*, 1993; Greub *et al.*, 1995). In particular the strong dependence

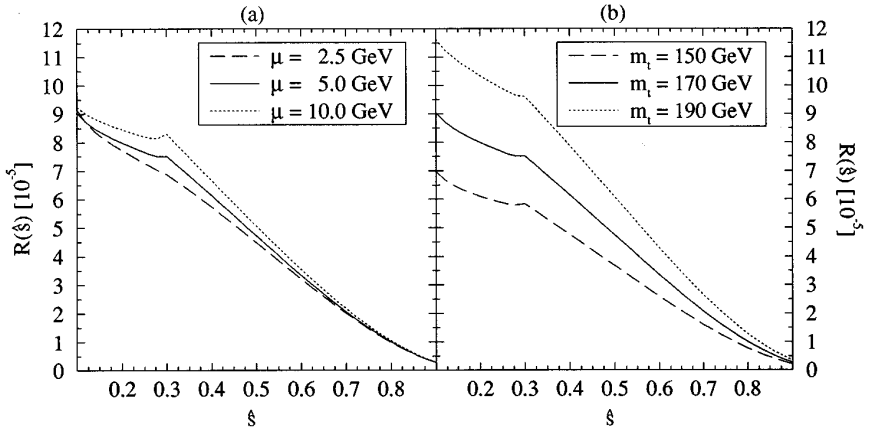

FIG. 22. μ and m_t dependence of $R(\hat{s})$. (a) $R(\hat{s})$ for m_t=170 GeV, $\Lambda^{(5)}_{\overline{\rm MS}}$=225 MeV, and differents values of μ. (b) $R(\hat{s})$ for μ=5 GeV, $\Lambda^{(5)}_{\overline{\rm MS}}$=225 MeV, and various values of m_t.

of $B\to X_s e^+e^-$ on m_t has been stressed by Hou *et al.* (1987). It is clear that, once $B\to X_s e^+e^-$ has been observed, it will offer a useful test of the standard model and its extensions. To this end the relevant branching ratio, the dilepton-invariant mass distribution, and other distributions of interest should be calculated with sufficient precision. In particular the QCD effects should be properly taken into account.

The central element in any analysis of $B\to X_s e^+e^-$ is the effective Hamiltonian for this decay which is given in Sec. X, where a detailed analysis of the Wilson coefficients has been presented. However, the actual calculation of $B\to X_s e^+e^-$ involves not only the evaluation of Wilson coefficients of the relevant local operators but also the calculation of the corresponding matrix elements of these operators relevant for $B\to X_s e^+e^-$. The latter part of the analysis can be done in the spectator model, which, as indicated by the heavy-quark expansion, should offer a good approximation to QCD for B decays. One can also include the nonperturbative $\mathcal{O}(1/m_b^2)$ corrections to the spectator model, which enhance the rate for $B\to X_s e^+e^-$ by roughly 10% (Falk *et al.*, 1994). A realistic phenomenological analysis should also include the long-distance contributions which are mainly due to the J/ψ and ψ' resonances (Deshpande *et al.*, 1989; Lim *et al.*, 1989; O'Donnell and Tung, 1991). Since in this review we are mainly interested in the next-to-leading-order short-distance QCD effects, we will not include these complications in what follows. This section closely follows the work of Buras and Münz (1995), except that the numerical results in Figs. 22–24 have been slightly changed in accordance with the input parameters of the Appendix.

We stress again that, in a consistent NLO analysis of the decay $B\to X_s e^+e^-$, one should calculate the Wilson coefficient of the operator $Q_{9V}=(\bar{s}b)_{V-A}(\bar{e}e)_V$ including leading-order and next-to-leading-order logarithms, but only keep leading-order logarithms in the remaining Wilson coefficients. Only then a scheme-independent amplitude can be obtained. As already discussed in Sec. X, this special treatment of Q_9 is related to the fact that, strictly speaking, in the leading logarithmic approximation only this operator contributes to $B\to X_s e^+e^-$. The contributions of the usual current-current operators, QCD penguin operators, magnetic penguin operators, and $Q_{10A}=(\bar{s}b)_{V-A}(\bar{e}e)_A$ enter only at the NLO level, and to be consistent only the leading contributions to the corresponding Wilson coefficients should be included.

B. The differential decay rate

Introducing

$$\hat{s}=\frac{(p_{e^+}+p_{e^-})^2}{m_b^2},\quad z=\frac{m_c}{m_b}, \tag{23.1}$$

and calculating the one-loop matrix elements of Q_i using the spectator model in the NDR scheme, one finds (Buras and Münz, 1995; Misiak, 1995)

$$\begin{aligned}R(\hat{s})&\equiv\frac{d/d\hat{s}\,\Gamma(b\to s e^+e^-)}{\Gamma(b\to c e\bar{\nu})}\\&=\frac{\alpha^2}{4\pi^2}\left|\frac{V_{ts}}{V_{cb}}\right|^2\frac{(1-\hat{s})^2}{f(z)\kappa(z)}\Bigg[(1+2\hat{s})(|\tilde{C}_9^{\rm eff}|^2\\&\quad+|\tilde{C}_{10}|^2)+4\left(1+\frac{2}{\hat{s}}\right)|C_{7\gamma}^{(0)\rm eff}|^2\\&\quad+12C_{7\gamma}^{(0)\rm eff}{\rm Re}\tilde{C}_9^{\rm eff}\Bigg],\end{aligned} \tag{23.2}$$

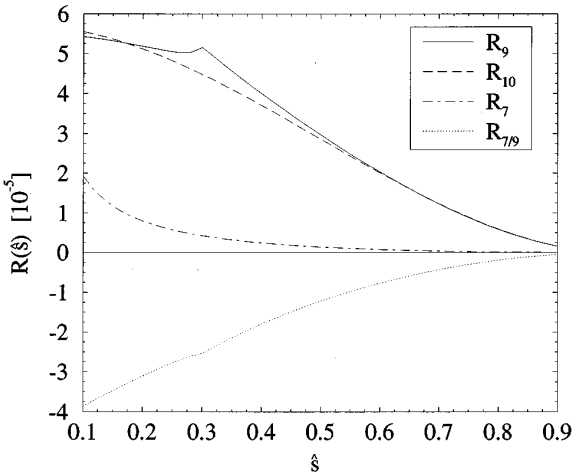

FIG. 23. Comparison of the four different contributions to $R(\hat{s})$ according to Eq. (23.2).

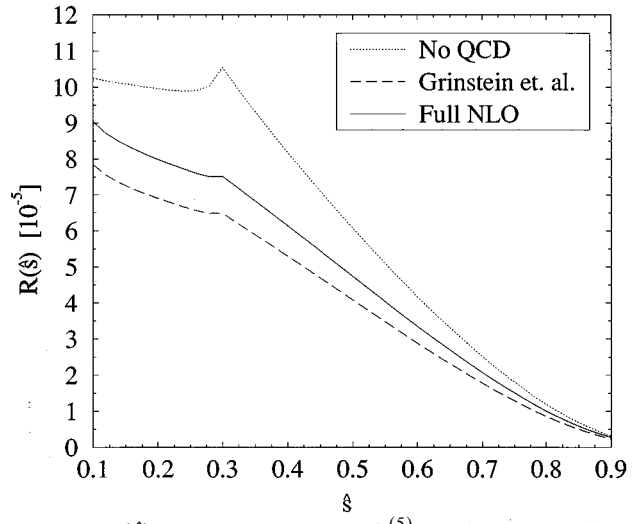

FIG. 24. $R(\hat{s})$ for m_t=170 GeV, $\Lambda^{(5)}_{\overline{\rm MS}}$=225 MeV, and μ=5 GeV.

where

$$\tilde{C}_9^{\rm eff}=\tilde{C}_9^{\rm NDR}\tilde{\eta}(\hat{s})+h(z,\hat{s})(3C_1^{(0)}+C_2^{(0)}+3C_3^{(0)}+C_4^{(0)}+3C_5^{(0)}+C_6^{(0)})-\tfrac{1}{2}h(1,\hat{s})(4C_3^{(0)}+4C_4^{(0)}+3C_5^{(0)}+C_6^{(0)})-\tfrac{1}{2}h(0,\hat{s})(C_3^{(0)}+3C_4^{(0)})+\tfrac{2}{9}(3C_3^{(0)}+C_4^{(0)}+3C_5^{(0)}+C_6^{(0)}). \tag{23.3}$$

Equation (23.2) with $\kappa(z)$=1 was first presented by Grinstein *et al.* (1989), who, in their approximate leading-order renormalization-group analysis, kept only the operators $Q_1,Q_2,Q_{7\gamma},Q_{9V},Q_{10A}$.

The various entries in Eq. (23.2) are given as follows,

$$h(z,\hat{s})=-\frac{8}{9}\ln\frac{m_b}{\mu}-\frac{8}{9}\ln z+\frac{8}{27}+\frac{4}{9}x-\frac{2}{9}(2+x)|1-x|^{1/2}\begin{cases}\left(\ln\left|\dfrac{\sqrt{1-x}+1}{\sqrt{1-x}-1}\right|-i\pi\right) & \text{for } x\equiv 4z^2/\hat{s}<1\\ 2\arctan\dfrac{1}{\sqrt{x-1}}, & \text{for } x\equiv 4z^2/\hat{s}>1,\end{cases} \tag{23.4}$$

$$h(0,\hat{s})=\frac{8}{27}-\frac{8}{9}\ln\frac{m_b}{\mu}-\frac{4}{9}\ln\hat{s}+\frac{4}{9}i\pi, \tag{23.5}$$

$$f(z)=1-8z^2+8z^6-z^8-24z^4\ln z, \tag{23.6}$$

$$\kappa(z)=1-\frac{2\alpha_s(\mu)}{3\pi}\left[\left(\pi^2-\frac{31}{4}\right)(1-z)^2+\frac{3}{2}\right], \tag{23.7}$$

$$\tilde{\eta}(\hat{s})=1+\frac{\alpha_s(\mu)}{\pi}\omega(\hat{s}), \tag{23.8}$$

with

$$\omega(\hat{s})=-\frac{2}{9}\pi^2-\frac{4}{3}\mathrm{Li}_2(s)-\frac{2}{3}\ln s\ln(1-s)-\frac{5+4s}{3(1+2s)}\ln(1-s)-\frac{2s(1+s)(1-2s)}{3(1-s)^2(1+2s)}\ln s+\frac{5+9s-6s^2}{6(1-s)(1+2s)}. \tag{23.9}$$

Here $f(z)$ is the phase-space factor for $b\to ce\bar{\nu}$ and $\kappa(z)$ is the corresponding single-gluon QCD correction (Cabibbo and Maiani, 1978) in the approximation of Kim and Martin (1989). $\tilde{\eta}$, on the other hand, represents single-gluon corrections to the matrix element of Q_9 with m_s=0 (Jezabek and Kühn, 1989; Misiak, 1995). For consistency reasons this correction should only multiply the leading-logarithmic-order term in $\tilde{C}_9^{\rm NDR}$.

In the HV scheme the one-loop matrix elements are different, and one finds an additional explicit contribution to Eq. (23.3) given by (Buras and Münz, 1995)

$$-\xi^{\rm HV}\tfrac{4}{9}(3C_1^{(0)}+C_2^{(0)}-C_3^{(0)}-3C_4^{(0)}). \tag{23.10}$$

However, $\tilde{C}_9^{\rm NDR}$ has to be replaced by $\tilde{C}_9^{\rm HV}$ given in Eqs. (10.5) and (10.9), and consequently $\tilde{C}_9^{\rm eff}$ is the same in both schemes.

The first term in the function $h(z,\hat{s})$ in Eq. (23.4) represents the leading μ dependence in the matrix elements. It is canceled by the μ dependence present in the leading-order logarithm in $\tilde{C}_9$. This is precisely the type of cancellation of the μ dependence that one would like to achieve in the case of $B\to X_s\gamma$. The μ dependence present in the coefficients of the other operators can only be cancelled by going to still higher order in the RG-improved perturbation theory. To this end the matrix elements of four-quark operators should be evaluated at two-loop level. Also, certain unknown three-loop anomalous dimensions should be included in the evaluation of $C_{7\gamma}^{\rm eff}$ and C_{9V}. Certainly this is beyond the scope of this review, and we will only investigate the leftover μ dependence below.

C. Numerical analysis

A detailed numerical analysis of the formulas above has been presented by Buras and Münz (1995). We give here a brief account of this work. We first set $|V_{ts}/V_{cb}|$=1, which, in view of Eq. (22.7), is a good approximation. We keep in mind that, for $\hat{s}\approx m_\psi^2/m_b^2$, $\hat{s}\approx m_{\psi'}^2;2/m_b^2$, etc., the spectator model cannot be the full story and additional long-distance contributions discussed by Deshpande *et al.* (1989), Lim *et al.* (1989), and O'Donnell and Tung (1991) have to be taken into account in a phenomenological analysis. Similarly, we do not include $1/m_b^2$ corrections calculated by Falk *et al.* (1994), which typically enhance the differential rate by about 10%.

In Fig. 22(a) we show $R(\hat{s})$ for m_t=170 GeV, $\Lambda_{\overline{\rm MS}}$ = 225 MeV, and different values of μ. In Fig. 22(b) we set μ=5 GeV and vary m_t from 150 GeV to 190 GeV. The remaining μ dependence is rather weak and

amounts to at most $\pm 8\%$ in the full range of parameters considered. The m_t dependence of $R(\hat{s})$ is sizable. Varying m_t between 150 GeV and 190 GeV changes $R(\hat{s})$ by typically 60–65%, which, in this range of m_t, corresponds to $R(\hat{s}) \sim m_t^2$. It is easy to verify that this strong m_t dependence originates in the coefficient $\tilde{C}_{10}$ given in Eq. (10.3), as already stressed by several authors in the past (Bertolini *et al.*, 1987; Hou *et al.* 1987; Grinstein *et al.*, 1989; Jaus and Wyler, 1990; Ali *et al.*, 1991, 1995; Deshpande *et al.*, 1993; Greub *et al.*, 1995).

We do not show the $\Lambda_{\overline{\rm MS}}$ dependence, as it is very weak. Typically, changing $\Lambda_{\overline{\rm MS}}$ from 140 MeV to 310 MeV decreases $R(\hat{s})$ by about 5%.

$R(\hat{s})$ is governed by three coefficients, $\tilde{C}_9^{\rm eff}$, $\tilde{C}_{10}$, and $C_{7\gamma}^{(0)\rm eff}$. The importance of various contributions has been investigated by Buras and Münz (1995). To this end one sets $\Lambda_{\overline{\rm MS}}^{5}=225$ GeV, $m_t=170$ GeV, and $\mu=5$ GeV. In Fig. 23 we show $R(\hat{s})$, keeping only $\tilde{C}_9^{\rm eff}$, $\tilde{C}_{10}$, $C_{7\gamma}^{(0)\rm eff}$, and the $C_{7\gamma}^{(0)\rm eff}$–$\tilde{C}_9^{\rm eff}$ interference term, respectively. Denoting these contributions by R_9, R_{10}, R_7, and $R_{7/9}$, we observe that the term R_7 plays only a minor role in $R(\hat{s})$. On the other hand, the presence of $C_{7\gamma}^{(0)\rm eff}$ cannot be ignored because the interference term $R_{7/9}$ is significant. In fact the presence of this large interference term could be used to measure experimentally the relative sign of $C_{7\gamma}^{(0)\rm eff}$ and $\mathrm{Re}\tilde{C}_9^{\rm eff}$ (Grinstein *et al.*, 1989; Jaus and Wyler, 1990; Ali *et al.*, 1991, 1995; Greub *et al.*, 1995), which, as seen in Fig. 23, is negative in the standard model. However, the most important contributions are R_9 and R_{10} in the full range of $\hat{s}$ considered. For $m_t \approx 170$ GeV these two contributions are roughly of the same size. Due to a strong m_t dependence of R_{10}, this contribution dominates for higher values of m_t and is less important than R_9 for $m_t<170$ GeV.

Next, in Fig. 24 we show $R(\hat{s})$ for $\mu=5$ GeV, $m_t=170$ GeV, and $\Lambda_{\overline{\rm MS}} = 225$ MeV, compared to the case of no QCD corrections and to the results Grinstein *et al.* (1989) would obtain for our set of parameters using their approximate leading-order formulae.

The discussion of the definition of m_t used here is identical to the one in the case of $K_L \to \pi^0 e^+ e^-$ and will not be repeated here. On the basis of the arguments given there, we believe that if $m_t=\bar{m}_t(m_t)$ is chosen, the additional short-distance QCD corrections to $B(B \to X_s e^+ e^-)$ should be small.

XXIV. THE DECAYS $K^+ \to \pi^+ \nu\bar{\nu}$ AND $K_L \to \pi^0 \nu\bar{\nu}$

A. General remarks on $K^+ \to \pi^+ \nu\bar{\nu}$

The rare decay $K^+ \to \pi^+ \nu\bar{\nu}$ is one of the cleanest decays from a theoretical standpoint. As such it is very well suited for the determination of CKM parameters, in particular of the element V_{td}. $K^+ \to \pi^+ \nu\bar{\nu}$ is CP conserving and receives contributions from both internal top and charm exchanges. The inclusion of next-to-leading-order QCD corrections incorporated in the effective Hamiltonian in Eq. (11.4) and discussed in detail in Sec. XI.B reduces considerably the theoretical uncertainties due to the choice of the renormalization scales present in the leading-order expressions. We will illustrate this below. Since the relevant hadronic matrix element of the weak current $(\bar{s}d)_{V-A}$ can be measured in the leading decay, $K^+ \to \pi^0 e^+ \nu$, the resulting theoretical expression for $B(K^+ \to \pi^+ \nu\bar{\nu})$ is only a function of the CKM parameters, the QCD scale $\Lambda_{\overline{\rm MS}}$, and the quark masses m_t and m_c. The long-distance contributions to $K^+ \to \pi^+ \nu\bar{\nu}$ have been found to be very small—a few percent of the charm contribution to the amplitude at most, which is safely negligible (Hagelin and Littenberg, 1989; Rein and Sehgal, 1989; Lu and Wise, 1994).

TABLE XLIV. The function $P_0(X)$ for various $\Lambda_{\overline{\rm MS}}^{(4)}$ m_c.

	$P_0(X)$		
$\Lambda_{\overline{\rm MS}}^{(4)} \backslash m_c$	1.25 GeV	1.30 GeV	1.35 GeV
215 MeV	0.402	0.436	0.472
325 MeV	0.366	0.400	0.435
435 MeV	0.325	0.359	0.393

Conventionally, the branching fraction $B(K^+ \to \pi^+ \nu\bar{\nu})$ is related to the experimentally well-known quantity $B(K^+ \to \pi^0 e^+ \nu)$ using isospin symmetry. Corrections to this approximation have recently been studied by Marciano and Parsa (1995). The breaking of isospin is due to quark-mass effects and electroweak radiative corrections. In the case of $K^+ \to \pi^+ \nu\bar{\nu}$ these effects result in a decrease of the branching ratio by 10%. The corresponding corrections in $K_L \to \pi^0 \nu\bar{\nu}$ lead to a 5.6% reduction of $B(K_L \to \pi^0 \nu\bar{\nu})$. We have checked the analysis of Marciano and Parsa (1996) and agree with their findings. Once calculated, the inclusion of these effects is straightforward, as they only amount to an overall factor for the branching ratio and do not affect the short-distance structure of $K \to \pi\nu\bar{\nu}$. We shall neglect the isospin-violating corrections in the following chapters, where the focus is primarily on the short-distance physics. The effects are, however, incorporated in the final prediction quoted in the summary table in Sec. XXVII.

In the following we shall concentrate on a discussion of $K^+ \to \pi^+ \nu\bar{\nu}$ within the framework of the standard model. The impact of various scenarios of new physics on this decay has been considered, for instance, by Bigi and Gabbiani (1991).

B. Master formulas for $K^+ \to \pi^+ \nu\bar{\nu}$

Using the effective Hamiltonian [Eq. (11.4)] and summing over the three neutrino flavors, one finds

$$B(K^+ \to \pi^+ \nu\bar{\nu}) = \kappa_+ \left[\left(\frac{\mathrm{Im}\lambda_t}{\lambda^5} X(x_t) \right)^2 + \left(\frac{\mathrm{Re}\lambda_c}{\lambda} P_0(X) + \frac{\mathrm{Re}\lambda_t}{\lambda^5} X(x_t) \right)^2 \right], \tag{24.1}$$

$$\kappa_+ = \frac{3\alpha^2 B(K^+ \to \pi^0 e^+ \nu)}{2\pi^2 \sin^4\Theta_W} \lambda^8 = 4.57 \times 10^{-11}, \tag{24.2}$$

where we have used

$$\alpha=\frac{1}{129},\quad \sin^2\Theta_W=0.23,$$

$$B(K^+\to\pi^0 e^+\nu)=4.82\times10^{-2}. \tag{24.3}$$

Here $\lambda_i = V_{is}^* V_{id}$ with λ_c being real to a very high accuracy. The function X of Eq. (11.5) can also be written as

$$X(x)=\eta_X X_0(x),\quad \eta_X=0.985, \tag{24.4}$$

where η_X summarizes the NLO corrections discussed in Sec. XI.B. With $m_t\equiv\bar m_t(m_t)$ the QCD factor η_X is practically independent of m_t and $\Lambda_{\overline{\rm MS}}$. Next

$$P_0(X)=\frac{1}{\lambda^4}\left[\frac{2}{3}X_{NL}^e+\frac{1}{3}X_{\rm NL}^\tau\right] \tag{24.5}$$

with the numerical values for $X_{\rm NL}^l$ given in Table XXXIII. The corresponding values for $P_0(X)$ as a function of $\Lambda_{\overline{\rm MS}}$ and $m_c\equiv\bar m_c(m_c)$ are collected in Table XLIV. We remark that a negligibly small term $\sim(X_{\rm NL}^e - X_{\rm NL}^\tau)^2$ ($\sim$0.2% effect on the branching ratio) has been discarded in Eq. (24.1).

Using the improved Wolfenstein parametrization and the approximate Eqs. (2.23)–(2.25), we can next write

$$B(K^+\to\pi^+\nu\bar\nu)=4.57\times10^{-11}A^4X^2(x_t)\times\frac{1}{\sigma}[(\sigma\bar\eta)^2+(\varrho_0-\bar\varrho)^2], \tag{24.6}$$

where

$$\sigma=\left(\frac{1}{1-\frac{\lambda^2}{2}}\right)^2. \tag{24.7}$$

The measured value of $B(K^+\to\pi^+\nu\bar\nu)$ then determines an ellipse in the $(\bar\varrho,\bar\eta)$ plane centered at $(\varrho_0,0)$ with (Buras, Lautenbacher, and Ostenmaier, 1994)

$$\varrho_0=1+\frac{P_0(X)}{A^2X(x_t)} \tag{24.8}$$

and having the squared axes

$$\bar\varrho_1^2=r_0^2,\quad \bar\eta_1^2=\left(\frac{r_0}{\sigma}\right)^2, \tag{24.9}$$

where

$$r_0^2=\frac{1}{A^4X^2(x_t)}\left[\frac{\sigma\cdot\mathcal{B}(K^+\to\pi^+\nu\bar\nu)}{4.57\times10^{-11}}\right]. \tag{24.10}$$

The departure of ϱ_0 from unity measures the relative importance of the internal charm contributions.

The ellipse defined by r_0, ϱ_0, and σ given above intersects with the circle [Eq. (2.32)]. This allows one to determine $\bar\varrho$ and $\bar\eta$ with

$$\bar\varrho=\frac{1}{1-\sigma^2}\left(\varrho_0-\sqrt{\sigma^2\varrho_0^2+(1-\sigma^2)(r_0^2-\sigma^2R_b^2)}\right),$$

$$\bar\eta=\sqrt{R_b^2-\bar\varrho^2}, \tag{24.11}$$

and consequently

$$R_t^2=1+R_b^2-2\bar\varrho, \tag{24.12}$$

where $\bar\eta$ is assumed to be positive.

In the leading order of the Wolfenstein parametrization

$$\sigma\to1,\quad \bar\eta\to\eta,\quad \bar\varrho\to\varrho, \tag{24.13}$$

and $B(K^+\to\pi^+\nu\bar\nu)$ determines a circle in the (ϱ,η) plane centered at $(\varrho_0,0)$ and having the radius r_0 of Eq. (24.10) with σ=1. Equations (24.11) and (24.12) then simplify to (Buchalla and Buras, 1994a)

$$R_t^2=1+R_b^2+\frac{r_0^2-R_b^2}{\varrho_0}-\varrho_0,\quad \varrho=\frac{1}{2}\left(\varrho_0+\frac{R_b^2-r_0^2}{\varrho_0}\right). \tag{24.14}$$

Given $\bar\varrho$ and $\bar\eta$ one can determine V_{td}:

$$V_{td}=A\lambda^3(1-\bar\varrho-i\bar\eta),\quad |V_{td}|=A\lambda^3R_t. \tag{24.15}$$

Before proceeding to the numerical analysis a few remarks are in order:

(i) The determination of $|V_{td}|$ and of the unitarity triangle requires the knowledge of V_{cb} (or A) and of $|V_{ub}/V_{cb}|$. Both values are subject to theoretical uncertainties present in the existing analyses of tree-level decays. Whereas the dependence on $|V_{ub}/V_{cb}|$ is rather weak, the very strong dependence of $B(K^+\to\pi^+\nu\bar\nu)$ on A or V_{cb} makes a precise prediction for this branching ratio difficult at present. We will return to this below.

(ii) The dependence of $B(K^+\to\pi^+\nu\bar\nu)$ on m_t is also strong. However m_t should be known by the end of this decade to within $\pm5\%$, and consequently the uncertainty in m_t will soon be less serious for $B(K^+\to\pi^+\nu\bar\nu)$ than the corresponding uncertainty in V_{cb}.

(iii) Once ϱ and η are known precisely from CP asymmetries in B decays, some of the uncertainties present in Eq. (24.6) related to $|V_{ub}/V_{cb}|$ (but not to V_{cb}) will be removed.

(iv) A very clean determination of $\sin2\beta$ without essentially any dependence on m_t and V_{cb} can be made by combining $B(K^+\to\pi^+\nu\bar\nu)$ with $B(K_L\to\pi^0\nu\bar\nu)$ discussed below. We will present an analysis of this type in Sec. XXIV.H.

C. Numerical analysis of $K^+\to\pi^+\nu\bar\nu$

1. Renormalization-scale uncertainties

We will now investigate the uncertainties in $X(x_t)$, $X_{\rm NL}$, $B(K^+\to\pi^+\nu\bar\nu)$, $|V_{td}|$, and in the determination of the unitarity triangle related to the choice of the renormalization scales μ_t and μ_c (see Sec. XI.B). To this end we will fix the remaining parameters as follows:

$$m_c\equiv\bar m_c(m_c)=1.3\ \text{GeV},\quad m_t\equiv\bar m_t(m_t)=170\ \text{GeV}, \tag{24.16}$$

$$V_{cb}=0.040,\quad |V_{ub}/V_{cb}|=0.08. \tag{24.17}$$

In the case of $B(K^+\to\pi^+\nu\bar\nu)$ we need the values of both $\bar\varrho$ and $\bar\eta$. Therefore in this case we will work with

$$\bar{\varrho}=0, \quad \bar{\eta}=0.36, \tag{24.18}$$

rather than with $|V_{ub}/V_{cb}|$. Finally, we will set $\Lambda^{(4)}_{\overline{\rm MS}}=0.325$ GeV and $\Lambda^{(5)}_{\overline{\rm MS}}=0.225$ GeV for the charm part and top part, respectively. We then vary the scales μ_c and μ_t, entering $m_c(\mu_c)$ and $m_t(\mu_t)$ respectively, in the ranges

$$1 \text{ GeV} \leqslant \mu_c \leqslant 3 \text{ GeV}, \quad 100 \text{ GeV} \leqslant \mu_t \leqslant 300 \text{ GeV}. \tag{24.19}$$

In Fig. 25 we show the charm function $X_{\rm NL}$ (for $m_l=0$) compared to the leading-logarithmic-order result X_L and the case without QCD, as functions of μ_c. We observe the following features

(i) The residual slope of $X_{\rm NL}$ is considerably reduced in comparison to X_L, which exhibits a quite substantial dependence on the unphysical scale μ_c. The variation of X [defined as $(X(1\text{ GeV})-X(3\text{ GeV}))/X(m_c)$] is 24.5% in NLLA compared to 56.6% in LLA.

(ii) The suppression of the uncorrected function through QCD effects is somewhat less pronounced in NLLA.

(iii) The next-to-leading-order effects amount to a $\sim$10% correction relative to X_L at $\mu=m_c$. However, the size of this correction strongly depends on μ due to the scale ambiguity of the leading-order result. This means that the question of how large the next-to-leading-order effects are compared to the LLA cannot be answered uniquely. Therefore the relevant result is actually the reduction of the μ dependence in NLLA.

In Fig. 26 we show the analogous results for the top function $X(x_t)$ as a function of μ_t. We observe

(i) Due to $\mu_t \geqslant \mu_c$ the scale dependences in the top function are substantially smaller than in the case of charm. Note in particular how the still appreciable, scale dependence of X_0 gets flattened out almost perfectly when the $\mathcal{O}(\alpha_s)$ effects are taken into account. The total variation of $X(x_t)$ with 100 GeV$\leqslant\mu_t\leqslant$300 GeV is around 1% in NLLA compared to 10% in LLA.

(ii) As already stated following Eq. (24.4), with the choice $\mu_t=m_t$ the NLO correction is very small. It is substantially larger for μ_t very different from m_t. Using Eq. (24.1) and varying $\mu_{c,t}$ in the ranges of Eq. (24.19), we find that, for the above choice of the remaining parameters, the uncertainty in $B(K^+\to\pi^+\nu\bar{\nu})$

$$0.76\times10^{-10} \leqslant B(K^+\to\pi^+\nu\bar{\nu}) \leqslant 1.20\times10^{-10} \tag{24.20}$$

present in the leading order is reduced to

$$0.88\times10^{-10} \leqslant B(K^+\to\pi^+\nu\bar{\nu}) \leqslant 1.02\times10^{-10} \tag{24.21}$$

including NLO corrections. Similarly, we obtain

$$8.24\times10^{-3} \leqslant |V_{td}| \leqslant 10.97\times10^{-3} \quad \text{LLA}, \tag{24.22}$$

$$9.23\times10^{-3} \leqslant |V_{td}| \leqslant 10.10\times10^{-3} \quad \text{NLLA}, \tag{24.23}$$

where we have set $B(K^+\to\pi^+\nu\bar{\nu})=1\times10^{-10}$. We observe that including the full next-to-leading-order corrections reduces the uncertainty in the determination of $|V_{td}|$ from $\pm14\%$ (LLA) to $\pm4.6\%$ (NLLA) in the present example. The main bulk of this theoretical error stems from the charm sector. Indeed, keeping $\mu_c=m_c$ fixed and varying only μ_t, the uncertainties in the determination of $|V_{td}|$ would shrink to $\pm4.7\%$ (LLA) and $\pm0.6\%$ (NLLA). Similar comments apply to $B(K^+\to\pi^+\nu\bar{\nu})$, where, as seen in Eqs. (24.20) and (24.21), the theoretical uncertainty due to $\mu_{c,t}$ is reduced from $\pm22\%$ (LLA) to $\pm7\%$ (NLLA).

Finally, in Fig. 27 we show the position of the point $(\bar{\varrho},\bar{\eta})$ that determines the unitarity triangle. To this end we have fixed all parameters as stated above except for R_b, for which we have chosen three representative numbers, R_b=0.25, 0.36, and 0.47. The full and the reduced ranges represent LLA and NLLA respectively. The impact of the inclusion of NLO corrections on the accuracy of determining the unitarity triangle is clearly visible.

2. Expectations for $B(K^+\to\pi^+\nu\bar{\nu})$

The purely theoretical uncertainties discussed so far should be distinguished from the uncertainties coming from the input parameters such as m_t, V_{cb}, $|V_{ub}/V_{cb}|$, etc. As we will see, the latter uncertainties are still rather large to date. Consequently the progress achieved by the NLO calculations (Buchalla and Buras, 1994a) cannot yet be fully exploited phenomenologically at present. However, the determination of the relevant parameters should improve in the future. Once the precision in the input parameters has attained the desired level, the gain in accuracy of the theoretical prediction for $K^+\to\pi^+\nu\bar{\nu}$ in NLLA by a factor of more than 3 compared to the LLA will become very important.

Using the standard set of input parameters specified in the Appendix and the constraints implied by the analysis of ε_K and B_d-$\bar{B}_d$ mixing as described in Sec. XVIII, we find for the $K^+\to\pi^+\nu\bar{\nu}$ branching fraction the range

$$0.6\times10^{-10} \leqslant B(K^+\to\pi^+\nu\bar{\nu}) \leqslant 1.5\times10^{-10}. \tag{24.24}$$

Equation (24.24) represents the current Standard-Model expectation for $B(K^+\to\pi^+\nu\bar{\nu})$ (neglecting small isospin-breaking corrections). To obtain this estimate we have allowed for a variation of the parameters m_t, $|V_{cb}|$, $|V_{ub}/V_{cb}|$, B_K, $F_B^2B_B$, and x_d within their uncertainties, as summarized in the Appendix. The uncertainties in m_c and $\Lambda_{\overline{\rm MS}}$, on the other hand, are small in comparison and have been neglected in this context. The above range would be reduced to

$$0.8\times10^{-10} \leqslant B(K^+\to\pi^+\nu\bar{\nu}) \leqslant 1.0\times10^{-10} \tag{24.25}$$

if the uncertainties in the input parameters could be decreased as assumed by the "future" scenario in the Appendix.

It should be remarked that the x_d constraint, excluding a part of the second quadrant for the CKM phase δ, plays an essential role in obtaining the upper bounds given above, without essentially any effect on the lower bounds. Without the x_d constraint the upper bounds in Eqs. (24.24) and (24.25) are relaxed to 2.3×10^{-10} and 1.6×10^{-10}, respectively.

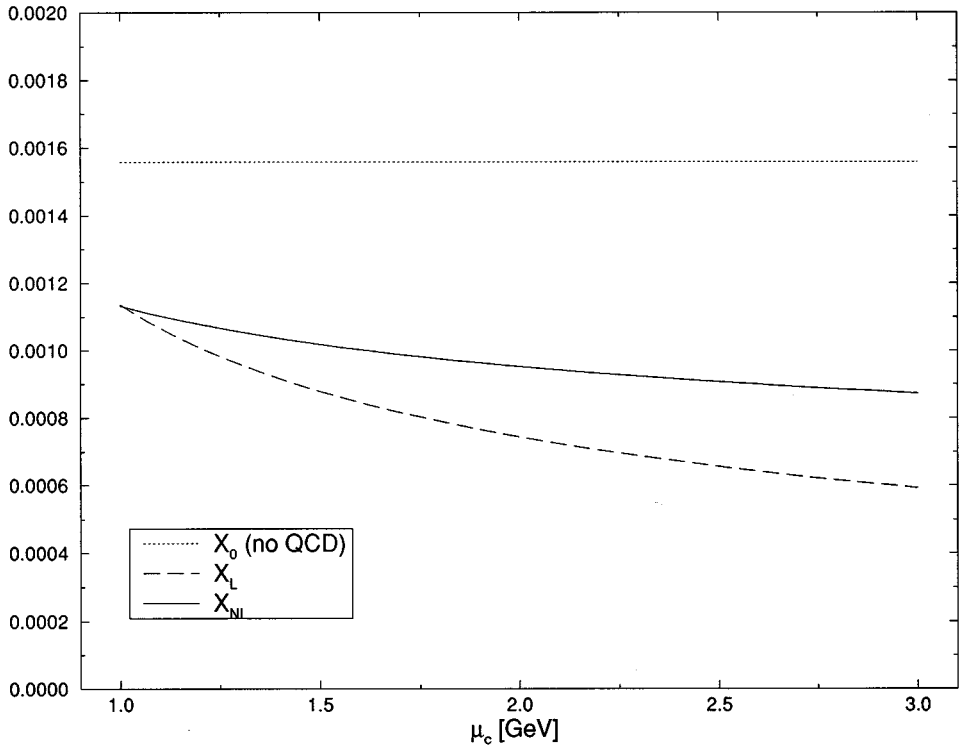

FIG. 25. Charm-quark function X_{NL} (for m_l=0), compared to the leading-logarithmic-order result X_L and the case without QCD, as functions of μ_c.

D. General remarks on $K_L \to \pi^0 \theta \bar{\nu}$

The rare decay $K_L \to \pi^0 \nu \bar{\nu}$ is even cleaner than $K^+ \to \pi^+ \nu \bar{\nu}$. It proceeds almost entirely through direct CP violation (Littenberg, 1989a) and is completely dominated by short-distance loop diagrams with top-quark exchanges. In fact the m_t dependence of $B(K_L \to \pi^0 \nu \bar{\nu})$ is again described by $X(x_t)$. Since the charm contribution can be fully neglected, the theoretical uncertainties present in $K^+ \to \pi^+ \nu \bar{\nu}$ due to m_c,

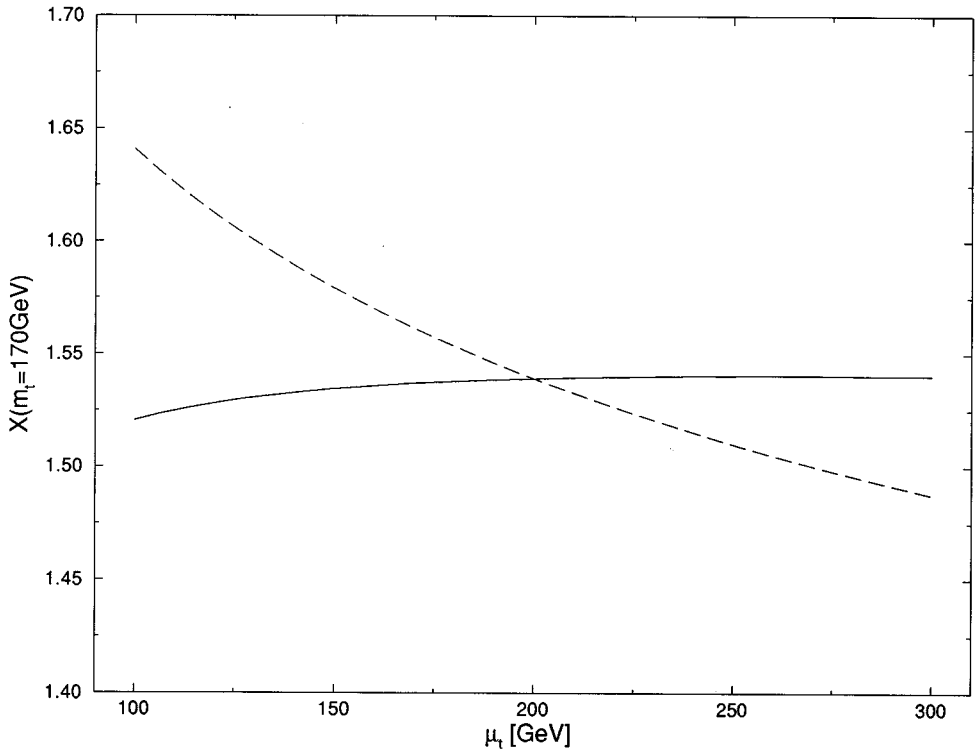

FIG. 26. Top-quark function $X(x_t)$ as a function of μ_t for fixed m_t=170 GeV with (solid curve) and without (dashed curve) $\mathcal{O}(\alpha_s)$ corrections.

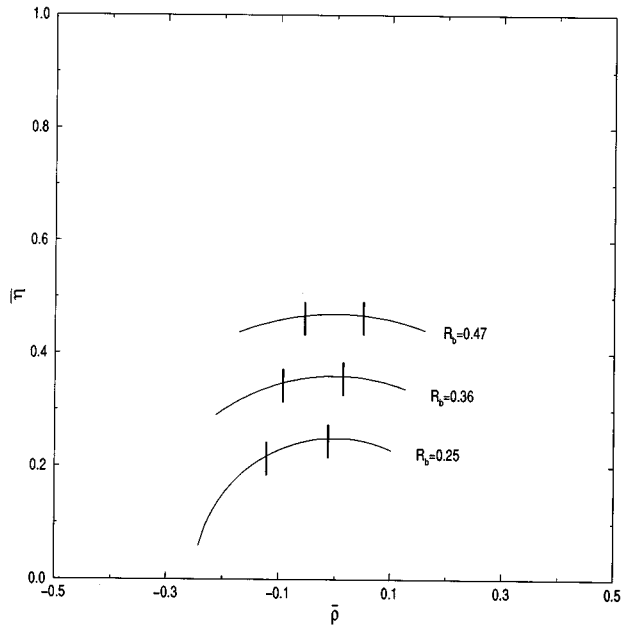

FIG. 27. The theoretical uncertainties in the determination of the unitarity triangle (UT) in the $(\bar{\varrho},\bar{\eta})$ plane from $B(K^+\to\pi^+\nu\bar{\nu})$. With fixed input parameters the vertex of the UT has to lie on a circle around the origin with radius R_b. A variation of the scales μ_c, μ_t within 1 GeV$\leqslant\mu_c\leqslant$3 GeV and 100 GeV$\leqslant\mu_t\leqslant$300 GeV then yields the indicated ranges in LLA (full) and NLLA (reduced). We show the cases R_b=0.25, 0.36, and 0.47.

μ_c, and $\Lambda_{\overline{\rm MS}}$ are absent here. For this reason $K_L\to\pi^0\nu\bar{\nu}$ is very well suited for the determination of CKM parameters, in particular the Wolfenstein parameter η.

E. Master formulas for $K_L\to\pi^0\nu\bar{\nu}$

Using the effective Hamiltonian [Eq. (11.56)] and summing over three neutrino flavors, one finds

$$B(K_L\to\pi^0\nu\bar{\nu})=\kappa_L\left(\frac{\mathrm{Im}\lambda_t}{\lambda^5}X(x_t)\right)^2, \tag{24.26}$$

$$\kappa_L=\kappa_+\frac{\tau(K_L)}{\tau(K^+)}=1.91\times10^{-10} \tag{24.27}$$

with κ_+ given in Eq. (24.2). Using the Wolfenstein parametrization, we can rewrite Eq. (24.26) as

$$B(K_L\to\pi^0\nu\bar{\nu})=1.91\times10^{-10}\eta^2A^4X^2(x_t) \tag{24.28}$$

or

$$B(K_L\to\pi^0\nu\bar{\nu})=3.48\times10^{-5}\eta^2|V_{cb}|^4X^2(x_t). \tag{24.29}$$

A few remarks are in order:

(i) The determination of η using $B(K_L\to\pi^0\nu\bar{\nu})$ requires the knowledge of V_{cb} and m_t. The very strong dependence on V_{cb} or A makes a precise prediction for this branching ratio difficult at present.

(ii) It has been pointed out (Buras, 1994) that the strong dependence of $B(K_L\to\pi^0\nu\bar{\nu})$ on V_{cb}, together with the clean nature of this decay, can be used to determine this element without any hadronic uncertainties. To this end η and m_t have to be known with sufficient precision in addition to $B(K_L\to\pi^0\nu\bar{\nu})$. η should be measured accurately in CP asymmetries in B decays and the value of m_t known to better than ±5 GeV from TEVATRON and future LHC experiments. Inverting Eq. (24.29) and using a very accurate approximation for $X(x_t)$ [valid for $m_t=\bar{m}_t(m_t)$], as given by Eqs. (24.4) and (14.6),

$$X(x_t)=0.65x_t^{0.575}, \tag{24.30}$$

one finds

$$V_{cb}=39.3\times10^{-3}\sqrt{0.39/\eta}\left[\frac{170\ \mathrm{GeV}}{m_t}\right]^{0.575}\times\left[\frac{B(K_L\to\pi^0\nu\bar{\nu})}{3\times10^{-11}}\right]^{1/4}. \tag{24.31}$$

We note that the weak dependence of V_{cb} on $B(K_L\to\pi^0\nu\bar{\nu})$ allows one to achieve a high precision for this CKM element even when $B(K_L\to\pi^0\nu\bar{\nu})$ is known with only relatively moderate accuracy, e.g., 10–15%. Needless to say, any measurement of $B(K_L\to\pi^0\nu\bar{\nu})$ is extremely challenging. A numerical analysis of Eq. (24.31) can be found in the work of Buras (1994).

F. Numerical analysis of $K_L\to\pi^0\nu\bar{\nu}$

1. Renormalization-scale uncertainties

The scale ambiguities present in the function $X(x_t)$ have already been discussed in connection with $K^+\to\pi^+\nu\bar{\nu}$. After the inclusion of NLO corrections they are so small that they can be neglected for all practical purposes. Effectively they could also be taken into account by introducing an additional error $\Delta m_t\leqslant\pm1$ GeV. At the level of $B(K_L\to\pi^0\nu\bar{\nu})$ the ambiguity in the choice of μ_t is reduced from $\pm10\%$ (LLA) down to $\pm1\%$ (NLLA), which considerably increases the predictive power of the theory. Varying μ_t according to Eq. (24.19) and using the input parameters of Sec. XXIV.C, we find that the uncertainty in $B(K_L\to\pi^0\nu\bar{\nu})$

$$2.68\times10^{-11}\leqslant B(K_L\to\pi^0\nu\bar{\nu})\leqslant3.26\times10^{-11} \tag{24.32}$$

present in the leading order is reduced to

$$2.80\times10^{-11}\leqslant B(K_L\to\pi^0\nu\bar{\nu})\leqslant2.88\times10^{-11} \tag{24.33}$$

after including NLO corrections. This means that the theoretical uncertainty in the determination of η amounts to only $\pm0.7\%$ in NLLA, which is safely negligible. The reduction of the scale ambiguity for $B(K_L\to\pi^0\nu\bar{\nu})$ is further illustrated in Fig. 28.

2. Expectations for $B(K_L\to\pi^0\nu\bar{\nu})$

From an analysis of $B(K_L\to\pi^0\nu\bar{\nu})$ similar to the one described for $K^+\to\pi^+\nu\bar{\nu}$ in Sec. XXIV.C.2, we obtain the standard-model expectation

$$1.1\times10^{-10}\leqslant B(K_L\to\pi^0\nu\bar{\nu})\leqslant5.0\times10^{-11}, \tag{24.34}$$

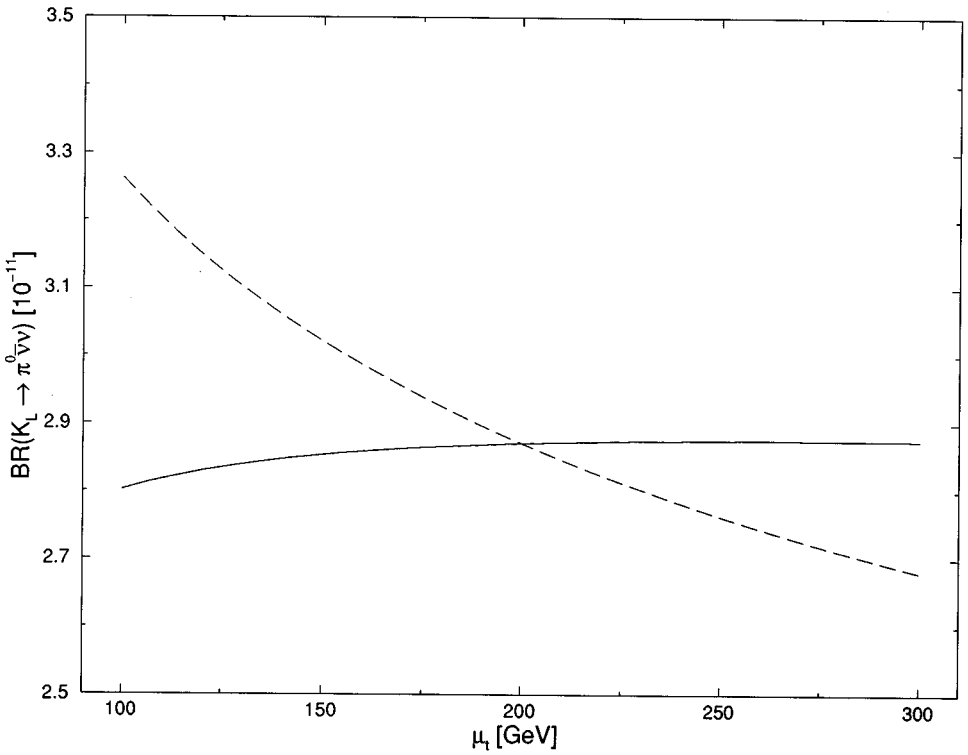

FIG. 28. The μ_t dependence of $B(K_L\to\pi^0\nu\bar{\nu})/10^{-11}$ with (solid curve) and without (dashed curve) $\mathcal{O}(\alpha_s)$ corrections for m_t=170 GeV, $|V_{cb}|$=0.04, and $\bar{\eta}$=0.36.

corresponding to present-day errors in the relevant input parameters. This would change to

$$2.2\times10^{-11}\leqslant B(K_L\to\pi^0\nu\bar{\nu})\leqslant 3.6\times10^{-11} \tag{24.35}$$

if the parameter uncertainties would decrease as anticipated by the "future" scenario defined in the Appendix.

G. Unitarity triangle from $K\to\pi\nu\bar{\nu}$

The measurement of $B(K^+\to\pi^+\nu\bar{\nu})$ and $B(K_L\to\pi^0\nu\bar{\nu})$ can determine the unitarity triangle completely, provided m_t and V_{cb} are known. Using these two branching ratios simultaneously allows one to eliminate $|V_{ub}/V_{cb}|$ from the analysis, which removes considerable uncertainty. Indeed it is evident from Eqs. (24.1) and (24.26) that, given $B(K^+\to\pi^+\nu\bar{\nu})$ and $B(K_L\to\pi^0\nu\bar{\nu})$, one can extract both $\mathrm{Im}\lambda_t$, and $\mathrm{Re}\lambda_t$. We get

$$\mathrm{Im}\lambda_t=\lambda^5\frac{\sqrt{B_2}}{X(x_t)}, \tag{24.36}$$

$$\mathrm{Re}\lambda_t=-\lambda^5\frac{(\mathrm{Re}\,\lambda_c/\lambda)P_0(X)+\sqrt{B_1-B_2}}{X(x_t)},$$

where we have defined the "reduced" branching ratios

$$B_1=\frac{B(K^+\to\pi^+\nu\bar{\nu})}{4.57\times10^{-11}},\quad B_2=\frac{B(K_L\to\pi^0\nu\bar{\nu})}{1.91\times10^{-10}}. \tag{24.37}$$

Using the expressions for $\mathrm{Im}\lambda_t$, $\mathrm{Re}\lambda_t$, and $\mathrm{Re}\lambda_c$ given in Eqs. (2.23)–(2.25), we find

$$\bar{\varrho}=1+\frac{P_0(X)-\sqrt{\sigma(B_1-B_2)}}{A^2X(x_t)},\quad \bar{\eta}=\frac{\sqrt{B_2}}{\sqrt{\sigma}A^2X(x_t)} \tag{24.38}$$

with σ defined in Eq. (24.7). An exact treatment of the CKM matrix shows that the formulas [Eq. (24.38)] are rather precise (Buchalla and Buras, 1994c). The error in $\bar{\eta}$ is below 0.1%, and $\bar{\varrho}$ may deviate from the exact expression by at most $\Delta\bar{\varrho}$=0.02 with essentially negligible error for $0\leqslant\bar{\varrho}\leqslant0.25$.

As an illustrative example, let us consider the following scenario. We assume that the branching ratios are known to within ±10%

$$B(K^+\to\pi^+\nu\bar{\nu})=(1.0\pm0.1)\times10^{-10},$$
$$B(K_L\to\pi^0\nu\bar{\nu})=(2.5\pm0.25)\times10^{-11}. \tag{24.39}$$

Next we take $[m_i\equiv\bar{m}_i(m_i)]$

$$m_t=(170\pm5)\ \text{GeV},\quad m_c=(1.30\pm0.05)\ \text{GeV},$$
$$V_{cb}=0.040\pm0.001, \tag{24.40}$$

where the quoted errors are quite reasonable if one keeps in mind that it will take at least ten years to achieve the accuracy assumed in Eq. (24.39). Finally, we use

$$\Lambda^{(4)}_{\overline{\mathrm{MS}}}=(200\text{–}350)\ \text{MeV},\quad \mu_c=(1\text{–}3)\ \text{GeV}, \tag{24.41}$$

where μ_c is the renormalization scale present in the analysis of the charm contribution. Its variation gives an

TABLE XLV. $\bar{\eta}$, $|V_{td}|$, and $\bar{\varrho}$ determined from $K^+\to\pi^+\nu\bar{\nu}$ and $K_L\to\pi^0\nu\bar{\nu}$ for the scenario described in the text and the uncertainties related to various parameters.

		Δ(BR)	$\Delta(m_t,V_{cb})$	$\Delta(m_c,\Lambda^{(4)}_{\overline{\rm MS}})$	$\Delta(\mu_c)$	$\Delta_{\rm total}$
$\bar{\eta}$	0.33	±0.02	±0.03	±0.00	±0.00	±0.05
$\lvert V_{td}\rvert/10^{-3}$	9.3	±0.6	±0.6	±0.5	±0.4	±2.1
$\bar{\varrho}$	0.00	±0.08	±0.09	±0.06	±0.04	±0.27

indication of the theoretical uncertainty involved in the calculation. In comparison to this error we neglect the effect of varying $\mu_W=\mathcal{O}(M_W)$, the high-energy matching scale at which the W boson is integrated out, as well as the very small scale dependence of the top-quark contribution. As reference parameters we use the central values in Eqs. (24.39) and (24.40) and $\Lambda^{(4)}_{\overline{\rm MS}}=300$ MeV and $\mu_c=m_c$. The results that would be obtained in such a scenario for $\bar{\eta}$, $|V_{td}|$, and $\bar{\varrho}$ are collected in Table XLV.

There we have also displayed separately the associated symmetrized errors (Δ) coming from the uncertainties in the branching ratios, m_t and V_{cb}, m_c and $\Lambda^{(4)}_{\overline{\rm MS}}$, and μ_c, as well as the total uncertainty.

We observe that respectable determinations of $\bar{\eta}$ and $|V_{td}|$ can be obtained. On the other hand, the determination of $\bar{\varrho}$ is rather poor. We also note that a sizable part of the total uncertainty results in each case from the strong dependence of both branching ratios on m_t and V_{cb}. There is, however, one important quantity for which the strong dependence of $B(K^+\to\pi^+\nu\bar{\nu})$ and $B(K_L\to\pi^0\nu\bar{\nu})$ on m_t and V_{cb} does not matter at all.

H. sin 2β from $K\to\pi\nu\bar{\nu}$

Using Eq. (24.38), one finds (Buchalla and Buras, 1994c)

$$r_s=r_s(B_1,B_2)\equiv\frac{1-\bar{\varrho}}{\bar{\eta}}=\cot\beta,\quad \sin2\beta=\frac{2r_s}{1+r_s^2} \tag{24.42}$$

with

$$r_s(B_1,B_2)=\sqrt{\sigma}\,\frac{\sqrt{\sigma(B_1-B_2)}-P_0(X)}{\sqrt{B_2}}. \tag{24.43}$$

Thus, within the approximation of Eq. (24.38), $\sin2\beta$ is independent of V_{cb} (or A) and m_t. An exact treatment of the CKM matrix confirms this finding to a high accuracy. The dependence on V_{cb} and m_t enters only at order $\mathcal{O}(\lambda^2)$, and, as a numerical analysis shows, this dependence can be fully neglected.

It should be stressed that $\sin2\beta$ determined this way depends only on two measurable branching ratios and on the function $P_0(X)$, which is completely calculable in perturbation theory. Consequently, this determination is free from any hadronic uncertainties, and its accuracy can be estimated with a high degree of confidence. To this end we use the input given in Eqs. (24.39)–(24.41) to find

$$\sin2\beta=0.60\pm0.06\pm0.03\pm0.02, \tag{24.44}$$

where the first error comes from $B(K^+\to\pi^+\nu\bar{\nu})$ and $B(K_L\to\pi^0\nu\bar{\nu})$, the second from m_c and $\Lambda_{\overline{\rm MS}}$, and the last one from the uncertainty due to μ_c. We note that the largest partial uncertainty results from the branching ratios themselves. It can probably be reduced with time, as is the case with the ±0.03 uncertainty related to $\Lambda_{\overline{\rm MS}}$ and m_c. Note that the theoretical uncertainty represented by $\Delta(\mu_c)$, which ultimately limits the accuracy of the analysis, is small. This reflects the clean nature of the $K\to\pi\nu\bar{\nu}$ decays. However, the small uncertainty of ±0.02 is only achieved by including next-to-leading-order QCD corrections. In the leading logarithmic approximation the corresponding error would amount to ±0.05, larger than the one coming from m_c and $\Lambda_{\overline{\rm MS}}$.

The accuracy to which $\sin2\beta$ can be obtained from $K\to\pi\nu\bar{\nu}$ is, in this example, comparable to the one expected in determining $\sin2\beta$ from CP asymmetries in B decays prior to LHC experiments. In this case $\sin2\beta$ is determined best by measuring the time-integrated CP violating asymmetry in $B^0_d\to\psi K_S$, which is given by

$$A_{CP}(\psi K_S)=\frac{\int_0^\infty[\Gamma(B\to\psi K_S)-\Gamma(\bar{B}\to\psi K_S)]dt}{\int_0^\infty[\Gamma(B-\psi K_S)+\Gamma(\bar{B}\to\psi K_S)]dt}$$

$$=-\sin2\beta\,\frac{x_d}{1+x_d^2}, \tag{24.45}$$

where $x_d=\Delta m/\Gamma$ gives the size of B^0_d-$\bar{B}^0_d$ mixing. Combining Eqs. (24.42) and (24.45), we obtain an interesting connection between rare K decays and B physics

$$\frac{2r_s(B_1,B_2)}{1+r_s^2(B_1,B_2)}=-A_{CP}(\psi K_S)\,\frac{1+x_d^2}{x_d}, \tag{24.46}$$

which must be satisfied in the standard model. We stress that, except for $P_0(X)$ given in Table XLIV, all quantities in Eq. (24.46) can be directly measured in experiment and this relationship is essentially independent of m_t and V_{cb}.

XXV. THE DECAYS $K_L\to\mu^+\mu^-$ AND $K^+\to\pi^+\mu^+\mu^-$

A. General remarks on $K_L\to\mu^+\mu^-$

The rare decay $K_L\to\mu^+\mu^-$ is CP conserving, and, in addition to its short-distance part, receives important contributions from the two-photon intermediate state, which is difficult to calculate reliably (Geng and Ng, 1990; Bélanger and Geng, 1991; Ko, 1992).

This latter fact is rather unfortunate because the short-distance part is, similar to $K^+\to\pi^+\nu\bar{\nu}$, free of hadronic uncertainties and, if extracted from the data, would give a useful determination of the Wolfenstein parameter ϱ. The separation of the short-distance from the long-distance piece in the measured rate is very difficult, however.

In spite of all this we will present the analysis of the short-distance contribution. On one hand it may turn out to be useful one day for $K_L\to\mu^+\mu^-$, and additionally it also plays an important role in a parity-violating asymmetry, which can be measured in $K^+\to\pi^+\mu^+\mu^-$. We will discuss this latter topic later on in this section.

The analysis of $(K_L\to\mu^+\mu^-)_{\rm SD}$ proceeds in essentially the same manner as for $K^+\to\pi^+\nu\bar{\nu}$. The only difference enters through the lepton line in the box contribution. This change introduces two new functions $Y_{\rm NL}$ and $Y(x_t)$ for the charm and top contributions, respectively (Sec. XI.C), which will be discussed in detail below.

B. Master formulas for $(K_L\to\mu^+\mu^-)_{\rm SD}$

Using the effective Hamiltonian of Eq. (11.44) and relating $\langle 0|(\bar{s}d)V_{-A}|K_L\rangle$ to $B(K^+\to\mu^+\nu)$, we find

$$B(K_L\to\mu^+\mu^-)_{\rm SD}=\kappa_\mu\left[\frac{{\rm Re}\lambda_c}{\lambda}P_0(Y)+\frac{{\rm Re}\lambda_t}{\lambda^5}Y(x_t)\right]^2, \tag{25.1}$$

$$\kappa_\mu=\frac{\alpha^2 B(K^+\to\mu^+\nu)}{\pi^2\sin^4\Theta_W}\frac{\tau(K_L)}{\tau(K^+)}\lambda^8=1.68\times10^{-9}, \tag{25.2}$$

where we have used

$$\alpha=\frac{1}{129},\quad \sin^2\Theta_W=0.23,\quad B(K^+\to\mu^+\nu)=0.635. \tag{25.3}$$

The function $Y(x)$ of Eq. (11.45) can also be written as

$$Y(x)=\eta_Y Y_0(x),\quad \eta_Y=1.026\pm0.006, \tag{25.4}$$

where η_Y summarizes the NLO corrections discussed in Sec. XI.C. With $m_t\equiv\bar{m}_t(m_t)$ this QCD factor depends only very weakly on m_t. The range in Eq. (25.4) corresponds to 150 GeV$\leq m_t\leq$190 GeV. The dependence on $\Lambda_{\overline{\rm MS}}$ can be neglected. Next

$$P_0(Y)=\frac{Y_{\rm NL}}{\lambda^4} \tag{25.5}$$

with $Y_{\rm NL}$ calculated in Sec. XI.C. Values for $P_0(Y)$ as a function of $\Lambda_{\overline{\rm MS}}$ and $m_c\equiv\bar{m}_c(m_c)$ are collected in Table XLVI.

Using the improved Wolfenstein parametrization and the approximate formulas of Eqs. (2.23)–(2.25), we can next write

$$B(K_L\to\mu^+\mu^-)_{\rm SD}=1.68\times10^{-9}A^4Y^2(x_t)\frac{1}{\sigma}(\bar{\varrho}_0-\bar{\varrho})^2 \tag{25.6}$$

with

$$\bar{\varrho}_0=1+\frac{P_0(Y)}{A^2Y(x_t)},\quad \sigma=\left(\frac{1}{1-\frac{\lambda^2}{2}}\right)^2. \tag{25.7}$$

The "experimental" value of $B(K_L\to\mu^+\mu^-)_{\rm SD}$ determines the value of $\bar{\varrho}$ given by

$$\bar{\varrho}=\bar{\varrho}_0-\bar{r}_0,\quad \bar{r}_0^2=\frac{1}{A^4Y^2(x_t)}\left[\frac{\sigma B(K_L\to\mu^+\mu^-)_{\rm SD}}{1.68\times10^{-9}}\right]. \tag{25.8}$$

Similar to r_0 in the case of $K^+\to\pi^+\nu\bar{\nu}$, the value of $\bar{r}_0$ is fully determined by the top contribution, which has only a very weak renormalization-scale ambiguity after the inclusion of $\mathcal{O}(\alpha_s)$ corrections. The main scale ambiguity resides in $\bar{\varrho}_0$, whose departure from unity measures the relative importance of the charm contribution.

C. Numerical analysis of $(K_L\to\mu^+\mu^-)_{\rm SD}$

1. Renormalization-scale uncertainties

We will now investigate the uncertainties in $Y(x_t)$, $Y_{\rm NL}$, $B(K_L\to\mu^+\mu^-)_{\rm SD}$, and $\bar{\varrho}$ related to the dependence of these quantities on the choice of the renormalization scales μ_t and μ_c. To this end we proceed as in Sec. XXIV.C.1. We fix all the remaining parameters as given in Eqs. (24.16) and (24.17), and we vary μ_c and μ_t within the ranges stated in Eq. (24.19).

Figure 29 shows the charm function $Y_{\rm NL}$ compared to the leading-logarithmic-order result Y_L and the case without QCD as a function of μ_c. We note the following points,

(i) The residual slope of $Y_{\rm NL}$ is considerably smaller than in Y_L, although it is still sizable. The variation of Y with μ defined as $[Y(1\ {\rm GeV})-Y(3\ {\rm GeV})]/Y(m_c)$ is 53% in NLLA compared to 92% in LLA.

(ii) There is a strong enhancement of Y_0 through QCD corrections, in contrast to the suppression found in the case of X_0.

In Fig. 30 we show the analogous results for $Y(x_t)$ as a function of μ_t. The observed features are similar to the ones found in the case of $X(x_t)$:

(i) Considerable reduction of the scale uncertainties in NLLA relative to the LLA with a tiny residual uncertainty after the inclusion of NLO corrections.

(ii) Small NLO correction for the choice $\mu_t=m_t$ as summarized by η_Y in Eq. (25.4). Using Eq. (25.1) and varying $\mu_{c,t}$ in the ranges of Eq. (24.19), we find that, for this choice of input parameters, the uncertainty in $B(K_L\to\mu^+\mu^-)_{\rm SD}$

$$0.816\times10^{-9}\leq B(K_L\to\mu^+\mu^-)_{\rm SD}\leq1.33\times10^{-9} \tag{25.9}$$

present in the leading order is reduced to

$$1.02\times10^{-9}\leq B(K_L\to\mu^+\mu^-)_{\rm SD}\leq1.25\times10^{-9} \tag{25.10}$$

after including NLO corrections. Here we have assumed $\bar{\varrho}=0$.

Similarly, we find

$$-0.117\leq\bar{\varrho}\leq0.165\quad {\rm LLA}, \tag{25.11}$$

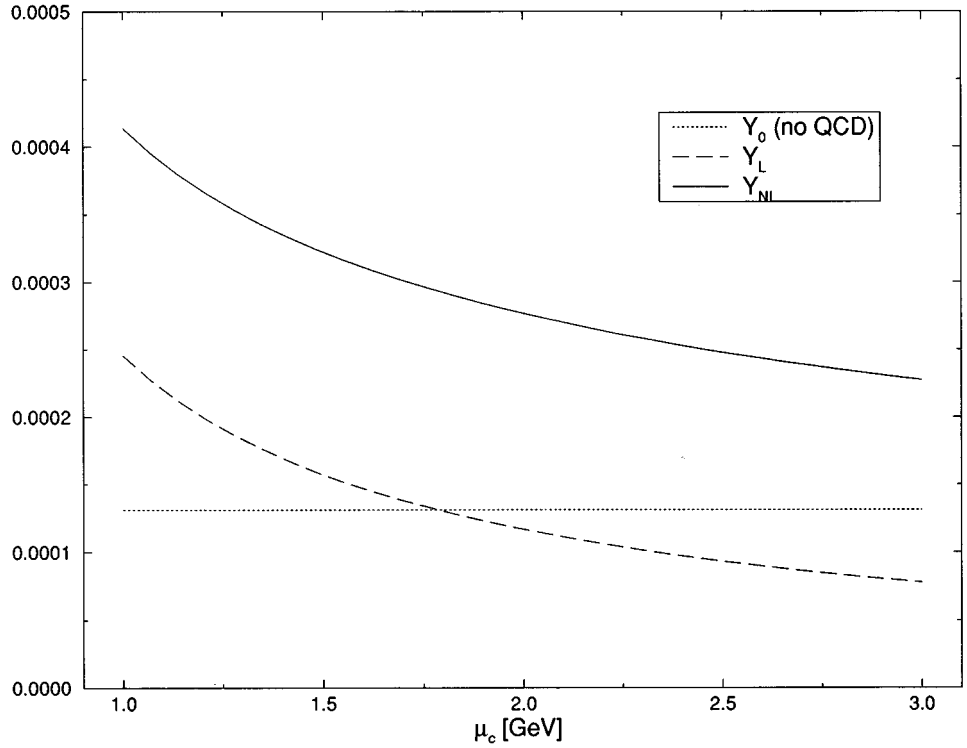

FIG. 29. Charm-quark function $Y_{\rm NL}$, compared to the leading-log result Y_L and the case without QCD, as functions of μ_c.

$$0.011 \leqslant \bar{\varrho} \leqslant 0.134 \quad \text{NLLA}, \tag{25.12}$$

where we have set $B(K_L \to \mu^+\mu^-)_{\rm SD}=1\times10^{-9}$. We observe again a considerable reduction of the theoretical error when the NLO effects are included in the analyses. Also, in this case the remaining ambiguity is largely dominated by the uncertainty in the charm sector.

2. Expectations for $B(K_L \to \mu^+\mu^-)_{\rm SD}$

We finally quote the standard-model expectation for the short-distance contribution to the $K_L \to \mu^+\mu^-$ branching ratio. Using the analysis of ε_K and the constraint implied by B_d-$\bar{B}_d$ mixing in analogy to the case of $K^+ \to \pi^+ \nu\bar{\nu}$ described in Sec. XXIV.C.2, we find

$$0.6\times10^{-9} \leqslant B(K_L \to \mu^+\mu^-)_{\rm SD} \leqslant 2.0\times10^{-9} \tag{25.13}$$

and

$$0.9\times10^{-9} \leqslant B(K_L \to \mu^+\mu^-)_{\rm SD} \leqslant 1.2\times10^{-9} \tag{25.14}$$

for present parameter uncertainties and the "future" scenario, respectively. The relevant sets of input parameters and their errors are collected in the Appendix. Removing the x_d constraint would increase the upper bounds in Eqs. (25.13) and (25.14) to 3.5×10^{-9} and 2.2×10^{-9}, respectively.

D. General remarks on $K^+ \to \pi^+\mu^+\mu^-$

Obviously, the short distance effective Hamiltonian of Eq. (11.44) also gives rise to an amplitude for the transition $K^+ \to \pi^+\mu^+\mu^-$. This amplitude, however, is three orders of magnitude smaller than the dominant contribution to $K^+ \to \pi^+\mu^+\mu^-$ given by the one-photon exchange diagram (Ecker *et al.*, 1987) and is therefore negligible in the total decay rate. On the other hand, the coupling to the muon pair is purely vectorlike for the one-photon amplitude, whereas it contains an axial-vector part in the case of the SD contribution mediated by Z^0 penguin and W box diagrams. Thus, as was pointed out by Savage and Wise (1990) and discussed in detail by Lu *et al.* (1992), the *interference* of the one-photon and the SD contribution, which is odd under parity, generates a parity-violating longitudinal muon polarization asymmetry

$$\Delta_{LR} = \frac{\Gamma_R - \Gamma_L}{\Gamma_R + \Gamma_L} \tag{25.15}$$

in the decay $K^+ \to \pi^+\mu^+\mu^-$. Here Γ_R (Γ_L) denotes the rate of producing a right- (left-) handed μ^+, that is a μ^+ with spin along (opposite) its three-momentum direction. In this way a measurement of the asymmetry Δ_{LR} could probe the phenomenologically interesting short-distance physics that is not visible in the total rate.

The $K^+ \to \pi^+\gamma^*$ vertex is described by a form factor $f(s)$ (s being the invariant mass squared of the muon pair), that determines the one-photon amplitude and hence the total rate of $K^+ \to \pi^+\mu^+\mu^-$, but also enters the asymmetry Δ_{LR}. This form factor has been analyzed in detail by Ecker *et al.* (1987) within the framework of chiral perturbation theory. The imaginary part $\mathrm{Im}\, f(s)$ turns out to be much smaller than $\mathrm{Re} f(s)$ and can safely be neglected in the calculation of Δ_{LR}. For this reason

$f(s) \approx \mathrm{Re} f(s)$, which depends on a constant not fixed by chiral perturbation theory, may also be directly extracted from experimental data on $K^+ \to \pi^+ e^+ e^-$ (Alliegro *et al.*, 1992), sensitive to $|f(s)|$. We follow Lu *et al.* (1992) in adopting this procedure.

The dominance of $\mathrm{Re}\, f(s)$ further implies that Δ_{LR} actually measures the real part of the short-distance amplitude. As emphasized by Bélanger *et al.* (1993), Δ_{LR} is therefore closely related to the short-distance part of $K_L \to \mu^+ \mu^-$ and could possibly yield useful information on this contribution, which is difficult to extract from experimental results on $K_L \to \mu^+ \mu^-$. Like $(K_L \to \mu^+ \mu^-)_{\mathrm{SD}}$, Δ_{LR} is in particular a measure of the Wolfenstein parameter ϱ.

Lu *et al.* (1992) have also considered potential long-distance contributions to Δ_{LR} originating from two-photon exchange amplitudes. Unfortunately, these are very difficult to calculate in a reliable manner. The discussion by Lu *et al.* (1992) indicates, however, that they are likely to be much smaller than the short-distance contributions considered above. We will focus here on the short-distance part, keeping in mind the uncertainty due to possible non-negligible long-distance corrections.

One should stress that the short-distance part by itself, although calculable in a well-defined perturbative framework, is not completely free from theoretical uncertainty. The natural context to discuss this issue is a next-to-leading-order analysis, which, for Δ_{LR}, has been presented by Buchalla and Buras (1994b), who generalize the previous leading logarithmic-order calculations (Savage and Wise, 1990; Lu *et al.*, 1992; Bélanger *et al.*, 1993). We will summarize the results of Buchalla and Buras (1994b) below.

Finally we mention that other asymmetries in $K^+ \to \pi^+ \mu^+ \mu^-$, which are odd under time reversal and are also sensitive to short-distance contributions, have been discussed in the literature (Savage and Wise, 1990; Agrawal *et al.*, 1991, 1992; Lu *et al.*, 1992). They involve both the μ^+ and μ^- polarizations and are considerably more difficult to measure than Δ_{LR}. Possibilities for measuring the polarization of muons from $K^+ \to \pi^+ \mu^+ \mu^-$ in future experiments, based on studying the angular distribution of $e^\pm$ from decay, are described by Kuno (1992).

E. Master formulas for Δ_{LR}

The absolute value of the asymmetry Δ_{LR} can be written as

$$|\Delta_{LR}| = r |\mathrm{Re}\, \xi|. \tag{25.16}$$

The factor r arises from phase-space integrations. It depends only on the particle masses m_K, m_π, and m_μ, on the form factors of the matrix element $\langle \pi^+ | (\bar{s} d)_{V-A} | K^+ \rangle$, and the form factor of the $K^+ \to \pi^+ \gamma^*$ transition, which is relevant for the one-photon amplitude. In addition r depends on a possible cut which may be imposed on θ, the angle between the three-momenta of the μ^- and the pion in the rest frame of the $\mu^+ \mu^-$ pair. Without any cuts one has $r = 2.3$ (Lu *et al.*, 1992). If $\cos\theta$ is restricted to lie in the region $-0.5 \leqslant \cos\theta \leqslant 1.0$, this factor is increased to

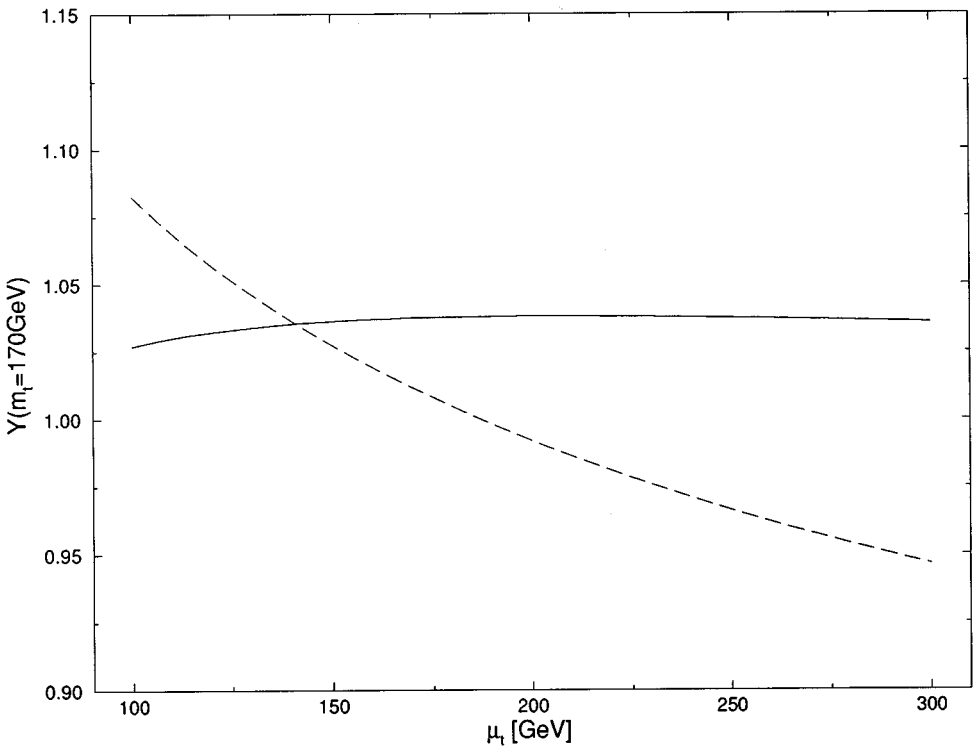

FIG. 30. Top-quark function $Y(x_t)$ as a function of μ_t for fixed $m_t = 170$ GeV with (solid curve) and without (dashed curve) $\mathcal{O}(\alpha_s)$ corrections.

TABLE XLVI. The function $P_0(Y)$ for various $\Lambda_{\overline{\rm MS}}^{(4)}$ and m_c.

	$P_0(Y)$		
$\Lambda_{\overline{\rm MS}}^{(4)}/m_c$	1.25 GeV	1.30 GeV	1.35 GeV
215 MeV	0.132	0.141	0.151
325 MeV	0.140	0.149	0.159
435 MeV	0.145	0.156	0.166

r=4.1. As discussed by Lu *et al.* (1992), such a cut in $\cos\theta$ could be useful since it enhances Δ_{LR} by 80% with only a 22% decrease in the total number of events.

Reξ is a function containing the information on the short-distance physics. It depends on CKM parameters, the QCD scale $\Lambda_{\overline{\rm MS}}$, the quark masses m_t and m_c, and is given by

$$\mathrm{Re}\xi=\kappa\left[\frac{\mathrm{Re}\lambda_c}{\lambda}P_0(Y)+\frac{\mathrm{Re}\lambda_t}{\lambda^5}Y(x_t)\right], \tag{25.17}$$

$$\kappa=\frac{\lambda^4}{2\pi\sin^2\Theta_W(1-\lambda^2/2)}=1.66\times10^{-3}. \tag{25.18}$$

Here $\lambda=|V_{us}|=0.22$, $\sin^2\Theta_W=0.23$, $x_t=m_t^2/M_W^2$, $\lambda_i=V_{is}^*V_{id}$, and

$$P_0(Y)=\frac{Y_{\rm NL}}{\lambda^4}. \tag{25.19}$$

The functions $Y_{\rm NL}$ and $Y(x_t)$ represent the charm and the top contribution, respectively. They are accurate to next-to-leading logarithmic order as given in Eqs. (11.48) and (11.45) and have already been discussed in Sec. XI.C and in the previous sections on the phenomenology of $(K_L\to\mu^+\mu^-)_{\rm SD}$. Numerical values for $P_0(Y)$ can be found in Table XLVI. From Eqs. (25.16) and (25.17) we can obtain $\mathrm{Re}\lambda_t$ expressed as a function of $|\Delta_{LR}|$:

$$\mathrm{Re}\lambda_t=-\lambda^5\frac{|\Delta_{LR}|/r\kappa-\left(1-\frac{\lambda^2}{2}\right)P_0(Y)}{Y(x_t)}. \tag{25.20}$$

Since $\mathrm{Re}\lambda_t$ is related to the Wolfenstein parameter $\bar\varrho$ (see Sec. II), one may use Eq. (25.20) to extract $\bar\varrho$ from a given value of $|\Delta_{LR}|$.

F. Numerical analysis of Δ_{LR}

To illustrate the phenomenological implications of the next-to-leading-order calculation, let us consider the following scenario. We assume a typical value for Δ_{LR}, allowing for an uncertainty of $\pm10\%$

$$\Delta_{LR}=(6.0\pm0.6)\times10^{-3}. \tag{25.21}$$

Here a cut on $\cos\theta$, $-0.5\leqslant\cos\theta\leqslant1.0$, is understood. Next we take $[m_i\equiv\bar m_i(m_i)]$

$$m_t=(170\pm5)\ \text{GeV},\quad m_c=(1.30\pm0.05)\ \text{GeV},$$

$$V_{cb}=0.040\pm0.001, \tag{25.22}$$

$$\Lambda_{\overline{\rm MS}}^{(4)}=(300\pm50)\ \text{MeV}. \tag{25.23}$$

Table XLVII shows the central value of $\bar\varrho$ that is extracted from Δ_{LR} in our example, together with the uncertainties associated to the relevant input. Combined errors due to a simultaneous variation of several parameters can be obtained to a good approximation by simply adding the errors in Table XLVII.

These errors should be compared with the purely theoretical uncertainty of the short-distance calculation, estimated by a variation of the renormalization scales μ_c and μ_t. Varying these scales as given in Eq. (24.19) and keeping all other parameters at their central values, we find

$$-0.15\leqslant\bar\varrho\leqslant-0.03\quad\text{(NLLA)}, \tag{25.24}$$

$$-0.31\leqslant\bar\varrho\leqslant0.02\quad\text{(LLA)}. \tag{25.25}$$

We observe that at NLO the scale ambiguity is reduced by almost a factor of 3 compared to the LLA. However, even in the NLLA the remaining uncertainty is still sizable, though moderate in comparison with the errors in Table XLVII. Note that the remaining error in Eq. (25.24) is almost completely due to the charm sector, since the scale uncertainty in the top contribution is practically eliminated at NLO.

We remark that for definiteness we have incorporated the numerically important piece $x_c/2$ in the leading logarithmic-order expression for the charm function Y, although this is strictly speaking a next-to-leading-order term. This procedure corresponds to a central value of $\bar\varrho=-0.12$ in LLA. Omitting the $x_c/2$ term and employing the strict leading-logarithmic-order result shifts this value to $\bar\varrho=-0.20$. Within NLLA this ambiguity is avoided in a natural way.

Finally, we give the standard-model expectation for Δ_{LR}, based on the short-distance contribution in Eq. (25.16), for the Wolfenstein parameter ϱ in the range $-0.25\leqslant\varrho\leqslant0.25$, $V_{cb}=0.040\pm0.004$, and $m_t=(170\pm20)$ GeV. Including the uncertainties due to m_c, $\Lambda_{\overline{\rm MS}}$, μ_c, and μ_t and imposing the cut $-0.5\leqslant\cos\theta\leqslant1$, we find

$$3.0\times10^{-3}\leqslant|\Delta_{LR}|\leqslant9.6\times10^{-3}, \tag{25.26}$$

employing next-to-leading-order formulas. Anticipating improvements in V_{cb}, m_t, and ϱ, we also consider a future scenario in which $\varrho=0.00\pm0.02$, $V_{cb}=0.040\pm0.001$, and $m_t=(170\pm5)$ GeV. The very precise determination of ϱ used here should be achieved through measuring CP asymmetries in B decays in the LHC era (Buras, 1994). Then Eq. (25.26) reduces to

TABLE XLVII. $\bar\varrho$ determined from $\Delta_{\rm LR}$ for the scenario described in the text and the uncertainties related to various input parameters.

		$\Delta(\Delta_{\rm LR})$	$\Delta(m_t)$	$\Delta(V_{cb})$	$\Delta(m_c)$	$\Delta(\Lambda_{\overline{\rm MS}})$
$\bar\varrho$	−0.06	±0.13	±0.05	±0.06	±0.01	±0.00

$$4.8\times10^{-3}\leq|\Delta_{LR}|\leq6.6\times10^{-3}. \tag{25.27}$$

One should mention that, although the top contribution dominates the short-distance prediction for $|\Delta_{LR}|$, the charm part is still important and should not be neglected, as Bélanger *et al.* (1993) did. It is easy to convince oneself that the charm sector contributes to $\bar{\varrho}$ the sizable amount $\Delta\bar{\varrho}_{\rm charm}\approx0.2$. Furthermore, as we have shown above, the charm part is the dominant source of theoretical uncertainty in the short-distance calculation of Δ_{LR}.

To summarize, we have seen that the scale ambiguity in the perturbative short-distance contribution to Δ_{LR} can be considerably reduced by incorporating next-to-leading-order QCD corrections. The corresponding theoretical error in the determination of $\bar{\varrho}$ from an anticipated measurement of $|\Delta_{LR}|$ is then decreased by a factor of 3, in a typical example. Unfortunately, the remaining scale uncertainty is quite visible even at NLO. In addition there are further uncertainties due to various input parameters and possibly to long-distance effects. Together this implies that the accuracy to which $\bar{\varrho}$ can be extracted from Δ_{LR} appears to be limited and Δ_{LR} cannot fully compete with the $K\to\pi\nu\bar{\nu}$ decay modes. Still, a measurement of Δ_{LR} might give interesting constraints on SM parameters, $\bar{\varrho}$ in particular, and we feel it is worthwhile to further pursue this interesting additional possibility.

XXVI. THE DECAYS $B\to X\nu\bar{\nu}$ AND $B\to\mu^+\mu^-$

A. General remarks

The rare decays, $B\to X_s\nu\bar{\nu}$, $B\to X_d\nu\bar{\nu}$ and $B_s\to\mu^+\mu^-$, $B_d\to\mu^+\mu^-$, are fully dominated by internal top-quark contributions. The relevant effective Hamiltonians are given in Eqs. (11.56) and (11.57), respectively. Only the top functions $X(x_t)$ and $Y(x_t)$ enter these expressions, and the uncertainties due to m_c and $\Lambda_{\overline{\rm MS}}$ affecting $K^+\to\pi^+\nu\bar{\nu}$ and $K_L\to\mu^+\mu^-$ are absent here. Consequently these two decays are theoretically very clean. In particular the residual renormalization-scale dependence of the relevant branching ratios, though sizable in leading order, can essentially be neglected after the inclusion of next-to-leading-order corrections. On the other hand a measurement of these rare B decays, in particular of $B\to X_s\nu\bar{\nu}$ and $B\to X_d\nu\bar{\nu}$, is experimentally very challenging. In addition, as we will see below, $B(B_s\to\mu^+\mu^-)$ and $B(B_d\to\mu^+\mu^-)$ are subject to the uncertainties in the values of the B-meson decay constants F_{B_s} and F_{B_d}, which hopefully will be removed one day.

B. The decays $B\to X_s\nu\bar{\nu}$ and $B\to X_d\nu\bar{\nu}$

The branching fraction for $B\to X_s\nu\bar{\nu}$ is given by

$$\frac{B(B\to X_s\nu\bar{\nu})}{B(B\to X_ce\bar{\nu})}=\frac{3\alpha^2}{4\pi^2\sin^4\Theta_W}\frac{|V_{ts}|^2}{|V_{cb}|^2}\frac{X^2(x_t)}{f(z)}\frac{\bar{\eta}}{\kappa(z)}. \tag{26.1}$$

Here $f(z)$, $z=m_c/m_b$, is the phase-space factor for $B\to X_ce\bar{\nu}$ defined already in Eq. (22.6), and $\kappa(z)$ is the corresponding QCD correction (Cabibbo and Maiani, 1978) given in Eq. (23.7). The factor $\bar{\eta}$ represents the QCD correction to the matrix element of the $b\to s\nu\bar{\nu}$ transition due to virtual and bremsstrahlung contributions and is given by the well-known expression

$$\bar{\eta}=\kappa(0)=1+\frac{2\alpha_s(m_b)}{3\pi}\left(\frac{25}{4}-\pi^2\right)\approx0.83. \tag{26.2}$$

For the numerical analysis we will use $\Lambda^{(5)}_{\rm QCD}=225$ MeV, Eq. (24.3), $|V_{ts}|=|V_{cb}|$, $m_t=170$ GeV, $B(B\to X_ce\bar{\nu})=0.104$, $f(z)=0.49$, and $\kappa(z)=0.88$, keeping in mind the QCD uncertainties in $B\to X_ce\bar{\nu}$ discussed in Sec. XVII.

Varying μ_t as in Eq. (24.19) we find that the ambiguity

$$3.82\times10^{-5}\leq B(B\to X_s\nu\bar{\nu})\leq4.65\times10^{-5} \tag{26.3}$$

present in the leading order is reduced to

$$3.99\times10^{-5}\leq B(B\to X_s\nu\bar{\nu})\leq4.09\times10^{-5} \tag{26.4}$$

after the inclusion of QCD corrections (Buchalla and Buras, 1993a).

It should be noted that $B(B\to X_s\nu\bar{\nu})$ as given in Eq. (26.1) is, in view of $|V_{ts}/V_{cb}|^2\approx0.95\pm0.03$, essentially independent of the CKM parameters and the main uncertainty resides in the value of m_t. Setting all parameters as given above and in the Appendix and using Eq. (24.30), we have

$$B(B\to X_s\nu\bar{\nu})=4.1\times10^{-5}\frac{|V_{ts}|^2}{|V_{cb}|^2}\left[\frac{m_t(m_t)}{170\ \text{GeV}}\right]^{2.30}. \tag{26.5}$$

In view of a new interest in this decay (Grossman *et al.*, 1995) we quote the standard-model expectation for $B(B\to X_s\nu\bar{\nu})$ based on the input parameters collected in the Appendix. We find

$$3.1\times10^{-5}\leq B(B\to X_s\nu\bar{\nu})\leq4.9\times10^{-5} \tag{26.6}$$

for the ''present day'' uncertainties in the input parameters and

$$3.6\times10^{-5}\leq B(B\to X_s\nu\bar{\nu})\leq4.2\times10^{-5} \tag{26.7}$$

for the ''future'' scenario.

In the case of $B\to X_d\nu\bar{\nu}$ one has to replace V_{ts} by V_{td}, which results in a decrease of the branching ratio by roughly an order of magnitude.

C. The decays $B_s\to\mu^+\mu^-$ and $B_d\to\mu^+\mu^-$

The branching ratio for $B_s\to l^+l^-$ is given by Buchalla and Buras (1993a)

$$B(B_s\to l^+l^-)=\tau(B_s)\frac{G_F^2}{\pi}\left(\frac{\alpha}{4\pi\sin^2\Theta_W}\right)^2F_{B_s}^2m_l^2m_{B_s}\times\sqrt{1-4m_l^2/m_{B_s}^2}|V_{tb}^*V_{ts}|^2Y^2(x_t), \tag{26.8}$$

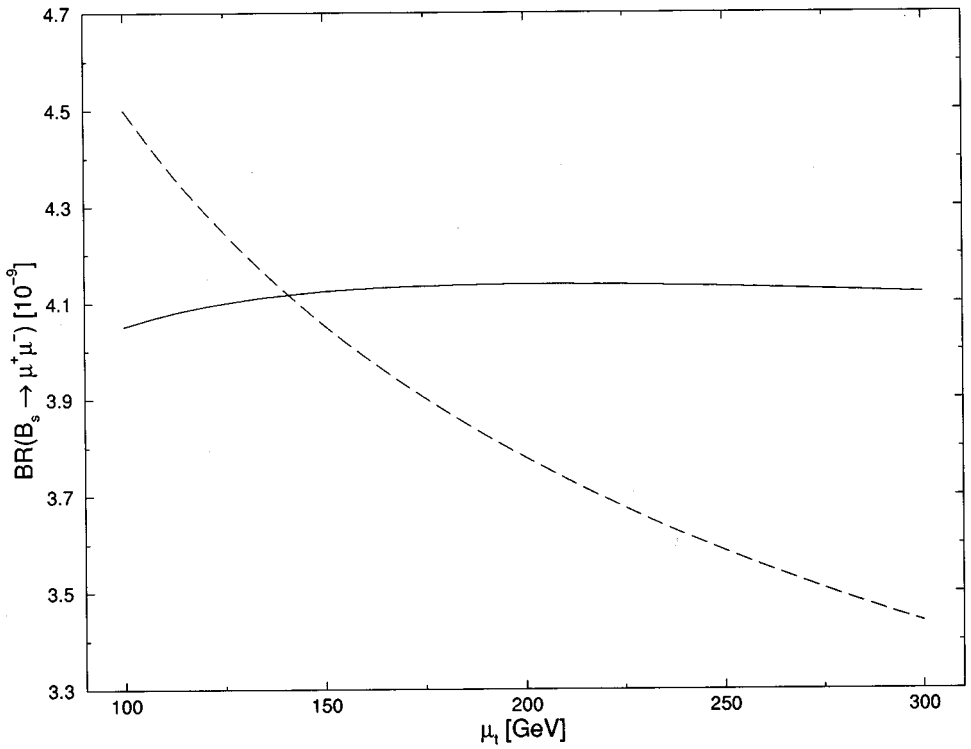

FIG. 31. The μ_t dependence of $B(B_s \to \mu^+\mu^-)[10^{-9}]$ with (solid curve) and without (dashed curve) $\mathcal{O}(\alpha_s)$ corrections for fixed parameter values as described in the text.

where B_s denotes the flavor eigenstate $(\bar{b}s)$ and F_{B_s} is the corresponding decay constant (normalized as F_π=131 MeV). Using Eqs. (24.3), (25.4), and (14.6), we find in the case of $B_s \to \mu^+\mu^-$

$$B(B_s \to \mu^+\mu^-) = 4.18\times 10^{-9}\left[\frac{\tau(B_s)}{1.6\ \text{ps}}\right]\left[\frac{F_{B_s}}{230\ \text{MeV}}\right]^2 \times\left[\frac{|V_{ts}|^2}{0.040}\right]^2\left[\frac{m_t(m_t)}{170\ \text{GeV}}\right]^{3.12}, \quad (26.9)$$

which approximates the next-to-leading-order result.

Taking the central values for $\tau(B_s)$, F_{B_s}, $|V_{ts}|$, and m_t and varying μ_t as in Eq. (24.19), we find that the uncertainty

$$3.44\times 10^{-9} \leqslant B(B_s \to \mu^+\mu^-) \leqslant 4.50\times 10^{-9} \quad (26.10)$$

present in the leading order is reduced to

$$4.05\times 10^{-9} \leqslant B(B_s \to \mu^+\mu^-) \leqslant 4.14\times 10^{-9} \quad (26.11)$$

when the QCD corrections are included. This feature is once more illustrated in Fig. 31.

Finally, we quote the Standard-Model expectation for $B(B_s \to \mu^+\mu^-)$ based on the input parameters collected in the Appendix. We find

$$1.7\times 10^{-9} \leqslant B(B_s \to \mu^+\mu^-) \leqslant 8.4\times 10^{-9} \quad (26.12)$$

using present day uncertainties in the parameters and $F_{B_s}=230\pm 40$ MeV. With reduced errors for the input quantities, corresponding to the second scenario as defined in the Appendix, and $F_{B_s}=230\pm 10$ MeV, this range would shrink to

$$3.1\times 10^{-9} \leqslant B(B_s \to \mu^+\mu^-) \leqslant 5.0\times 10^{-9}. \quad (26.13)$$

For the case of $B_d \to \mu^+\mu^-$ similar formulas hold with obvious replacements of labels $(s \to d)$. Provided the decay constants F_{B_s} and F_{B_d} will have been calculated reliably by nonperturbative methods or measured in leading leptonic decays one day, the rare processes $B_s \to \mu^+\mu^-$ and $B_d \to \mu^+\mu^-$ should offer clean determinations of $|V_{ts}|$ and $|V_{td}|$. The accuracy of the related analysis will profit considerably from the reduction of theoretical ambiguity achieved through the inclusion of short-distance QCD effects. In particular $B(B_s \to \mu^+\mu^-)$, which is expected to be $\mathcal{O}(4\times 10^{-9})$, should be attainable at hadronic machines such as HERA-B, Tevatron, and LHC.

XXVII. SUMMARY

In this review we have described in detail the present status of higher-order QCD corrections to weak decays of hadrons. We have emphasized that during the last few years considerable progress has been made in this field through the calculation of the next-to-leading-order QCD corrections to essentially all of the most interesting and important processes. This effort reduced considerably theoretical uncertainties, which will improve the accuracy of the CKM parameters to be determined in future experiments. We have illustrated this with several examples.

In this review we have concentrated on weak decays in the standard model. The structure of weak decays in

TABLE XLVIII. Summary of standard model (SM) theoretical predictions and experimental results for the rare and CP-violating processes discussed in this review. The entry "input" indicates that the corresponding measurement is used to determine or to constrain CKM parameters needed for the calculation of other decays. For $B(K_L\to\mu^+\mu^-)$ the theoretical value refers only to the short-distance contribution. In the case of $B(K_L\to\pi^0e^+e^-)$ the SM prediction corresponds to the contribution from direct CP violation. The SM predictions for $K^+\to\pi^+\nu\bar{\nu}$ and $K_L\to\pi^0\nu\bar{\nu}$ include the isospin-breaking corrections considered by Marciano and Parsa (1996).

Quantity	SM prediction	Experiment	Exp. reference
		K Decays	
$\lvert\epsilon_K\rvert$	input	$(2.266\pm0.023)\times10^{-3}$	(Particle Data Group, 1994)
ϵ'/ϵ	$(5.6\pm7.7)\times10^{-4}$	$(15\pm8)\times10^{-4}$	(Particle Data Group, 1994)
$B(K_L\to\pi^0e^+e^-)$	$(4.5\pm2.8)\times10^{-12}$ [$CP_{\rm dir}$]	$<4.3\times10^{-9}$	(Harris *et al.*, 1993)
$B(K^+\to\pi^+\nu\bar{\nu})$	$(1.0\pm0.4)\times10^{-10}$	$<2.4\times10^{-9}$	(Adler *et al.*, 1996)
$B(K_L\to\pi^0\nu\bar{\nu})$	$(2.9\pm1.9)\times10^{-11}$	$<5.8\times10^{-5}$	(Weaver *et al.*, 1994)
$B(K_L\to\mu^+\mu^-)$	$(1.3\pm0.7)\times10^{-9}$ [SD]	$(7.4\pm0.4)\times10^{-9}$	(Particle Data Group, 1994)
$\lvert\Delta_{\rm LR}(K^+\to\pi^+\mu^+\mu^-)\rvert$	$(6\pm3)\times10^{-3}$	—	—
		B Decays	
x_d	input	0.75 ± 0.06	(Browder and Honscheid, 1995)
$B(B\to X_s\gamma)$	$(2.8\pm0.8)\times10^{-4}$	$(2.32\pm0.67)\times10^{-4}$	(Alam *et al.*, 1995)
$B(B\to X_s\nu\bar{\nu})$	$(4.0\pm0.9)\times10^{-5}$	$<7.7\times10^{-4}$	(ALEPH Collaboration, 1996)
$B(B_s\to\tau^+\tau^-)$	$(1.1\pm0.7)\times10^{-6}$	—	—
$B(B_s\to\mu^+\mu^-)$	$(5.1\pm3.3)\times10^{-9}$	$<8.4\times10^{-6}$	(Kroll *et al.*, 1995)
$B(B_s\to e^+e^-)$	$(1.2\pm0.8)\times10^{-13}$	—	—
$B(B_d\to\mu^+\mu^-)$	$\sim10^{-10}$	$<1.6\times10^{-6}$	(Kroll *et al.*, 1995)
$B(B_d\to e^+e^-)$	$\sim10^{-14}$	$<5.9\times10^{-6}$	(Ammar *et al.*, 1994)

extensions of the standard model will generally have to be modified. Although we do not expect substantial effects due to "new physics" in tree-level decays, the picture of loop-induced processes, such as rare and CP-violating decays, may turn out to be different from the one presented here. The basic structure of QCD calculations will remain valid, however. In certain extensions of the standard model, in which no new local operators occur, only the initial conditions to the renormalization-group evolution will have to be modified. In more complicated extensions additional operators may be present and, in addition to the change of the initial conditions, the evolution matrix may also have to be generalized.

In order to be able to decide whether modifications of the standard theory are required by the data, it is essential that the theoretical calculations within the standard model itself reach the necessary precision. As far as the short-distance contributions are concerned, we think that in most cases such a precision has been already achieved.

Important exceptions are the $b\to s\gamma$ and $b\to sg$ transitions for which the complete NLO corrections are not yet available. On the other hand, the status of long-distance contributions, represented by the hadronic matrix elements of local operators or equivalently by various B_i parameters, is much less satisfactory. This is in particular the case for nonleptonic decays, where the progress is very slow. Yet without these difficult nonperturbative calculations it is impossible to give reliable theoretical predictions for nonleptonic decays even if the Wilson coefficients of the relevant operators have been calculated with high precision. Moreover, these coefficients have unphysical renormalization-scale and renormalization-scheme dependences that can only be canceled by the corresponding dependences in the hadronic matrix elements. All efforts should be made to improve the status of nonperturbative calculations.

The next ten years should be very exciting for the field of weak decays. The experimental efforts in several laboratories will provide many new results for the rare and CP-violating decays, which will offer new tests of the standard model and possibly signal some "new physics." As we have stressed in this review, the NLO calculations presented here will undoubtedly play an important role in these investigations. Let us just imagine that B_s^0-$\bar{B}_s^0$ mixing and the branching ratios for $K^+\to\pi^+\nu\bar{\nu}$, $K_L\to\pi^0\nu\bar{\nu}$, $B\to X_s\nu\bar{\nu}$, and $B_s\to\mu^+\mu^-$ have been measured to an acceptable accuracy. Having additionally at our disposal accurate values of $\lvert V_{ub}/V_{cb}\rvert$, $\lvert V_{cb}\rvert$, m_t, F_B, B_B, and B_K, as well as respectable results for the angles (α,β,γ) from the CP asymmetries in B decays, we could get a great insight into the physics of quark mixing and CP violation. One should hope that this progress on the experimental side will be paralleled by the progress in calculations of hadronic matrix elements as well as by calculations of QCD corrections in potential extensions of the standard model.

We would like to end this review with a summary of theoretical predictions and present experimental results for the rare and CP violating decays discussed by us. This summary is given in Table XLVIII.

Let us hope that the next ten years will bring a further reduction of uncertainties in the theoretical predictions and will provide us with accurate measurements of various branching ratios, for which, as seen in Table XLVIII, only upper bounds are available at present.

TABLE XLIX. Input parameters with present and "future" errors.

Quantity	Central	Present	Future
$\|V_{cb}\|$	0.040	± 0.003	± 0.001
$\|V_{ub}/V_{cb}\|$	0.08	± 0.02	± 0.01
B_K	0.75	± 0.15	± 0.05
$\sqrt{B_d}F_{B_d}$	200 MeV	± 40 MeV	± 10 MeV
x_d	0.75	± 0.06	± 0.03
m_t	170 GeV	± 15 GeV	± 5 GeV

ACKNOWLEDGMENTS

We would like to thank M. Jamin for extensive discussions and numerical checks in Secs. VII and XIX, M. Münz for providing the updated figures in Secs. XXII and XXIII, and S. Herrlich and U. Nierste for valuable comments on Sec. XII. Thanks are also due to W. Bardeen, M. Beneke, G. Burdman, I. Dunietz, A. El-Khadra, B. Gough, C. Greub, C. Hill, B. Kayser, W. Kilian, A. Kronfeld, A. Lenz, L. Littenberg, M. Misiak, T. Onogi, S. Parke, J. Simone, and B. Winstein for useful discussions.

M.E.L. acknowledges support by the Deutsche Forschungsgemeinschaft (DFG) and the hospitality of the SLAC theory group during parts of this work. This work has been supported by the German Bundesministerium für Bildung und Forschung under contract 06 TM 743, the CEC Science project SC1-CT91-0729, and DFG Contracts La 924/1-1 and ESMEX Li 519/2-1. Fermilab is operated by Universities Research Association, Inc., under Contract DE-AC02-76CHO3000 with the United States Department of Energy.

APPENDIX: COMPILATION OF NUMERICAL INPUT PARAMETERS

For the convenience of the reader we give a compilation of input parameters that were used in the numerical parts of this review.

Running quark masses:

$$\bar{m}_d(m_c)=8 \text{ MeV}, \quad \bar{m}_s(m_c)=(170\pm 20) \text{ MeV},$$

$$\bar{m}_c(m_c)=1.3 \text{ GeV},$$

$$\bar{m}_b(m_b)=4.4 \text{ GeV}, \quad m_b^{(\text{pole})}=4.8 \text{ GeV}.$$

Scalar meson masses and decay constants:

$$m_\pi=135 \text{ MeV}, \quad F_\pi=131 \text{ MeV},$$

$$m_K=498 \text{ MeV}, \quad F_K=160 \text{ MeV},$$

$$m_{B_d}=5.28 \text{ GeV}, \quad \tau(B_d)=1.6\times 10^{-12} \text{ s},$$

$$m_{B_s}=5.38 \text{ GeV}, \quad \tau(B_s)=1.6\times 10^{-12} \text{ s}.$$

QCD and electroweak parameters:

$$\alpha_s(M_Z)=0.117\pm 0.007, \quad \Lambda_{\overline{\text{MS}}}^{(5)}=(225\pm 85) \text{ MeV},$$

$$\alpha=1/129, \quad M_W=80.2 \text{ GeV},$$

$$\sin^2\Theta_W=0.23.$$

CKM elements:

$$|V_{us}|=0.22, \quad |V_{ud}|=0.975.$$

K decays, K^0-$\bar{K}^0$, and B^0-$\bar{B}^0$ mixing:

$$\tau(K_L)=5.17\times 10^{-8} \text{ s}, \quad \tau(K^+)=1.237\times 10^{-8} \text{ s},$$

$$BR(K^+\to\pi^0 e^+\nu)=0.0482,$$

$$|\varepsilon_K|=(2.266\pm 0.023)\times 10^{-3},$$

$$\Delta M_K=3.51\times 10^{-15} \text{ GeV},$$

$$\text{Re}A_0=3.33\times 10^{-7} \text{ GeV},$$

$$\text{Re}A_2=1.50\times 10^{-8} \text{ GeV},$$

$$\Omega_{\eta\eta'}=0.25,$$

$$\eta_1=1.38, \quad \eta_2=0.57,$$

$$\eta_3=0.47, \quad \eta_B=0.55.$$

The values for $\text{Re}A_{0,2}$ have been obtained from the Particle Data Group (PDG) using isospin analysis.

Hadronic matrix element parameters for $K\to\pi\pi$:

$$B_{2,\text{LO}}^{(1/2)}(m_c)=5.7\pm 1.1,$$

$$B_{2,NDR}^{(1/2)}(m_c)=6.6\pm 1.0, \quad \text{for } \Lambda_{\overline{\text{MS}}}^{(4)}=325 \text{ MeV}$$

$$B_{2,\text{HV}}^{(1/2)}(m_c)=6.2\pm 1.0,$$

$$B_3^{(1/2)}=B_5^{(1/2)}=B_6^{(1/2)}=B_7^{(1/2)}=B_8^{(1/2)}$$
$$=B_7^{(3/2)}=B_8^{(3/2)}=1 \quad \text{(central values)}.$$

For illustrative purposes we have sometimes used present as well as estimated future errors for various input parameters in our numerical calculations. In Table XLIX below this is indicated by labels "present" and "future."

REFERENCES

Abachi, S., *et al.*, 1995, Phys. Rev. Lett. **74**, 2632.
Abada, A., *et al.*, 1992, Nucl. Phys. B **376**, 172.
Abe, F., *et al.*, 1994a, Phys. Rev. D **50**, 2966.
Abe, F., *et al.*, 1994b, Phys. Rev. Lett **73**, 225.
Abe, F., *et al.*, 1994c, Phys. Rev. D **51**, 4623.
Adel, K., and Y. P. Yao, 1993, Mod. Phys. Lett. A **8**, 1679.
Adel, K., and Y. P. Yao, 1994, Phys. Rev. D **49**, 4945.
Adler, S., *et al.*, 1996, Phys. Rev. Lett. **76**, 1421.
Agrawal, P., J. Ng, G. Bélanger, and C. Geng, 1991, Phys. Rev. Lett. **67**, 537.
Agrawal, P., J. Ng, G. Bélanger, and C. Geng, 1992, Phys. Rev. D **45**, 2383.
ALEPH Collaboration, 1996, Contribution to the International Conference on High Energy Physics, Warsaw, Poland.
Alam, M. S., *et al.*, 1995, Phys. Rev. Lett. **74**, 2885.
Ali, A., G. F. Giudice, and T. Mannel, 1995, Z. Phys. C **67**, 417.
Ali, A., and C. Greub, 1991a, Z. Phys. C **49**, 431.
Ali, A., and C. Greub, 1991b, Phys. Lett. B **259**, 182.
Ali, A., and C. Greub, 1993, Z. Phys. C **60**, 433.
Ali, A., and C. Greub, 1995, Phys. Lett. B **361**, 146.

Ali, A., and D. London, 1995, Z. Phys. C **65**, 431.
Ali, A., T. Mannel, and T. Morozumi, 1991, Phys. Lett. B **273**, 505.
Alliegro, C., *et al.*, 1992, Phys. Rev. Lett. **68**, 278.
Allton, C. R., M. Ciuchini, M. Crisafulli, V. Lubicz, and G. Martinelli, 1994, Nucl. Phys. B **431**, 667.
Altarelli, G., G. Curci, G. Martinelli, and S. Petrarca, 1981, Nucl. Phys. B **187**, 461.
Altarelli, G. and L. Maiani, 1974, Phys. Lett. B **52**, 351.
Altarelli, G., and S. Petrarca, 1991, Phys. Lett. B **261**, 303.
Ammar, R., *et al.*, 1993, Phys. Rev. Lett. **71**, 674.
Ammar, R., *et al.*, 1994, Phys. Rev. D **49**, 5701.
Antonelli, V., S. Bertolini, M. Fabrichesi, and E. I. Lashin, 1996, Nucl. Phys. B **469**, 181.
Ashmore, J. F., 1972, Lett. Nuovo Cimento **4**, 289.
Bagan, E., P. Ball, V. Braun, and H. G. Dosch, 1992, Phys. Lett. B **278**, 457.
Bagan, E., P. Ball, V. Braun, and P. Gosdzinsky, 1994, Nucl. Phys. B **432**, 3.
Bagan, E., P. Ball, V. Braun, and P. Gosdzinsky, 1995, Phys. Lett. B **342**, 362.
Bagan, E., P. Ball, V. Braun, and P. Gosdzinsky, 1996, Phys. Lett. B **374**, 363(E).
Bagan, E., P. Ball, B. Fiol, and P. Gosdzinsky, 1995, Phys. Lett. B **351**, 546.
Ball, P., M. Beneke, and V. M. Braun, 1995a, Phys. Rev. D **52**, 3929.
Ball, P., M. Beneke, and V. M. Braun, 1995b, Nucl. Phys. B **452**, 563.
Ball, P., and U. Nierste, 1994, Phys. Rev. D **50**, 5841.
Barbieri, R., and G. F. Giudice, 1993, Phys. Lett. B **309**, 86.
Bardeen, W. A., A. J. Buras, D. W. Duke, and T. Muta, 1978, Phys. Rev. D **18**, 3998.
Bardeen, W. A., A. J. Buras, and J.-M. Gérard, 1987a, Phys. Lett. B **192**, 138.
Bardeen, W. A., A. J. Buras, and J.-M. Gérard, 1987b, Nucl. Phys. B **293**, 787.
Bardeen, W. A., A. J. Buras, and J.-M. Gérard, 1988, Phys. Lett. B **211**, 343.
Barger, V., M. S. Berger, and R. J. N. Phillips, 1993, Phys. Rev. Lett. **70**, 1368.
Barr, G. D., *et al.*, 1992, Phys. Lett. B **284**, 440.
Barr, G. D., *et al.*, 1993, Phys. Lett. B **317**, 233.
Baxter, R. M., *et al.*, 1994, Phys. Rev. D **49**, 1594.
Bélanger, G., and C. Q. Geng, 1991, Phys. Rev. D **43**, 140.
Bélanger, G., C. Q. Geng, and P. Turcotte, 1993, Nucl. Phys. B **390**, 253.
Beneke, M., and V. Braun, 1994, Nucl. Phys. B **426**, 301.
Beneke, M., and V. Braun, 1995, Phys. Lett. B **348**, 513.
Bernard, C., J. Labrenz, and A. Soni, 1994, Phys. Rev. D **49**, 2536.
Bernard, C., and A. Soni, 1991, Nucl. Phys. (Proc. Suppl.) **9**, 155.
Bertolini, S., F. Borzumati, and A. Masiero, 1987, Phys. Rev. Lett. **59**, 180.
Bertolini, S., F. Borzumati, A. Masiero, and G. Ridolfi, 1991, Nucl. Phys. B **353**, 591.
Bertolini, S., J. O. Eeg, and M. Fabbrichesi, 1995a, Nucl. Phys. B **449**, 197.
Bertolini, S., J. O. Eeg, and M. Fabbrichesi, 1995b, "A new estimate of $\varepsilon^1/\varepsilon$," SISSA preprint, SISSA 103/95/EP.
Bethke, S., 1994, talk presented at the QCD '94 Conference, Montpellier, France.
Bigi, I. I., B. Blok, M. Shifman, N. G. Uraltsev, and A. I. Vainshtein, 1994, in *B-Decays* (2nd Edition), edited by S. L. Stone (World Scientific, Singapore), (1994), p. 132; (1992), p. 610.
Bigi, I. I., B. Blok, M. Shifman, and A. Vainshtein, 1994, Phys. Lett. B **323**, 408.
Bigi, I. I., *et al.*, 1993, Phys. Rev. Lett. **71**, 496.
Bigi, I. I., and F. Gabbiani, 1991, Nucl. Phys. B **367**, 3.
Bigi, I. I., M. Shifman, N. G. Uraltsev, and A. I. Vainshtein, 1994a, Int. J. Mod. Phys. A **9**, 2467.
Bigi, I. I., M. Shifman, N. G. Uraltsev, and A. I. Vainshtein, 1994b, Phys. Rev. D **50**, 2234.
Bigi, I. I., and N. G. Uraltsev, 1994, Z. Phys. C **62**, 623.
Bigi, I. I., N. G. Uraltsev, and A. I. Vainshtein, 1992, Phys. Lett. B **293**, 430; 1993, **297**, 477(E).
Bijnens, J., J.-M. Gérard, and G. Klein, 1991, Phys. Lett. B **257**, 191.
Bijnens, J., and J. Prades, 1995, Nucl. Phys. B **444**, 523.
Bijnens, J., and M. B. Wise, 1984, Phys. Lett. B **137**, 245.
Bjorken, J. D., I. Dunietz, and J. Taron, 1992, Nucl. Phys. B **371**, 111.
Blok, B., L. Koyrakh, M. Shifman, and A. I. Vainshtein, 1994, Phys. Rev. D **49**, 3356.
Blok, B., and M. Shifman, 1993, "Lifetimes of charmed hadrons revisited. Facts and fancy," hep-ph/9311331.
Bollini, C. G., and J. J. Giambiagi, 1972a, Phys. Lett. B **40**, 566.
Bollini, C. G., and J. J. Giambiagi, 1972b, Nuovo Cimento B **12**, 20.
Borzumati, F. M., 1994, Z. Phys. C **63**, 291.
Boyd, C. G., B. Grinstein, and R. Lebed, 1995, Phys. Rev. Lett. **74**, 4603.
Breitenlohner, P., and D. Maison, 1977, Commun. Math. Phys. **52**, 11, 39, 55.
Broadhurst, D. J., and A. Grozin, 1991, Phys. Lett. B **267**, 105.
Brodsky, S. J., G. P. Lepage, and P. B. Mackenzie, 1983, Phys. Rev. D **28**, 228.
Browder, T. E., and K. Honscheid, 1995, Prog. Part. Nucl. Phys. **35**, 81.
Bruno, C., and J. Prades, 1993, Z. Phys. C **57**, 585.
Buchalla, G., 1993, Nucl. Phys. B **391**, 501.
Buchalla, G., 1996, "Renormalization of ΔB=2 transitions in the static limit beyond leading logarithms," hep-ph/9608232.
Buchalla, G., and A. J. Buras, 1993a, Nucl. Phys. B **400**, 225.
Buchalla, G., and A. J. Buras, 1993b, Nucl. Phys. B **398**, 285.
Buchalla, G., and A. J. Buras, 1994a, Nucl. Phys. B **412**, 106.
Buchalla, G., and A. J. Buras, 1994b, Phys. Lett. B **336**, 263.
Buchalla, G., and A. J. Buras, 1994c, Phys. Lett. B **333**, 221.
Buchalla, G., A. J. Buras, and M. K. Harlander, 1990, Nucl. Phys. B **337**, 313.
Buchalla, G., A. J. Buras, and M. K. Harlander, 1991, Nucl. Phys. B **349**, 1.
Buchalla, G., I. Dunietz, and H. Yamamoto, 1995, Phys. Lett. B **364**, 188.
Buras, A. J., 1980, Rev. Mod. Phys. **52**, 199.
Buras, A. J., 1993, Phys. Lett. B **317**, 449.
Buras, A. J., 1994, Phys. Lett. B **333**, 476.
Buras, A. J., 1995, Nucl. Phys. B **434**, 606.
Buras, A. J., and J.-M. Gérard, 1987, Phys. Lett. B **192**, 156.
Buras, A. J., and M. K. Harlander, 1992, in *Heavy Flavours*, edited by A. J. Buras and M. Lindner (World Scientific, Singapore), p. 58.
Buras, A. J., Jamin, and M. E. Lautenbacher, 1993a, Nucl. Phys. B **400**, 75.

Buras, A. J., M. Jamin, and M. E. Lautenbacher, 1993b, Nucl. Phys. B **408**, 209.
Buras, A. J., M. Jamin, M. E. Lautenbacher, and P. H. Weisz, 1992, Nucl. Phys. B **370**, 69; **375**, 501(A).
Buras, A. J., M. Jamin, M. E. Lautenbacher, and P. H. Weisz, 1993, Nucl. Phys. B **400**, 37.
Buras, A. J., M. Jamin, and P. H. Weisz, 1990, Nucl. Phys. B **347**, 491.
Buras. A. J., and M. E. Lautenbacher, 1993, Phys. Lett. B **318**, 212.
Buras, A. J., M. E. Lautenbacher, M. Misiak, and M. Münz, 1994, Nucl. Phys. B **423**, 349.
Buras, A. J., M. E. Lautenbacher, and G. Ostermaier, 1994, Phys. Rev. D **50**, 3433.
Buras, A. J., M. Misiak, M. Münz, and S. Pokorski, 1994, Nucl. Phys. B **424**, 374.
Buras, A. J., and M. Münz, 1995, Phys. Rev. D **52**, 186.
Buras, A. J., and P. H. Weisz, 1990, Nucl. Phys. B **333**, 66.
Burdman, G., and J. Kambor, 1996, "Dispersive approach to semi-leptonic form factors in heavy-to-light meson decays," FERMILAB preprint FERMILAB-PUB-96-033-T, hep-ph/9602353.
Cabibbo, N., and L. Maiani, 1978, Phys. Lett. B **79**, 109.
Callan Jr, C. G., 1970, Phys. Rev. D **2**, 1541.
Cella, G., G. Curci, G. Ricciardi, and A. Viceré, 1990, Phys. Lett. B **248**, 181.
Cella, G., G. Curci, G. Ricciardi, and A. Viceré, 1994a, Phys. Lett. B **325**, 227.
Cella, G., G. Curci, G. Ricciardi, and A. Viceré, 1994b, Nucl. Phys. B **431**, 417.
Cella, G., G. Ricciardi, and A. Viceré, 1991, Phys. Lett. B **258**, 212.
Chay, J., H. Georgi, and B. Grinstein, 1990, Phys. Lett. B **247**, 399.
Chetyrkin, K. G., C. A. Dominguez, D. Pirjol, and K. Schilcher, 1995, Phys. Rev. D **51**, 5090.
Cho, P., and M. Misiak, 1994, Phys. Rev. D **49**, 5894.
Cicuta, G. M., and E. Montaldi, 1972, Lett. Nuovo Cimento **4**, 329.
Ciuchini, M., E. Franco, and V. Giménez, 1996, "Next-to-leading order renormalization of the ΔB=2 operators in the static theory," hep-ph/9608204.
Ciuchini, M., E. Franco, G. Martinelli, and L. Reina, 1993a, Phys. Lett. B **301**, 263.
Ciuchini, M., E. Franco, G. Martinelli, and L. Reina, 1994a, Nucl. Phys. B **415**, 403.
Ciuchini, M., E. Franco, G. Martinelli, L. Reina, and L. Silvestrini, 1993b, Phys. Lett. B **316**, 127.
Ciuchini, M., E. Franco, G. Martinelli, L. Reina, and L. Silvestrini, 1994b, Phys. Lett. B **334**, 137.
Ciuchini, M., E. Franco, G. Martinelli, L. Reina, and L. Silvestrini, 1995, Z. Phys. C **68**, 239.
Ciuchini, M., E. Franco, L. Reina, and L. Silvestrini, 1994, Nucl. Phys. B **421**, 41.
Cohen, A. G., G. Ecker, and A. Pich, 1993, Phys. Lett. B **304**, 347.
Cohen, A. G., and A. Manohar, 1984, Phys. Lett. B **143**, 481.
Crisafulli, M., *et al.*, 1996, Phys. Lett. B **369**, 225.
Datta, A., J. Fröhlich, and E. A. Paschos, 1990, Z. Phys. C **46**, 63.
Datta, A., E. A. Paschos, J.-M. Schwarz, and M. N. S. Roy, 1995, "QCD corrections for the K^0-$\bar{K}^0$ and B^0-$\bar{B}^0$ system," hep-ph/9509420, University of Dortmund preprint, DO-TH 95/12.
Deshpande, N. G., and X.-G. He, 1995, Phys. Rev. Lett. **74**, 26; **74**, 4099 (E).
Deshpande, N. G., X.-G. He, and J. Trampetić, 1995, Phys. Lett. B **345**, 547.
Deshpande, N. G., X.-G. He, and J. Trampetić, 1996, Phys. Lett. B **367**, 362.
Deshpande, N. G., P. Lo, J. Trampetić, G. Eilam, and P. Singer, 1987, Phys. Rev. Lett. **59**, 183.
Desphpande, N. G., K. Panose, and J. Trampetić, 1993, Phys. Lett. B **308**, 322.
Deshpande, N. G., J. Trampetić, and K. Panose, 1989, Phys. Rev. D **39**, 1461.
Dib, C. O., I. Dunietz, and F. J. Gilman, 1989a, Phys. Lett. B **218**, 487.
Dib, C. O., I. Dunietz, and F. J. Gilman, 1989b, Phys. Rev. D **39**, 2639.
Dib, C. O., I. Dunietz, and F. J. Gilman, 1991, Mod. Phys. Lett. A **6**, 3573.
Dib, C. O., I. Dunietz, F. J. Gilman, and Y. Nir, 1990, Phys. Rev. D **41**, 1522.
Dikeman, R. D., M. Shifman, and N. G. Uraltsev, 1996, Int. J. Mod. Phys. A **11**, 571.
Donoghue, J. F., and F. Gabbiani, 1995, Phys. Rev. D **51**, 2187.
Donoghue, J. F., E. Golowich, and B. R. Holstein, 1982, Phys. Lett. B **119**, 412.
Donoghue, J. F., E. Golowich, B. R. Holstein, and J. Trampetić, 1986, Phys. Lett. B **179**, 361.
Draper, T., and C. McNeile, 1994, Nucl. Phys. B (Proc. Suppl.) **34**, 453.
Dugan, M. J., and B. Grinstein, 1991, Phys. Lett. B **256**, 239.
Duncan, A., E. Eichten, J. Flynn, B. Hill, G. Hockney, and H. Thacker, 1995, Phys. Rev. D **51**, 5101.
Ecker, G., A. Pich, and E. de Rafael, 1987, Nucl. Phys. B **291**, 692.
Ecker, G., A. Pich, and E. de Rafael, 1988, Nucl. Phys. B **303**, 665.
Eeg, J. O., and I. Picek, 1988, Phys. Lett. B **214**, 651.
Ellis, J., and J. S. Hagelin, 1983, Nucl. Phys. B **217**, 189.
Falk, A. F., M. Luke, and M. J. Savage, 1994, Phys. Rev. D **49**, 3367.
Falk, A. F., M. Wise, and I. Dunietz, 1995, Phys. Rev. D **51**, 1183.
Fleischer, R., 1994a, Z. Phys. C **62**, 81.
Fleischer, R., 1994b, Phys. Lett. B **332**, 419.
Floratos, E. G., D. A. Ross, and C. T. Sachrajda, 1977, Nucl. Phys. B **129**, 66.
Flynn, J. M., 1990, Mod. Phys. Lett. A **5**, 877.
Flynn, J. M., O. Hernńdez, and B. Hill, 1991, Phys. Rev. D **43**, 3709.
Flynn, J. M., and L. Randall, 1989a, Nucl. Phys. B **326**, 31.
Flynn, J. M., and L. Randall, 1989b, Phys. Lett. B **224**, 221; **235**, 412(E).
Franco, E., L. Maiani, G. Martinelli, and A. Morelli, 1989, Nucl. Phys. B **317**, 63.
Fröhlich, J., J. Heinrich, E. A. Paschos, and J.-M. Schwarz, 1991, "An improved estimate of direct CP violation," University of Dortmund preprint, DO-TH 02/91.
Gaillard, M. K., and B. W. Lee, 1974a, Phys. Rev. Lett. **33**, 108.
Gaillard, M. K., and B. W. Lee, 1974b, Phys. Rev. D **10**, 897.
Gell-Mann, M., and F. E. Low, 1954, Phys. Rev. **95**, 1300.
Geng, C. Q., and J. N. Ng, 1990, Phys. Rev. D **41**, 2351.
Georgi, H., 1991, in *Proceedings of TASI-91*, edited by R. K. Ellis *et al.* (World Scientific, Singapore), p. 589.

Gérard, J.-M., 1990, Acta Phys. Pol. B **21**, 257.
Gibbons, L. K., *et al.*, 1993, Phys. Rev. Lett. **70**, 1203.
Gilman, F. J., and M. B. Wise, 1979, Phys. Rev. D **20**, 2392.
Gilman, F. J., and M. B. Wise, 1980, Phys. Rev. D **21**, 3150.
Gilman, F. J., and M. B. Wise, 1983, Phys. Rev. D **27**, 1128.
Giménez, V., 1993, Nucl. Phys. B **401**, 116.
Greub, C., A. Ioannissian, and D. Wyler, 1995, Phys. Lett. B **346**, 149.
Grigjanis, R., P. J. O'Donnell, M. Sutherland, and H. Navelet, 1988, Phys. Lett. B **213**, 355.
Grigjanis, R., P. J. O'Donnell, M. Sutherland, and H. Navelet, 1989, Phys. Lett. B **223**, 239.
Grigjanis, R., P. J. O'Donnell, M. Sutherland, and H. Navelet, 1992, Phys. Lett. B **286**, 413(E).
Grinstein, B., 1989, Phys. Lett. B **229**, 280.
Grinstein, B., 1991, in *High Energy Phenomenology*, edited by R. Huerta and M. A. Péres (World Scientific, Singapore), p. 161.
Grinstein, B., M. J. Savage, and M. B. Wise, 1989, Nucl. Phys. B **319**, 271.
Grinstein, B., R. Springer, and M. B. Wise, 1990, Nucl. Phys. B **339**, 269.
Gross, D., 1976, in *Methods In Field Theory* (Les Houches 1975, Proceedings), edited by R. Balian and J. Zinn-Justin (North-Holland, Amsterdam), p. 141.
Grossman, Y., Z. Ligeti, and E. Nardi, 1996, Nucl. Phys. B **465**, 369; Erratum: hep-ph/9510378.
Guberina, B., and R. D. Peccei, 1980, Nucl. Phys. B **163**, 289.
Hagelin, J. S., and L. S. Littenberg, 1989, Prog. Nucl. Phys. **23**, 1.
Harris, D. A., *et al.*, 1993, Phys. Rev. Lett. **71**, 3918.
Harris, G. R., and J. L. Rosner, 1992, Phys. Rev. D **45**, 946.
Hayashi, T., M. Matsuda, and M. Tanimoto, 1993, Prog. Theor. Phys. **89**, 1047.
Heiliger, P., and L. Sehgal, 1993, Phys. Rev. D **47**, 4920.
Heinrich, J., E. A. Paschos, J.-M. Schwarz, and Y. L. Wu, 1992, Phys. Lett. B **279**, 140.
Herrlich, S., 1994, Ph.D. thesis, Munich Technical University.
Herrlich, S., and U. Nierste, 1994; Nucl. Phys. B **419**, 292.
Herrlich, S., and U. Nierste, 1995a, Phys. Rev. D **52**, 6505.
Herrlich, S., and U. Nierste, 1995b, Nucl. Phys. B **455**, 39.
Herrlich, S., and U. Nierste, 1996, "The Complete $|\Delta S| = 2$ Hamiltonian in the next-to-leading order," TUM-T31-86/96, hep-ph/9604330.
Hewett, J. L., 1993, Phys. Rev. Lett. **70**, 1045.
Hokim, Q., and X. Pham, 1983, Phys. Lett. B **122**, 297.
Hokim, Q., and X. Pham, 1984, Ann. Phys. (N.Y.) **155**, 202.
Hou, W. S., R. I. Willey, and A. Soni, 1987, Phys. Rev. Lett. **58**, 1608.
Inami, T., and C. S. Lim, 1981, Prog. Theor. Phys. **65**, 297.
Isgur, N., and M. Wise, 1989, Phys. Lett. B **232**, 113.
Isgur, N., and M. Wise, 1990, Phys. Lett. B **237**, 527.
Isgur, N., and M. Wise, 1992, in *Heavy Flavours*, edited by A. J. Buras and M. Lindner (World Scientific, Singapore), p. 234.
Ishizuka, N., 1993, Phys. Rev. Lett. **71**, 24.
Jamin, M., and M. Münz, 1995, Z. Phys. C **66**, 633.
Jamin, M., and A. Pich, 1994, Nucl. Phys. B **425**, 15.
Jaus, W., and D. Wyler, 1990, Phys. Rev. D **41**, 3405.
Jezabek, M., and J. H. Kühn, 1989, Nucl. Phys. B **320**, 20.
Ji, X., and M. Musolf, 1991, Phys. Lett. B **257**, 409.
Kambor, J., J. Missimer, and D. Wyler, 1990, Nucl. Phys. B **346**, 17.
Kambor, J., J. Missimer, and D. Wyler, 1991, Phys. Lett. B **261**, 496.
Kapustin, A., and Z. Ligeti, 1995, Phys. Lett. B **355**, 318.
Kapustin, A., Z. Ligeti, and H. D. Politzer, 1995, Phys. Lett. B **357**, 653.
Kaufman, W. A., H. Steger, and Y. P. Yao, 1989, Mod. Phys. Lett. A **3**, 1479.
Kilcup, G. W., 1991, Nucl. Phys. B (Proc. Suppl.) **20**, 417.
Kilian, W., and T. Mannel, 1993, Phys. Lett. B **301**, 382.
Kim, C. S., and A. D. Martin, 1989, Phys. Lett. B **225**, 186.
Ko, P., 1992, Phys. Rev. D **45**, 174.
Köhler, G. O., and E. A. Paschos, 1995, Phys. Rev. D **52**, 175.
Kroll, J., *et al.*, 1995, "Search for the decay $B^0 \to \mu^+ \mu^-$," Fermilab preprint, FERMILAB-CONF-95/229-E.
Kuno, Y., 1992, in *Proceedings of the 10th International Symposium on High Energy Spin Physics*, Nagoya, Japan, p 769; KEK-preprint 92-190.
Lim, C. S., T. Morozumi, and A. I. Sanda, 1989, Phys. Lett. B **218**, 343.
Littenberg, L. S., 1989a, Phys. Rev. D **39**, 3322.
Littenberg, L. S., 1989b, in *Proceedings of the Workshop on CP Violation at a Kaon Factory*, edited by J. N. Ng (publisher, city), p. 19.
Littenberg, L. S., and G. Valencia, 1993, Annu. Rev. Nucl. Part. Sci. **43**, 729.
Lu, M., and M. B. Wise, 1994, Phys. Lett. B **324**, 461.
Lu, M., M. B. Wise, and M. J. Savage, 1992, Phys. Rev. D **46**, 5026.
Luke, M., and M. J. Savage, 1994, Phys. Lett. B **321**, 88.
Luke, M., M. J. Savage, and M. B. Wise, 1995, Phys. Lett. B **343**, 329.
Lusignoli, M., 1989, Nucl. Phys. B **325**, 33.
Mannel, T., 1993, in *QCD—20 Years Later*, edited by P. M. Zerwas and H. A. Kastrup (World Scientific, Singapore), p. 634.
Mannel, T., 1994, Nucl. Phys. B **413**, 396.
Mannel, T., W. Roberts, and Z. Ryzak, 1992, Nucl. Phys. B **368**, 204.
Manohar, A. V., and M. B. Wise, 1994, Phys. Rev. D **49**, 1310.
Marciano, W., and Z. Parsa, 1996, Phys. Rev. D **53**, R1.
Misiak, M., 1991, Phys. Lett. B **269**, 161.
Misiak, M., 1993, Nucl. Phys. B **393**, 23.
Misiak, M., 1994, Phys. Lett. B **321**, 113.
Misiak, M., 1995, Nucl. Phys. B **439**, 461(E).
Misiak, M., and M. Münz, 1995, Phys. Lett. B **344**, 308.
Narison, S., 1994, Phys. Lett. B **322**, 247.
Neubert, M., 1992, Phys. Rev. D **45**, 2451.
Neubert, M., 1994a, Phys. Lett. B **338**, 84.
Neubert, M., 1994b, Phys. Rev. D **49**, 4623.
Neubert, M., 1994c, Phys. Rep. **245**, 259.
Neubert, M., and B. Stech, 1991, Phys. Rev. D **44**, 775.
Nierste, U., 1995, Ph.D. Thesis (Munich Technical University); hep-ph/9510323.
Nir, Y., 1989, Phys. Lett. B **221**, 184.
Nir, Y., 1992, in *Proceedings of the the 20th Annual SLAC Summer Institute on Particle Physics*, Stanford, California, 1992, p. 81.
Novikov, V. A., A. I. Vainshtein, V. I. Zakharov, and M. A. Shifman, 1977, Phys. Rev. D **16**, 223.
O'Donnell, P. J., and H. K. K. Tung, 1991, Phys. Rev. D **43**, R2067.
Ohl, K. E., *et al.*, 1990, Phys. Rev. Lett. **64**, 2755.
Ovsyannikov, L. V., 1956, Dokl. Acad. Nauk SSSR **109**, 1112.

Palmer, W. F., and B. Stech, 1993, Phys. Rev. D **48**, 4174.
Papadimitriou, V., *et al.*, 1991, Phys. Rev. D **44**, 573.
Particle Data Group, 1994, Phys. Rev. D **50**.
Patterson, J. R., 1995, in *Proceedings of the XXVII International Conference on High Energy Physics*, Glasgow, 1994, edited by P. J. Bussey and I. G. Knowles (IOP Publications Ltd., Bristol), p. 149.
Peccei, R. D., and K. Wang, 1995, Phys. Lett. B **349**, 220.
Pich, A., and E. de Rafael, 1985, Phys. Lett. B **158**, 477.
Pich, A., and E. de Rafael, 1991, Nucl. Phys. B **358**, 311.
Politzer, H. D., and M. B. Wise, 1988a, Phys. Lett. B **206**, 681.
Politzer, H. D., and M. B. Wise, 1988b, Phys. Lett. B **208**, 504.
Ponce, W. A., 1981, Phys. Rev. D **23**, 1134.
Pott, N., 1996, Phys. Rev. D **54**, 938.
Prades, J., C. Dominguez, J. Penarrocha, A. Pich, and E. de Rafael, 1991, Z. Phys. C **51**, 287.
Rein, D., and L. M. Sehgal, 1989, Phys. Rev. D **39**, 3325.
Ritchie, J. L., and S. G. Wojcicki, 1993, Rev. Mod. Phys. **65**, 1149.
Rosner, J. L., 1992, in *B-Decays*, edited by S. L. Stone (World Scientific, Singapore).
Sachrajda, C. T., 1992, in *Heavy Flavours*, edited by A. J. Buras and M. Lindner (World Scientific, Singapore), p. 415.
Sachrajda, C. T., 1994, in *B-Decays* (2nd Edition), edited by S. L. Stone (World Scientific, Singapore), p. 602.
Savage, M. J., and M. Wise, 1990, Phys. Lett. B **250**, 151.
Schmidtler, M., and K. R. Schubert, 1992, Z. Phys. C **53**, 347.
Sharpe, S. R., 1991, Nucl. Phys. B (Proc. Suppl.) **20**, 429.
Sharpe, S. R., 1994, Nucl. Phys. B (Proc. Suppl.) **34**, 403.
Shifman, M., N. G. Uraltsev, and A. I. Vainshtein, 1995, Phys. Rev. D **51**, 2217.
Simone, J. N., 1996, Nucl. Phys. B (Proc. Suppl.) **47**, 17.
Soares, J. M., 1996, Phys. Rev. D **53**, 241.
Soni, A., 1995, "Weak matrix elements on the lattice-circa 1995," preprint, hep-lat 9510036.
Stueckelberg, E. C. G., and A. Petermann, 1953, Helv. Phys. Acta **26**, 499.
Symanzik, K., 1970, Commun. Math. Phys. **18**, 227.
't Hooft, G., 1973, Nucl. Phys. B **61**, 455.
't Hooft, G., and M. Veltman, 1972a, Nucl. Phys. B **50**, 318.
't Hooft, G., and M. Veltman, 1972b, Nucl. Phys. B **44**, 189.
Tanimoto, M., 1992, Phys. Lett. B **274**, 463.
Thorndike, E., 1995, talk presented at the EPS-HEP Conference, Brussels, Belgium, 1995.
Vainshtein, A. I., V. I. Zakharov, V. A. Novikov, and M. A. Shifman, 1976, Sov. J. Nucl. Phys. **23**, 540.
Vainshtein, A. I., V. I. Zakharov, and M. A. Shifman, 1977, Joint Euro. Jorus Publ. JET P **45**, 670.
Voloshin, M. B., 1995, Phys. Rev. D **51**, 3948.
Voloshin, M. B., and M. Shifman, 1987, Sov. J. Nucl. Phys. **45**, 292.
Vysotskij, M. I., 1980, Sov. J. Nucl. Phys. **31**, 797.
Weaver, M., *et al.*, 1994, Phys. Rev. Lett. **72**, 3758.
Webber, B. R., 1994, talk presented at the International Conference on High Energy Physics, Glasgow, Scotland.
Weinberg, S., 1973, Phys. Rev. D **8**, 3497.
Wilson, K. G., and W. Zimmermann, 1972, Commun. Math. Phys. **24**, 87.
Winstein, B., and L. Wolfenstein, 1993, Rev. Mod. Phys. **65**, 1113.
Witten, E., 1977, Nucl. Phys. B **122**, 109.
Wolfenstein, L., 1964, Phys. Rev. Lett. **13**, 562.
Wolfenstein, L., 1983, Phys. Rev. Lett. **51**, 1841.